Light and taste

Third plane side-view combined with Complex Fenestration System atmospheres under midday Clear Sky at restaurants

Urtza Uriarte Otazua
UPC 2016

Light and taste

Third plane side-view combined with Complex Fenestration System atmospheres under midday Clear Sky at restaurants

By

Urtza Uriarte Otazua

PhD thesis supervised by Dr. Joan Lluís Zamora i Mestre and Rufino Javier Hernández Minguillón

Presented at *Universitat Politècnica de Catalunya*

In the program of *Àmbits de Recerca en l'Energia i el Medi Ambient a l'Arquitectura*

Escola Tècnica Superior d'Arquitectura del Vallès

Department of Tecnologia de l´Aquitectura (753-TA)

2016 November

Acknowledgements

Firstly, I would like to thank my family for their support and encouragement throughout this project. Without their help, hardly I could have finished. In particular, I want to thank my deceased brother for encouraging me to enter the *Escola Tècnica Superior d'Arquitectura de Barcelona*.

Following, I would like to thank my thesis supervisors, Professor Joan Lluís Zamora and Professor Rufino Javier Hernández, for their unconditional support. I am also grateful to Professor Helena Coch and deceased Professor Rafael Serra for teaching the fundamental principles of daylighting, and especially to Professor Antonio Isalgue for his generosity and inexhaustible patience in teaching me everything I needed to know about the aspects of building physics. I cannot forget Professor Jaume Roset and his wise advice and all my colleagues at the *Laboratori d'Innovació i Tecnologia de l'Arquitectura* (LiTA), *Calidad de Vida en Arquitectura* (CAVIAR) and *Arquitectura Energia i Medi Ambient* (AIEM).

Continuing, I want to thank Professor André De Herde for hosting at the *Architecture et Climat* and to all the research team for their exceptional welcome. I am particularly grateful to Professor Magali Bodart and Dr. Coralie Cauwerts for teaching the fundamental principles of Radiance and Complex Fenestration Systems.

In addition, I want to thank the Radiance Community for the enormous help offered, and especially the great scientist Greg Ward for his continued support and Dr. Jan Wienold for his technical advice. I want to thank Alstan Jakubiec for his support in DIVA.

Finally, I would like to thank the *Universitat Politècnica de Catalunya-BarcelonaTech* (UPC), *Euskal Herriko Unibertsitatea* (UPV/EHU) and *Université Catholique de Louvain* (UCL) for giving me the opportunity to prepare this thesis. Furthermore, I would like to thank the Basque Government's Department of Education, Language Policy and Culture for funding the PhD as a predoctoral training program (FPI), because without the financial support it would have been impossible to undertake this project.

Abstract

This thesis deals with sunny side-lit indoor atmospheres, in which an outdoor view is required and a calm environment to enhance concentration. Different window systems were compared: a single fully glazed façade and complex façades. The complex façades were composed of large or small windows that combined a light shelf and prismatic film complex fenestration systems.

The luminance and illuminance distribution parameters were selected to assess the light atmosphere. The Daylight Glare Probability (DGP) index was used to evaluate the luminance distribution and the Daylight Autonomy (DA) index was used to evaluate the illuminance distribution. The simulation method was selected to validate the hypothesis. Evalglare, which is a tool for performing a glare analysis of a Radiance-based HDR scene, was used to obtain the DGP index and the Three-Phase Method was used to simulate complex fenestration with Radiance to obtain the DA index. In addition, DIVA, Radiance's based plugin for Rhino, was used to obtain reference illuminance data and the DA of window systems without Complex Fenestration Systems (CFS).

Furthermore, one point of view usually contains more than two workplanes; a down view (e.g. to a tablet, paper, etc.), a front view (e.g. to a monitor, other person, etc.) and a far view (e.g. to the outside, open-plan, etc.). Therefore, a third workplane was proposed in addition to the source and background planes. In consequence, the mean DGP of three workplanes was proposed as a simple way to obtain the overall glare perception. The mean DA was also proposed to obtain a reference value throughout the space and standard deviation was used to obtain more information about illuminance distribution throughout the space.

The restaurant was proposed as case study because in recent years the demand for an outside view whilst dining has grown considerably. In this context, the selected point of view was that of a person seated at a table next to the façade, with another person in front of him or her. Therefore, the workplanes were the table, the person and the window. These three workplanes were tested by the DGP index and the workplane of the table spread along the room was tested by the DA index.

The results show, on one hand according to the luminance distribution results, the contribution of the different workplanes, as the third plane, the source plane and the background plane, could help to get closer to the final glare perception, because it takes into account aspects of adaptation. Three workplanes combination could allow differentiating more extreme luminance values than having only two workplanes. The small window tends to provide less probability of daylight glare than the large window, but also provides less light and more local contrast. On the other hand, according to illuminance distribution results, if redirecting systems are added to the façade

composition and the light source that probably causes the glare is avoided, light that it is better distributed throughout the workplanes can be achieved.

In conclusion, the small window combined with a Complex Fenestration System can provide less indoor sidelight, but, intimate and comfortable atmosphere where users can enjoy a good concentration level. When the two functions of an outdoor view and light supplied from a glazed façade are separated, they may work better. A complex daylight design, combining an outside view, redirected light, indirect light and direct light with the workplanes could provide a different atmosphere with an accurate light balance, according to the activity.

Keywords: daylighting, side-view, visual comfort, window, Complex Fenestrations Systems, Radiance, Building Performance Simulation

Resumen

La tesis trata sobre ambientes interiores en días soleados con iluminación natural lateral, en el cual la vista exterior es requerida y un ambiente tranquilo para mejorar la concentración. Diferentes sistemas de ventanas fueron comparados; una simple fachada totalmente vidriada y unas fachadas complejas. Las fachadas complejas están compuestas por una ventana grande o pequeña combinada por sistemas complejos de ventanas como un estante de luz o una película prismática.

Los parámetros como la distribución de luminancias y la distribución de iluminancias fueron seleccionados para evaluar el ambiente lumínico. El índice Daylight Glare Probability (DGP) fue utilizado para evaluar la distribución de luminancias y el índice Daylight Autonomy (DA) fue utilizado para evaluar la distribución de iluminancias. El método de simulación fue elegido para validar la hipótesis. Evalglare, el cual es una herramienta para realizar el análisis de deslumbramiento de escenas de HDR basados en Radiance, fue utilizado para obtener el índice DGP y Three-Phase Method fue utilizado para simular el índice DA con los sistemas complejos de ventanas con Radiance. Igualmente, DIVA, programa adicional basado en Radiance para Rhino, fue utilizado para obtener datos de referencia de iluminancia y el DA para sistemas de ventanas sin sistemas complejos de ventanas (CFS).

Asimismo, normalmente un punto de vista contiene más de dos planos de trabajo; una vista inferior (p. ej. hacia una pantalla, papel, etc.), una vista frontal (p. ej. hacia un monitor, otra persona, etc.) y una vista lejana (p. ej. hacia un exterior, espacio abierto, etc.). Por lo tanto, un tercer plano de trabajo fue propuesto para añadir a los planos de trabajo de la fuente y el fondo. En consecuencia, la media del DGP de los tres planos de trabajo fue propuesto de una forma sencilla para obtener la percepción global del deslumbramiento. La media de DA también fue propuesto para conseguir un valor de referencia a lo largo del espacio y la medida de desviación de estándar fue utilizado para obtener más información sobre la distribución de la iluminancia a lo largo del espacio.

El restaurante fue propuesto como caso de estudio, porque en los últimos años en la actividad de comer la demanda de las vistas exteriores ha incrementado considerablemente. En este contexto, el punto de vista seleccionado es adyacente a la fachada desde una persona sentada comiendo con una mesa compartida por una persona de en frente. Por lo tanto, los planos de trabajo son la mesa, la persona y la ventana. Estos tres planos están testeados por el índice DGP y el plano de trabajo de la mesa expandido a lo largo de la sala está testeado por el índice DA.

Los resultados demuestran, por un lado conforme a los resultados de la distribución de luminancias, la contribución de diferentes planos de trabajo, como el tercer plano, el plano de la fuente y el plano del fondo, podría aproximar más a la percepción global de

deslumbramiento, porque tiene en cuenta aspectos de la adaptación. La combinación de los tres planos de trabajo puede permitir una diferenciación mayor de las luminancias extremas que la combinación de dos planos de trabajo. La ventana pequeña tiene tendencia a proporcionar menos probabilidad de deslumbramiento que la ventana grande pero menos cantidad de luz y más contraste local. Por otro lado, conforme a los resultados de la distribución de iluminancias, si los sistemas de redirección se incorporan a la composición de la fachada y la probabilidad de deslumbramiento de la fuente de luz se evita, se puede conseguir una iluminación mejor distribuida a lo largo de los planos de trabajo se.

En conclusión, la ventana en combinación con sistemas complejos de ventanas es capaz de proporcionar menos la iluminación natural lateral pero sí una atmósfera interior confortable e íntima mediante en el cual los usuarios pueden disfrutar de un buen nivel de concentración. Cuando las dos funciones de la fachada vidriada como la vista exterior y la aportación de iluminación son separadas, las dos funciones pueden trabajar mejor. Un complejo diseño de la iluminación natural, combinando la vista exterior, la luz redirigida, la luz indirecta y la luz directa con los planos de trabajo, podría proporcionar una atmósfera diferente con un adecuado balance lumínico en función de la actividad.

Palabras clave: iluminación natural, vista lateral, confort visual, ventana, sistemas complejos de ventanas, Radiance, simulación del comportamiento del edificio

Index

List of Figures

List of Tables

Chapter I

INTRODUCTION

1.1 Context

The thesis addresses the design of daylight atmospheres according to visual comfort. It examines the luminance and illuminance distribution of the side-view through a split façade, taking into account the composition of the window and a Complex Fenestration System (CFS) under high outdoor luminance. The selected case study is a restaurant, as restaurants have a high demand for side-views.

Daylighting is a design parameter that allows different indoor atmospheres to be created with low energy consumption. It is a useful resource to design a space, and especially to design quality atmospheres, because it provides well-being for the users. We could say that daylight is a forgotten design resource.

Activities that use side-lit spaces are very common. Side-lighting is one of the oldest lighting applications, owing to the fact that it is easy, practical and nearby side opening. Usually, this light enters through the façade and is complemented by the outside view. This kind of view could be called a side-view.

In recent years, looking at the outdoors through a side-view has become a valued experience. The side view turns into so important that users prefer not to have any obstructions. In this case, daylight control becomes a problem to solve, as well as the combination of side-view and lighting. Combining outdoor view, redirect light, indirect light and direct light in the same atmosphere could be a complex daylighting design, but comfortable visual performance can probably be attained.

The side-view in a context of high outdoor luminance is relevant, mainly when the current façade are highly glazed façade. Therefore, a split façade could better control the daylight and the combination between side-view and lighting.

The amount of daylight that enters plays a determining role in users' concentration on activities. The design of the indoor light atmosphere affects the productivity and well-being of users. Calm and quite indoor atmospheres tend to be associated with a good level of concentration. Therefore, the façade design should achieve a good balance between side-view and concentration on the activity.

This research is about luminance and illuminance distribution of split façade that includes a side-view and is comprised of different window systems. The window systems include small and large windows, a light shelf and 3M prismatic film Complex Fenestration Systems. The Daylight Glare Probability (DGP) index will be used to assess luminance distribution and the Daylight Autonomy (DA) index will be used to evaluate illuminance distribution.

To obtain a detailed assessment, from a point of view, three workplanes will be defined that contributed to the overall task. Then, in a simple way, the mean DGP is

proposed to determine the contribution of each workplane to the overall perception, to avoid extreme situations and to consider aspects of adaptation. Moreover, regarding illuminance distribution, mean and standard deviation measures for each window system will be tested to obtain more accurate information on distribution.

The simulation will be used to obtain the DGP and DA indexes. Radiance software will be used to calculate both indexes. Rhinoceros software will be used to obtain virtual models. To check the luminance distribution and visualizations, DIVA, Radiance's plugin for Rhino, will be used. Evalglare, which is a tool for performing a glare analysis of a Radiance-based HDR scene, will be used to obtain the DGP index. To check the illuminance distribution given by the DA index, DIVA for window systems without Complex Fenestration Systems and the Three-Phase Method for all window systems will be used.

A restaurant is proposed for the cases study due to its side-view and indoor quality atmosphere high demand. During dining, it is of interest to have a comfortable vision perception. In recent years, restaurant light designs have been innovative, but many of them have involved electric lighting. The addition of daylight to indoor light performance would be enriching, and would achieve better comfortable vision perception with low energy consumption.

Figure 1. 1 Outside view demand with fully glazed façade. *Mirador de Ulía* restaurant, picture obtained from the website, http://www.donosticlick.com/restaurante-mirador-de-ulia-sansebastian/

In this context, if users are able to taste the light, it is because the atmosphere has comfortable vision quality. Thus, good lighting improves users' well-being and contributes to decreasing the energy consumption, as in bioclimatic guidelines.

In the context of the study, in recent years the value of outside views has increased notably. In consequence, the main façade of restaurants is usually oriented to appreciate the outdoor views. In addition, customers seem to sit looking out at the scenery. Furthermore, the value of visual events is so high that a gallery market has become visually attractive.

Figure 1. 2 Restaurant at gallery. Antwerpen. 2015

In restaurants with a façade that provides an outdoor view, costumers choose to sit next to the façade with a side-view position. It seems that usually these places are used to create an intimate environment.

Figure 1. 3 Restaurant with sidelighting. Ghent. 2015

Usually, façade design reflects the architectural style of each historical time. In ancient times, a window was an aperture in the wall to provide fresh air and a connection to the outside. However, from medieval times to modernism, the window became increasingly complex. Each part of the window has its function, so that users can get the most out of it. This kind of façade can be called a split façade. It has many advantages, and helps to provide a quality indoor atmosphere. In addition, all of the strategies are considered in the design, and consequently follow passive system guidelines, with low energy consumption. Furthermore, the complexity can offer more possibilities to satisfy the different needs of each user.

Figure 1. 4 Restaurant with modernism style. Brussels. 2015

In this way, following the style before rationalism, façades have incorporated many light management criteria. Regarding the indoor atmosphere provided by these techniques, daylight is used to create the atmosphere. The paths of light throughout the room are considered. This aspect could be called luminance distribution, and focuses only on the intensity of the light.

Figure 1. 5 Intimated indoor atmospehere at *Hostal Bofill* restaurant. Viladrau. 2015

The possibility of light reaching the deeper areas of the room is another aspect that classical windows have taken into account. The most common strategy is to have high windows and some parts of the wall that redirect light. We can use the term illuminance distribution to describe this aspect: the light level throughout the room.

However, since rationalism times, the façade has ceased to be a bearing wall and artificial systems have begun to be implemented. As a result, fully glazed façades have been created, always in response to the demand for external views. Sometimes, these façades cause discomfort. Usually, a large outside view prevails over a comfortable light balance indoors.

1.2 Problem statement

After observing side-view light atmospheres, in a context of high outdoor luminance, discomfort in light perception is detected. Despite the large, glazed transparent surfaces, a good outdoor view is not guaranteed, or a high level of concentration on the activity. Moreover, unbalanced indoor light distribution is observed.

Some new or retrofit restaurants' façades are checked to determine current façade designs. The aim is to observe whether the façades are highly glazed.

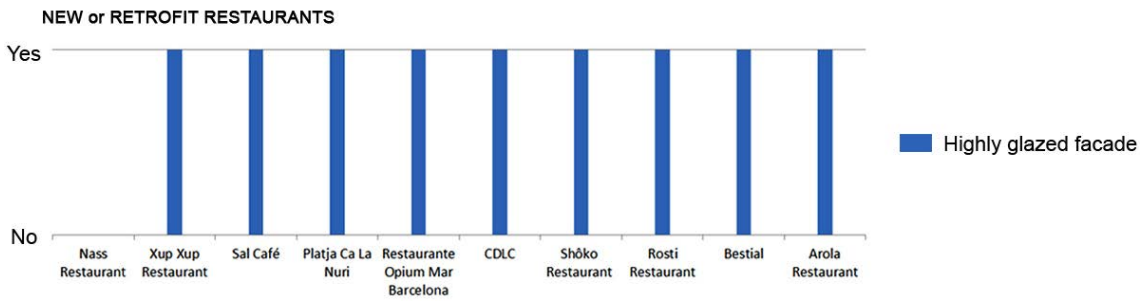

Figure 1. 6 Some retrofit restaurants at Barceloneta, Barcelona (Spain), with highly glazed façade

Ten new or retrofit restaurants were selected on the seafront of Barcelona. A total of 90% of them had a highly glazed façade. The percentage is high, but in most current restaurants, highly glazed façade designs are observed. In many cases, the façade is comprised of a large, homogeneous piece of glass. It is difficult to find a split façade in current architecture design.

Figure 1. 7 Fully glazed façade at *Platja Ca la Nuri*. Barceloneta. 2014

The loss and the lack of direct sunlight strategies cause an obstructed side-view with filtering systems. The problem is that restaurant customers prefer a side-view without any obstructions. In addition, customers tend to wear sunglasses at these tables, which confirm that the light conditions are glaring. Moreover, the large transparent glass surfaces do not cover undesirable outdoor elements. With the loss of a frame, landscape selection is lost.

Figure 1. 8 Shading systems to block direct sunlight. Barceloneta. 2014

Figure 1. 9 Sunglasses for reduce side-view brightness. Barceloneta. 2014

Figure 1. 10 Some undesirable elements in outdoor view. Barceloneta. 2014

A simple side opening creates unbalanced indoor light distribution. A lack of light redirecting systems causes high light contrast between the inside and outside areas. When the sky is clear, there is considerable direct light and more shadows appear.

Figure 1. 11 High light contrast between indoors and outdoors, especially caused by the high directionality of the sunlight. Barceloneta. 2014

Therefore, there are problems with the side-view, when the advantages of a split façade are not considered, and there are problems with the indoor light atmosphere. Particularly, there are problems with luminance and illuminance distributions, which cause glaring and non-uniform perception.

According to specific problems of tools to assess luminance distribution and illuminance distribution, add that the glare metrics are used for one workplane. However, it seems that checking only one part of overall visual field is not representative enough to evaluate overall visual perception. Specially, when this one workplane is an extreme, local visual field of overall perception such as side-view, it has extreme luminance values. Thus, this workplane should not be representative of overall perception, because it should consider the mean of different local visual fields. In this context, Daylight Glare Probability index is selected to check the luminance distribution of each workplane.

Furthermore, the simulation of illuminance distribution by Daylight Autonomy index has some complications. The performance of Complex Fenestration Systems cannot be obtained accurately by classical Radiance commands, and the Three Phase Method must be implemented. So, this method allows a scattering description of Complex Fenestration Systems to be taken into account, as they are considered as light sources.

1.3 Research objectives

In the context of high outdoor luminance and side-view without obstructions such as a filter, the general objective of the thesis is to demonstrate that:

· **A split façade could improve the indoor light atmosphere**, and consequently the indoor light perception for a particular situation.

Luminance and illuminance distribution are assessed to evaluate indoor light perception:

· Regarding the side-view, the aim is to demonstrate that a split window creates a calm atmosphere, by decreasing the view of large bright surfaces outside, and consequently reducing the glare probability and the view of unnecessary elements outdoors.

· Regarding the Complex Fenestration System, the aim is to assess whether they improve the light distribution on workplanes and throughout the space.

Therefore, the general objective is to enhance a calm atmosphere, to achieve a higher level of concentration, optimize transparent surfaces, and keep a good level of comfort combined with low energy consumption.

With reference to specific targets, the objective is to simulate the luminance and illuminance distribution parameters of various split façade window systems. Some measurements are planned to obtain reference data to calibrate the simulations:

· Regarding the luminance distribution parameter, the aim is to test the Daylight Glare Probability (DGP) index of different workplanes. Thus, the goal is to probe whether a small window provides less overall glare probability. In addition, taking into account that the overall glare prediction of one point of view is comprised of different workplanes, a detailed glare prediction for each workplane is wanted to do. Accordingly, the mean Daylight Glare Probability between the workplanes is tested. Thus, classical glare methods with an indoor luminance range for an outdoor view should result in very high glare. The aim is, in a simple way and taking into account different workplanes such as an intermediate workplane, to determine whether the overall glare prediction is closer to the real perception. In summary, the objective is to try to characterize the light performance of the third plane in addition to the source and background planes.

· According to the illuminance distribution parameter, the goal is to obtain the Daylight Autonomy (DA) index simulation of different window systems.

Specially, the aim is to obtain DA simulation of Complex Fenestration Systems using the Three-Phase Method, which is a specific method based on a Radiance simulator. Furthermore, the objective is to use DIVA, the Radiance program based plugin for Rhinoceros, to have reference illuminance data and the DA of window systems without Complex Fenestration Systems. Regarding Complex Fenestration Systems, the aim is to examine whether redirecting systems improve the light level throughout the space.

To sum up, the final objective is to obtain some design indicators and tools to contribute to the creation of more comfortable, side-lit indoor atmospheres. To achieve this, the goal is to examine whether the small window combined with Complex Fenestration System could provide such an atmosphere.

1.4 State of the art

In this section, the topics covered in this research are explained. Each topic is associated with a summary card on a publication that addresses the phenomena. The publication is listed, followed by an explanation of each topic.

First, the atmospheres provided by side-views and their workplanes are discussed. Frequently, other visual fields appear under a side-view, including a “toward to down” visual field and a “toward to out” visual field. These visual fields can be related with any outdoor or far vision connection, table task vision connection, or vertical communication connection. This combination of different workplanes will be explained in more detail in a subsection below, in the Material and Methods in Chapter 2. To date, side-lit has been tested mainly in offices or classrooms, and usually focusing on one workplane or visual field. Nevertheless, different activities with these three visual fields will have suitable atmospheres for side lighting requirements, particularly activities related with customer support or public spaces.

Figure 1. 12 Activities with three workplanes, especially tasks of customer support. Pictures obtained from the website; http://www.emprendepyme.net/cuanto-gana-una-recepcionista-de-hotel.html; http://www.mujeresdeempresa.com/servicio-hotelero-la-importancia-de-la-atencion-al-invitado/

1.4.1 Side-view

In open plan office environments, it has been shown that occupants generally want a visual connection to the outdoors (Card 2). In addition, daylighting, as well as, outdoors view increase efficiency in activity providing stress relief (Card 6). According to some psychological studies, it is easier to concentrate if there are fewer objects to pay attention to (Card 9). If occupants are not comfortable, the energy consumption will tend to increase, with higher electric lighting demand (Card 1).

In the restaurant industry, the main activities are eating, talking, and an outside view is very common. The restaurant is a significant environment, where the quality of the visual field is very important. However, not all façade designs can achieve an appropriate concentration level for the aforementioned activities. Although these activities of quality tourist areas are more tolerated socially, not all users experience a comfortable light atmosphere that promotes well-being (Card 7). Privacy is another factor to consider, providing a calm environment and an appropriate level of concentration (Card 8).

In the modern age, with the era of industrialization, the façade is no longer a structural element, and has become only a skin. In addition, electric lighting, HVAC systems and control over the physical environment have meant that the façade can be fully glazed (Card 3). At the same time, the interest of landscapes and cityscapes increases the need for a glazed façade.

In recent decades, the offer of outdoor views in restaurants has increased (Card 4). Looking at the scenery as cityscapes, landscapes and seascapes is a valued experience. In addition, the gastronomic sector has developed rapidly, and as a result, the dining experience has become part of our social lives (Card 5). Often these two activities are integrated. Therefore, restaurant customers prefer sitting where they have an outside side-view.

Figure 1. 13 Outside view demand with fully glazed façade. *Azurmendi* restaurant, picture obtained from the website, https://www.azurmendi.biz/

2016	card **1**
Topic	Side-view (electric lighting demand)
Title	Economic feasibility of maximising daylighting of a standard office building with efficient electric lighting
Author(s)	Fontoynont M. Ramananarivo K. Soreze T. Fernez G. Guldhammer Skov K
Organization	Danish Building Research Institute, Aalborg University Ministry of Justice, BEIO/OI Technical University of Denmark Quantity Surveyor, GIRUS
Source	Journal article (Energy and Buildings 2016; 110:435-442)
Information provided	· Light discomfort increases the demand of electric lighting

2013	card **2**
Topic	Side-view (glaring, fully glazed façade in an open-plan office building)
Title	Evaluating daylighting effectiveness and occupant visual comfort in a side-lit open-plan office building in San Francisco, California
Author(s)	Konis K
Organization	U.C. Berkeley
Source	Journal article (Building and Environment 2013; 59: 662-677)
Information provided	· Generally, occupants want visual connection to the outdoors · A fully glazed façade tend to provide uncomfortable atmospheres · Solar control systems improve light comfort

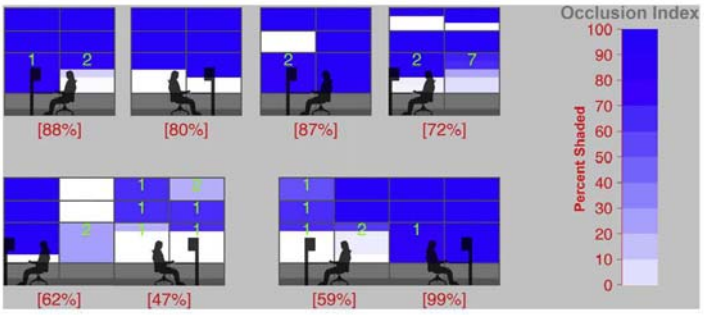

Figure 1. 14 Generally, occupants want visual connection to the outdoors (Konis 2013)

2012	card **3**
Topic	Side-view (electric lighting demand)
Title	Post-occupancy evaluation of green buildings: the measured impact of over-glazing
Author(s)	Byrd H.
Organization	School of Architecture & Planning, The University of Auckland
Source	Journal article (Architectural Science Review. 2012; 55:206-212)
Information provided	· The additional energy used for both cooling and artificial lighting results in high proportions of glazing being responsible for significantly greater energy consumption than predicted and a potential loss in productivity

2012	card **4**
Topic	Side-view (restaurants)
Title	Influence of restaurants atmospherics on patron satisfaction and behavioral intentions
Author(s)	Heung V. Gu T.
Organization	School of Hotel and Tourism Management, The Hong Kong Polytechnic University
Source	Journal article (International Journal of Hospitality Management 2012; 31:1167-1177)
Information provided	· The design of restaurants' indoor atmosphere is a determining factor in terms of customer satisfaction

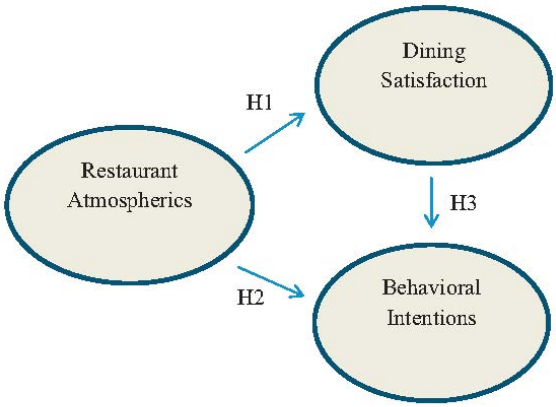

Figure 1. 15 Restaurant atmospherics a feature of dinner behaviour (Heung, Gu 2012)

2012 **card 5**

Topic	Side-view (restaurants)
Title	Restaurant's Atmospheric Elements: What the Customer Wants
Author(s)	Ariffin H.F. Bibon M.F. Abdullah R.P.S.R.
Organization	Faculty of Hotel and Tourism Management, Universiti Teknologi MARA
Source	Journal article (Procedia - Social and Behavioral Sciences 2012; 38:380-387)
Information provided	· Atmospheric elements contribute significantly to each representation of customer behaviour

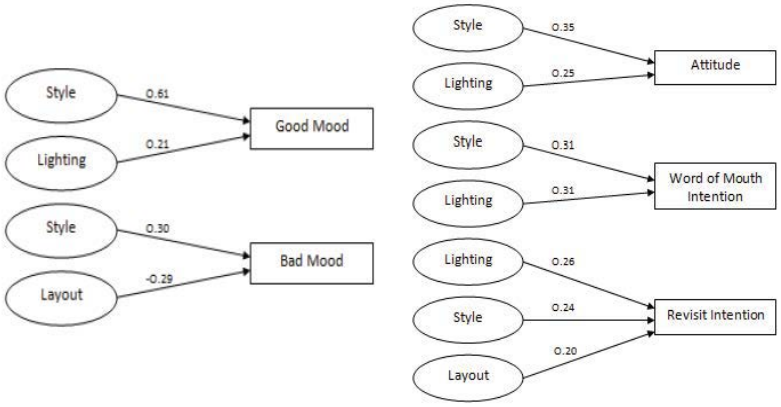

Figure 1. 16 Lighting as significant variable of atmospheric elements to customer behaviour (Ariffin, Bibon, Abdullah)

2010 **card 6**

Topic	Side-view (health benefits)
Title	Lighting, Well-being and Performance at Work
Author(s)	Silvester J
Organization	Centre for Performance at Work
Source	Report (City University London 2010)
Information provided	· A view of the outdoors increases the efficiency of an activity and provided stress relief

2006	card **7**
Topic	Side-view (atmosphere requirements)
Title	Peter Zumthor : atmospheres : architectural environments, surrounding objects
Author(s)	Zumthor P.
Organization	-
Source	Book (Birkhäuser 2006. ISBN 3764374950)
Information provided	· Indoor and light design helps to provide comfortable atmospheres

2005	card **8**
Topic	Side-view (atmosphere requirements)
Title	Cul zuffel e l'aura dado
Author(s)	Caminada G.
Organization	-
Source	Book (Luzern : Quart, cop. 2005. ISBN 3907631692)
Provided information	· Indoor and light design helps to create comfortable atmospheres (Photographs of Residència a Disentis. 2003)

Figure 1. 17 Indoor light atmospheres (Departament d'expressió gràfica arquitectònica 2009-2010)

1978	card **9**
Topic	Side-view (Concentration level)
Title	Salience, Attention, and Attribution: Top of the Head Phenomena
Author(s)	Taylor S.E. Fiske S.T.
Organization	Harvard Univeristy, Cambridge, Massachusetts
Source	Journal article (Advances in Experimental Social Psychology 1978; 11: 249-288)
Information provided	· It is easier to concentrate if there are fewer objects to pay attention to

1.4.2 Split façade

There are many studies on the split façade. Most of them deal with controlling and taking advantage of daylighting. The first aim of the split façade could be to block direct sunlight.

Diming (Card 12), venetian blinds, roller blinds and overhang (Card 10) strategies have been used to avoid direct sunlight and uncomfortable glare. Splitting the façade in different diming windows blocks light from workplanes, but allows light to enter in the space, increasing the mean light level.

Another objective of split façade could be to add a light redirecting system, as found in Complex Fenestration Systems. Complex Fenestration Systems could be created from simple light shelfs, parabolic mirrors or anidolic systems (Card 14) or prismatic films (Card 11). Redirecting lighting systems improve the light distribution indoors throughout the room. There many studies on the proportions and dimensions of split façades, and several of them are systematized in a window and Complex Fenestration System. Despite many studies of Complex Fenestration Systems in climates with low luminosity, there some split façade designs for climates with high luminosity (Card 13).

In addition, the bottom part of façade that is usually lower than the height of the tables' workplane does not help to light most workplanes. Therefore, this part does not need necessarily to be transparent to light.

Figure 1. 18 Split façade of *FOC BCN* restaurant. Picture obtained from the website, http://www.focbcn.com/

2010 card **10**

Topic	Split façade (exterior overhang)
Title	The Impact of Exterior Overhangs on the Daylighting Performance of Office Spaces
Author(s)	Rao S. Tzempelikos A.
Organization	School of Civil Engineering, Purdue University
Source	Congress paper (International High Performance Building Conference 2010)
Information provided	· Overhang dimensions · Direct sunlight will create glare problems for variable numbers of hours (depending on the overhang's geometrical characteristics) and therefore a combination of an overhang with other shading devices is recommended

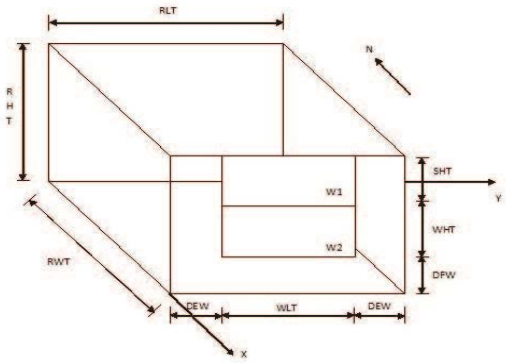

RHT = ROOM HEIGHT = 3m
RWT = ROOM WIDTH = 4 m
RLT = ROOM LENGTH = 4 m
WHT = WINDOW2 HEIGHT = 1.2 m
WLT = WINDOW2 LENGTH = 2.5 m
SHT = WINDOW1 HEIGHT = 1 m
SWT = OVERHANG LENGTH = 0.25 m to 1 m
WINDOW PANE THICKNESS = 6 mm
k = EXTINCTION COEFFICEINT = 7.76 m^{-1}
GROUND REFLECTANCE = 20%
CEILING REFLECTANCE = 80%
WALL REFLECTANCE = 70%
FLOOR REFLECTANCE = 40%
SPECULAR SHELF REFLECTANCE= 50%-90%

Figure 1. 19 Possible overhang and Windows dimensions (Spaces, Rao, Tzempelikos 2010)

2008 card **11**

Topic	Split façade (Laser cut panel and prismatic film CFS)
Title	Comparing Physical and Virtual Methods for Daylight Performance Modelling Including Complex Fenestration Systems
Author(s)	Thanachareonkit A.
Organization	Laboratoire d'énergie solaire et physique du bâtiment, École polytechnique fédérale de Lausanne
Source	Thesis
Information provided	· In redirecting systems, such as Complex Fenestration Systems, it is difficult to reproduce the light reflections · The results of real model with clear sky nearby CFS are not reliable and the results of virtual model are reliable without direct sunlight and with uniform sky

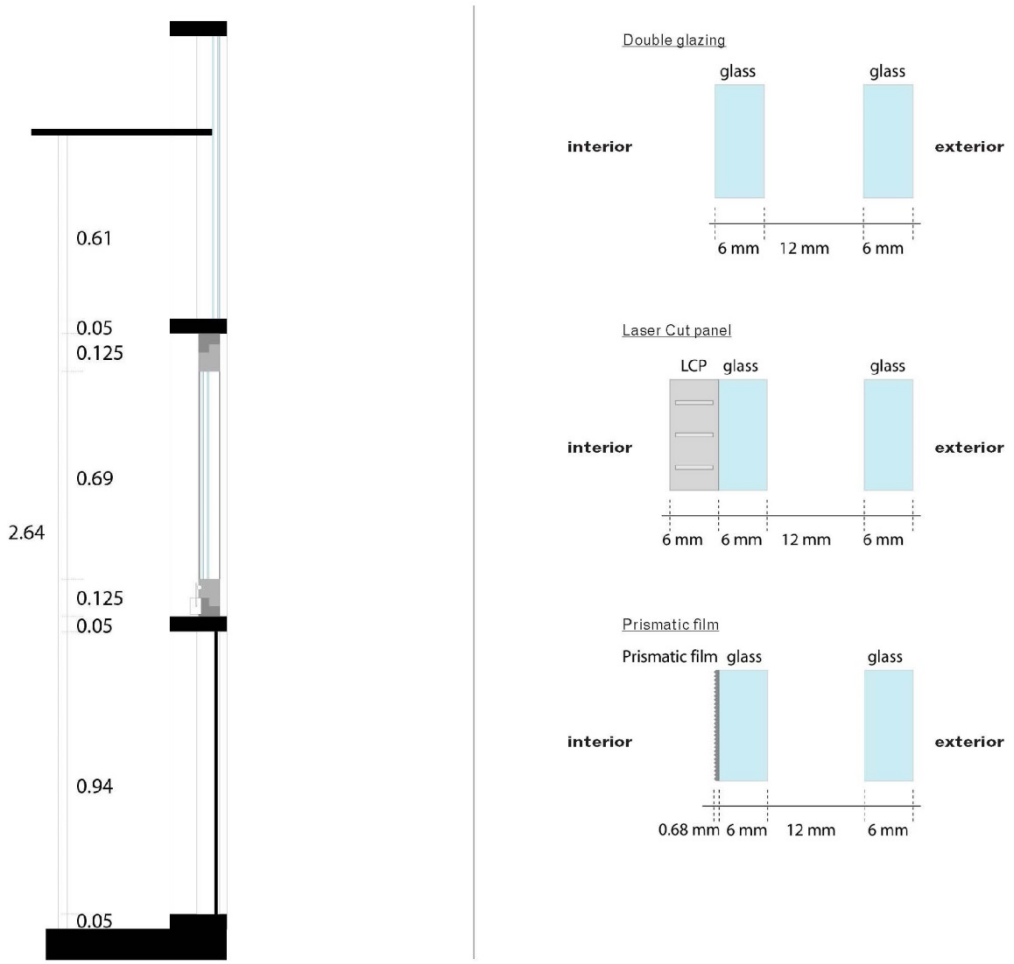

Figure 1. 20 Split façade dimensions and description of Laser Cut Panel and Prismatic Film Complex Fenestration Systems (Thanachareonkit 2008)

2006 card **12**

Topic	Split façade (electrochromic window)
Title	Advancement of electrochromic windows
Author(s)	Lee E. Selkowitz S. (Principal Investigator) (and others from Lawrence Berkeley National Laboratory)
Organization	Lawrence Berkeley National Laboratory
Source	Scientific report for California Energy Commission Public Interest Energy Research (PIER) Program
Information provided	· Façade split into different windows with electrochromic glass to block direct sunlight and to obtain a comfortable light balance

Figure 1. 21 Individual switchable EC window panes with an option to suit according to view, glare control, and privacy (Lawrence Berkeley National Laboratory, California Energy Commission 2006)

2006 card **13**

Topic	Split façade (CFS in highly luminous climates)
Title	Evaluating visual comfort and performance of three natural lighting systems for deep office buildings in highly luminous climates
Author(s)	Ochoa C.E. Guedi I.
Organization	Climate and Energy Laboratory in Architecture, Technion-Israel Institute of Technology
Source	Journal article (Building and Environment 2006; 41:1128-1135)
Information provided	·The proposal for the façade is to split it into three parts. The top part is to designed redirect sunlight, the central part to allow interaction with the outdoors; and the bottom part to protect from radiation

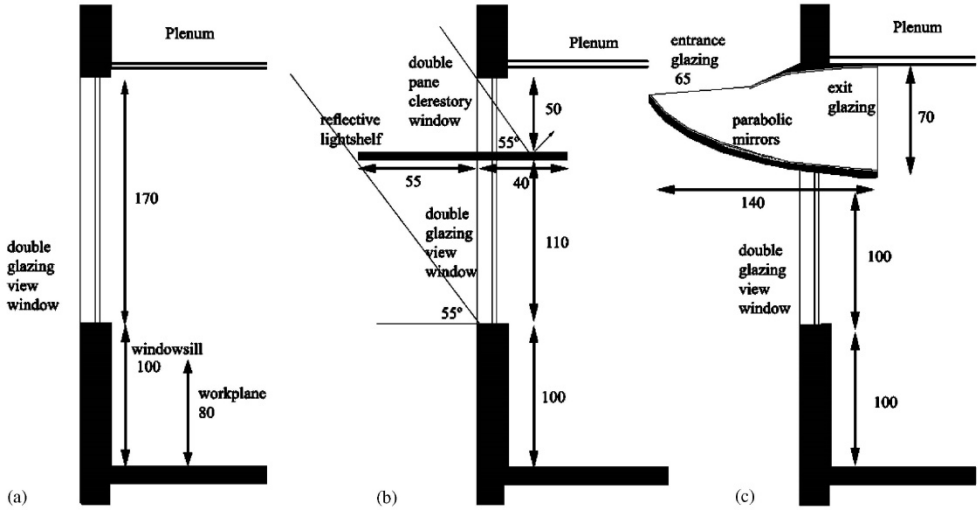

Figure 1. 22 Base case (a), light shelf (b) and anidolic (c) concentrator light conductor systems (Ochoa, Guedi 2006)

2002 card **14**

Topic	Split façade (redirecting systems)
Title	Anidolic daylighting systems
Author(s)	Scartezzini J.L. Courret G.
Organization	Swiss Federal Institute of Technology, Lausanne (EPFL)
Source	Journal article (Solar Energy 2002; 73-2:123-135)
Information provided	· Under clear sky conditions, sunlight control capabilities improve visual comfort and overall performance

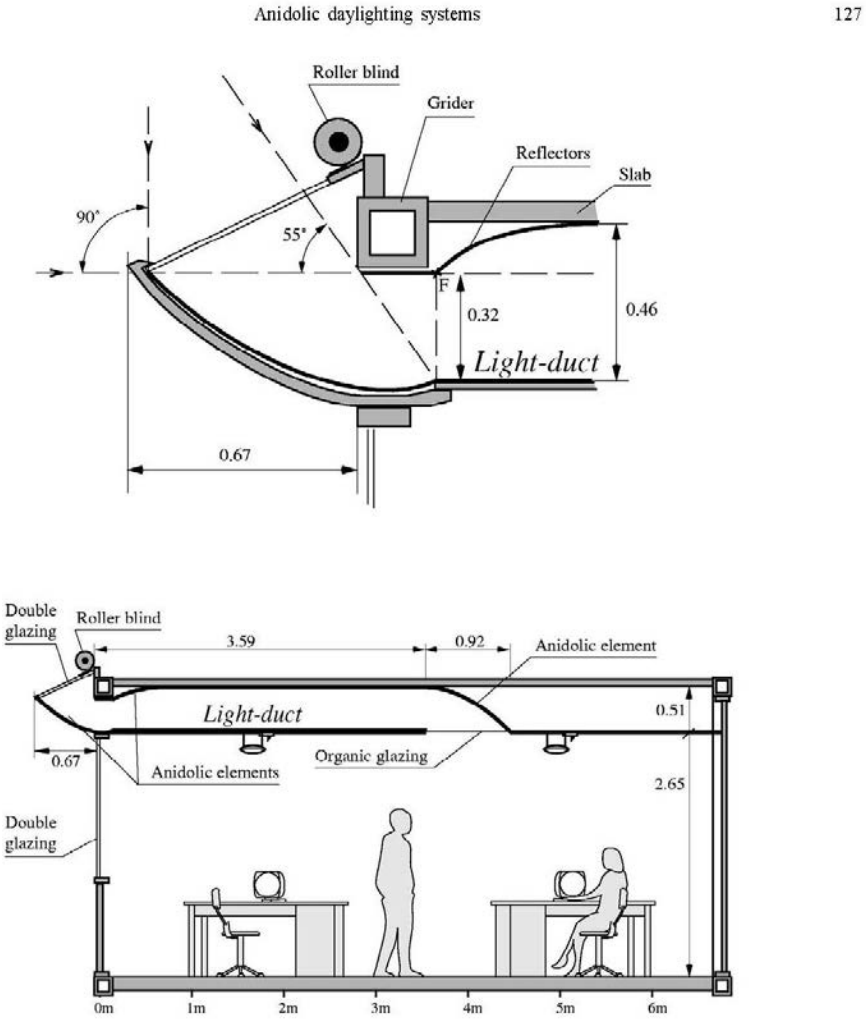

Figure 1. 23 Anidolic external collector and anidolic installed at ceiling (Scartezzini, Courret 2002)

1.4.3 Luminance distribution by a window

Luminance distribution evaluation is a difficult task, but it is an important aspect for visual comfort. How to balance luminance in a visual field is a topic that has been researched for many years. Regarding sidelight luminance distribution, many studies examine the luminance distribution perception caused by a window (Card 18). The size, geometry and thickness of a window are parameters that influence visual perception. Small windows can create significant local contrast, whereas large windows, up to a fully glazed façade, could create a more glare probability (Card 17). In addition, the position of a window depending on point of view is a parameter that influences visual perception. In the central point of view, the luminance has a greater impact than if the luminance source is in the lateral point, according to the visual field. In the central part, although both are important, the luminance value is considerable, and appears to be greater than the luminance source size (Card 15). However, in the lateral part, which has a lower luminance value, it seems that both the size and value are important. This concept has not been widely studied.

The problem becomes much complicated when the visual field is not considered static. Usually, in an activity there is more than one workplane, as mentioned in the introduction to this section. However, up to now, one visual field as a workplane has been considered to test luminance distributions. In each workplane, the mean luminance value and distribution may be different, and the transition between one workplane and another should be taken into account. In addition, considering that the brain does not work with absolute values, but by contrast, visual perception is a slightly more complex task. The mean luminance source value, size and position against the mean luminance background are influential parameters, as is the previous luminance value of the prior visual field. The luminance value is affected by adaptation of the previous luminance value. Therefore, the overall mean luminance distribution of an activity's different workplanes has been considered in this study.

The methods for assessing visual perception are related with glare (Card 21). Glare methods have been considered a way to evaluate the luminance distribution of a visual field. Two basic glare metrics (CGI, DGI, UGR, VCP and DGP) are designed to assess the glare from daylight: DGI (Card 20) and DGP. However, only DGP incorporates vertical eye illuminance as a non-contrast-based aspect of the metric. The Daylight Glare Probability index (DGP) is considered a more practical method, because the required data is the illuminance value at eye level, whereas the DGI index is a little more complex, owing to the required luminance value:

$$DGI = 1 \cdot \log\ 0.478 \sum_{i=1}^{n} \frac{L_s^{1.6} \cdot \Omega^{0.8}}{L_b + 0.07 \cdot\ \omega^{0.5} \cdot L_s}$$

Where,

L_s, source luminance in cd/m²

L_b, average background luminance in cd/m²

ω, angular size of the source in steradians as seen by the eye

Ω, solid angle subtended by the source, modified for the effect of the position of the observer in relation to the source in steradians

However according to the Jan Wienold manual, the Daylight Glare Probability (DGP) is defined as (Card 19):

$$DGP = c_1 \cdot E_v + c_2 \cdot log\left(1 + \sum_i \frac{L_{s,i}^2 \cdot \omega_{s,i}}{E_v^{a_1} \cdot P_i^2}\right) + c_3$$

Where:

E_v, vertical eye illuminance (lux)

L_s, luminance of source (cd/m2)

ω_s, solid angle of source (-)

P, position index (-)

$c_1 = 5.87 \cdot 10^{-5}$; $c_2 = 9.18 \cdot 10^{-2}$; $c_3 = 0.16$; $a_1 = 1.87$

Possible scaling of glare obtained by the DGP value:

Imperceptible, DGP ≤ 0.35

Perceptible, 0.35 < DGP ≤ 0.40

Disturbing, 0.40 < DGP ≤ 0.45

Intolerable, DGP > 0.45

Accordingly, the DGP index is selected to assess the luminance distribution simulation (Card 16), because it uses illuminance data as a reference value, and the measurement of light level is more practical than a luminance measurement. Apart from other indexes, the simulation of the DGP index can be obtained by Evalglare, which is explained in depth in the Material and Methods chapter. The mean DGP of different workplanes is proposed (a concept that has not been worked on extensively) to obtain the overall glare perception of an activity.

Figure 1. 24 Luminance distribution between outside view and inside view in relation with the activity, *El Peñón* restaurant

Figure 1. 25 Luminance distribution between outside view and inside view in relation with the activity, *La Branka* restaurant

2012 card **15**

Topic	Luminance distribution (luminance source position)
Title	Luminances and vision related to daylighting
Author(s)	Aguilar A. Uriarte U. Isalgue A. Coch H. Serra R.
Organization	Arquitectura Energia i Medi Ambient, Universitat Politècnica de Catalunya
Source	Congress paper (World Renewable Energy Forum 2012)
Information provided	· A reduction factor is proposed for a lateral luminance source, because lateral luminance perception is lower than central

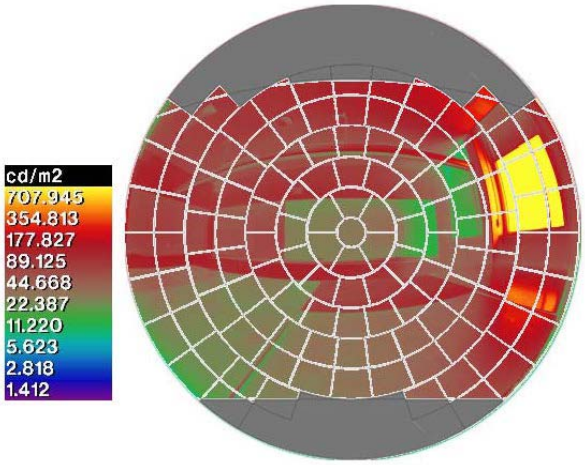

Figure 1. 26 The perception of lateral luminances is lower than central luminance perception
(Aguilar, Uriarte, Isalgue, Coch. Serra 2012)

2011 card **16**

Topic	Luminance distribution (simulation tools)
Title	The daylighting dashboard – A simulation based design analysis for daylit spaces
Author(s)	Reinhart C.F. Wienold J.
Organization	Centre Scientifique et Technique du Batiment Building Research Establishment of the DoE Institut Royal Meteorologiue de Belgique Bartlett School of Architecture and Planning, University College
Source	Journal Article (Building and Environment 2011; 46: 386-396)
Information provided	· Simulation tools for daylighting

2009 card **17**

Topic	Luminance distribution (window)
Title	El balcón y la celosía. Elementos de confort lumínico y térmico en el clima de la ciudad de Lima
Author(s)	Agüero R.
Organization	Universitat Politècnica de Catalunya
Source type	Master thesis (Arquitectura Energía y Medio Ambiente)
Information provided	· According to the window distribution, dimension and shape, the geometry is important for the outdoor view and the luminance balance

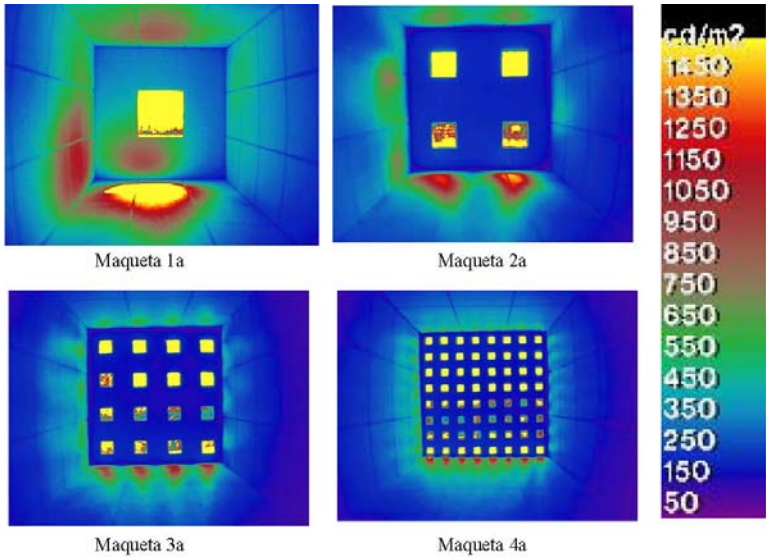

Figure 1. 27 Different windows provide different side-view perception and light distribution (Agüero 2009)

2009 card **18**

Topic	Luminance distribution (window)
Title	Re-interpretation of traditional architecture for visual comfort
Author(s)	Ruggiero F. Serra R. Dimundo A.
Organization	Dipartimento di Scienze dell'Ingegneria Civile e dell'Architettura, Politecnico di Bari Universitat Politècnica de Catalunya
Source	Journal Article (Building and Environment 2009; 44:1886–1891)
Information provided	· Depending on the window distribution, dimension and shape, the geometry is important for the outdoor view and the balance of luminance

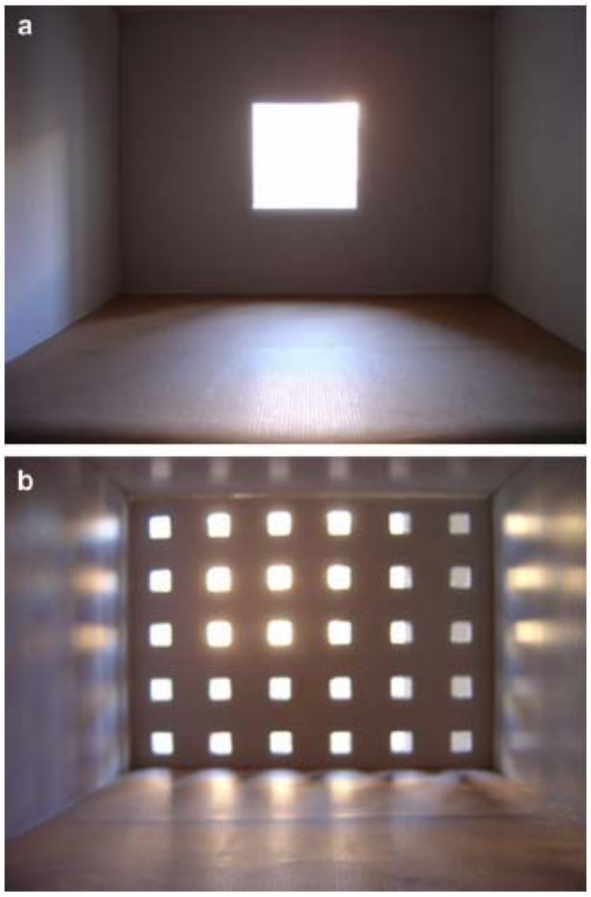

Figure 1. 28 Different light distribution according to different aperture (Ruggiero, Serra, Dimundo 2009)

2006	card **19**
Topic	Luminance distribution (Daylight Glare Probability index)
Title	Evaluation methods and development of a new glare prediction model for daylight environments with the use of CCD cameras
Author(s)	Wienold J. Christoffersen J.
Organization	Centre Scientifique et Technique du Batiment Building Research Establishment of the DoE Institut Royal Meteorologiue de Belgique Bartlett School of Architecture and Planning, University College
Source	Journal Article (Energy and Buildings 2006; 38: 743–757)
Information provided	· New glare prediction model

1998	card **20**
Topic	Luminance distribution (daylight glare source)
Title	Glare from windows: current views of the problem
Author(s)	Chauvel P. Collins J.B. Dogniaux R. Longmore J.
Organization	Centre Scientifique et Technique du Batiment Building Research Establishment of the DoE Institut Royal Meteorologiue de Belgique Bartlett School of Architecture and Planning, University College
Source	Journal Article (Lighting Research and Technology, 1998; 30: 89-93)
Information provided	· The discomfort glare from a single window (except for a rather small one) is practically independent of the size and distance from the observer, but is critically dependent on the sky luminance

1972	card **21**
Topic	Luminance distribution (glare source)
Title	Glare from daylighting in buildings
Author(s)	Hopkinson R.G.
Organization	University College London
Source	Journal Article (Applied Ergonomics 1972, 3-4: 206-215)
Information provided	· Glare is a direct function of both the size of the window and the brightness of the sky that is seen through it, and an inverse function of the brightness of the room's interior · Glare can be reduced by cutting down the size and brightness of the visible patch of sky and by increasing the interior brightness by the judicious use of highly reflective surface

1.4.4 Illuminance distribution by a Complex Fenestration System

Illuminance distribution is a topic that has been widely studied. Light level is another essential aspect to ensure visual comfort. It is a source of light for the space that combines light uniformity and contrast by daylighting. Light driving is a passive resource that has been widely used throughout history. Less, but better distributed, light is a guideline that has been used for many years (Card 24). The easy availability of electric lighting has meant that driving passive strategies are not needed. However, Complex Fenestration Systems have been developed and used in many sustainable buildings.

Many Complex Fenestration Systems can be used to obtain more uniform light distribution. The light shelf is simple, and one of the most commonly used light driving systems. Nevertheless, 3M prismatic film is currently being used for easy implementation in a glazed façade and in large windows (Card 22). These two systems combined with a framed window are proposed to analyse.

The illuminance point in time data along a workplane is a frequently used method to obtain the illuminance distribution in a workplane. The Daylight Factor (DF) is a very commonly used index for a uniform daylight context, as it can provide a uniform or overcast sky:

$$DF = 100 \cdot \frac{E_{in}}{E_{ext}}$$

Where,

E_{in}, inside illuminance at a fixed point in lux

E_{ext}, outside horizontal illuminance under an overcast (CIE sky) or uniform sky in lux

And the IES formula is:

$$DF_{m,\ IES} = \frac{A_{window} \varepsilon\ U \cdot 100}{A_{floor}}$$

DFm, IES = (Awindow ε U * 100) / (Afloor)

Accordingly, as the context of the study is high outdoor luminance and clear skies, the Daylight Autonomy index is used, although this is usually based on annual data. The index is used when there is a high percentage of clear sky throughout the year, so

Climate-Based Daylighting Modelling (CBDM) is applied. This is because there are many days where the direct sunlight performs differently. Thus, the percentage varies considerably every hour. The final percentage is the mean of the hourly percentage for the year overall. Therefore, Daylight Autonomy (DA) is defined as the percentage of annual daytime hours that is above a specified target illumination level at a given point in space:

$$E > E_{target} => DA = \frac{(\sum_{1}^{8760} n) \cdot 100}{8760 \cdot n}$$

$$E < E_{target} => DA = 0$$

Where,

E, inside illuminance at a sensor point in lux

E_{target}, illuminance comfort limit value

n, sensor point number

Consequently, the Daylight Autonomy index is used to describe the illuminance distribution. The aim of this index is to evaluate the illuminance distribution of a window comprised of CFS, with the Three-Phase Method simulation of Radiance (Card 23). The index is explained in depth in the Material and Methods chapter. Note that illuminance data is used to provide a reference. As well as DIVA, the Radiance program-based plugin for Rhinoceros, it is used for illuminance data and DA without Complex Fenestration Systems.

Figure 1. 29 Ununiformed illuminance distribution throughout the space, *Pez Vela* restaurant

2014 card **22**

Topic	Illuminance distribution (Complex Fenestration Systems)
Title	On advanced daylighting simulations and integrated performance assessment of complex fenestration systems for sunny climates
Author(s)	Basurto C.
Organization	Laboratoire d'énergie solaire et physique du bâtiment, École polytechnique fédérale de Lausanne
Source	Thesis
Information provided	· In many cases the standard glazing lead to a higher daylighting flux into the room, especially at Spring Equinox where the IR is significantly larger than those of the CFS. When comparing the performance of CFS, Film 3M, CFS3 and CFS2 appears to be the ones that perform better regarding the admission of daylight into the room. In Building B1, the Standard -glazing (τv 70%) and Film 3M present a better Illuminance Uniformity next to the window and in the centre of the room, while at the back of the room the LCP, Film 3M and CFS2 show better values. · In buildings located at low latitudes, the intensive use of daylighting represents a major risk for the visual and thermal comfort of the occupants. It has been however shown in this study that the use of an appropriate-selected CFS can improve the interior daylight distribution in buildings located in such regions (mostly dominated sunny climates); moreover their additional functioning as a shading device might also contribute to improve the visual and thermal comfort. However, it has also been evident that in regards to the mitigation of glare risks in some cases the effect of CFS is overcome by the overall building environment. In such cases, the use of additional sun shading becomes imperative in order to offer a satisfactory indoor environment quality to the occupants by reducing glare and overheating risks. Thus, the performance assessment of CFS combined with a simultaneous use of different configurations of shading devices (overhangs, exterior blinds, venetian blinds, fins, etc.) would be a relevant step in the direction of achieving an optimal interior daylighting in buildings located at low latitudes

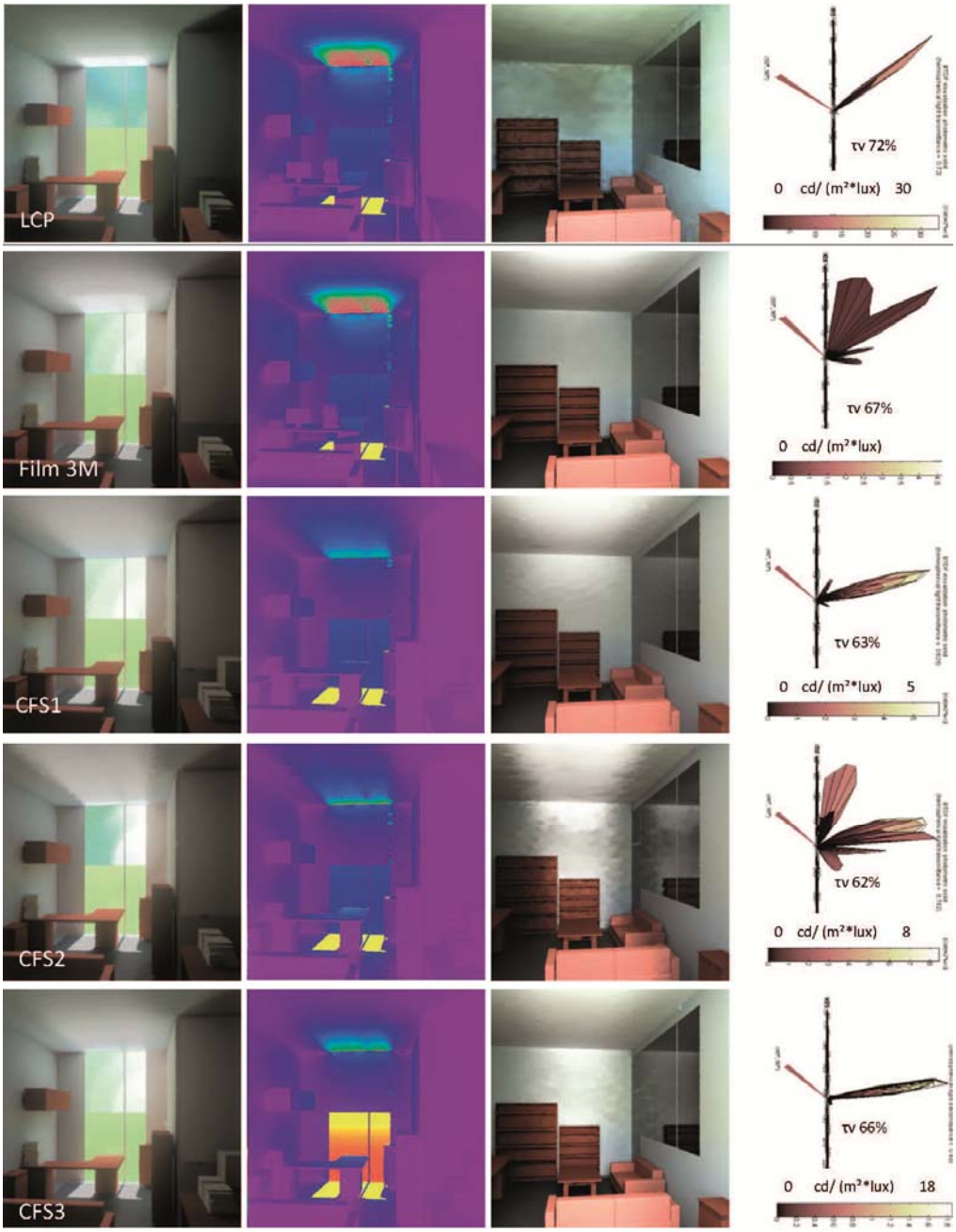

Figure 1. 30 The BTDF diagram os each Complex Fenestartion System (Basurto 2014)

2010 card **23**

Topic	Illuminance distribution (Complex Fenestration Systems Simulation)
Title	The Three-Phase Method for Simulating Complex Fenestration with Radiance
Author(s)	McNeil A.
Organization	Lawrence Berkeley National Laboratory
Source type	Tutorial
Information provided	· Matrix calculation can be performed very quickly enabling the user to simulate many sky conditions by Tregenza or Reinhart division schemes and fenestration transmission properties by Bi-directional Scattering Distribution Function in relation with Klems Angles Basis

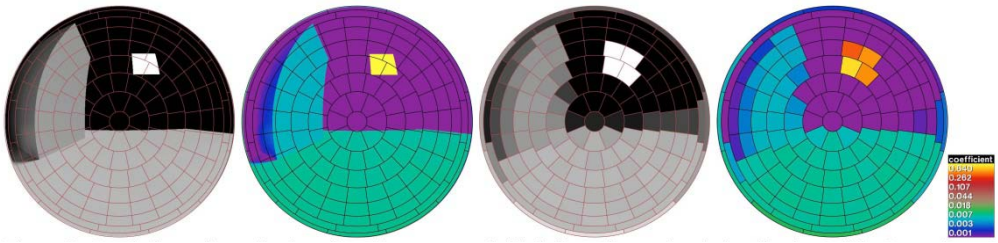

Figure 1. 31 Tregenza patch distribution to obtain D matrix coefficients (McNeil 2010)

1998 card **24**

Topic	Illuminance distribution (redirected lighting)
Title	The Mediterranean blind: Less light, better vision
Author(s)	Coch H. Serra R. Isalgué A.
Organization	Arquitectura Energia i Medi Ambient, Universitat Politècnica de Catalunya
Source	Journal Article (Renewable Energy 1998; 15:431-436)
Information provided	· Smaller light source perception and distributed light improve overall indoor light perception

Figure 1. 32 Different light distribution and local contrast with the opening without obstruction or with blind shut (Coch, Serra, Isalgué 1998)

1.5 Hypothesis

The general hypothesis of the thesis is that:

· **A split façade comprised of a window and a Complex Fenestration System can provide a comfortable, indoor side-lit atmosphere** to enhance good concentration and create a calm atmosphere.

· Moreover, it is predicted that complex window systems allow framing of outdoor scenery, which improves the quality of the side-view by selecting desirable visual elements.

The specific hypotheses are that:

· The window improves the luminance distribution decreasing the overall Daylight Glare Probability.

· A Complex Fenestration System improves the illuminance distribution increasing uniformity, which improves the light distribution on the workplanes, and in consequence the Daylight Autonomy throughout the space.

· The specific hypotheses that refer to the simulation are that:

  · The mean DGP of different workplanes could be a simple way to get closer to the overall visual perception, avoiding extreme luminance values and keeping each workplane's light contribution.

  · The simulation of Daylight Autonomy of Complex Fenestration Systems can be obtained by the Three-Phase Method. The results should be acceptable and indicative.

· Moreover, if outdoor view requirements are separated from lighting requirements, both functions will work more accurately separately. Luminance distribution at eye level could be better established without the need for large, bright surfaces. However, other light that enters combined with redirecting systems could be designed freely without any luminance condition, and provide enough light on workplanes.

Note that a split façade design that defines the height, divisions, geometry and position of each part could improve the indoor light perception for a specific activity. It seems that height is important to obtain good light redirection. Window size is significant to decrease glare and visual elements. Overhang position is key to avoid direct light and to permit redirected light to enter. Only to consider, indoor walls in a warm colour may be is important to increase the light comfort at low light levels. In addition, other light that enters could improve the light level and the indoor light perception accordingly. The indirect light that enters could improve the mean light level on workplanes and direct light that enters could improve the indoor light balance, and thus the light comfort perception.

Chapter II

MATERIAL AND METHODS

The proposed methodology to demonstrate that, within outdoor high luminance context, split façade comprised of a window and a Complex Fenestration System is better to have a good concentration and calm atmosphere is to analyse and compare luminance and illuminance distributions of fully glazed façade and split façade window systems.

For this propose, virtual models for case studies have been created to add window systems to each case the study and then to assess luminance and illuminance distribution of each system. Furthermore, for the selected case the study different workplanes of overall visual perception are defined.

Note that, for luminance distribution the methodology used up to now is False Colour Image method. Usually the luminance values are calibrated by luminance meter. Frequently from a vision field of office environment, in which appear all workplanes together, a False Colour Image is obtained often from HDR image. With reference to Daylight Glare Method, Evalglare tool is being used according to vertical eye level illuminance data. For illuminance distribution, the Point-in-Time illuminance data of Complex Fenestration Systems is being used by Bidirectional Scattering Distribution Function (BSDF) material type with Radiance common commands. However, for simulating the Daylight Autonomy of Complex Fenestration Systems Three or Five Phase Method are using. These methods are considered as references to propose the following material and method for assess luminance and illuminance distribution and to get indoor light atmosphere perception.

2.1 Workplanes and light requirements

As the proposal of different workplanes combination has been mentioning in the previous chapter, following the description of three types of workplanes is explained. The wokplanes that contributing in overall visual field are detailed:

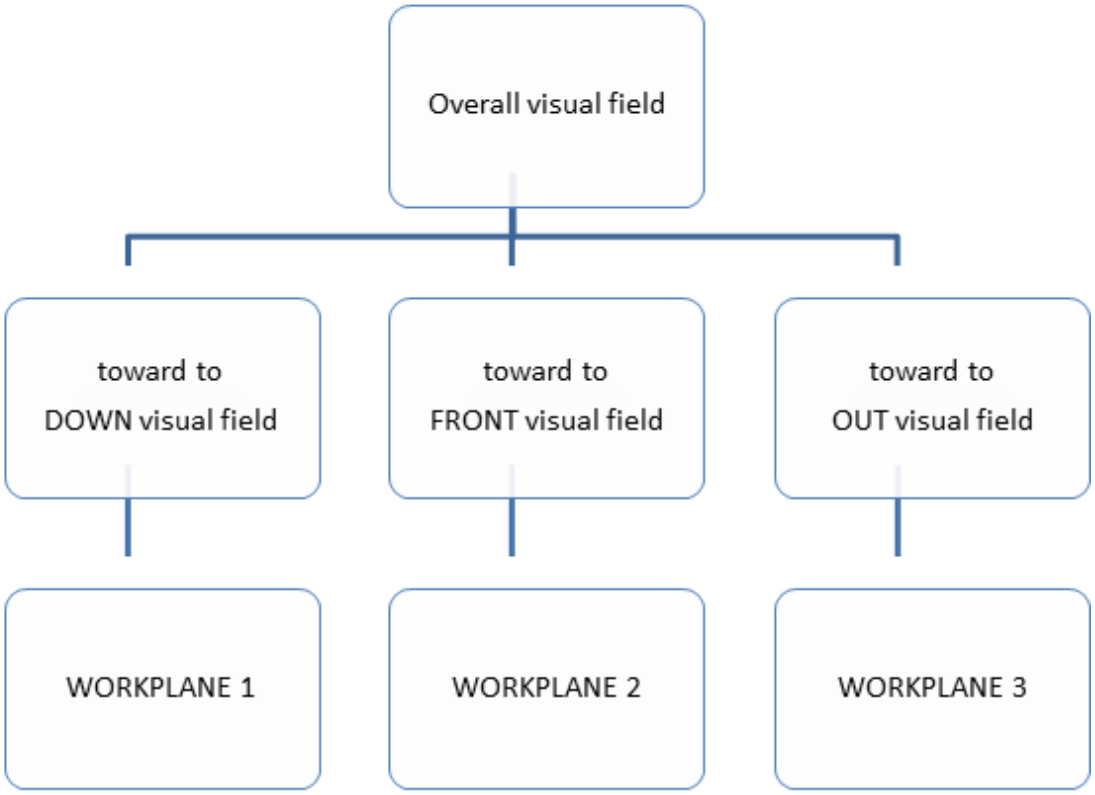

Figure 2. 1 Description of Down view, front view and far view workplanes

Note that, according to luminance distribution and proposed DGP index, for each workplane a False Colour Image and DGP with glare source image is planned to after get mean DPG index.

The activities with three main workplanes could follow the next light requirements:

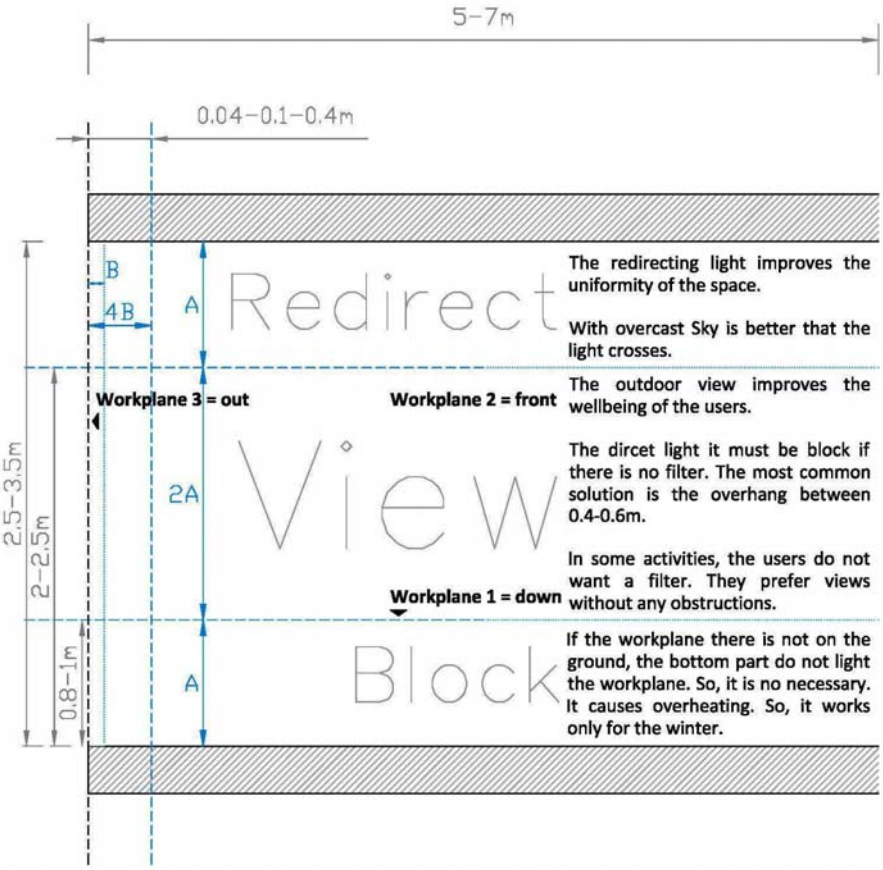

Figure 2. 2 Light requirements according to the height and deep

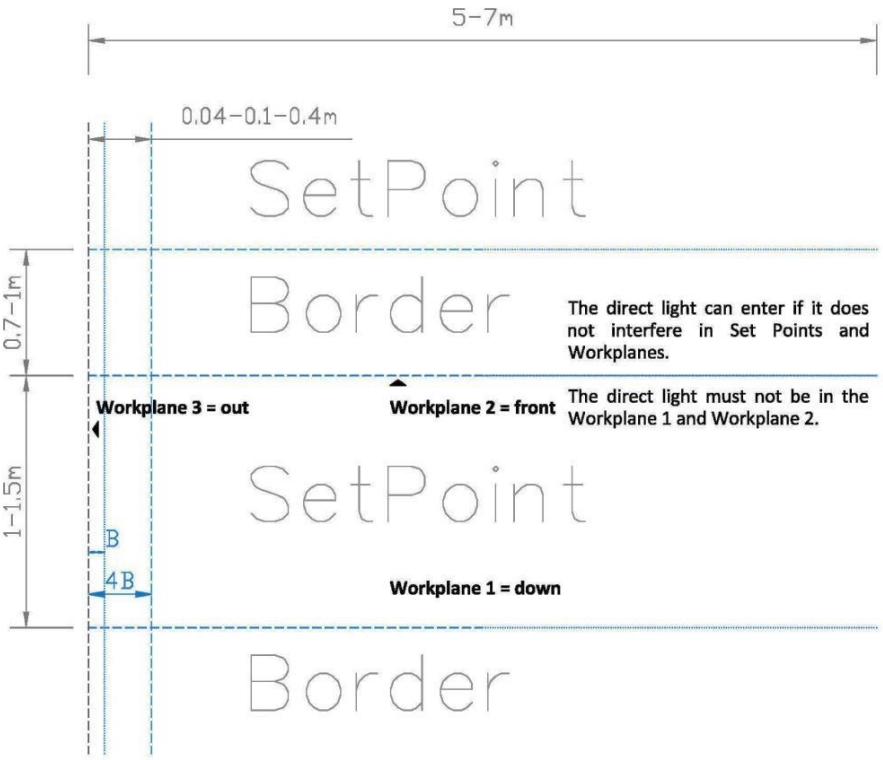

Figure 2. 3 Light requirements according to the with and deep

Once the workplanes of side lighting are defined the parameters should be explained. Before of precise description analyse, in the following diagram the parameters are presented:

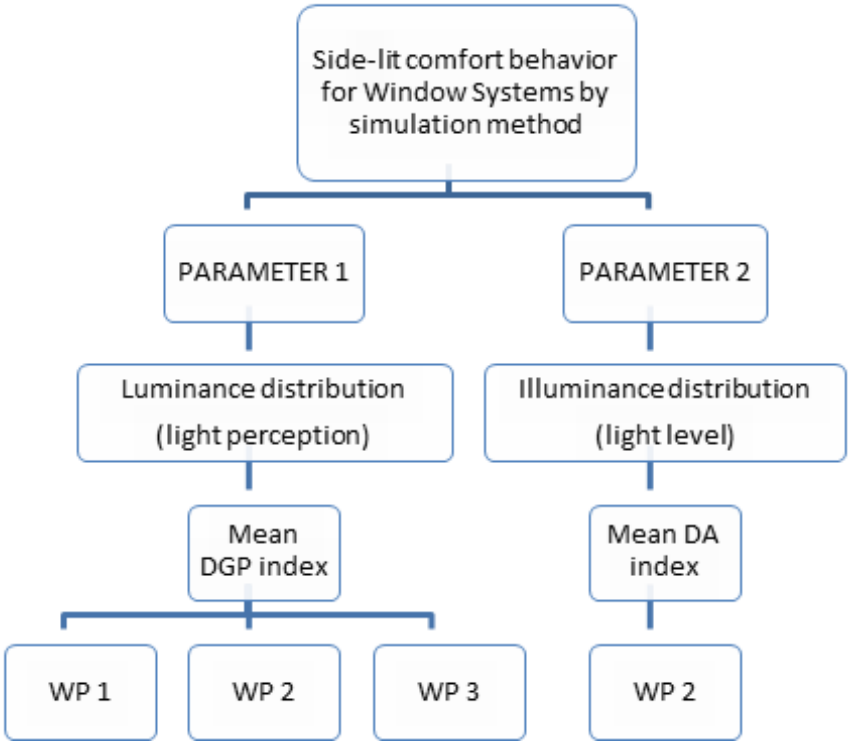

Figure 2. 4 Side-lit comfort behavior for window systems by simulation method

As in the image before is explained the simulation is selected to assess the hypothesis. Therefore, Rhinoceros, software tool to model in 3D based on NURBS, is selected to build virtual models and DIVA for Rhino, Radiance program(see Annex 1) based plugin, is used to get luminance and illuminance distribution simulations. Moreover, the three-Phase Method with Radiance is chosen for Simulating Complex Fenestration Systems. Note that, Greg Ward is an author of many programs of Radiance. In the following the methodology to evaluate luminance and illuminance distributions are presented.

2.2 Parameter 1: Luminance distribution by Daylight Glare Probability (DGP) index

Daylight Glare Probability (DGP) index is chosen to assess luminance distribution. Therefore, according to side-lit, that the overall glare probability of window may be lower than fully glazed façade will be assessed by DGP index. Already mentioned in state of the art section, the DGP index incorporates vertical eye illuminance as a non-contrast-based aspect of the metric.

The simulation has been used to get DGP index. Thus, Evalglare, a Radiance based tool for glare evaluation, has been used to calculate an index described in previous chapter. In addition, with this tool there is an option to get glare source image to check glaring surfaces of the scene.

The commands used for Evalglare program are the following ones and the Operative System selected was Linux Ubuntu 14.04, although it works with different OS as Windows:

The image must be equal or smaller than 800 x 800 pixels to be effective. Using *getinfo* command the image dimension can check:

```
$ getinfo –d FINAL_HDRI.hdr
```

To change the size of the image using the *pfilt* command:

```
$ pfilt –x /5.5 –y /5.5 FINAL_HDRI.hdr > FINAL_HDRI_small.hdr
```

To get DGP index of HDR image (-i parameter the externally measured vertical illuminance data can be added):

```
$ evalglare –i 2350 FINAL_HDRI_small.hdr
```

To get glare source with color:

```
$ evalglare –c FINAL_HDRI_small_test.pic FINAL_HDRI_small.hdr
```

Note that, the tool is valid for illuminance higher than or the same of 380lux and DGP index higher than or the same of 0.2.

The Daylight Glare Probability (DGP) will be applied to each workplane HDR image. Thus, in a simply way mean DGP of three workplanes is proposed. The extreme workplane luminance values are smoothed by intermediate workplane, in contrast to classical method of luminance source against background luminance. The adaptation of the vision and mind is important, so it could be interesting and more real to add

third plane of earlier workplane's luminance data to glaring methods. The dynamic state methods could be more approximated than the steady state methods to describe better the overall real visual field.

Therefore, describing the work scene by three workplanes is closer to real situation. It seems that taking into account different workplanes describes better the visual field than only taking account one workplane. Usually our brain works by contrasting values not with absolute values. So, to analyse just only extreme views does not make sense, because the luminance level is appreciated comparing with previous vision.

Regarding, simulation of DGP by DIVA plugin, add that each simulated visualization is compared and calibrated by real photographs. Following, the material and methods of DGP obtained by real photographs and DGP obtained by simulated visualization are explained.

2.2.1 Conditions for real photographs' DGP

First the specifications of real photographs are presented.

The photographs are made within specifications of; ISO 400; 3 lighting exposures, -2/0/+2; auto image style; auto white balance (see Annex 2); three shot serially by remote shutter release and a tripod; and 8.0M 3456x2304 image quality. The photos are made by a digital camera (Canon EOS 600D, with Canon objective EFS 18-55mm) fitted with a circular fisheye lens (Gloxy; Front Filter Size, 67 mm; conversion factor, 0.42x; thread Size, 46mm). The result of the photograph with this lens is circular picture inside the projection frame. The projection is hemispheric and is known as the "equisolid angle projection". Its unique feature is that it retains the proportions among the solid angles. The purpose of the use of fisheye projection is to simulate the visual field of the human eye.

The HDR images can be got by WebHDR online software of Axel Jacobs or by Greg Ward's *hdrgen* program:

```
$ hdrgen –o *.hdr -2exposure.JPG 0exposure.JPG +2exposure.JPG
```

Moreover, the illuminance measurement of each workplane is necessary to add as Evalglare parameter (-i) to calibrated DGP results. Then, the next required instrument is a device to measure illumination level (The Hagner Digital Photometer TP200). The measuring range is 0.1- 200,000 Ix. This devise has a simple luminance meter. The

luminance measurements are planned to use as only reference luminance data. The luminance measuring range is 0.01-20,000 fc and acceptance angle is approximately 1/30°. The limits are enough to verify the measurements taken in our study, as the margins have not been exceeded in any case.

Therefore, photographs and illuminance data of each workplane with each window system of each case study are proposed to get mean DGP index.

Note that the False Colour Image can be obtained by different options. One of them is by Radiance's *falsecolor* command. The False Colour Image can be obtained as follows:

Once the *.hdr picture is obtained, although the program works with *.pic format, the following parameters should be defined:

-s => to get different scales

-log => to get logarithmic mapping defining the decades

-n => to change the number of contours (and corresponding legend entries)

-lw => to set the width of the legend

-lh => to set the height of the legend

More program details in Annex 1. For instance, the command can be script as follows:

```
$ falsecolor –s 3000 –log 3 –n 10 –lw 400 –lh 800 –ip *.hdr > *_fc.hdr
```

As it is mentioned earlier, using the *pfilt* command the pixel number of the file *.hdr can be reduced and the balance of the brightness, as well.

Finally, using a ra_tiff program the *.hdr file can be become to *.tif file:

```
$ ra_tiff *_fc.hdr *_fc.tif
```

2.2.2 Conditions for virtual visualization DGP by DIVA for Rhino

Secondly, according to the DGP of simulated visualizations of each workplane with each window system of each case study, the specifications of simulation by DIVA for Rhino are presented:

Note that, the real point of view of each workplane vision field, measured illuminance data, and DGP obtained by real photographs are used as reference to simulated DGP. The following steps are planned to get simulated DGP:

1) Build the virtual model by Rhino by material specifications (or use Radiance scene description)

2) Set the point of view for each workplane (or use –vf file.vf with –vt* -vh –vv –vp -vd –vu parameters)

3) From Metrics tab of DIVA and then from Daylight Images tab get Point-in-Time Glare (or Annual Glare). The following conditions must be specified:

    · Image quality

    · Sky Condition

    · Date and Time

    · Camera Type

    · Select Camera Views

    · Radiance parameters according to earlier specifications:

    · -ps -pt -pj -dj -ds -dt -dc -dr -dp -st -ab -aa -ar -ad -as -lr -lw –vu

    · Image Size [x y]

    · Hide Dynamic Shading

    · Geometric Density

    · Cleanup Temporary Directory

(or use *oconv* and *rpict* Radiance programs to get an image in .pic format and then, use Evalglare program)

Note that, DIVA generate an image, glare source image and DGP index running internally Evalglare program. Sometimes the default Clear Sky with Sun (CIE Clear Sky), which is generate by *gensky* Radiance program, does not irradiance measured

horizontal illuminance (E_h) data, especially when in the view appears the sky. In this case *gendaylit* program is used (it is need to add to *_sky.rad file in DIVA's Temp folder). With this program by –E parameter can be added measured global-horizontal irradiation. To assess whether incoming illuminance data is the same that measured workplane's illuminance data the incoming illuminance data of visualization image can be tested by Evalglare –V parameter.

False Colour image is got from Visualization tab of Daylight Images tab. The visualization is obtained in *.pic and *.tif format but with DIVA's *wxFalsecolor* program the image can become false colour image (or by *falsecolor* program of Radiance, as well).

2.3 Parameter 2: Illuminance distribution by Daylight Autonomy (DA) index

Daylight Autonomy (DA) index is chosen to assess illuminance distribution, which uses advanced Climate Based Daylighting Modelling (CBDM). Therefore, according to side-lit, that the uniformity of Daylight Autonomy of façade by Complex Fenestration System is higher providing better illuminance distribution than fully glazed façade will be assessed by DA index.

Already mentioned in state of the art section, Daylight Autonomy (DA) is defined as a percentage of annual daytime hours that a given point in a space is above a specified illumination level. For predominantly daylight spaces it has become customary to assume a target illuminance of 300 lux.

In addition, the sky conditions of each hour are necessary, 8760 sky conditions. Thus, a major innovation since in considers geographic location specific weather information on an annual basis.

According to DA simulation of a workplane with each window system of each case study, the specifications of simulation are presented.

Note that, the objective of DA index is to check light level and light distribution throughout a space. So, usually the index at horizontal workplane as Down WP1 is calculated. Therefore, only Down WP1's DA of each window system of each case study is proposed to simulate. Furthermore, although Point-in-Time illuminance data of Complex Fenestration Systems can be calculated by DIVA's Metrics option the DA of Complex Fenestration System calculation cannot. Therefore, the DA of Complex Fenestration Systems is proposed simulated by Three-Phase Method. Following, both simulation methods are explained.

2.3.1 Conditions for DA simulation by DIVA for Rhino

The following steps should follow to get simulated DA:

1) Build the virtual model by Rhino by material specifications (or use Radiance scene description)

2) Set in Location tab sun and sky conditions by recorded climate data in the form of *.epw file, which is EnergyPlus weather data

3) Set sensor point of Down WP1 in nodes tab

4) From Metrics tab of DIVA, then from Daylight Grid-Based and finally from Climate-Based tab choose in Metric pull-down menu Daylight Autonomy specification, as well as, continuing the following conditions specifications:

   · Occupancy schedule: although the DA is orientated for annual daytime in this file, which is built by any text editor program, any daytime can be add. Including only summertime DA

   · Target illuminance

   · Units

   · Show Daysim Report

   · Use DGP Schedules

   · Radiance parameters according to earlier specifications: -ab -ad -as -ar –aa

   · Adaptive Visual Comfort

   · Geometric Density

   · Cleanup Temporary Directory

The metrics use Radiance and Daysim as their calculation engines. Moreover, using Radiance and Daysim programs DA can be simulated identically.

2.3.2 Conditions for DA simulation by Three-Phase Method

The Three-Phase Method for Simulating Complex Fenestration with Radiance is a method to get RGB irradiance values for each of the 8760 simulated time steps, which means it takes the all hours of entire year into account.

According to Andy MacNeil manual, this method is a means to perform annual simulation of Complex or Dynamic Fenestration Systems. Flux transfer is broken into the following three phases for independent simulations:

1) Sky to exterior of fenestration (D)

2) Transmission through fenestration (T)

3) Interior of fenestration into the simulated space (V)

A matrix is used to characterize each phase of light transport. The input condition, sky luminance, is a vector. The result: illuminance values or a rendering, is also vector. The result is achieved by multiplying the sun vector by each matrix representing each phase of flux transfer. This process is described by the following equation:

i = VTDs or

I = VTDS

where:

i = point in time illuminance or luminance result

I = matrix containing time series of illuminance or luminance result

V = view matrix, relating outgoing directions on window to desired results at interior

T = transmission matrix, relating incident window directions to exiting directions (BSDF)

D = daylight matrix, relating sky patches to incident directions on window

s = sky vector, assigning luminance values to patches representing sky directions

S = sky matrix, a collection of sky vectors

The **V** and **D** matrices are created with a Radiance simulation. The **T** matrix can be created using LBNL WINDOW software, by simulation (ie TracePro or Radiance

genBSDF) or can be measured with goniophotometer. The **s** vector is generated from a Radiance sky description.

Regarding DA point in time illuminance and luminance results (i) are not required, as well as, luminance matrix results and sky vector (s) for point in time results. Following, the matrices generations are explained:

Sky Matrix:

A sky matrix is a time series set of sky vectors. To generate a sky vector the sky is discretized using either the Tregenza or Reinhart division schemes. A sky vector is a list of overage RGB radiance values for each discretized patch of the sky. An annual hourly sky matrix contains 8760 sky vectors, one for each hour of the year. A sky matrix file can be generated as follows:

```
$ epw2wea *.epw *.wea

$ gendaymtx *.wea > *.smx
```

Transmission Matrix:

The transmission matrix is a Bi-directional Transmission Distribution Function (BTDF) which contains outgoing flux coefficients in all directions for each incident direction.

LBNL's WINDOW software can generate a transmission matrix for a fenestration system. It runs only in Windows (Microsoft operation system). The pre-release research version is WINDOW 7 and this version of software is proposed to get Transmission Matrix file. This WINDOW 7 format uses a Klems angle basis to describe incoming and outgoing angles.

Although Radiance, like most Unix software, does not pay attention to file extensions, the file extension of Transmission Matrix is *.xml .

Daylight Matrix:

The daylight matrix contains luminous flux transfer coefficients from the sky divisions to the window's incident Klems divisions. The daylight matrix includes a coefficient for the ground contribution.

The last Radiance program of Greg Ward to get Daylight Matrix is *rfluxmtx*. This program is used for front-end *rcontrib* program and for setting *.cal files. The *rfluxmtx* generalizes sampling for light pipes. It is composed by single sender

objects and one or more receiver objects. In addition, the program needs rendering parameters, as well.

The sender file has light pipe polygon description with Translucent_20 material description. The receiver file has source sky and ground description with glow material without texture description. However, the ground has “h=u” parameter as “uniform” hemispheric sampling description. The sky has “h=r4” as 4 divisions in each dimension of Reinhart’s sub-structuring of the Tregenza sky pattern and u=+Y as "up" direction for the hemisphere. Therefore, a Daylight Matrix file can be generated as follows (the rendering parameters are proposed as -ab 4 -lw 1e-4 -ad 1000):

```
$ rfluxmtx -v -n 2 -c 20000 -ff -ab 4 -lw 1e-4 -ad 1000 *sender.rad *reciver.rad \
-w *space_material.rad *space_geometry.rad > *.dmx
```

View Matrix

The view matrix characterizes the relationship between light leaving a window and arriving at a point. The program *rcontrib* is used again to generate the view matrix. To characterize this relationship first the fenestration material to the Radiance glow material type has to be changed. So, the fenestration emits light in all directions into the space. The surface normal of the windows must be faced into the space otherwise the light is emitted out the space.

On one hand, the octree scene description by *oconv* program with space texture, material and geometry description and window light source description must be generated.

On the other hand, *rcontrib* program is used to generate View Matrix with *.vmx file extension. This process needs description of sensor points, which is created as a text file. Moreover, the number of bins in which rays of the window will be collected (NKbins) and the window orientation for the klems bins (kbin*) is required. For that, the file klems_*.cal contains equations that allows *rcontrib* to bin rays hitting the window based on incident direction. kbinsS is for a window with a normal in the +y axis (South orientation) for the interior of the window. There is also kbinN kbinE and kbinW for other vertical window orientations and kbinD for flat skylights. Furthermore, there is a possibility to specify other window directions by adding them to the klems_in.cal file, or using the more general specification that takes normalized window normal and up vectors; kbin(nx,ny,nz,ux,uy,uz). This last option is proposed. Note that the rendering parameters are needed (-ab 2 -ad 1000 -lw 2e-5 proposed parameters).

Finally, a View Matrix file can be generated as follows:

```
$ oconv *space_material.rad *space_geometry.rad window*.rad > *_vmx.oct

$ rcontrib -f klems_int.cal -b kbin* -bn Nkbins -m windowglow -I+ -ab 2 -ad 1000 -lw 2e-5 *_vmx.oct < *.pts > *.vmx
```

Note that, all scripts are useful for Linux OS.

Results of annual illuminance data by *dctimestep* program

The *rmtxop* program is required to convert RGB irradiance values to illuminance data taking into account luminous efficacy for each colour (k_R = 179lm/w and I = $0.265I_R + 0.670I_G + 0.065I_B$). An annual illuminance data of each sensor point can generate as follows:

```
$ dctimestep *.vmx *.xml *.dmx *.smx | rmtxop -fa -c 47.4 119.9 11.6 - > *.dat
```

This last script is proposed to use by Windows OS. To get DA the illuminance data results processing by hand with an Excel is proposed.

2.4 Window Systems

The window systems can be composed by a window and a Complex Fenestration System. Following, different window systems and Complex Fenestration Systems are proposed.

2.4.1 Description of window systems

The window systems are defined as side-view frame and it is directly related with luminance distribution of vision field. According to, two frame systems, small and large, are proposed to compare with no frame fully glazed façade. The aim is to check the luminance and illuminance distribution of each window system on each workplane. In the following scheme the proposed window systems is detailed.

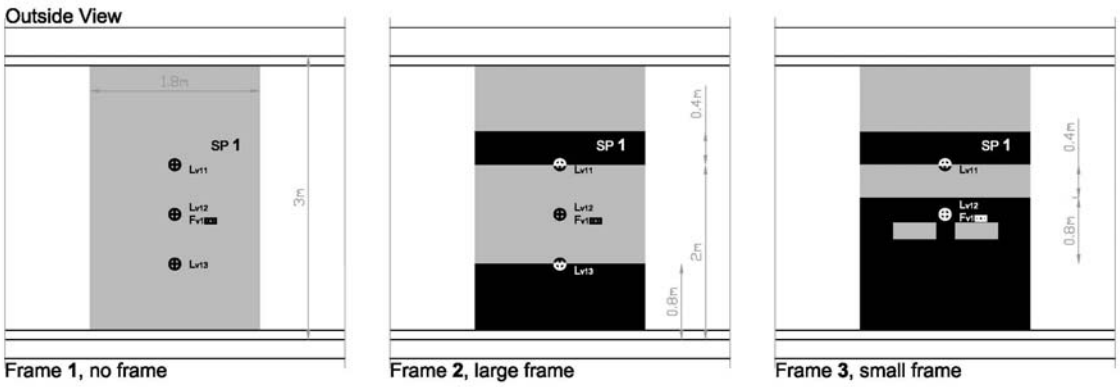

Figure 2. 5 The proposed No Frame, Large Frame and Small Frame window systems

2.4.2 Description of Complex Fenestration Systems

The Complex Fenestration Systems (CFS) are defined as light redirecting systems and it is directly related with illuminance distribution throughout the space. According to, two CFS, light shelf and 3M prismatic film, are proposed to compare with no CFS fully glazed façade. The aim is to check the illuminance distribution throughout the space of each window system and each case the study. In the following scheme the proposed Complex Fenestration Systems is detailed.

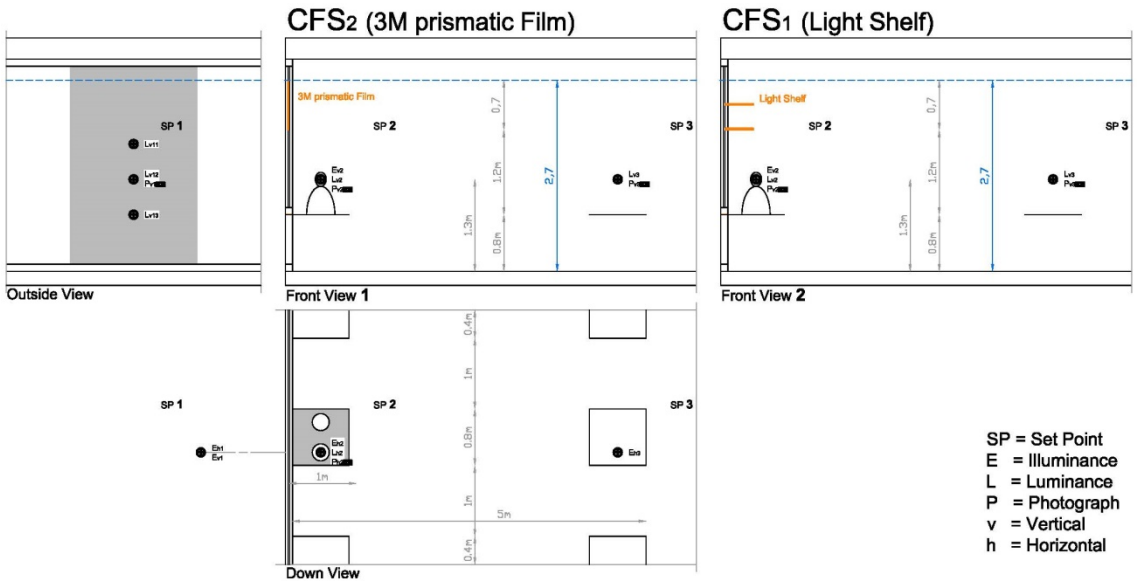

Figure 2. 6 The proposed 3M Prismatic Film and Light Shelf Complex Fenestration Systems

Chapter III

DAYLIGHT AND RESTAURANTS

As in the previous chapters is mentioned, the daylighting is very useful resource for humans. Thus, the presence of daylighting in architectonic inside spaces helps to human wellbeing. Daylight environments increase occupant productivity and comfort, and provide the mental and visual stimulation, necessary to regulate human circadian rhythms. The lighting requirements are very different for each human activity. Knowing the lighting requirements of each activity helps to design the space and taking advantage of free resource, daylighting, use. Therefore, defining lighting parameters there is high possibility to improve the user's visual comfort, to increase efficiency in activity providing stress relief, as well as, to reduce electric lighting consumption.

With reference to outside view high demand of the society, one of the most requested outdoor scenery is the seascape. In last years, many people usually go to boardwalks to enjoy the sea views.

Figure 3. 1 Costumers seated toward to seascape at restaurant in the seafront of Oostende, Belgium

Regarding façade environment, spilt façade with a window and a Complex fenestration Systems have been used in office or academic field. In those activities the main workplanes are a table, a monitor or a blackboard and an out connection. However, as in the presented study outdoor is a workplane, particularly side-view, the dining activity in restaurants is selected as case study. It seems that this outdoor workplane in this activity is more requested. Much it is, so that the users of dining activity prefer to have side-view without obstructions.

Therefore as currently the outdoor views are very important at restaurants and tasting different flavours have become cultural experience, the indoor design of restaurants is gaining relevance. Thus, the retrofitting market has been opportunities and façade

design according to daylighting. It can be useful tool to performance quality indoor atmospheres.

3.1 Previous analysis of restaurants from La Barceloneta and Zarautz

Once having the first intuition of poor side-view daylight design in the section of problem statement of the first Chapter, a field work of restaurants was conducted. La Barceloneta, neighbourhood of Barcelona, and Zarautz, town nearby Bilbao, were selected to observe façade designs and indoor light atmospheres. Both places have seascape side-view demand.

Figure 3. 2 The seafront of Barcelona

Figure 3. 3 The seafront of Zarautz. Modified picture of © 2010 – 2016 Randall St. Germain, Wolf Shield Publishing, Camino My Way.com — All Rights Reserved

On one hand, La Barceloneta is located in Mediterranean coast and in recent years has become the most neighbourhood of Barcelona with restaurants per area. First some details were observed by analysing 56 restaurants:

- Almost all offer outdoor views by a façade
- A third part are contemporary, another third are modernist and another third are traditional
- Almost all contemporary have fully glazed façade
- Almost all traditional have split façade
- In more than a half the tables nearby façade are aligned to outdoor views
- In almost all the costumers prefer the tables aligned to outdoor views
- The most common tables are for 2 or 4 dinners aligned to outdoor views
- Almost in half the ceiling works as light conductor
- Almost in half the wall woks as light conductor
- More than a half has a terrace in front of the view
- Less than a half offer views at night

After analysing 12 selected restaurants following details were observed:

- More than a half table has white tablecloth
- In contemporaries the white table mat is the most common
- Almost all have white dishes
- Almost all have transparent glasses
- Almost all have glossy cutlery
- The most common table size is 0.7m x 0.7m
- The most common direct sunlight protection is the awning, although there are some overhangs
- The awning obstructs the view
- Usually the awnings are white or clear colour
- Using filters, such as curtains or blinds, is not common

· The used curtains are white or clear colour

· There is not light redirecting system

· There is not protection for reflected light of pavement

· Sectored electric light is not common

· There is not electric light with dimming or temperature colour setting

Figure 3. 4 Ununiformed illuminance distribution, obstructed outside view and electric lighting consumption with outdoor high luminance context

After observed the restaurants of La Barceloneta some patterns are detected as 43% of all restaurants facades analysed are highly glazed. Among them 87% are located on the seafront and in addition all of them are placed on the ground floor.

Moreover, only 20% of Highly Glazed Facades are split. The most of them are divided into three parts, which all of them are not contemporary design. Mostly these segmentations follow the same guideline; top, central and bottom. Accordingly this design strategy responds to the required passive window functions; outside connexion, lighting and also ventilation.

On the other hand, Zarautz is located in Atlantic coast and in recent years has become one of the most towns with restaurants per area. In this area similar patterns are detected as 26% of all restaurants facades analysed are highly glazed. Among them 80% are located on the seafront and in addition 75 % are placed on the ground floor. There are fewer restaurants than La Barceloneta, but, the glazed façades tend to be not split.

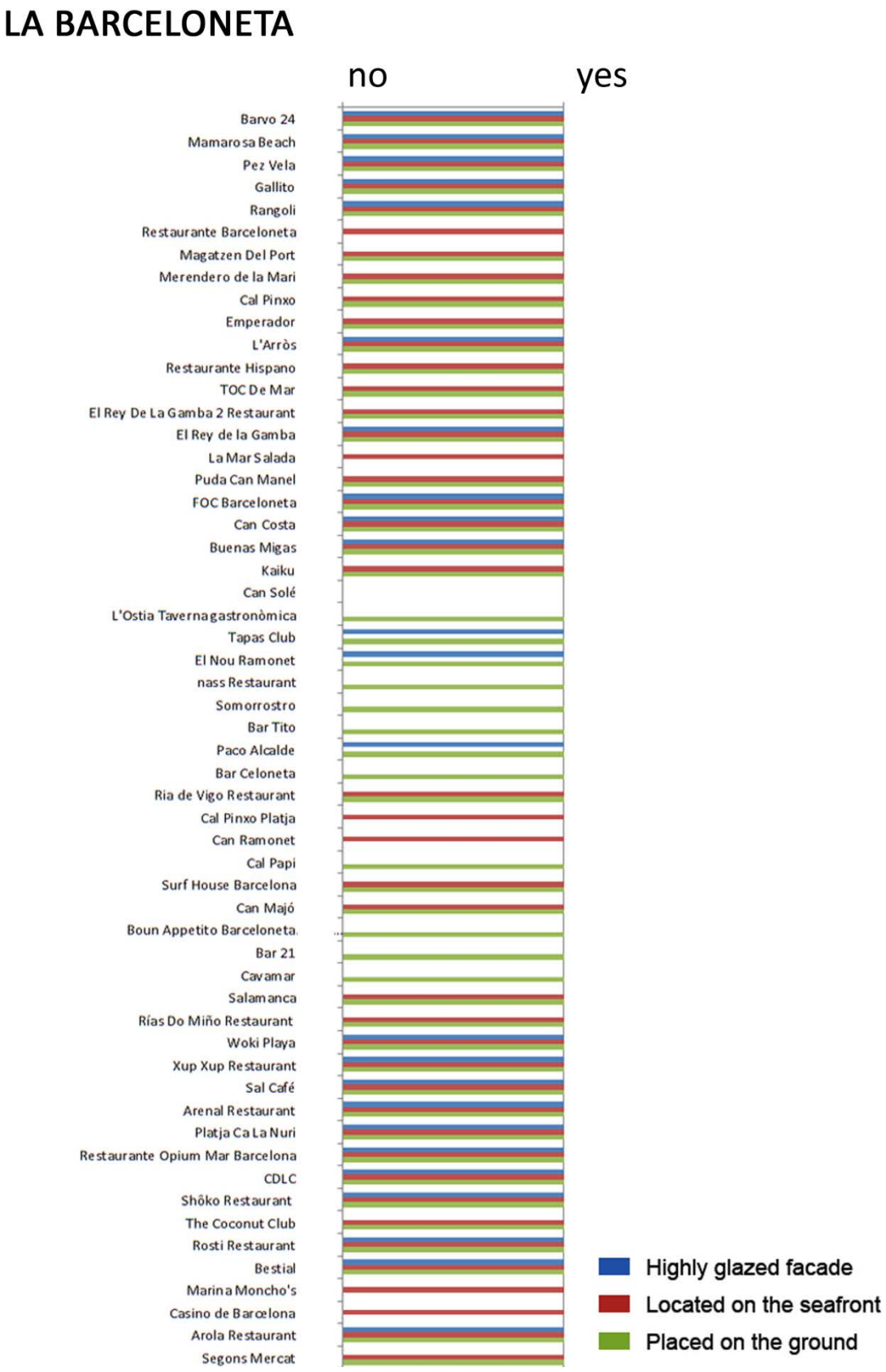

Figure 3. 5 Façade and location features of restaurants of La Barceloneta. The three parameters (façade, location and place) are tested if they are true with "Yes" or false with "No"

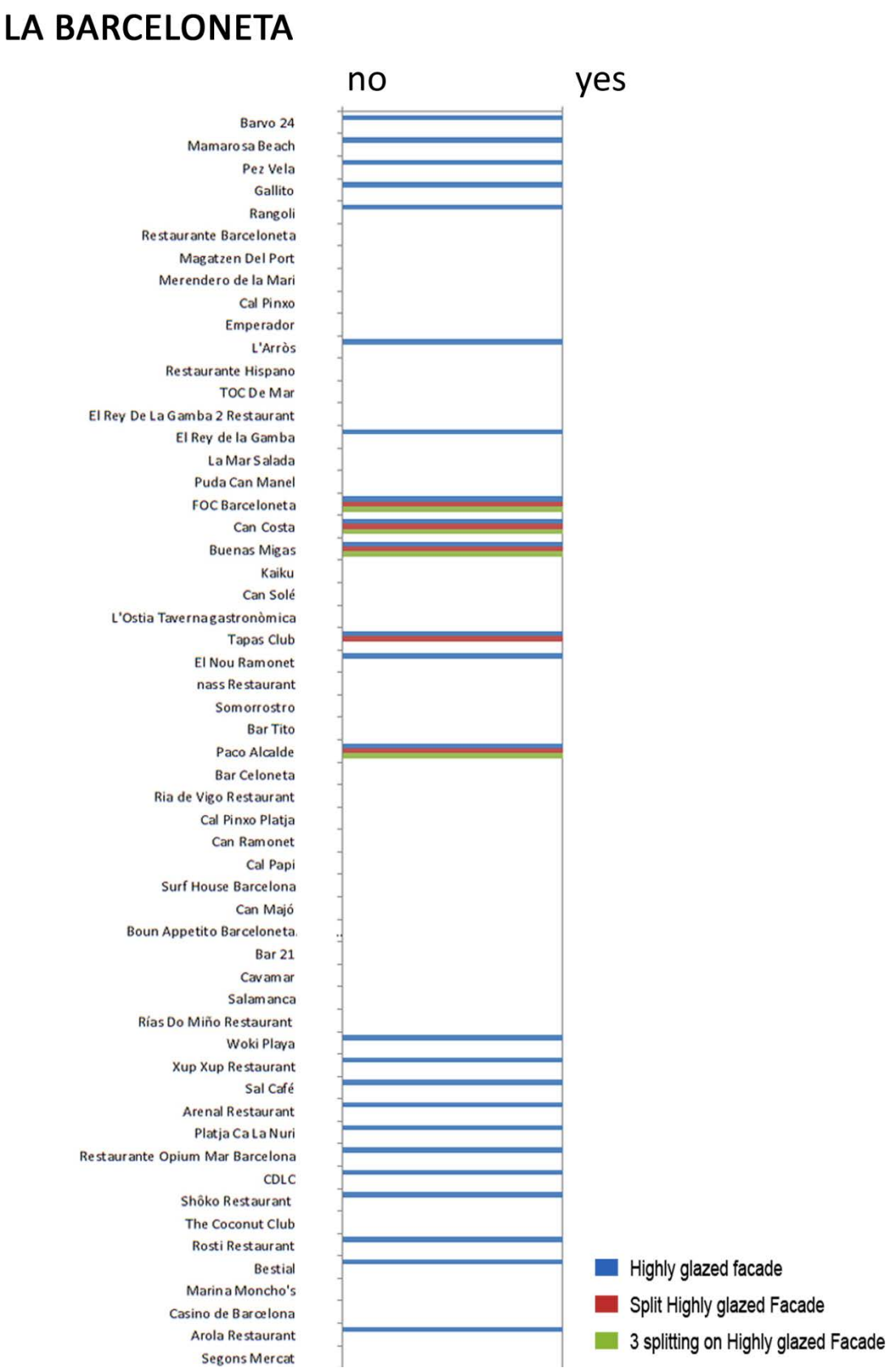

Figure 3. 6 Façade composition of restaurants of La Barceloneta. The three parameters (façade, split façade and 3 splitting on façade) are tested if they are true with "Yes" or false with "No"

Figure 3. 7 Façade picture of each analysed restaurant of La Barceloneta

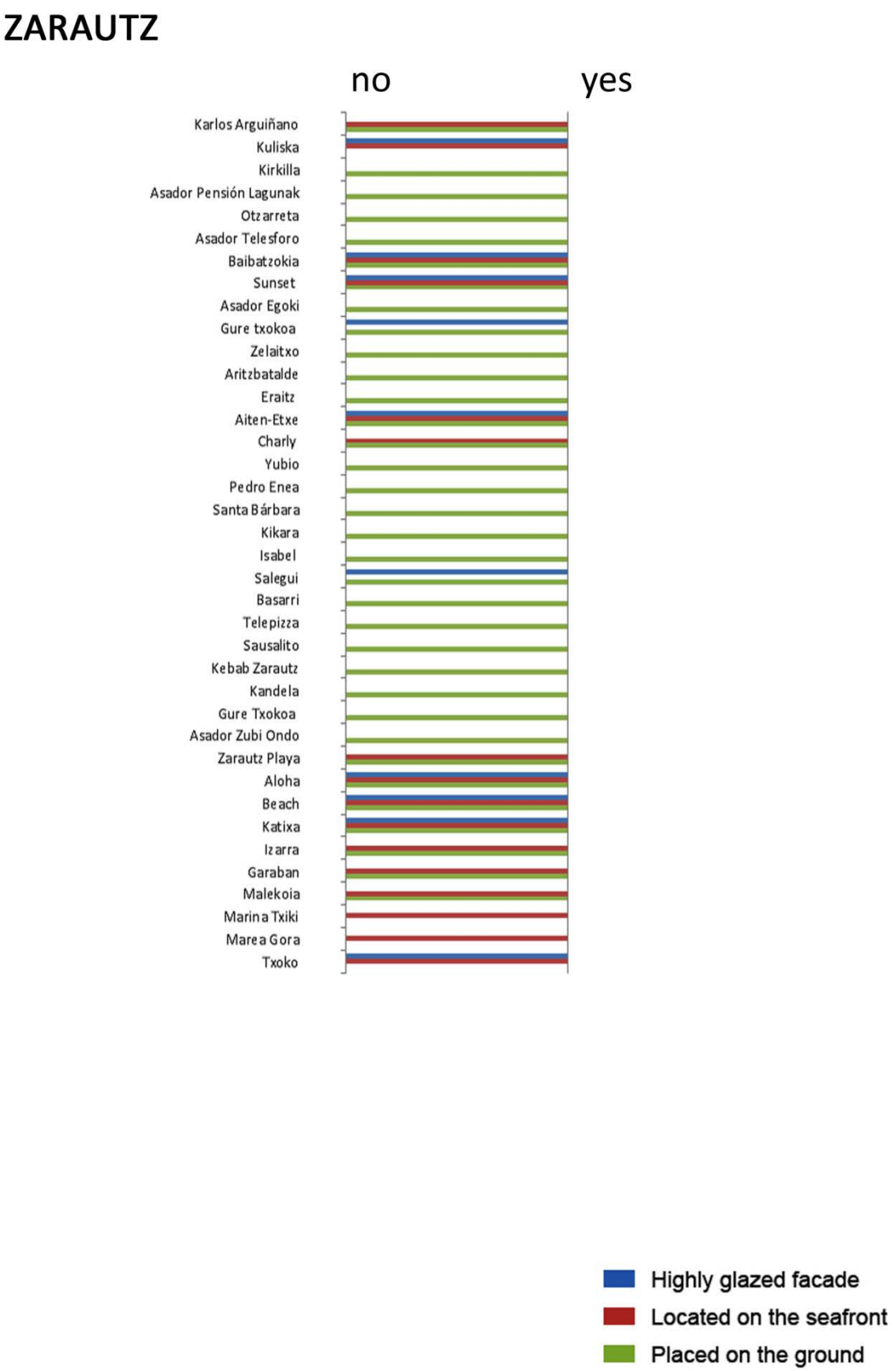

Figure 3. 8 Façade and location features of restaurants of Zarautz. The three parameters (façade, location and place) are tested if they are true with "Yes" or false with "No"

Figure 3. 9 Façade picture of each analysed restaurant of Zarautz

Finally, to end with the observation, two pictures of indoor atmosphere with glazed façade are added to MIT Scene Recognition tool. A restaurant of each location is selected to identify and to check if they are representative for indoor restaurant side-view atmosphere.

First, the restaurant *Ca La Nuri* located in La Barceloneta is added.

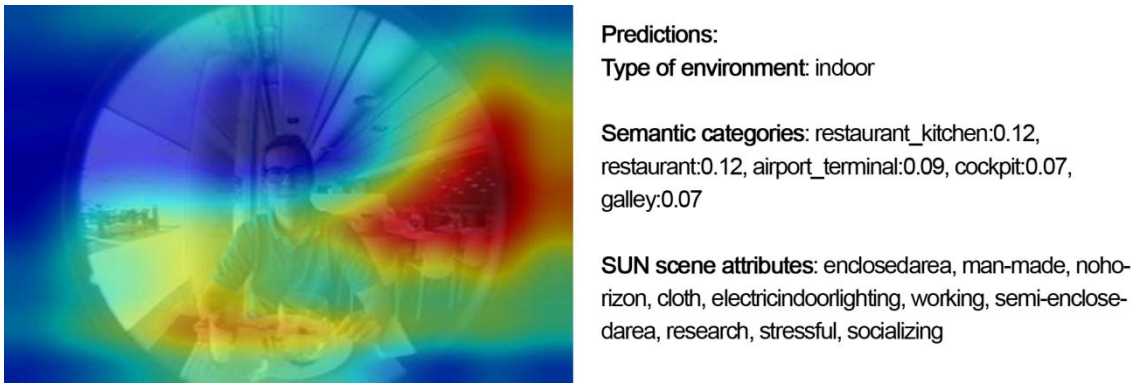

Figure 3. 10 MIT Scene Recognition tool's results of picture of *Ca La Nuri* restaurant

Second, the restaurant *Beach* located in Zarautz is added.

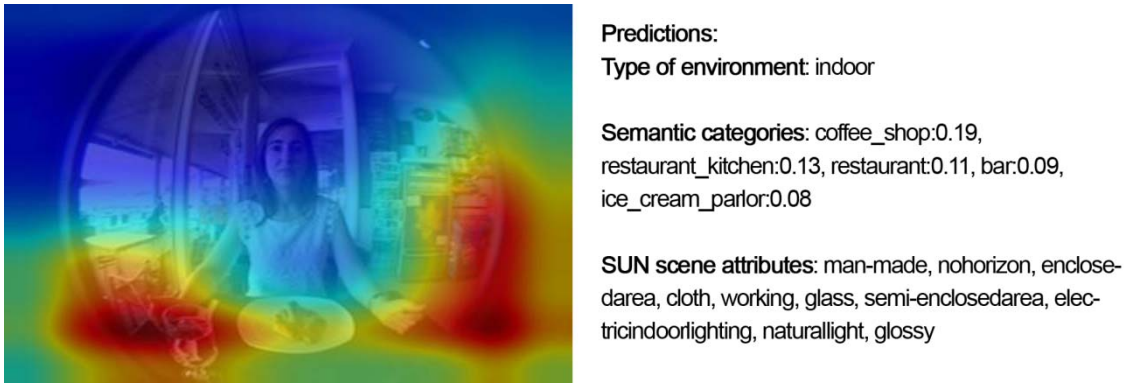

Figure 3. 11 MIT Scene Recognition tool's results of picture of *Beach* restaurant

Both case studies are recognized as a restaurant. In addiction they have features of; working; research; stressful; socializing; glass; and natural-light. The most information content used by the tool there is almost in the central part of the pictures. Therefore, recognition tool shows some indications that the pictures describe working and stressful spaces. So, fully glazed façades may provide fraught atmospheres and particularly at studied restaurants of quality tourist areas.

In consequence, the topic has relevance because there some problems without solution under outdoor high luminance context. The aspects of side-view, fully glazed façade, luminance distribution and illuminance distribution are considered to test in

this thesis. These problems are relevant because the side-view of fully glazed could cause inaccurate perception with undesirable elements, useless transparent surfaces for lighting, glare probability and ununiformed light distribution. Definitely, maybe no quality and discomfort indoor light atmosphere.

In the following sections the selected two restaurants, virtual restaurant prototype, case study's workplanes and light requirements are explained.

3.2 Restaurant 1, Sal Café, under Mediterranean climate

The selected Mediterranean restaurant is called Sal Café. It is located in Barcelona, east of Spain, under Mediterranean warm humid climate, Csa according Köppen-Geiger climate classification. The climate in Barcelona is the Mediterranean type. The Mediterranean climate is between 30° and 45° latitude and west of the continents. It is characterized by relatively wet and mild winters and dry summers. The rainy seasons are intermediate, autumn and spring. The most significant climate are the three to five months of dryness in the summer; when under the dominion of the subtropical anticyclone. Few days with extreme temperatures, hot or cold, so the maximum and minimum annual averages in Barcelona are moderate, typical of a mild Mediterranean climate. Overcast skies are not frequent, about 20% per year. Sun hours are many, about more than 2 500 hours per year.

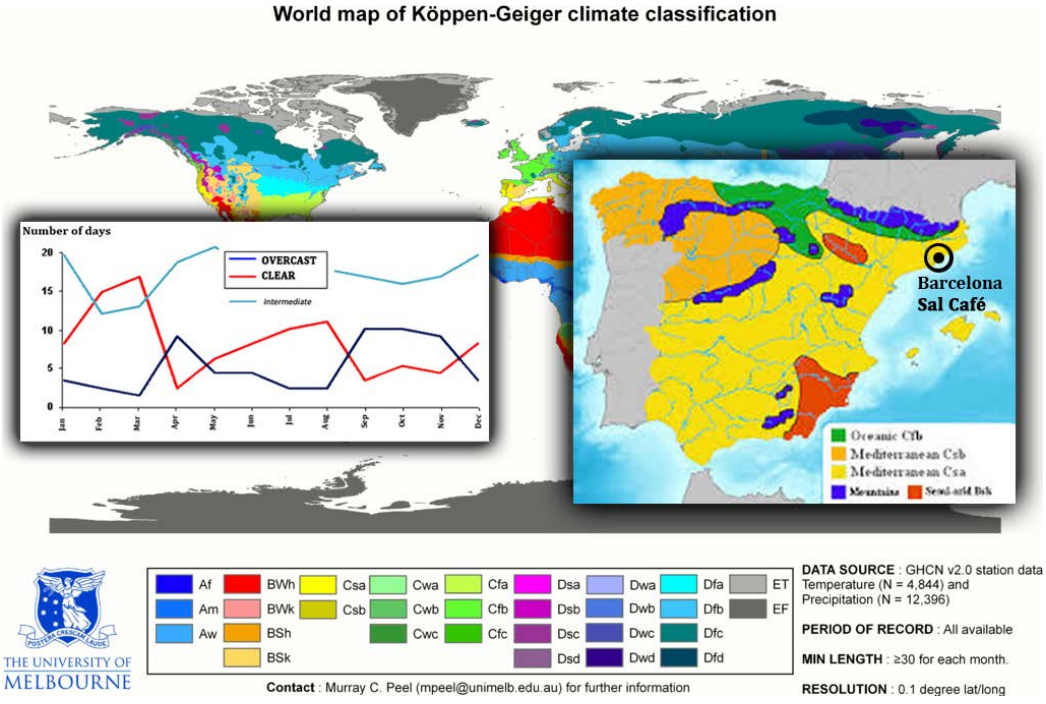

Figure 3. 12 Sky description and location of Sal Café restaurant in Köppen-Geiger climate classification

Sal Café restaurant is located on the seafront of Barcelona. The facade in which is intended to intervene is oriented to the southeast. The module has 2.7m height, 2m large and 5m deep. One 0.7m x 0.7m table with two 0.5m x 0.4m chairs. The roof is white to redirect daylight toward inside. The inside walls are black, diffuse surface, and there some mirrors, reflecting surfaces, in which reflected outside view and provide illumination.

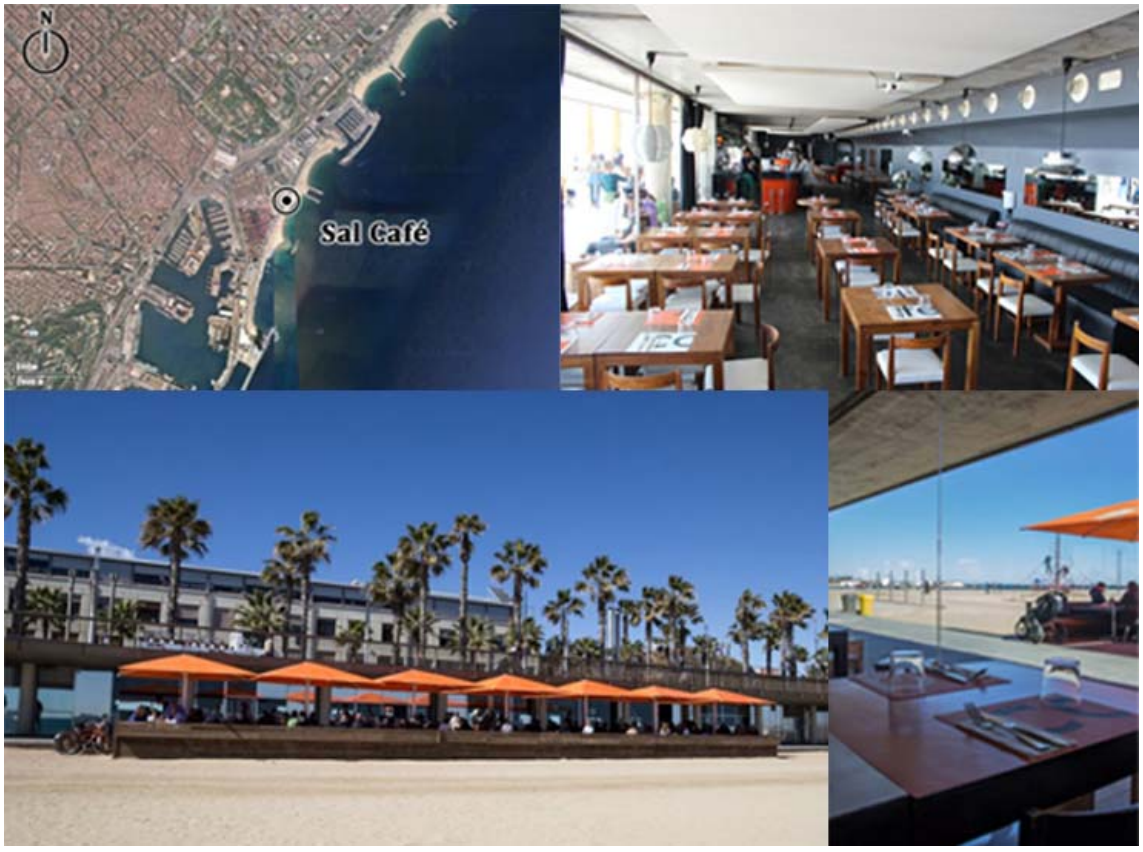

Figure 3. 13 Sal Café restaurant description

3.3 Restaurant 2, Azurmendi, under Atlantic climate

The selected Atlantic restaurant is called Azurmendi. It is located in Bilbao, north of Spain, under Cantabrian oceanic warm rainy climate, Cfb according Köppen-Geiger climate classification. The proximity to the Cantabrian Sea, makes its climate is classified as temperate oceanic with rainfall spread throughout the year, without a well-defined dry summer season. The Atlantic climate is about 43° latitude and north of the continent. The precipitation is abundant, and given the latitude and atmospheric dynamics, rainy days represent 45% of the annual total, to which must be added the

41% in which the sky is overcast. Around Bilbao overcast sky is very common. The rainy season occurs between October and April, noting November as the wettest. Rainfall usually occurs in the form of showers, very fine mists. This same proximity to the ocean makes that the two most defined seasons of winter-summer region and there they remain soft and low intensity thermal oscillations. The average maximum temperature in summer varies between 25 and 26 ° C, while the average minimum winter die between 6 and 7 ° C. The overcast skies are frequent, about 41% per year. Sun hours are not many, about 1 500 hours per year.

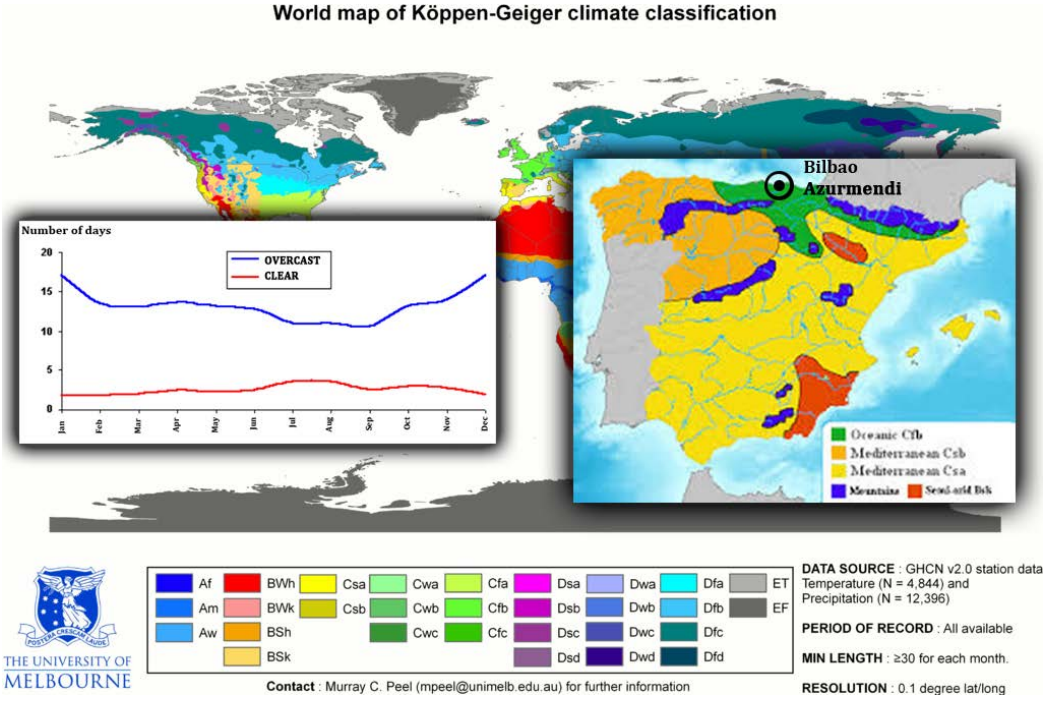

Figure 3. 14 Sky description and location of Azurmendi restaurant in Köppen-Geiger climate classification

Azurmendi restaurant is located near Bilbao. The facade in which is intended to intervene is oriented to the north. The module has 3m height, 2.5m large and 10m deep. One 1.2m x 1.2m table with two 0.5m x 0.4m chairs. The roof is grey don't to redirect too much daylight toward inside. Inside there are diffuse surface wood walls that warm the ambient and there are some mirrors, reflecting surfaces, in which reflected outside view and provide illumination.

Figure 3. 15 Azurmendi restaurant description

3.4 Virtual Restaurant Prototype

The virtual prototype is a simple room. The facade in which is intended to intervene is oriented to the south. The module has 2m in width, 5m in deep and 2.7m in height. There is a table with 0.7m x 0.7m and two chairs of 0.5m x 0.4m. There is some food on the table and a sit person. Inside there are white high reflecting ceiling, medium reflecting plane grey walls, low reflecting plane grey floor. In the following, there are the nine Window Systems proposed.

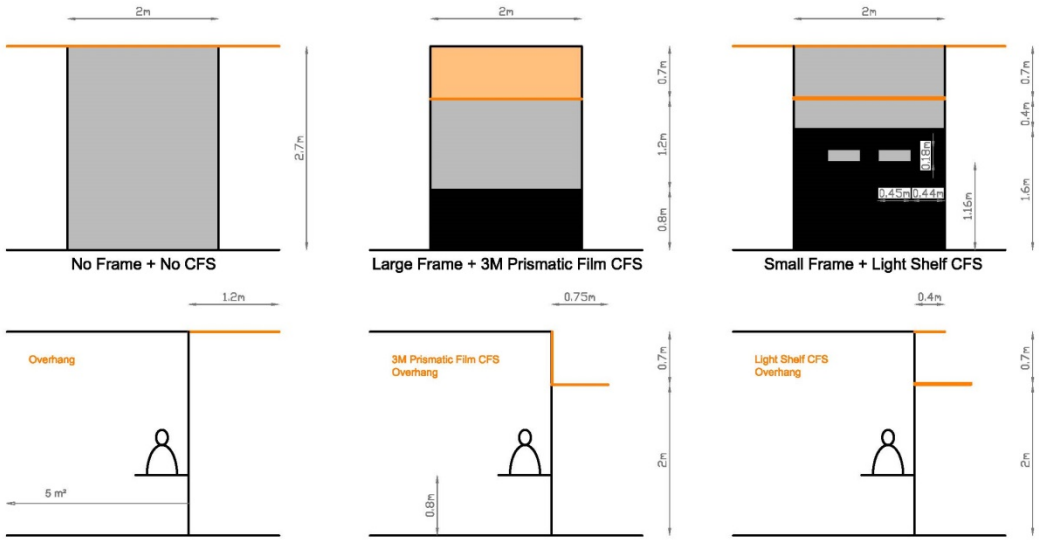

Figure 3. 16 Geometry description of proposed window systems for Virtual Restaurant Prototype

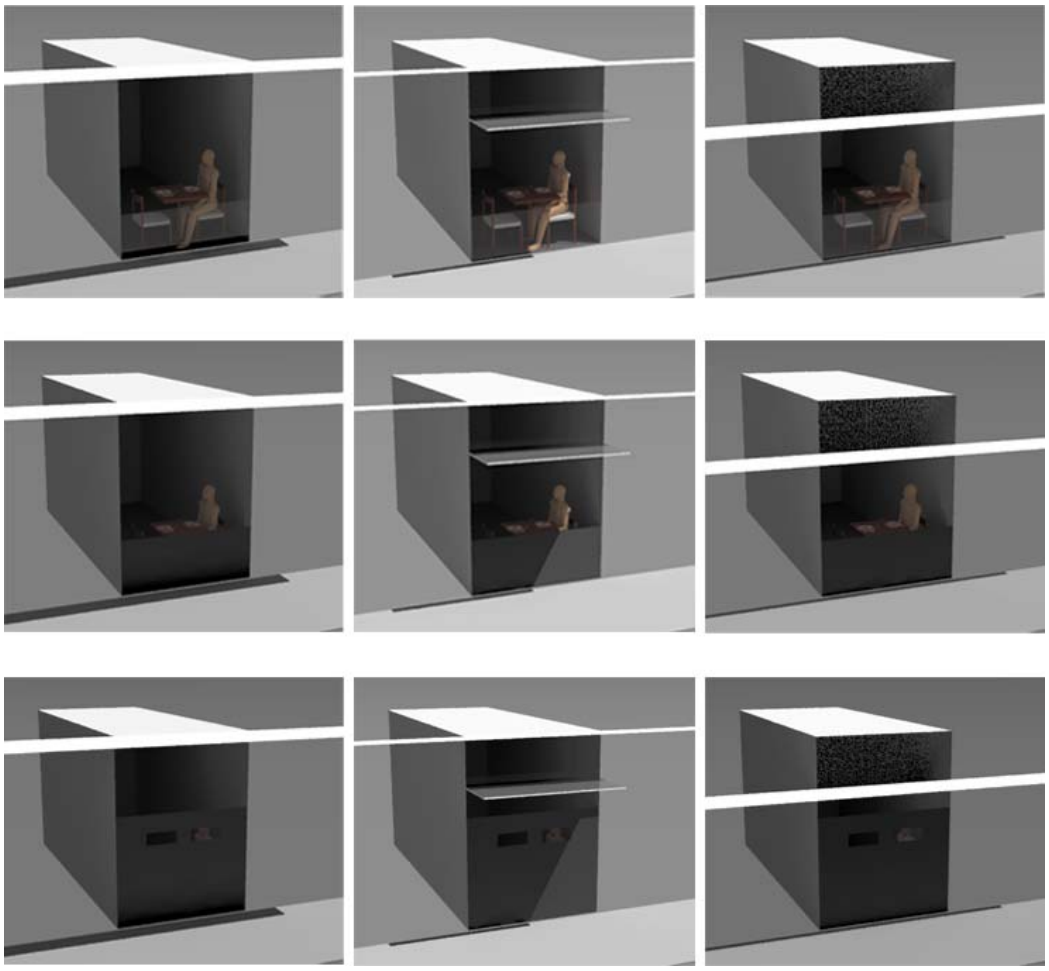

Figure 3. 17 Visualization of each proposed window system; No Frame, No Frame with Light Shelf CFS, No Frame with Prismatic Film CFS; Larger Frame, Large Frame with Light Shelf CFS, Large Frame with Prismatic Film CFS; and Small Frame, Small Frame with Light Shelf CFS and Small Frame with Prismatic Film CFS

3.5 Definition of Workplanes

The relevance of the definition of the most representative local visual fields that contribute to overall visual field is important to add. A good definition of workplanes will fit better user's light requirements and energy optimization.

After asking the managers of restaurants almost all customers prefer sitting with outside view. The workplanes for luminance distribution and the workplane for illuminance distribution have particular specifications. Therefore the workplanes of each parameter are explained apart.

3.5.1 Workplanes for luminance distribution

Tables adjacent to the façade are the most requested and usually the tables for two people have the features of; down view, toward to a table; front view toward to a person; and out view, toward to window. Accordingly, table adjacent to glazed façade for two people position is chosen.

Accordingly the Set Point 2 is selected as point of view to analyse luminance distribution. So, three workplane are defined to get overall mean Daylight Glare Probability. The results of interactions between different workplanes are more real owing to luminance adaptation. Therefore, the three workplanes are; table, person and window.

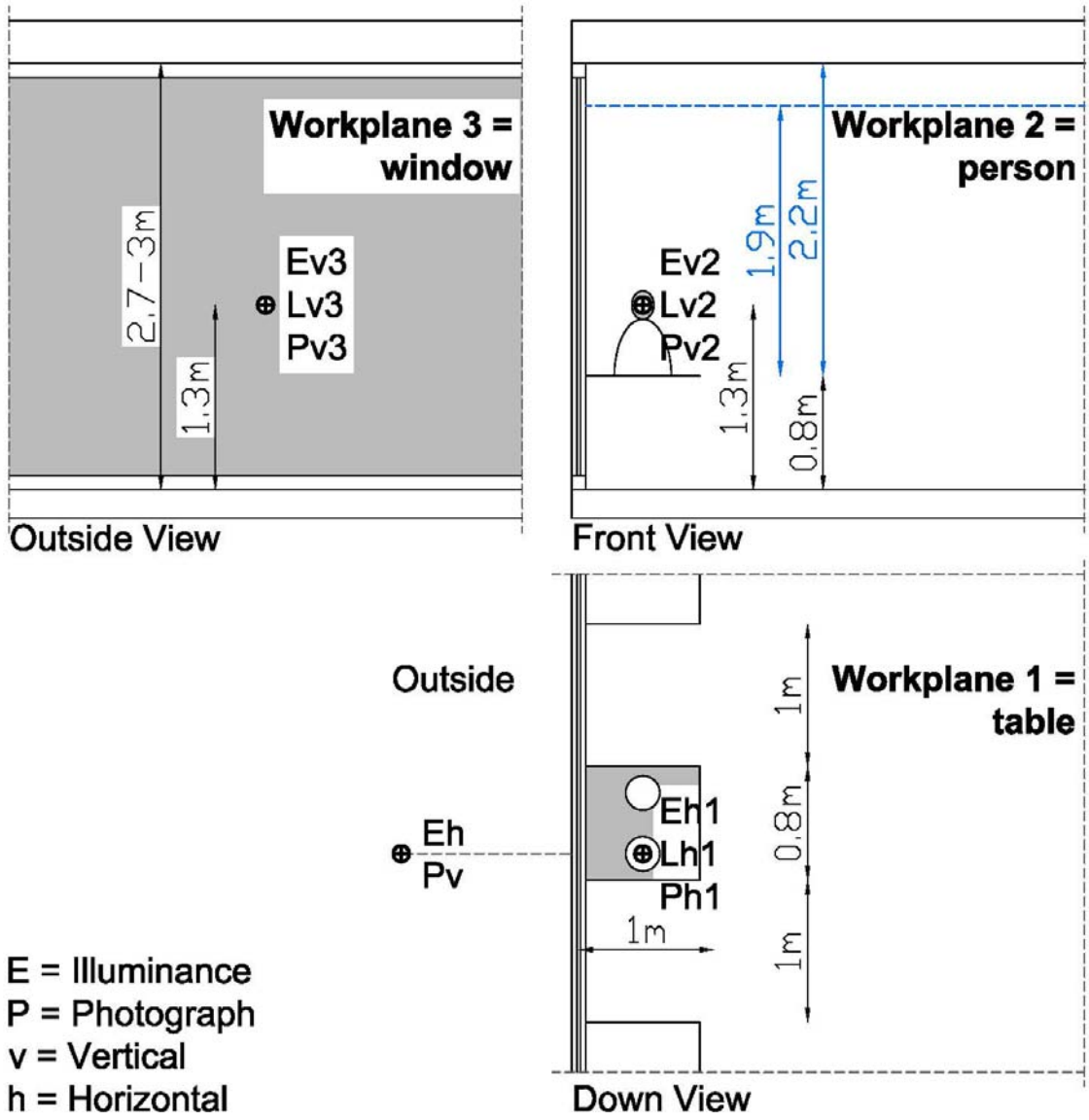

Figure 3. 18 Workplanes description of luminance distribution for the selected activity

3.5.2 Workplane for illuminance distribution

With reference to illuminance distribution, the workplane is a plane which sets the table throughout the 5m X 5m of the space. The goal is to check illuminance distribution along the space according to each window system.

This plane is set approximately by sensor points. This grid has 20cm between sensors and 30cm between walls, although some suggestion indicates 50cm between walls. This proposed grid totally has 576 sensor points. Each selected restaurant has some

sensor points less due to some furniture that hinders. So, the aim is to analyse Daylight Autonomy in each sensor point for each window system.

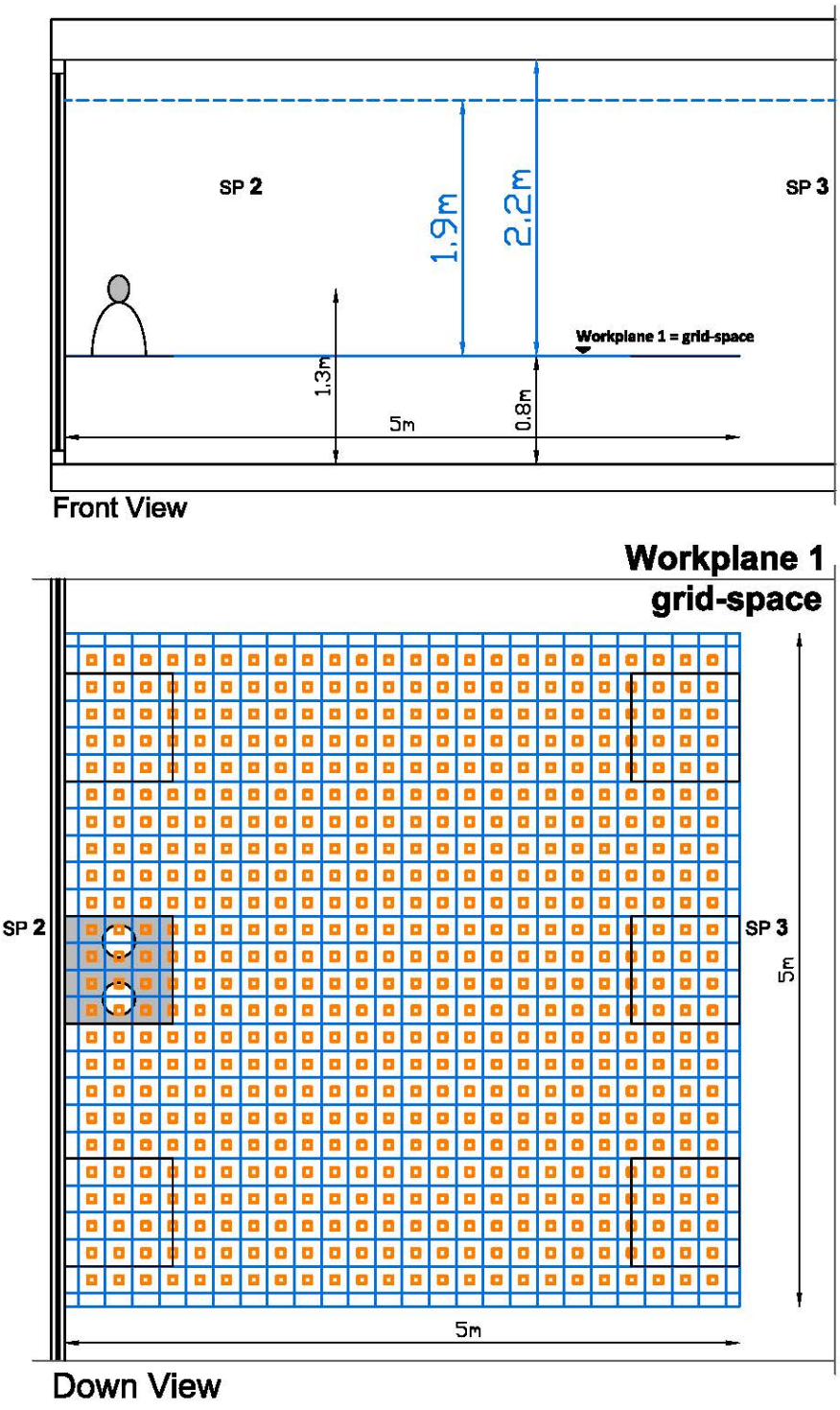

Figure 3. 19 Workplane by sensor-grid description for illuminance distribution and the selected activity

Chapter IV

RESULTS OF PARAMETER 1: luminance distribution evaluated by Daylight Glare Probability (DGP) index

This chapter deals with luminance distribution. The Daylight Glare Probability (DGP) index will be used for assess luminance distribution. The DGP will be applied to each workplane, to each window system and to each case study.

The virtual models of selected two restaurants, Sal Café and Azurmendi, have been created by Rhino. The aim is to get the DGP index of each simulated workplane visualization. In addition, real photographs of each workplane have been taken to get the simulation of DGP of real pictures. These DGPs have been used to calibrate the DGP's of virtual simulations.

Figure 4. 1 In the up row virtual model of Sal Café restaurant. In the down row virtual model of Azurmendi restaurant

Furthermore, as already in chapter before is mentioned, a virtual prototype of a restaurant has been created to get more accurate window systems' lighting performance. The DGP of each workplane and window system has been obtained.

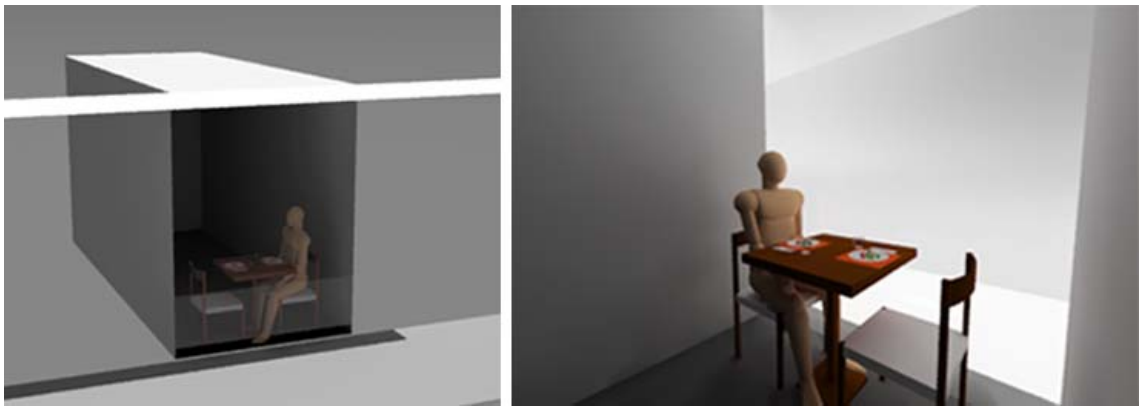

Figure 4. 2 Description of Virtual Restaurant Prototype

Finally, the mean DGP of each window systems has been get in order to evaluate luminance distribution perception. In the following table the all DGP calculations are explained:

Mean DGP (WP1, WP2 , WP3)	Restaurant 1 (Sal Café)	Restaurant 2 (Azurmendi)	Virtual Restaurant
Real pictures	x	x	-
Virtual pictures	x	x	x

Table 4. 1 Pictures that are tested by DGP index for each restaurant

The mean DGP is a simple way to get into account different workplanes to avoid extreme situation. There are more advanced methods as the view of each eye or Omnidirectional Stereo System (ODS) to get overall glare perception. However, the mean DGP could be useful to demonstrate that the absolute extreme luminance is not very important when you have another workplane or view to focus on, as well as the adaptation steps.

Note that, from the sit person point of view, which will be aligned to the façade and sharing a table with other person, the three workplanes, table, person and window, will be assessed. The DGP will be tested for different Window Systems as; No Frame, Large Frame, Small Frame and Light-Shelf and Prismatic Film Complex Fenestration Systems only for Virtual Restaurant Prototype.

4.1 Scripts of DGP simulation

In de following section the scripts that have been used are explained. The scripts for real pictures and virtual pictures will be explained separated:

Real pictures' DGP scripts process:

1) The HDR of different exposures of real pictures is necessary to get. For that WebHDR online application has been used. The medium size *.hdr file has been selected to use with Evalglare program.

Note that *hdrgen* is a program to get *.hdr file.

2) First should be checked the *.hdr file dimension. It must be lower than 800 x 800 pixels by Radiance-5.0.a.11-Linux *getinfo* program:

```
$ getinfo –d *.hdr
```

Note that, *pfilt* is the program to get smaller *.hdr file.

3) The Evalglare program has been used to get DGP index. –i parameter is used in the program to add measured illuminance data. The illuminance data of each workplane of real restaurants are the followings:

	Illuminance (E, lux) RESTAURANT 1 (Sal Café)		
	WP1 (table)	WP2 (person)	WP3 (window)
No Frame	2350	3500	9350
Large Frame	1810	2840	7840
Small Frame	780	1240	4073

Table 4. 2 The illuminance data of each workplane of Restaurant 1 (Sal Café)

	Illuminance (E, lux) RESTAURANT 2 (Azurmendi)		
	WP1 (table)	WP2 (person)	WP3 (window)
No Frame	2540	1860	4700
Large Frame	1639	1810	3790
Small Frame	1287	1350	2420

Table 4. 3 The illuminance data of each workplane of Restaurant 2 (Azurmendi)

Therefore the script of the first DGP has been the following:

```
$ evalglare –i 2350 *res1_wp1_nf.hdr
```

Note that, the DGP is used for indoor luminance range. In consequence, the out view workplane's DGP could be a little overestimated. In addition, the lens should be calibrated to get correct equisolid angle projection. In this work, the calibration has not been done.

4) With Evalglare program there is an option to get an image with glare source coloured. The colour has not importance and the –i value does not change the result. The script of the first Glare Source image has been the following:

```
$ evalglare –c *res1_wp1_nf_gs.pic *res1_wp1_nf.hdr
```

Sometimes the Glare Source image is necessary to apply *pfilt* command to get balanced brightness. The script could be the following:

```
$ pfilt *res1_wp1_nf_gs.pic > *res1_wp1_nf_gs-pfilt.pic
```

The last step to obtain Glare Source image is becoming *.pic file to *.tif file as in the following:

```
$ ra_tiff *res1_wp1_nf_gs-pfilt.pic *res1_wp1_nf_gs-pfilt.tif
```

5) The False Colour Image is useful for get luminance values distribution. For that WebHDR online application has been used. The parameters have been:

   · Logarithmic scale with 3 decades (*-log 3* for *falsecolor* program)

   · 10 number of contours (*-n 10* for *falsecolor* program)

   · 3000 cd/m^2 limit of scale value (*-s 3000* for *falsecolor* program)

   · The width (*-lw* for *falsecolor* program) and the height (*-lh* for *falsecolor* program) of the legend have been the default value of online application.

   Note that, *falsecolor* is the program to get False Colour Image.

6) Once the DGP of each workplane has been obtained the mean DGP of each restaurant is get. The mean DGP is calculated by the average of each workplane. The first mean DGP of Sal Café restaurant has been get as in the following:

Daylight Glare Probability (DGP) index			
WP1 (table)	WP2 (person)	WP3 (window)	MEAN
30	36	69	(30+36+69)/3=45

Table 4. 4 Description of the mean DGP calculation according to the DGP of the three workplanes

Virtual pictures' DGP scripts process by DIVA for Rhino:

1) Once the model is set by Rhino the viewpoints of workplanes are necessary to get. The viewpoints are the same as the real photographs. They can define by *Set View* tab.

2) Starting with DIVA, Radiance and Daysim program based plugin for Rhino. The program can be obtained from DIVA FOR RHINO website http://diva4rhino.com/ (The program for Windows OS is used for thesis's

visualizations). The DIVA plugin has 4 tabs; *Location*, *Nodes*, *Materials* and *Metrics*. To get DGP of visualizations the *Nodes* tab is not necessary:

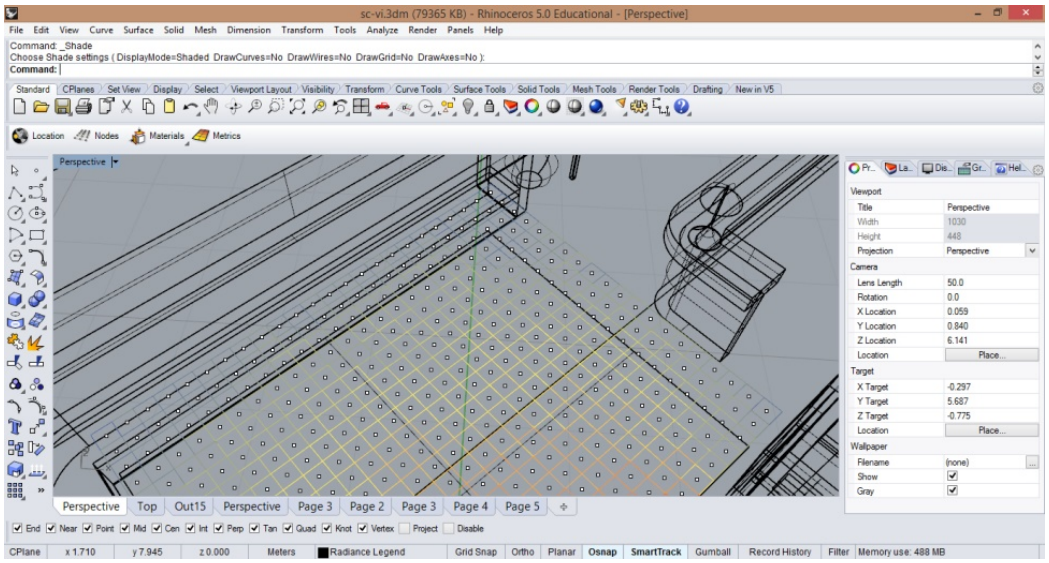

Figure 4. 3 DIVA plugin visualization into Rhinoceros program

· *Location* tab: The *.epw weather data file of the location is necessary; it could download from EnergyPlus website https://energyplus.net/weather . It must be put in DIVA's *WeatherData* folder as C:\DIVA\WeatherData. Once the location is set *-DIVA folder is created, where Rhino file is saved and DIVA's default files are saved.

· *Materials* tab: the materials specifications are defined as Radiance's material description. Other materials have been needed, so the material specifications have been added to *material.rad* file, where it is in Resources' folder in previous *-DIVA created folder. The file *.xml that has the scattering function must be placed in *lib* folder C:\DIVA\Radiance\lib.

· *Metrics* tab: In *Daylight Images* tab and then selecting *Point-in-Time Glare* tab the Visualization Image and the DGP index with Glare Sources Image of a particular moment is obtained.

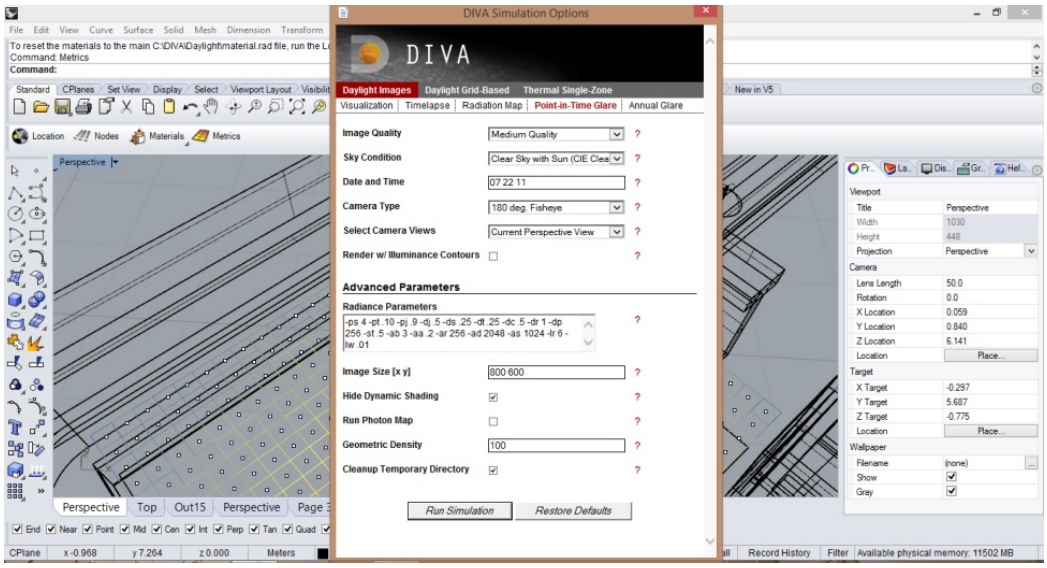

Figure 4. 4 The calculation options of Metrics tab

Therefore, the pictures in Visualization folder inside of *-DIVA folder are saved; the Visualization Image in *.pic and *.tif format file, Glare Sorce Image in *.tif format file and DGP index by Evalglare program in *.txt format file.

3) The parameters of Point-in-Time Glare have been the following:

· Image Quality: Medium Quality

· Sky Condition: Clear Sky with Sun (CIE Clear Sky) for Sal Café Mediterranean climate restaurant and Intermediate Sky with Sun for Azurmendi Atlantic climate restaurant. For the virtual prototype Clear Sky with Sun (CIE Clear Sky) is selected because there is not huge difference between both skies.

· Date and Time: Standards Time, 07 22 11 for Sal Café restaurant, 08 25 11 for Azurmendi restaurant and 07 22 11 for virtual prototype.

· Camera type: 180 deg. Fisheye

· Select Camera views: Current Perspective View

· Radiance parameters: All Radiance parameters are changeable:

```
-ps 4 -pt .10 -pj .9 -dj .5 -ds .25 -dt .25 -dc .5 -dr 1 -dp 256 -st .5 -ab 3 -aa .2 -ar 256 -ad 2048 -as 1024 -lr 6 -lw .01
```

Note that, for Workplane 1, Down vision, the View Up Vector (-vu *xd yd zd*) with vertical direction is needed; for Sal Café with southeast orientation, –vu 0.5 0.5 0 ; for Azurmendi north orientation, -vu 1 0 0; and for virtual prototype with south orientation, -vu 1 0 0. For example:

```
-ps 4 -pt .10 -pj .9 -dj .5 -ds .25 -dt .25 -dc .5 -dr 1 -dp 256 -st .5 -ab 3 -aa .2 -ar 256 -ad 2048 -as 1024 -lr 6 -lw .01 –vu 0.5 0.5 0
```

· Image Size [x y]: 800 600
· Geometry Density: 100
· Cleanup Temporary Directory

Note that, real fish eye projection is a little different to simulated fish eye projection owing to the real one takes 130º of field and the simulated fish eye projection takes fully 180º of field.

4) Add that, *gensky* command, Radiance program, is launched to get Sky simulation. Some visualization need outdoor horizontal illuminance data to suit better the virtual incoming illuminance data of pictures. *gensky* command has –B parameter option for Diffuse Horizontal Irradiance (DhI) data, whereas, *gendaylit* has –E parameter option for Global Horizontal Irradiance (GhI) data. The measured data is global illuminance data, so, for some visualization *gendaylit* command has been used. Then incoming illuminance data of pictures have been checked by Evalglare program and –V parameter. It has had to be similar to incoming measured illuminance data. The command *gendaylit* is launched from *_sky.rad file of Temp folder C:\DIVA\Temp . It can be launched from the script *.bat file directly in the same folder or using *oconv* and *rpict* programs of Radiance launching from MS-DOS Window and after Evalglare program.

The measured outdoor horizontal global illuminance data are the following:

	$E_{outdoor\ global\ horizontal\ illuminance}$ (lux=lm/m^2)	$GhI_{calculated}$ (w/m^2) *Dividing with luminous efficacy (k_R = 179lm/w)
RESTAURANT 1 (Sal café)	82 000	≈ 458
RESTAURANT 2 (Azurmendi)	73 500	≈ 410

Table 4. 5 Global horizontal irradiance obtained from measured horizontal global illuminance of each restaurant. At 12:00 local time in 22 July (Sal Café) and 25 August (Azurmendi)

Due to the visible sky patch through the window the incoming light varies widely. Accordingly, for few workplanes the irradiance value has had to be suited to approach measured incoming light level. The followed workplanes have been calibrated:

			-E parameter (outdoor global irradiance value w/m^2)
Sal Café	No Frame	WP1	410.61
		WP3	410.61
	Large Frame	WP3	410.61
Azurmendi	No Frame	WP1	250
	Large Frame	WP1	105
		WP3	105

Table 4. 6 The pictures run by *gendaylit* program and used global irradiance data

In addition, the overflows caused for the sun should be taken into account. In this case, the sun luminance should be changed for real luminance of sun. However, in this work it does not do it.

5) The False Colour Image of the virtual pictures as the same of real pictures serves to describe luminance distribution. DIVA has a program *wxFalsecolor*, which the visualizations in *.pic file format (*.hdr file format as well open) turn into in False Colour Image.

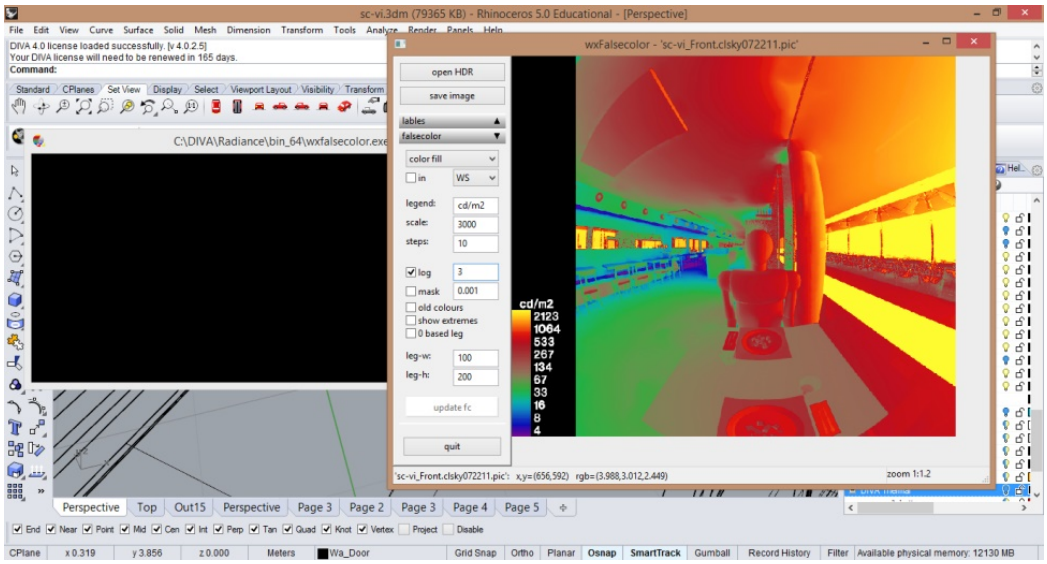

Figure 4. 5 The processing of False Colour Image by *wxFalsecolor* program from DIVA plugin

Therefore, selecting *falsecolor* tab the parameters can be set. The following one has been used, the same as real parameters of real photographs:

· scale: 3000

· steps: 10

· log: 3

Clicking *convert fc* option the virtual picture has been became in False Colour Image. There is an option to save in *.tif file format, as well.

4.2 Pictures, False Colour Images, Glare Source Images and DGP index

In this section the pictures of each Workplane, each Window Systems and restaurants. Each Workplane has a picture, a False Colour Image and Glare Source Image with DGP index. Note that the virtual prototype visualizations are of 22 of July at 11:00 Standard Time (12:00 Local Time) in Barcelona. That is because with Clear Sky there is not huge difference in daylight performance at Bilbao or Barcelona. The rendering parameters are the same as the others restaurants. In addition, the virtual prototype has Light Shelf and Prismatic Film Complex Fenestration Systems in some Window Systems.

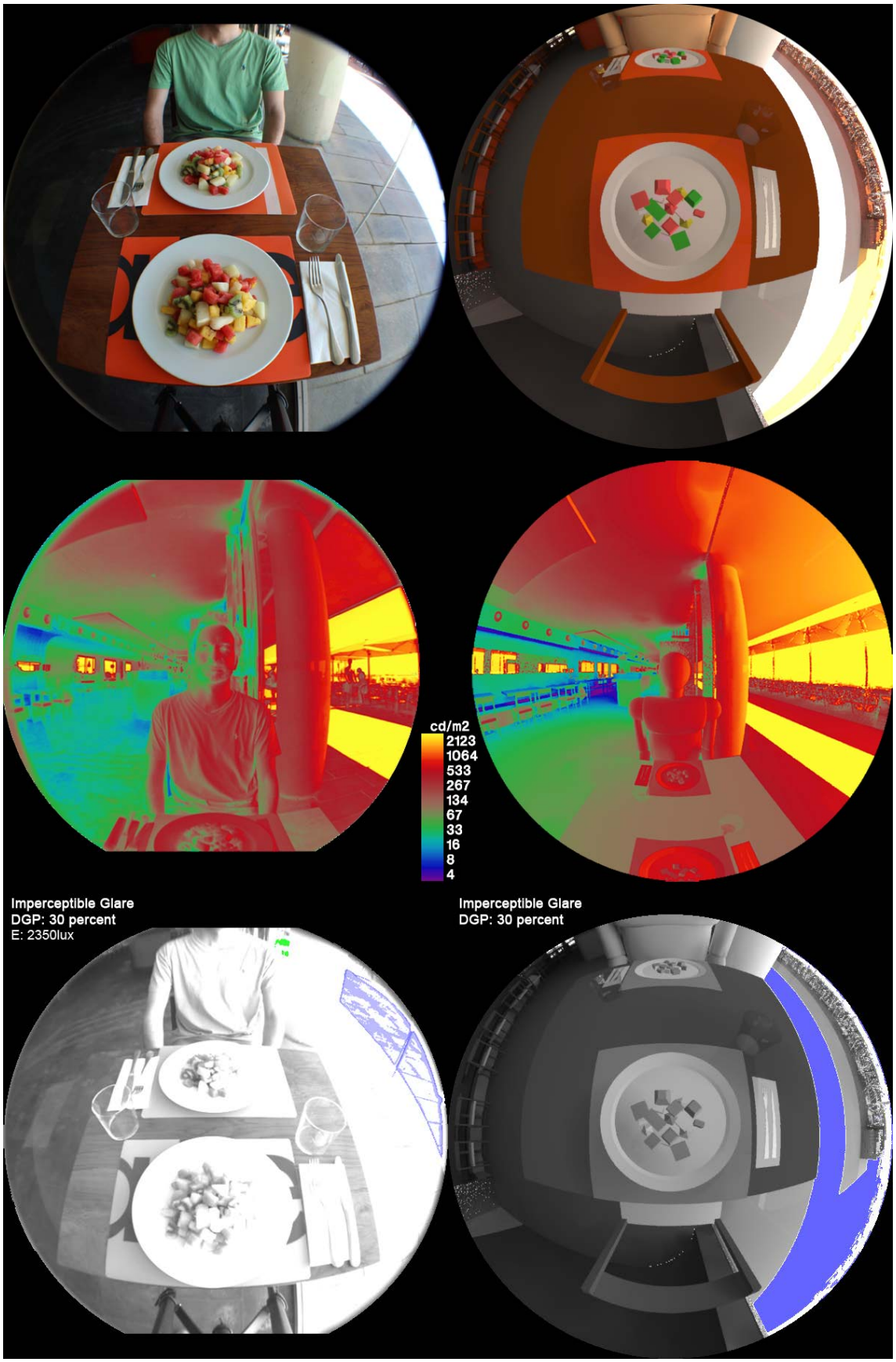

Figure 4. 6 Real and virtual Visualizations, False Colour Images and Glare Source Images with DGP index of WP1 (table) for No Frame Window System from Restaurant 1 (Sal Café)

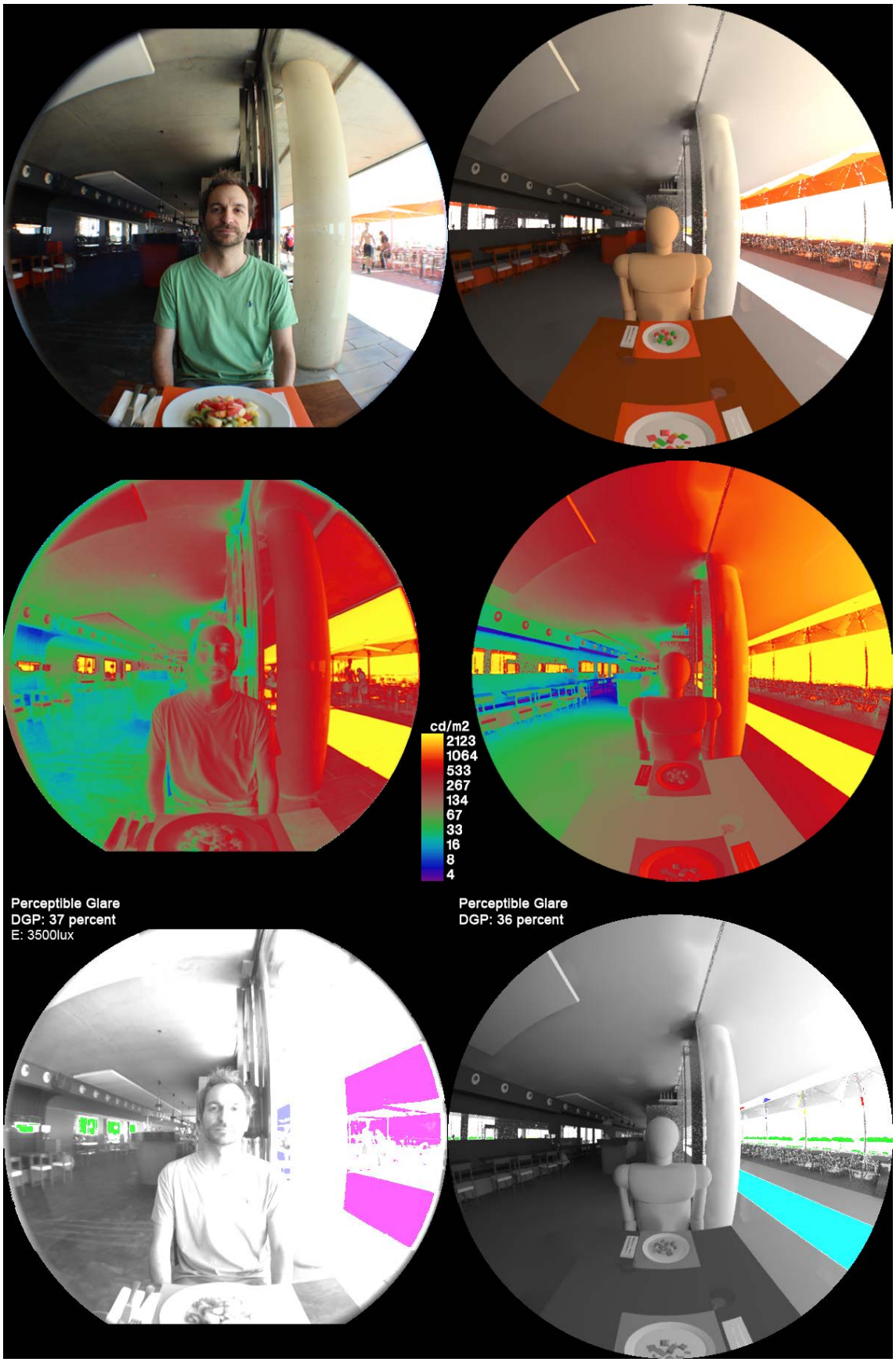

Figure 4. 7 Real and virtual Visualizations, False Colour Images and Glare Source Images with DGP index of WP2 (person) for No Frame Window System from Restaurant 1 (Sal Café)

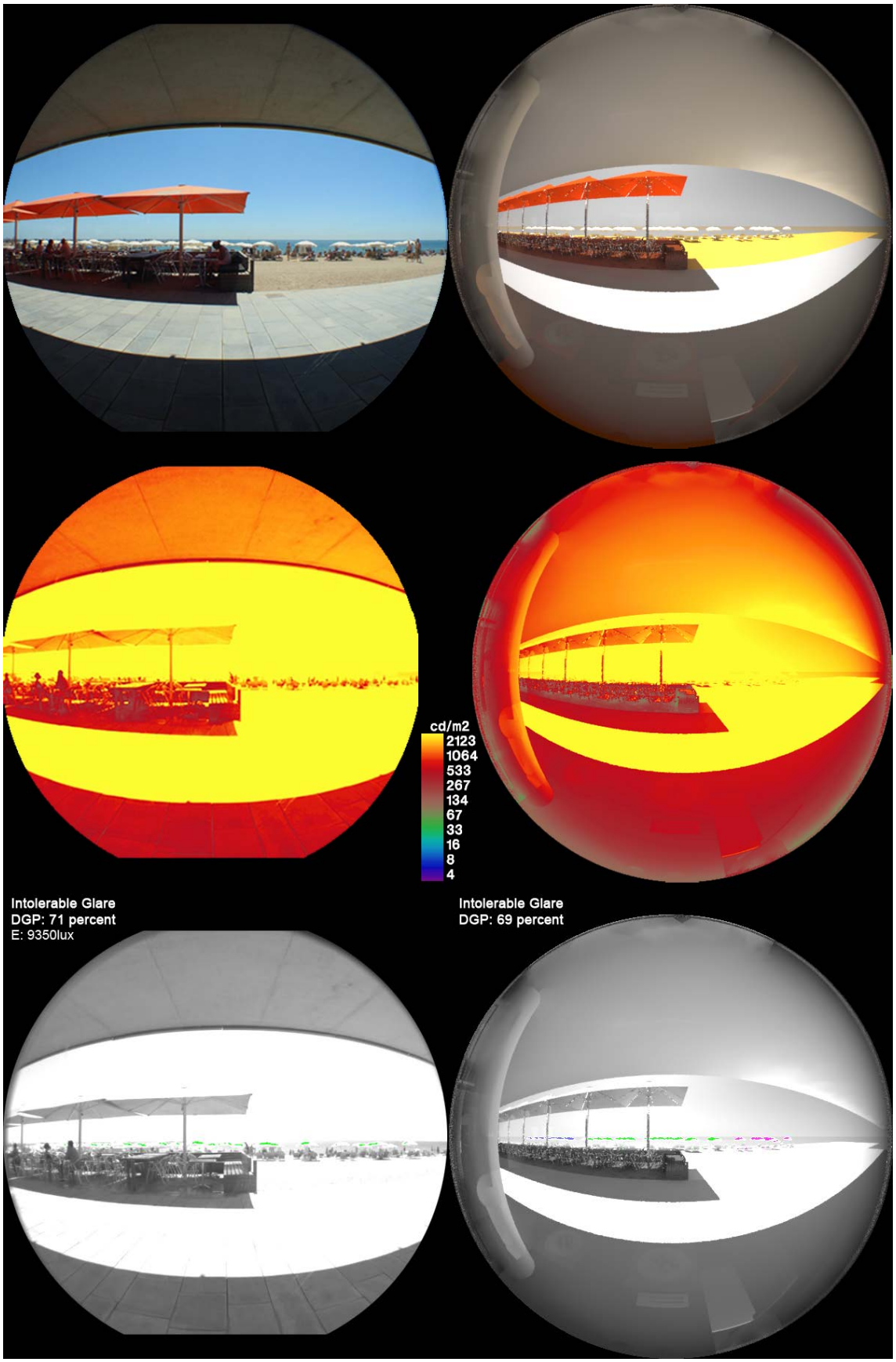

Figure 4. 8 Real and virtual Visualizations, False Colour Images and Glare Source Images with DGP index of WP3 (window) for No Frame Window System from Restaurant 1 (Sal Café)

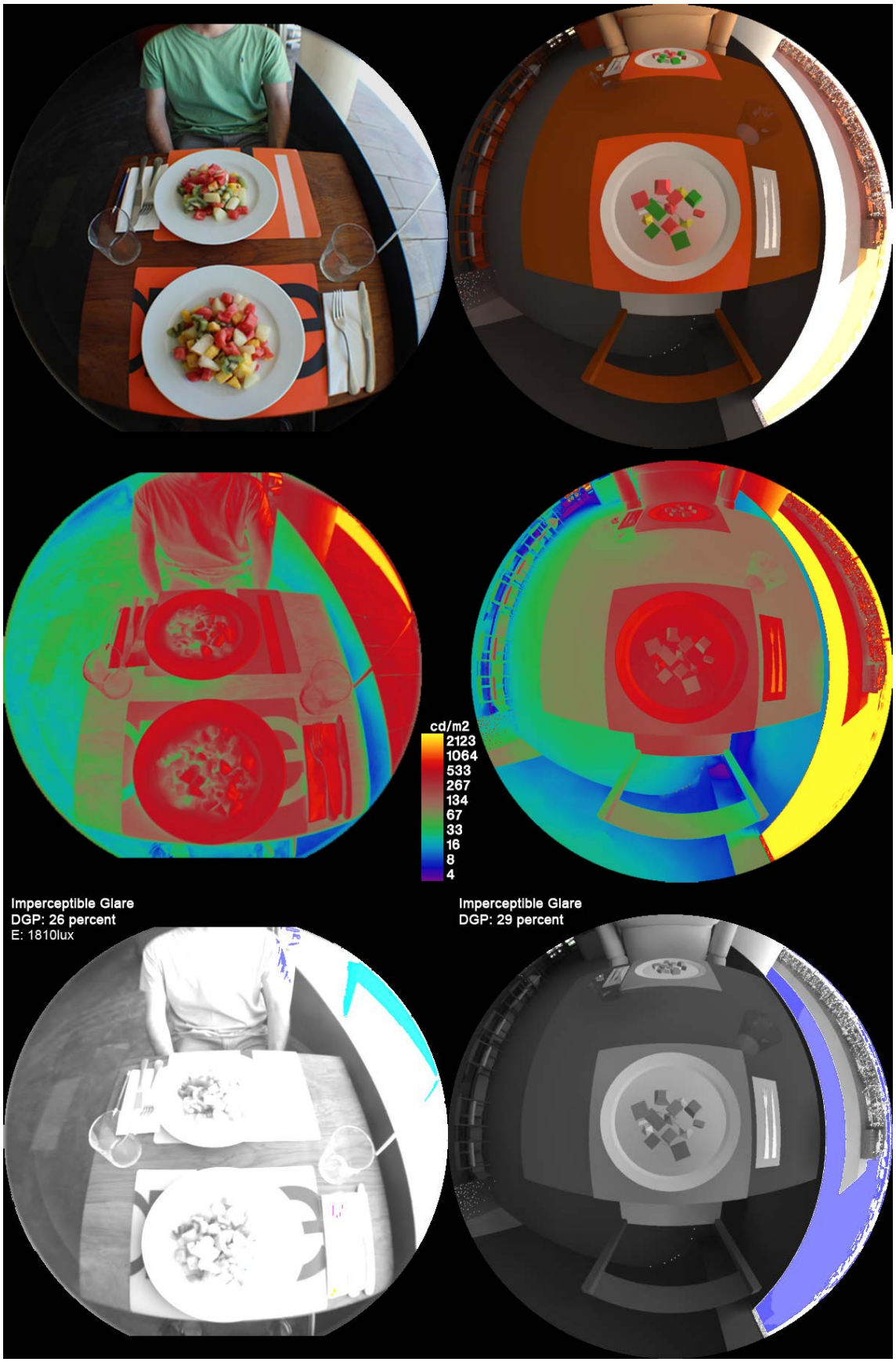

Figure 4. 9 Real and virtual Visualizations, False Colour Images and Glare Source Images with DGP index of WP1 (table) for Large Frame Window System from Restaurant 1 (Sal Café)

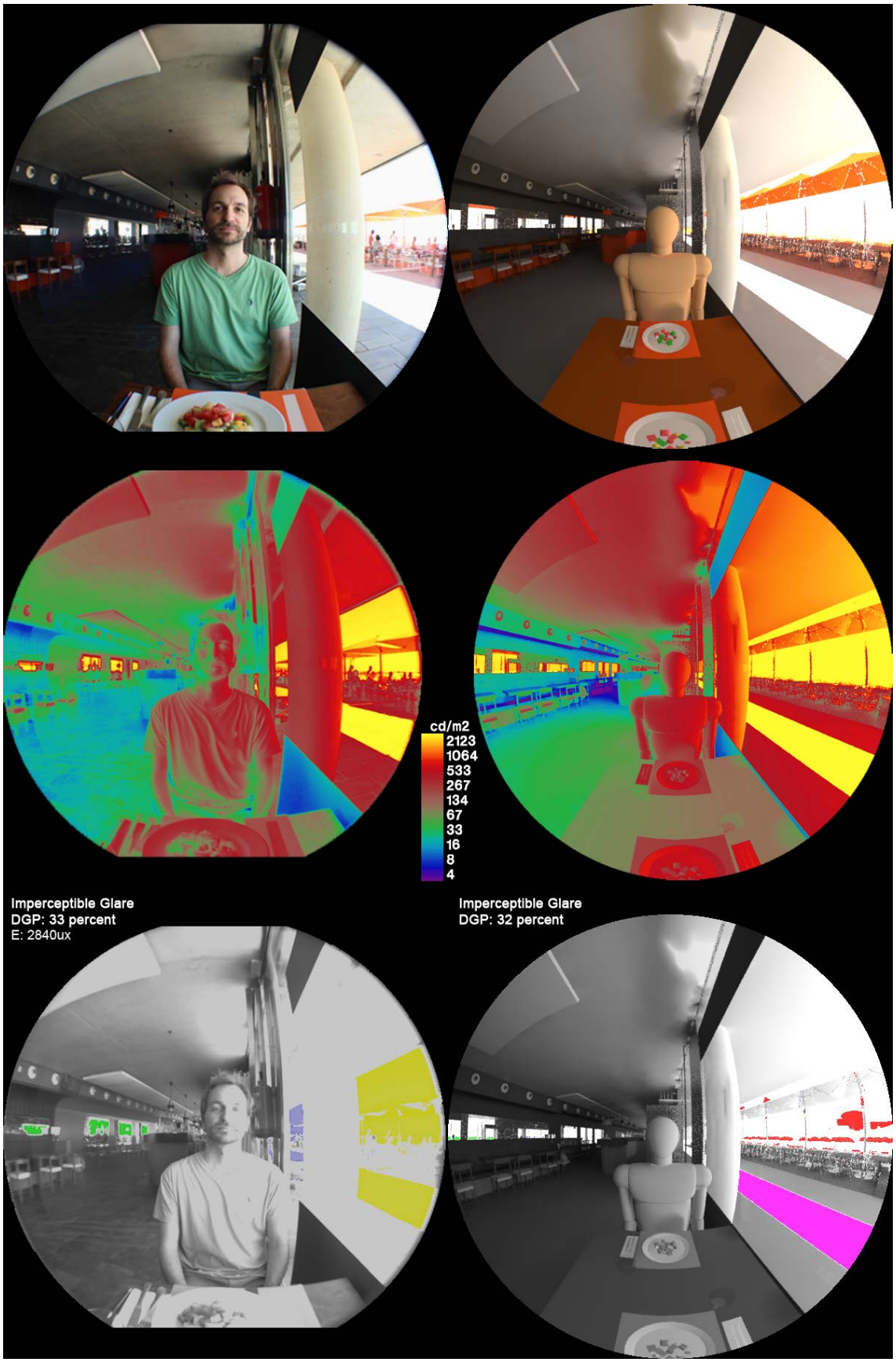

Figure 4. 10 Real and virtual Visualizations, False Colour Images and Glare Source Images with DGP index of WP2 (person) for Large Frame Window System from Restaurant 1 (Sal Café)

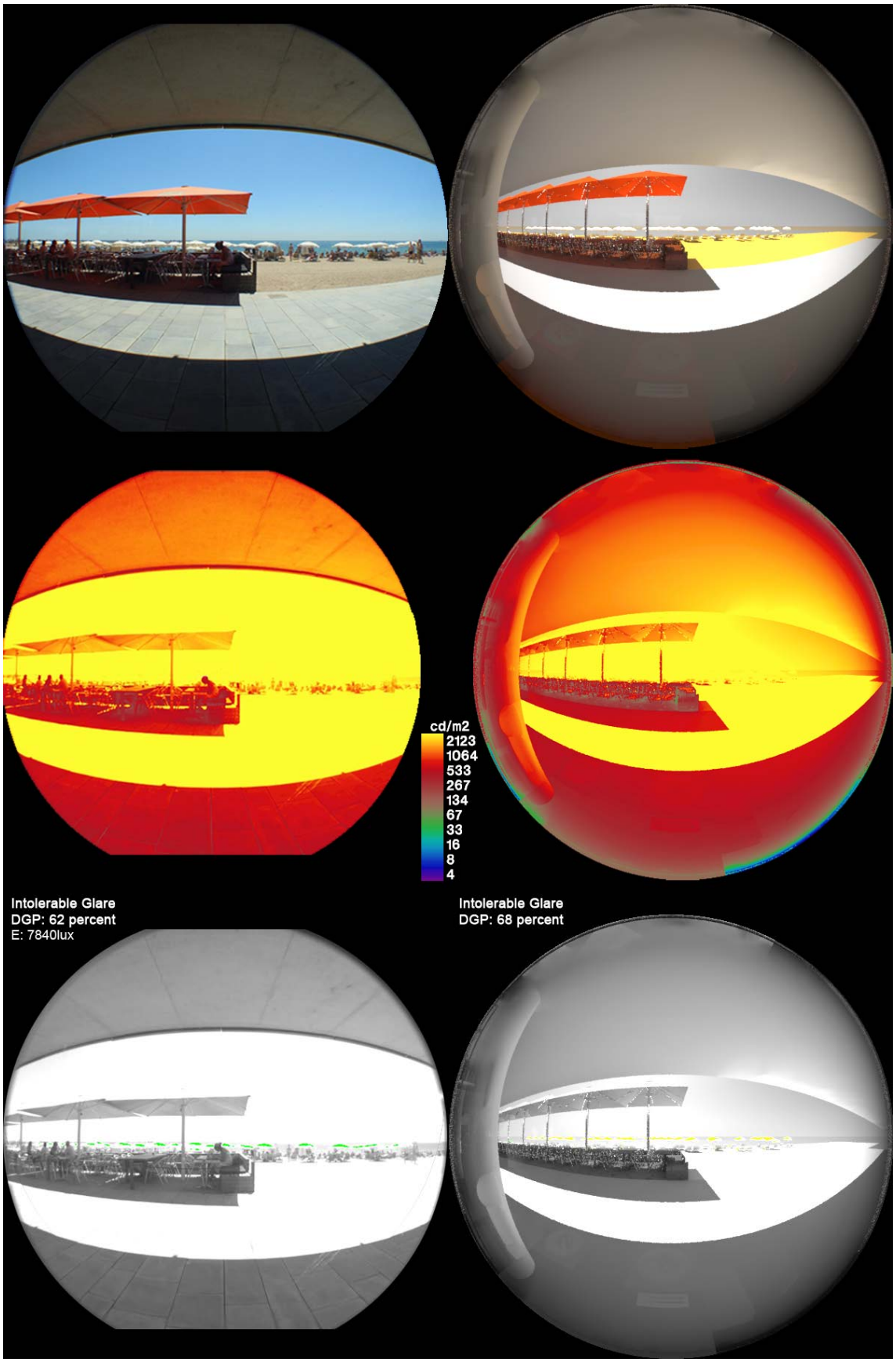

Figure 4. 11 Real and virtual Visualizations, False Colour Images and Glare Source Images with DGP index of WP3 (window) for Large Frame Window System from Restaurant 1 (Sal Café)

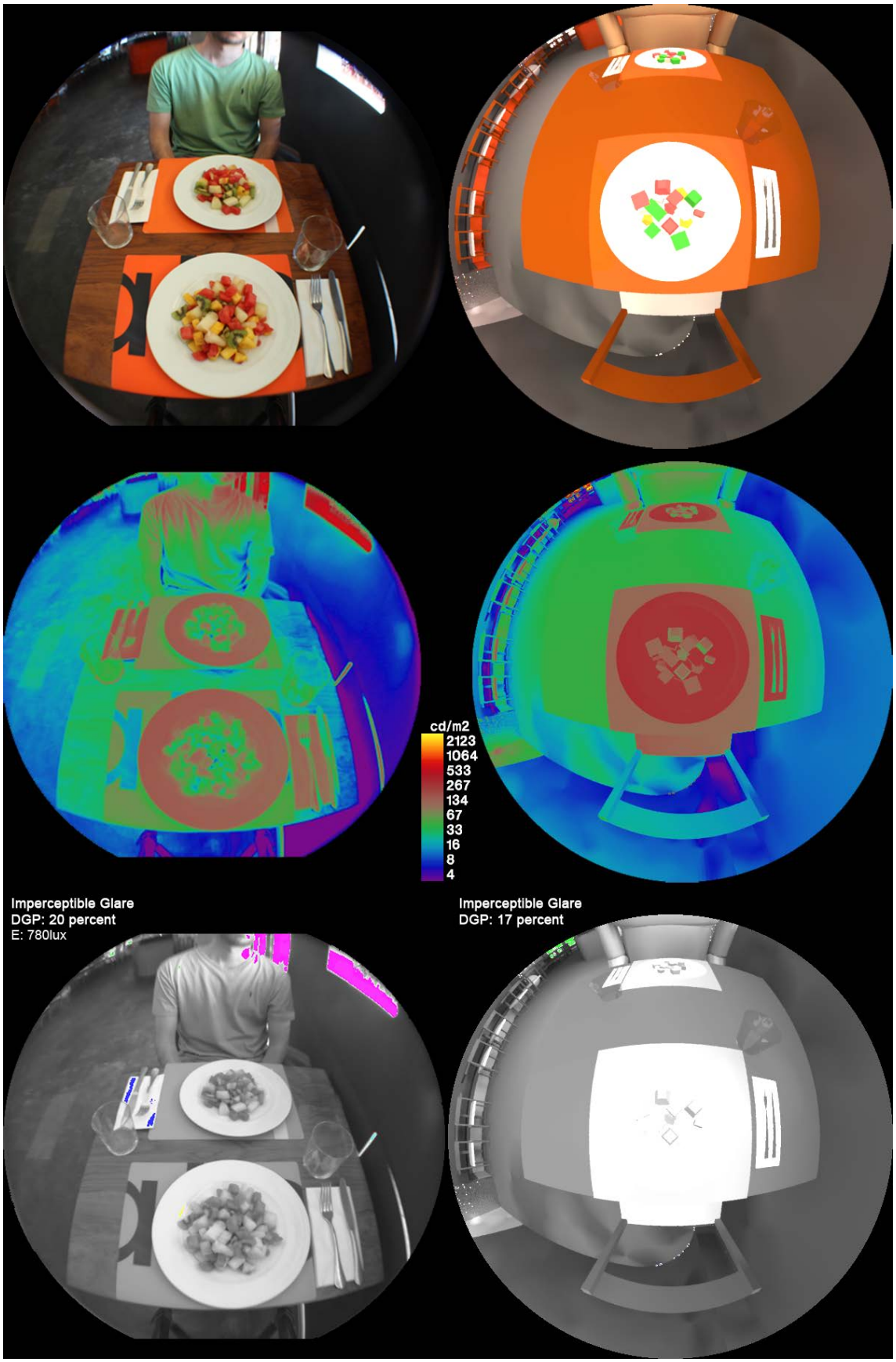

Figure 4. 12 Real and virtual Visualizations, False Colour Images and Glare Source Images with DGP index of WP1 (table) for Small Frame Window System from Restaurant 1 (Sal Café)

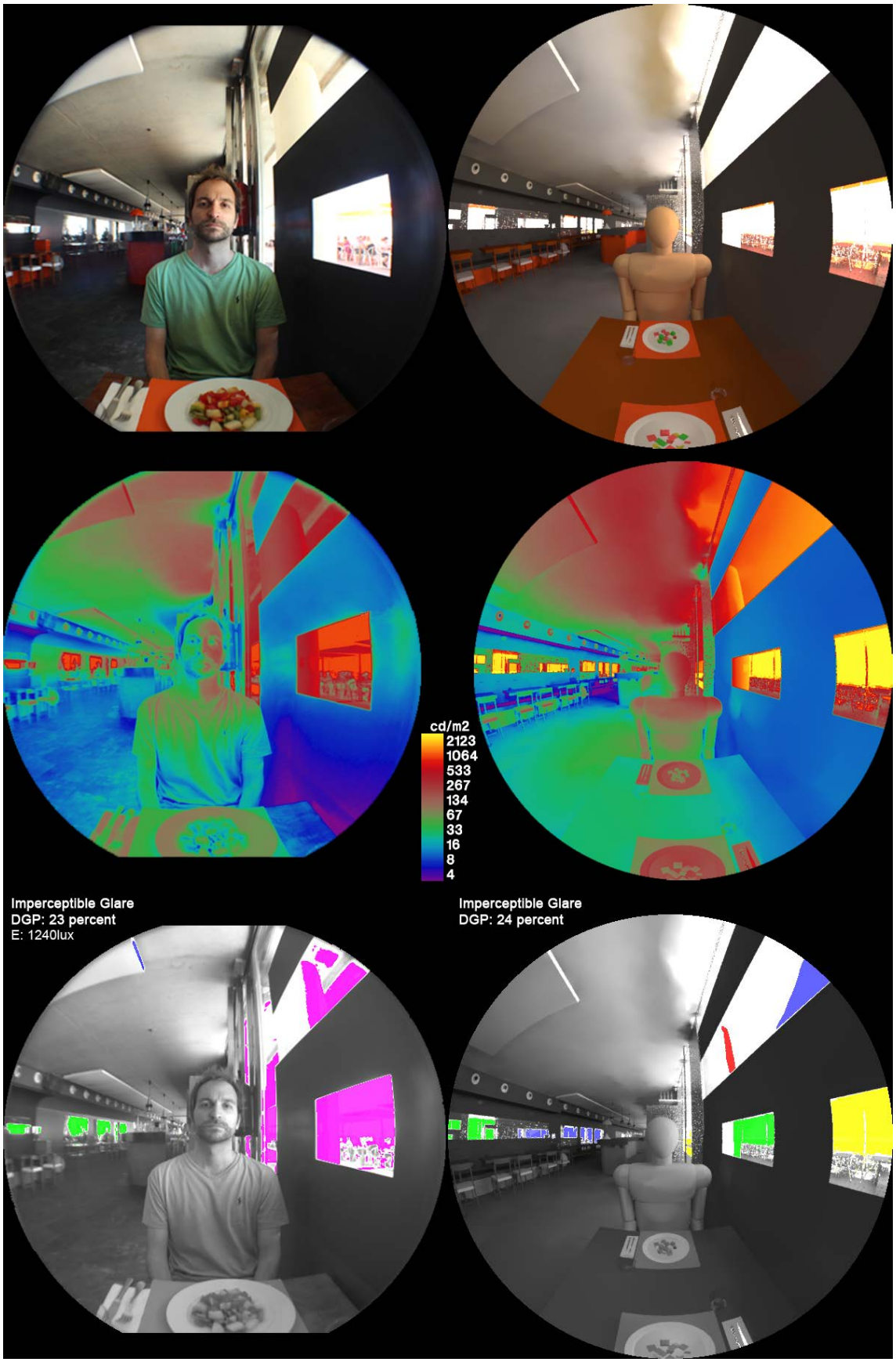

Figure 4. 13 Real and virtual Visualizations, False Colour Images and Glare Source Images with DGP index of WP2 (person) for Small Frame Window System from Restaurant 1 (Sal Café)

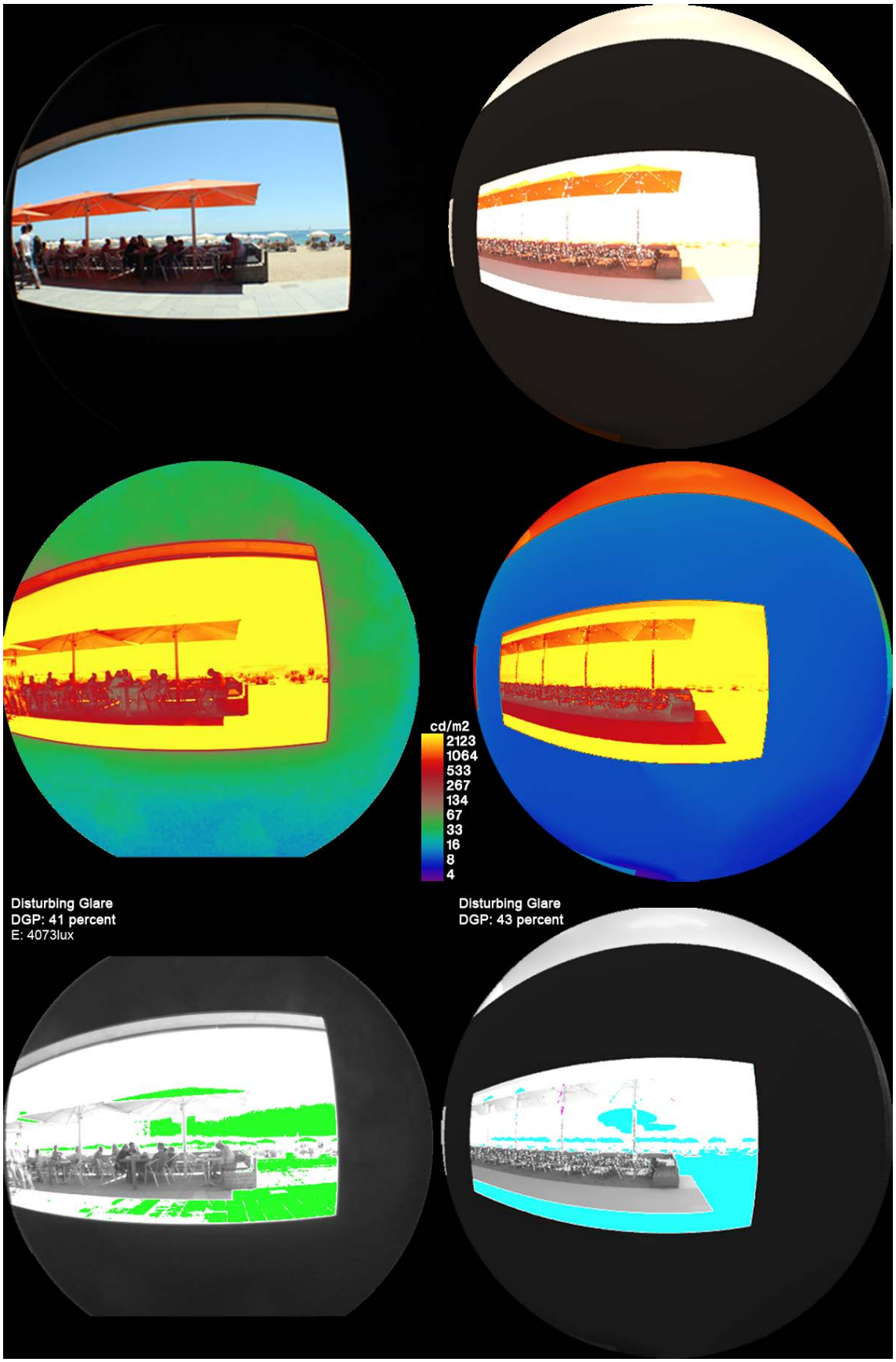

Figure 4. 14 Real and virtual Visualizations, False Colour Images and Glare Source Images with DGP index of WP3 (window) for Small Frame Window System from Restaurant 1 (Sal Café)

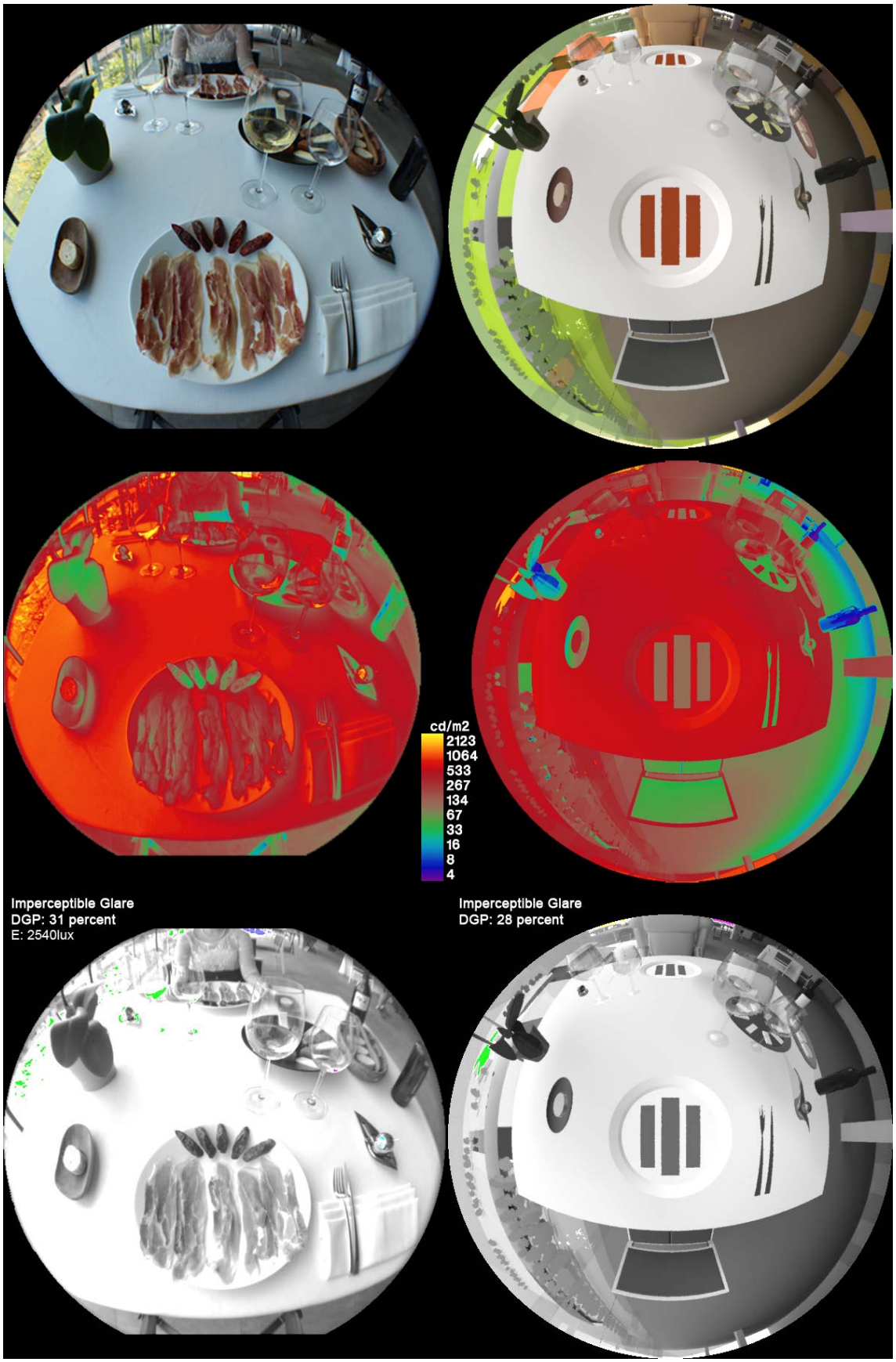

Figure 4. 15 Real and virtual Visualizations, False Colour Images and Glare Source Images with DGP index of WP1 (table) for No Frame Window System from Restaurant 2 (Azurmendi)

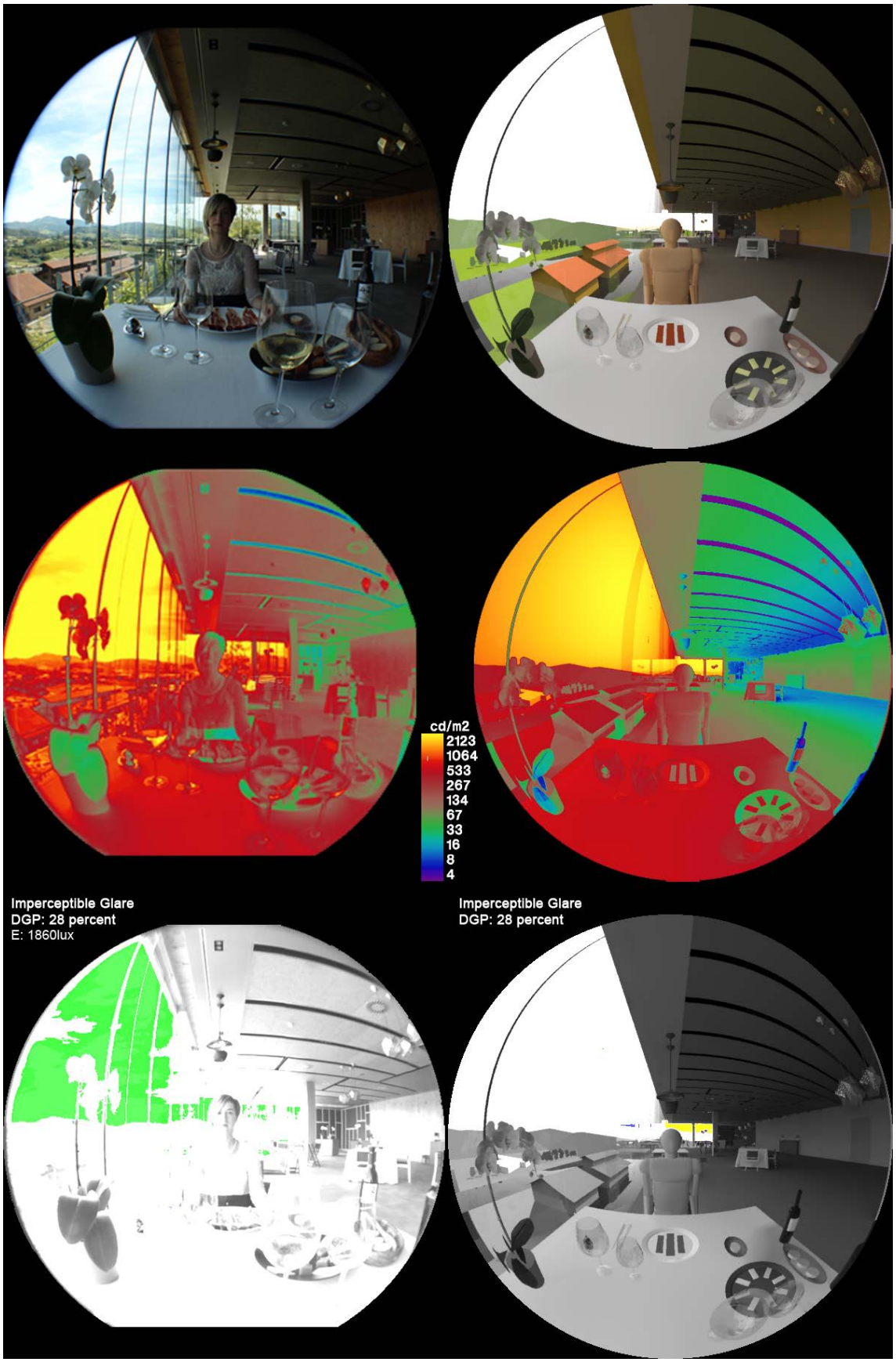

Figure 4. 16 Real and virtual Visualizations, False Colour Images and Glare Source Images with DGP index of WP2 (person) for No Frame Window System from Restaurant 2 (Azurmendi)

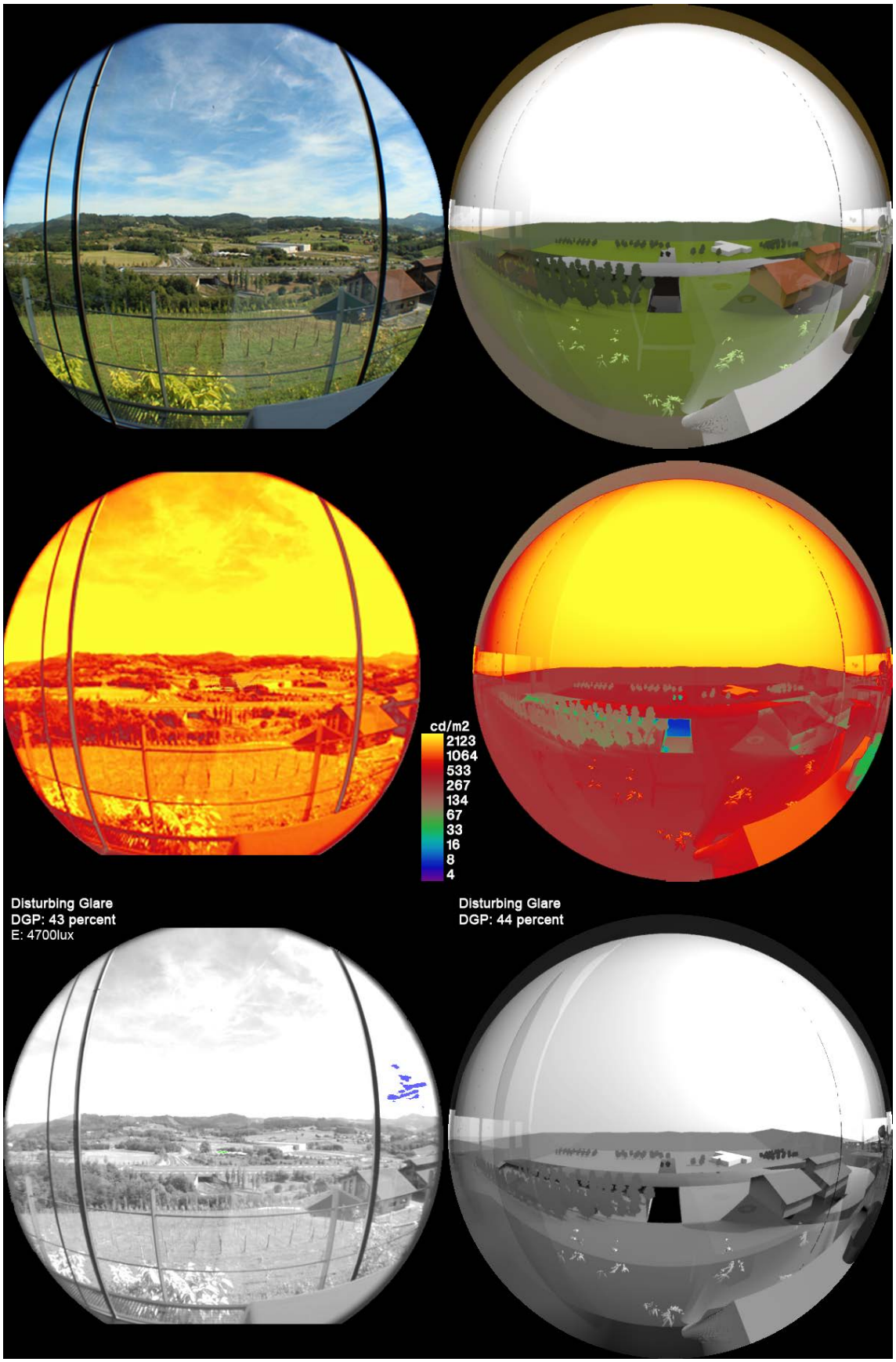

Figure 4. 17 Real and virtual Visualizations, False Colour Images and Glare Source Images with DGP index of WP3 (window) for No Frame Window System from Restaurant 2 (Azurmendi)

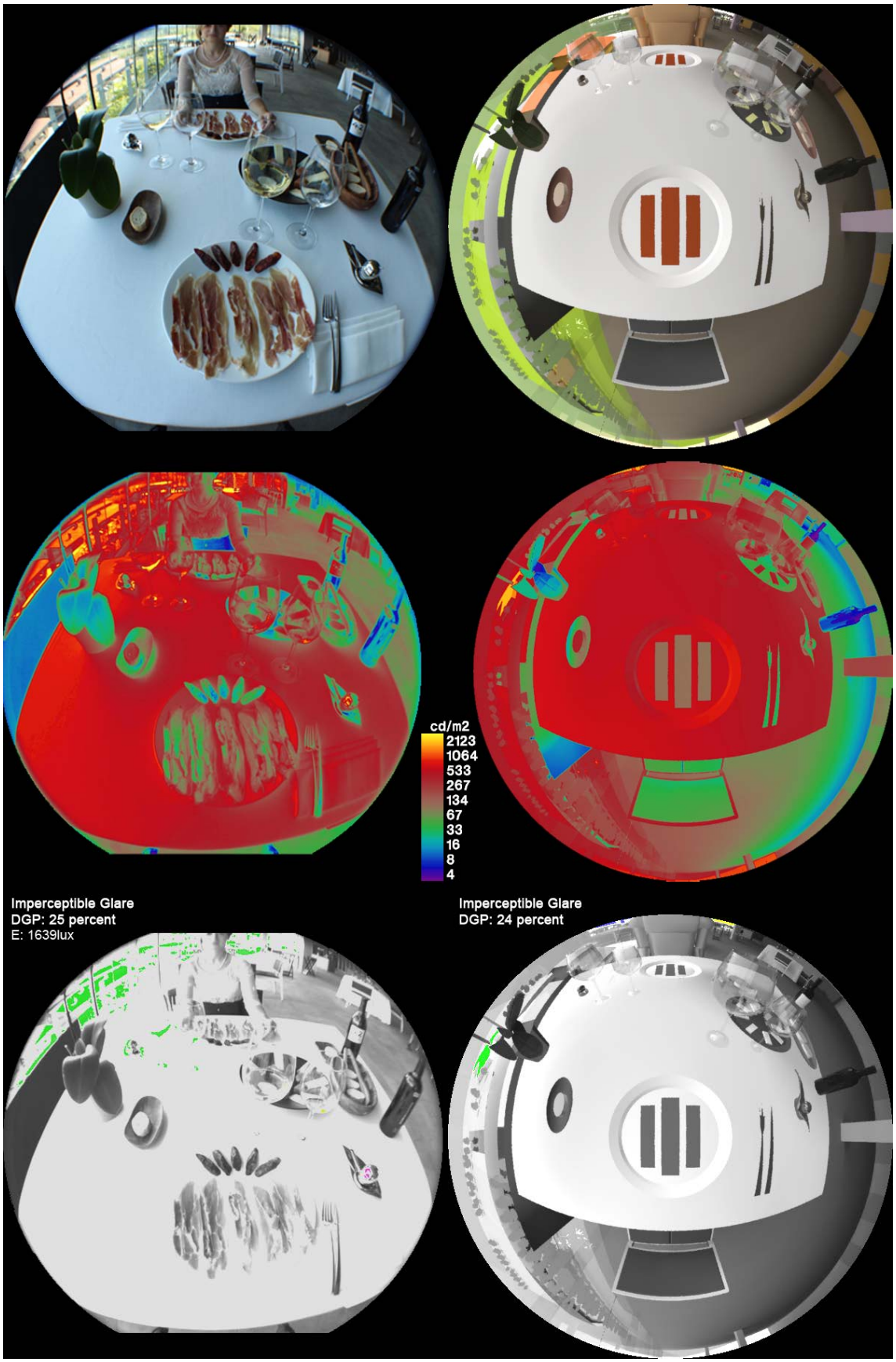

Figure 4. 18 Real and virtual Visualizations, False Colour Images and Glare Source Images with DGP index of WP1 (table) for Large Frame Window System from Restaurant 2 (Azurmendi)

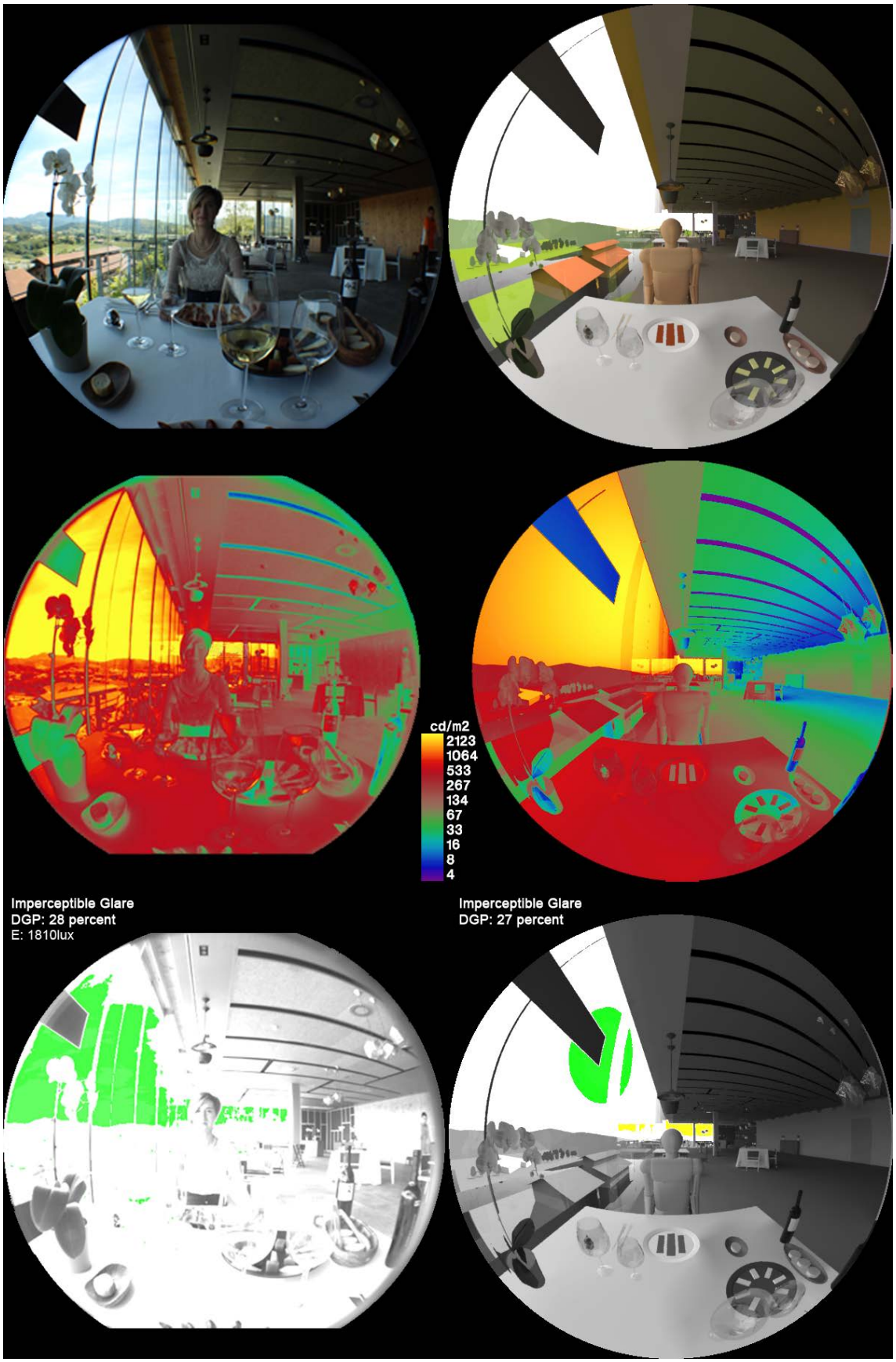

Figure 4. 19 Real and virtual Visualizations, False Colour Images and Glare Source Images with DGP index of WP2 (person) for Large Frame Window System from Restaurant 2 (Azurmendi)

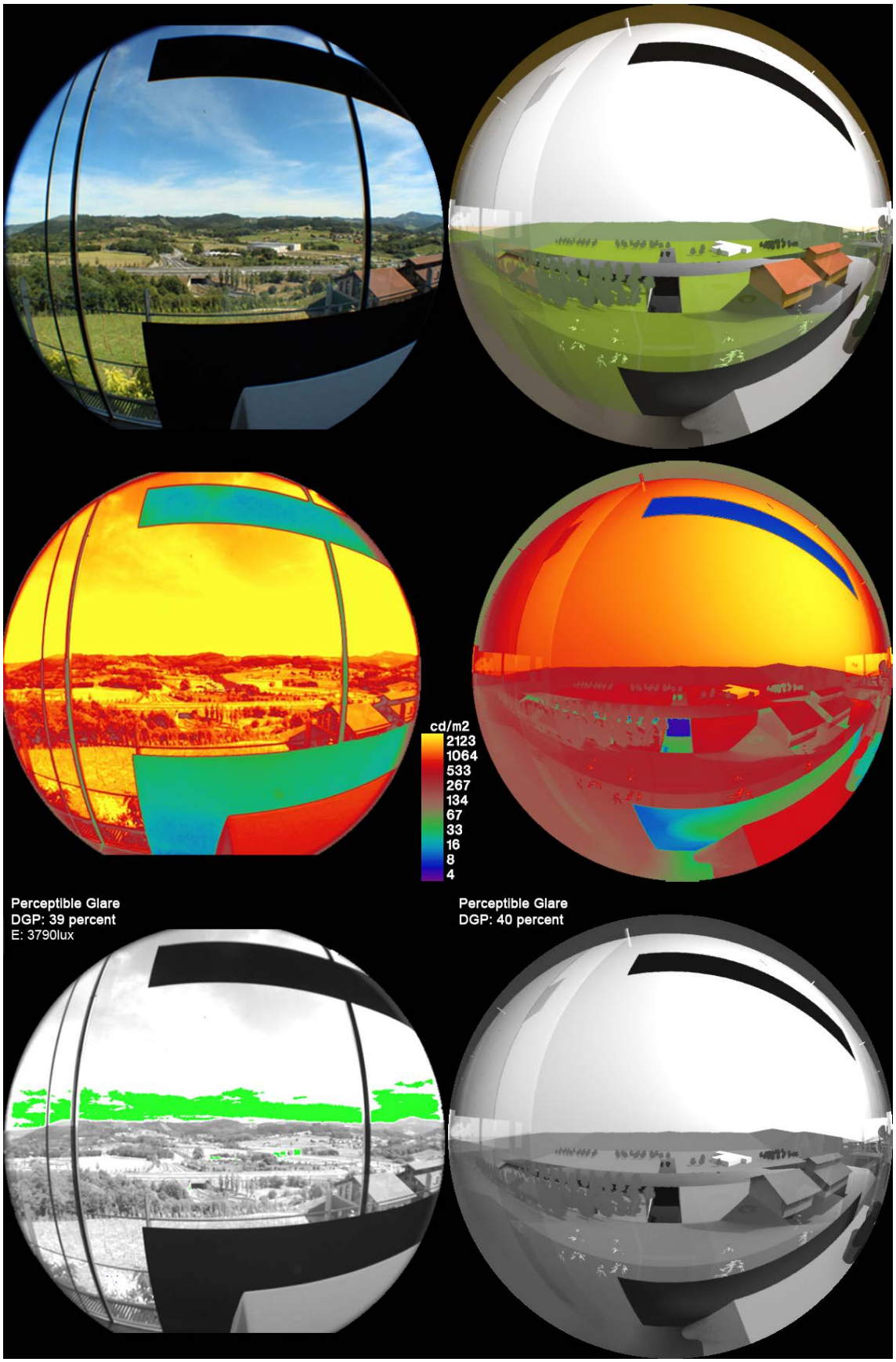

Figure 4. 20 Real and virtual Visualizations, False Colour Images and Glare Source Images with DGP index of WP3 (window) for Large Frame Window System from Restaurant 2 (Azurmendi)

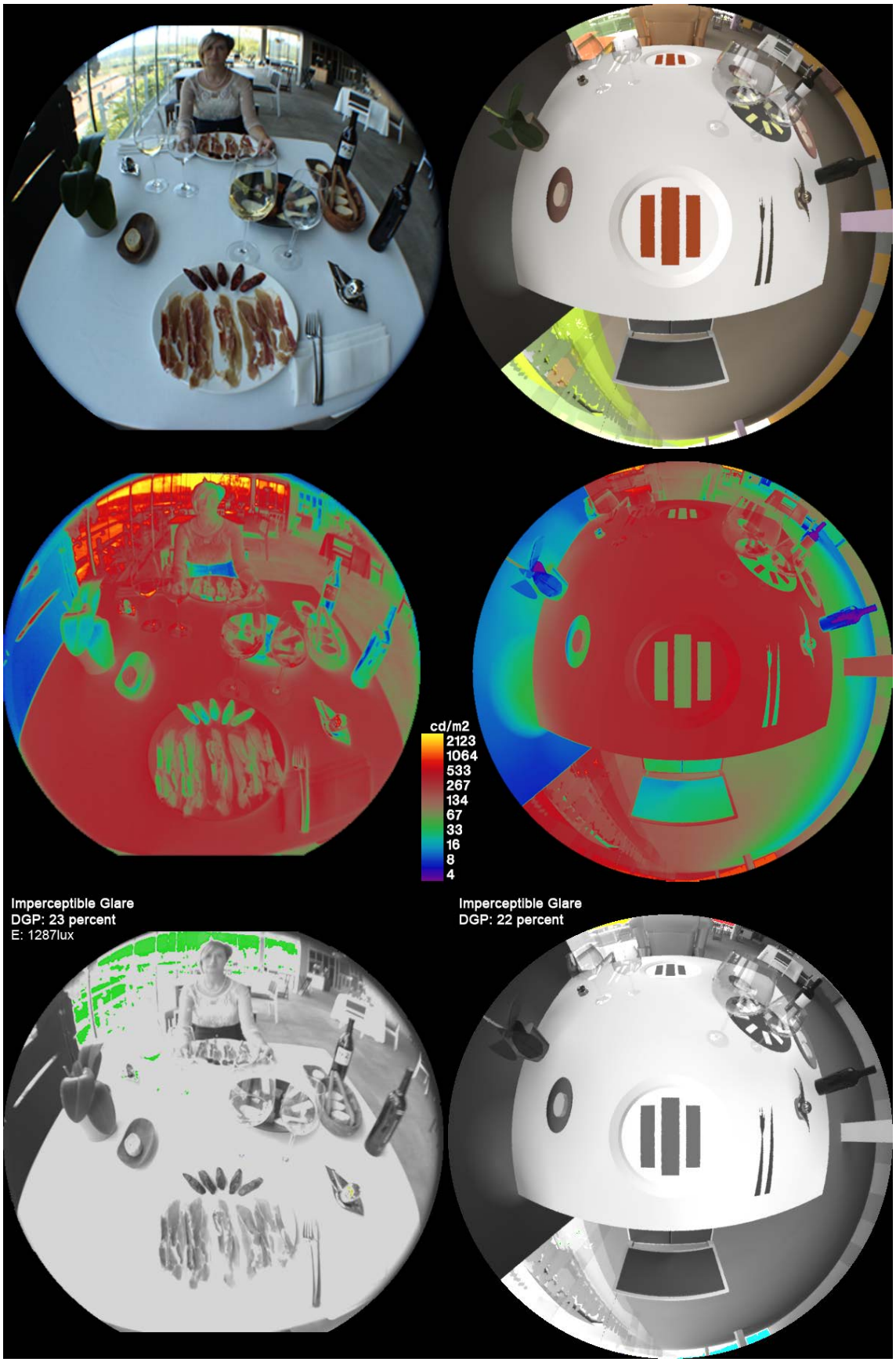

Figure 4. 21 Real and virtual Visualizations, False Colour Images and Glare Source Images with DGP index of WP1 (table) for Small Frame Window System from Restaurant 2 (Azurmendi)

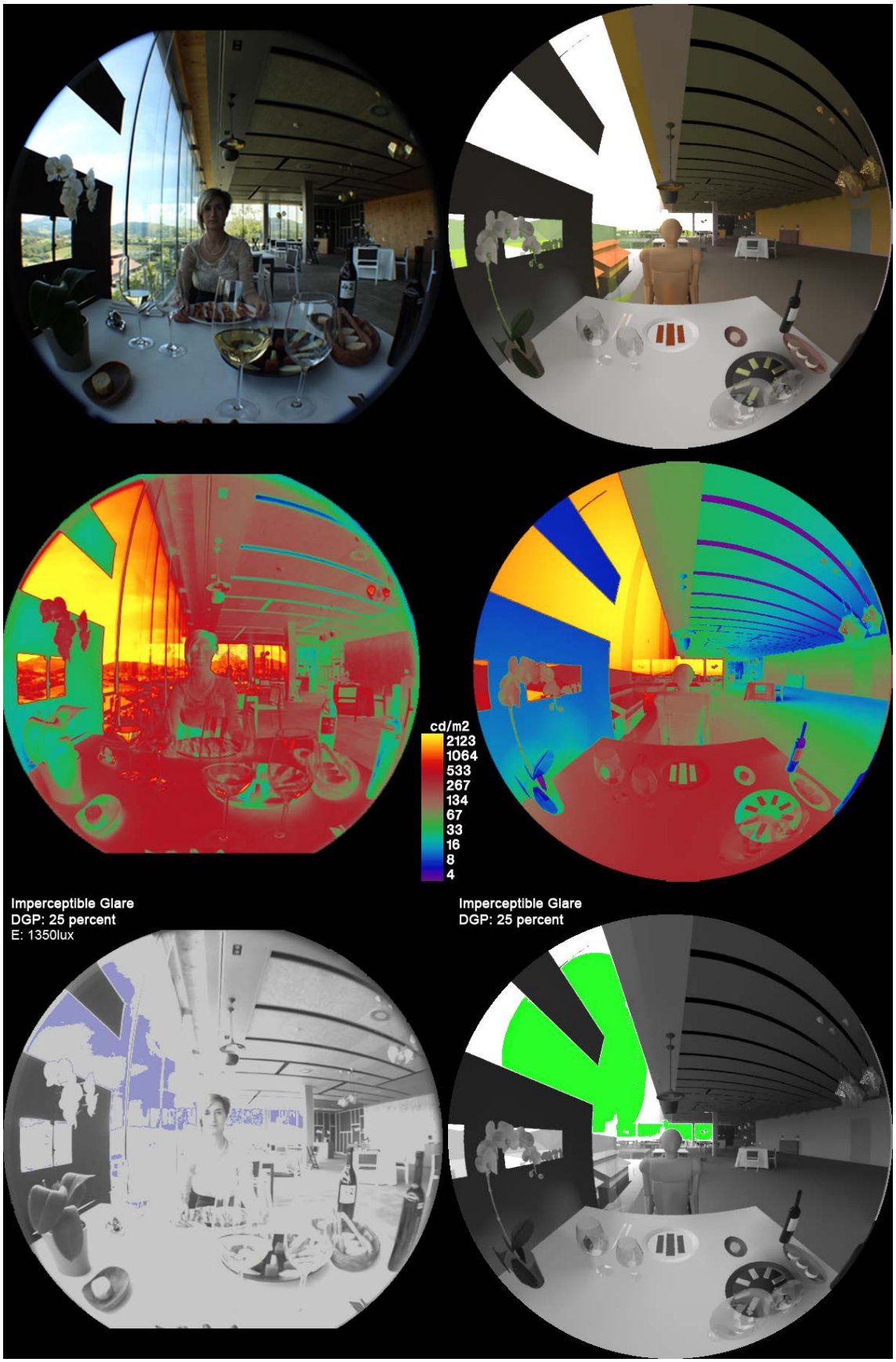

Figure 4. 22 Real and virtual Visualizations, False Colour Images and Glare Source Images with DGP index of WP2 (person) for Small Frame Window System from Restaurant 2 (Azurmendi)

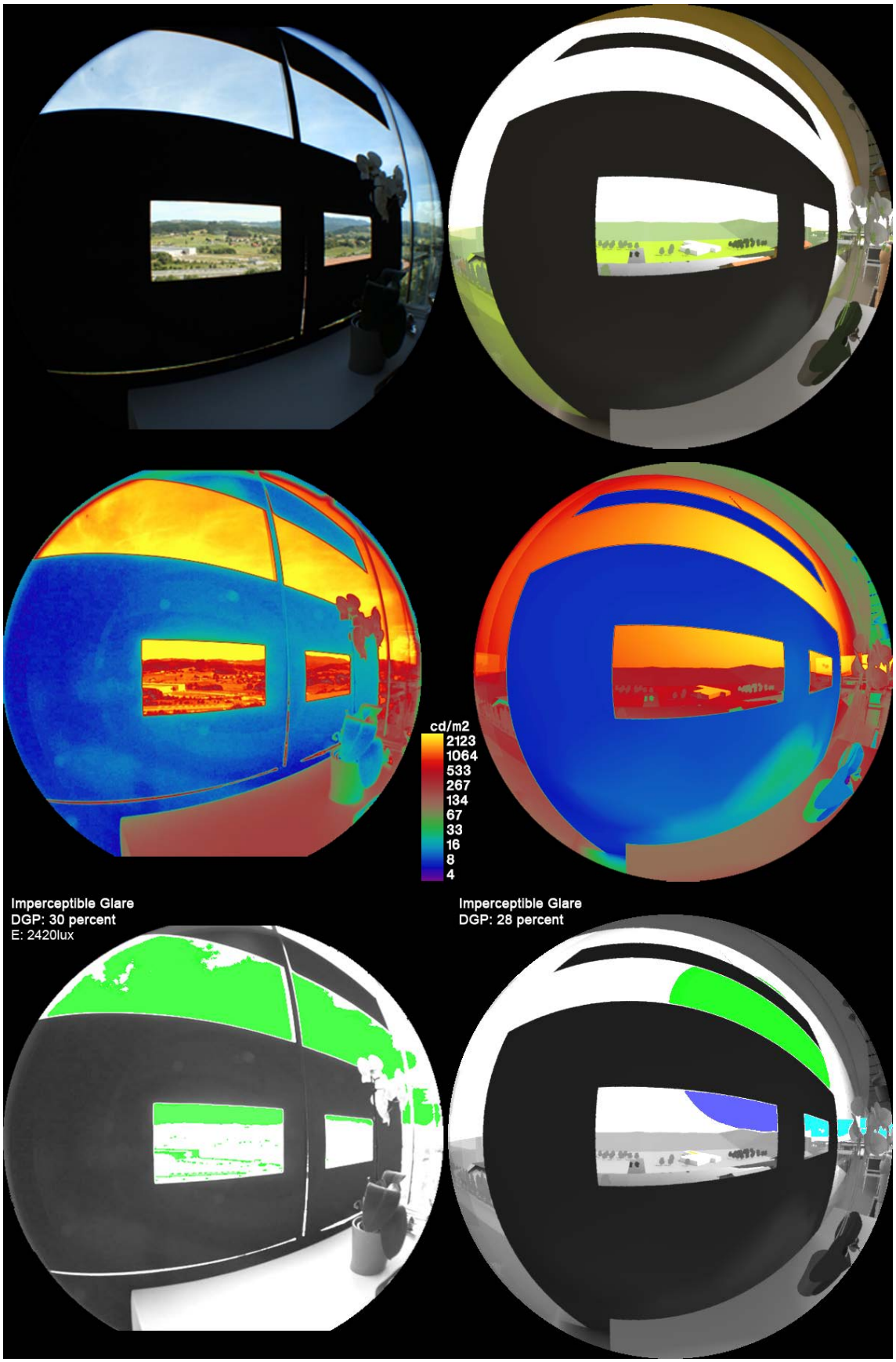

Figure 4. 23 Real and virtual Visualizations, False Colour Images and Glare Source Images with DGP index of WP3 (window) for Small Frame Window System from Restaurant 2 (Azurmendi)

The following pictures are of the virtual prototype. The location is not very important because all of pictures visualizations are under Clear Sky with Sun (CIE Clear Sky). However, the first Window Systems are tested in both, Barcelona and Bilbao. Therefore, the visualizations are at 22 of July at 11:00 Standard Time (12:00 Local Time) in Barcelona and Bilbao:

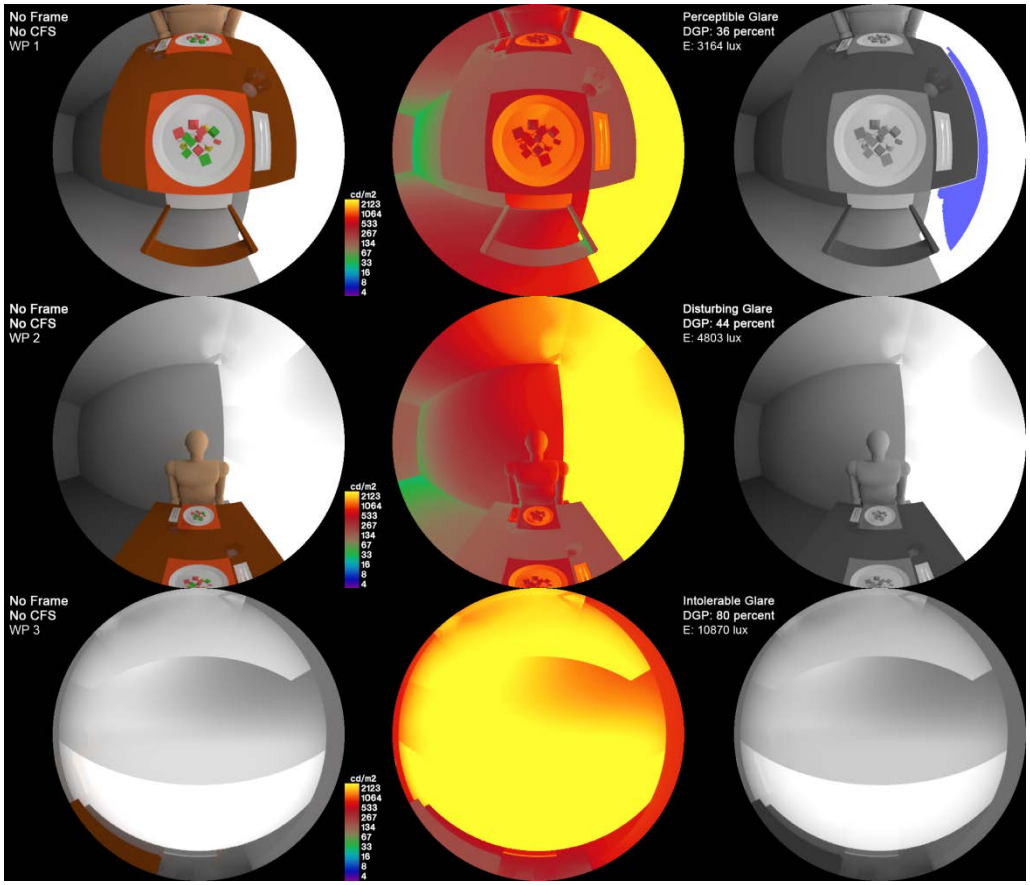

Figure 4. 24 Visualizations, False Colour Images and Glare Source Images with DGP index of WP1 (table), WP2 (person) and WP3 (window) for No Frame WS from Virtual Restaurant Prototype in Barcelona (12:00 LT, 22 July)

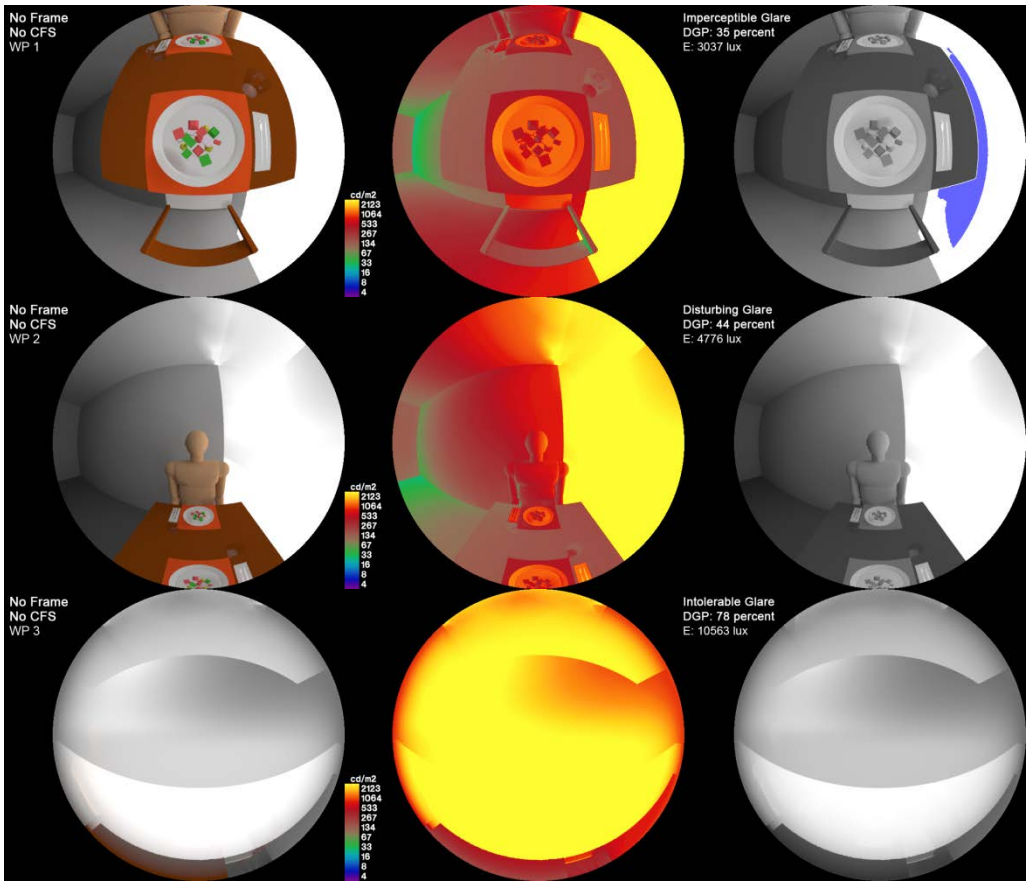

Figure 4. 25 Visualizations, False Colour Images and Glare Source Images with DGP index of WP1 (table), WP2 (person) and WP3 (window) for No Frame WS from Virtual Restaurant Prototype in Bilbao (12:00 LT, 22 July)

Virtual Restaurants	No Frame WS	No CFS	Daylight Glare Probability (DGP) index			
			WP1 (table)	WP2 (person)	WP3 (window)	**MEAN**
Barcelona			36	44	80	**53**
Bilbao			35	44	78	**52**

Table 4. 7 The DGP index results of Virtual Prototype at 12:00 local time at 22 July in Barcelona and Bilbao

In consequence there is very little difference between DGP results of Barcelona and Bilbao under the same Clear Sky with Sun (CIE Clear Sky). For the following pictures, the rendering parameters are the same as the others restaurants and the pictures are at 22 of July at 11:00 Standard Time (12:00 Local Time) in Barcelona. In addition, the virtual prototype has Light Shelf and Prismatic Film Complex Fenestration Systems in some Window Systems.

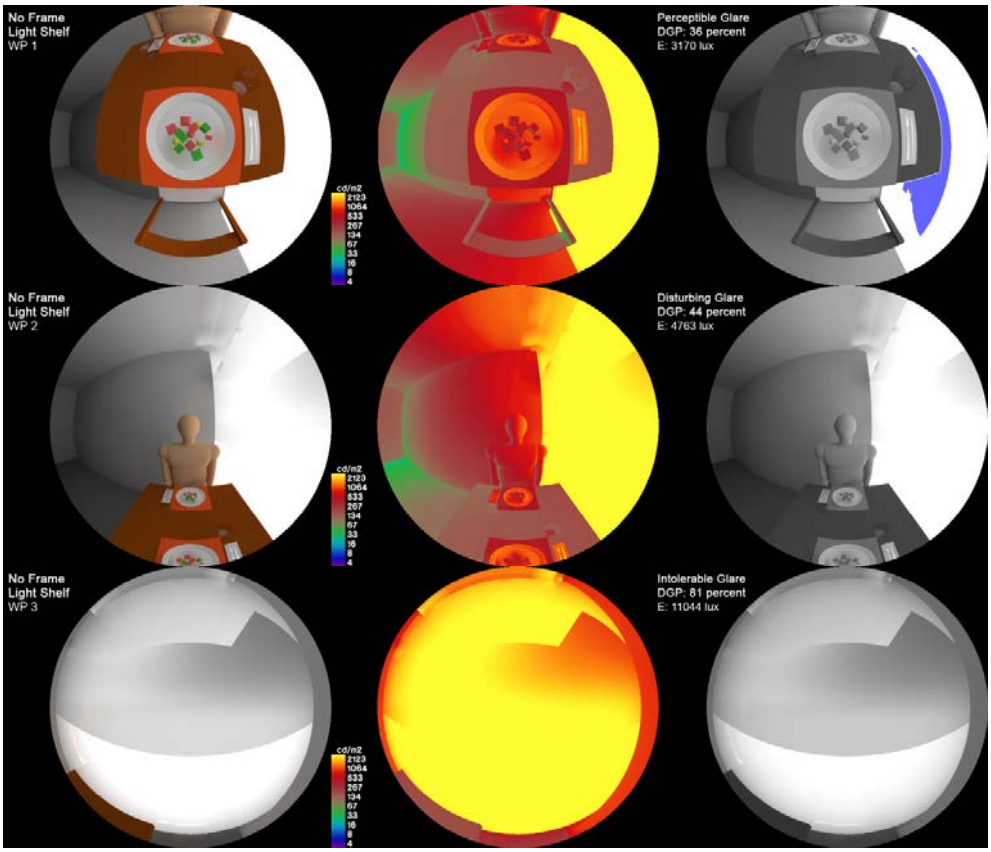

Figure 4. 26 The images of WP1, WP2 and WP3 for No Frame WS with Light Shelf CFS from VRP

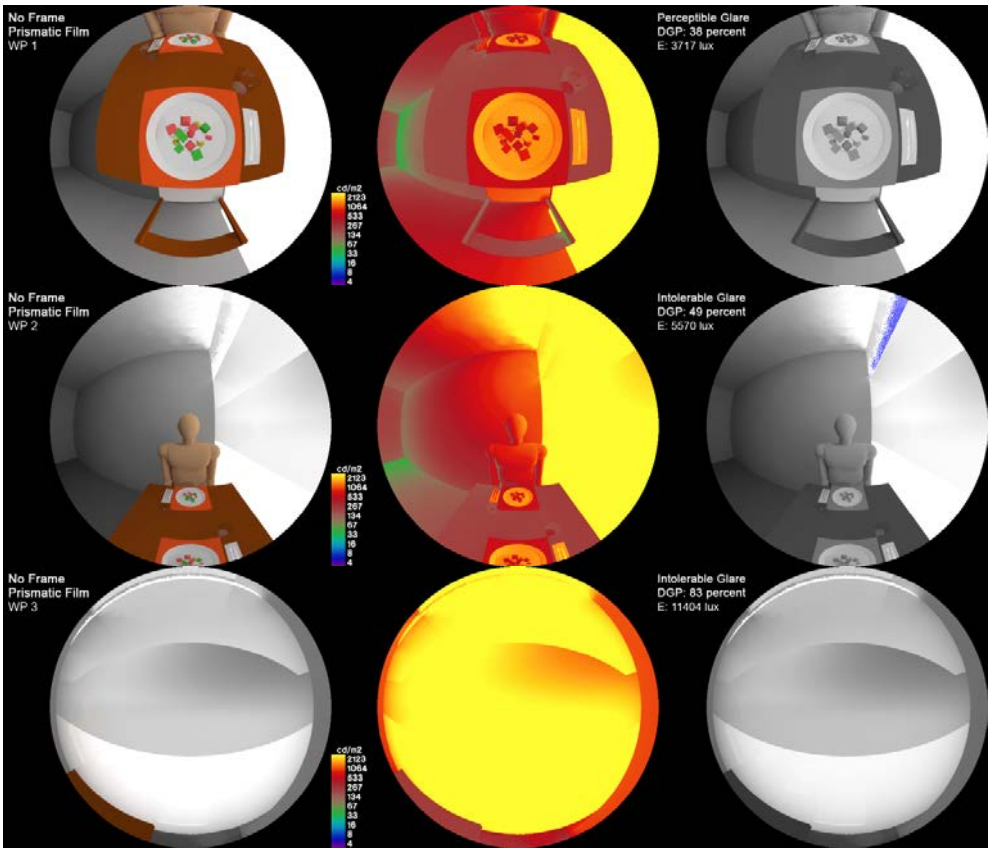

Figure 4. 27 The images of WP1, WP2 and WP3 for No Frame WS with Prismatic Film CFS from VRP

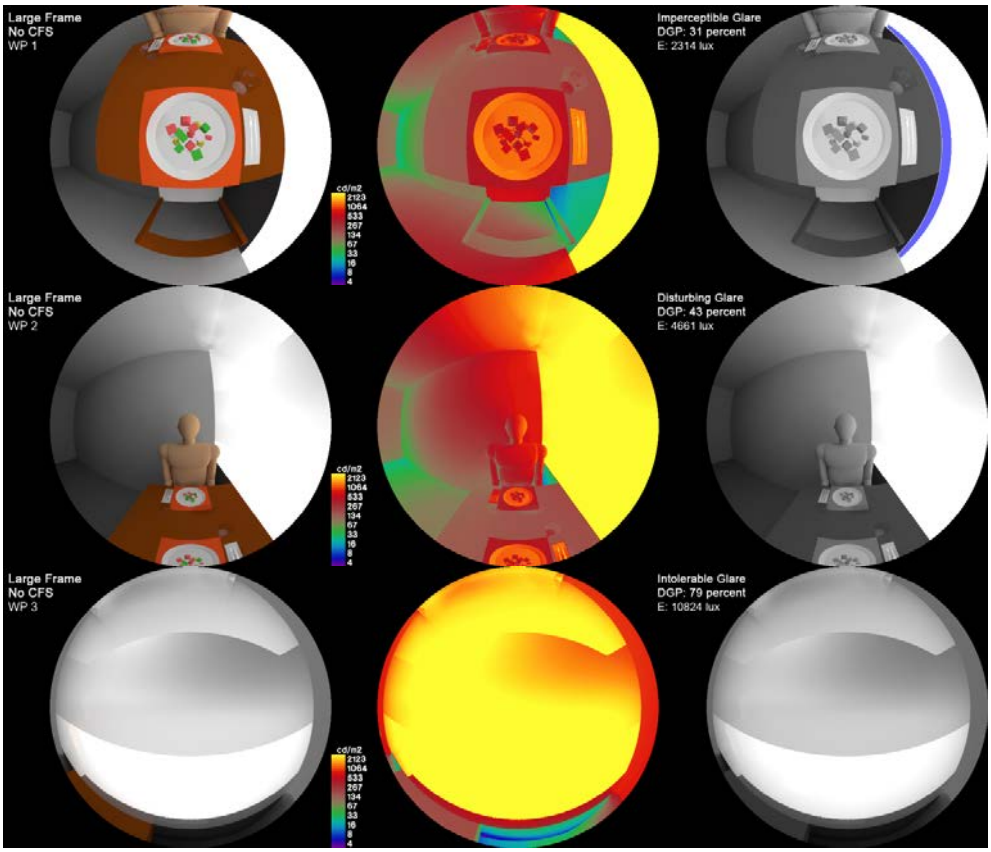

Figure 4. 28 The images of WP1, WP2 and WP3 for Large Frame WS from VRP

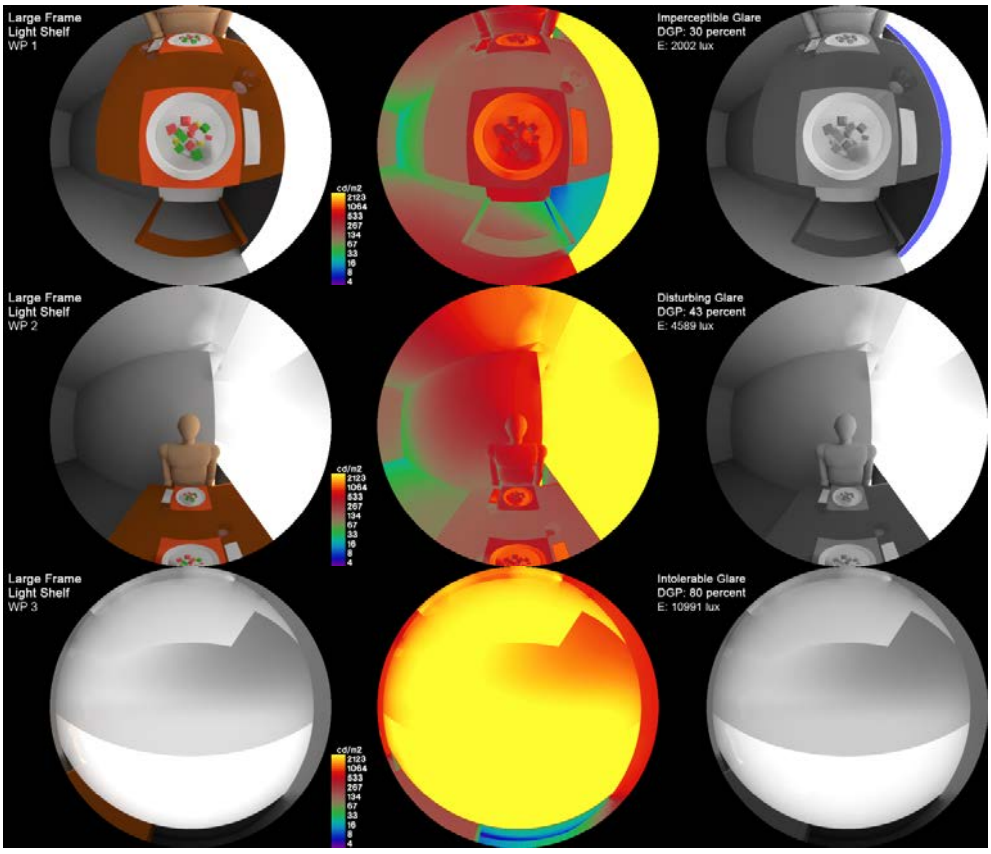

Figure 4. 29 The images of WP1, WP2 and WP3 for No Frame WS with Light Shelf CFS from VRP

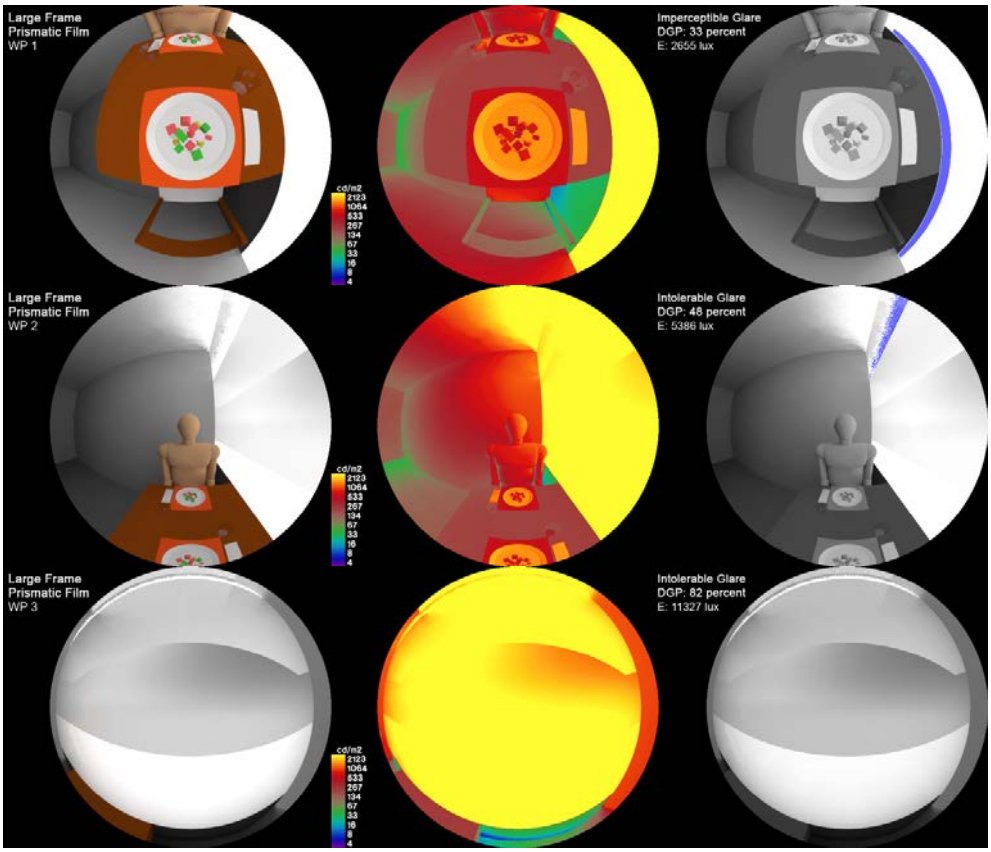

Figure 4. 30 The images of WP1, WP2 and WP3 for Large Frame WS with Prismatic Film CFS from VRP

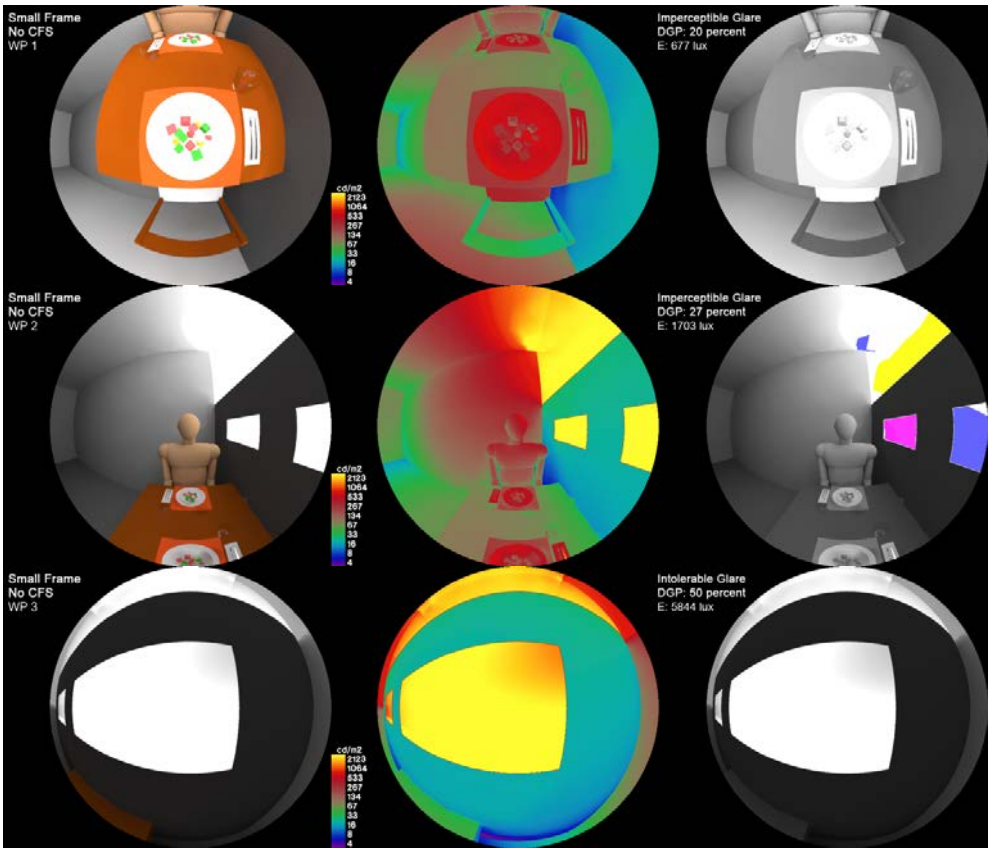

Figure 4. 31 The images of WP1, WP2 and WP3 for Small Frame WS from VRP

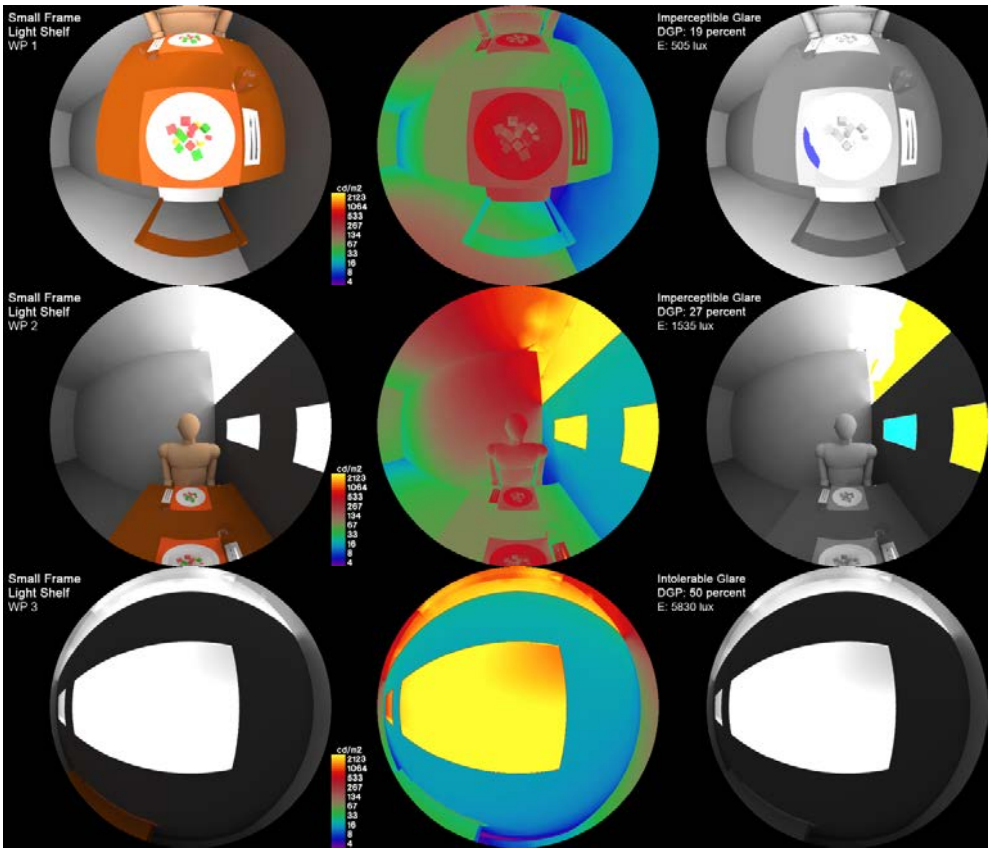

Figure 4. 32 The images of WP1, WP2 and WP3 for Small Frame WS with Light Shelf CFS from VRP

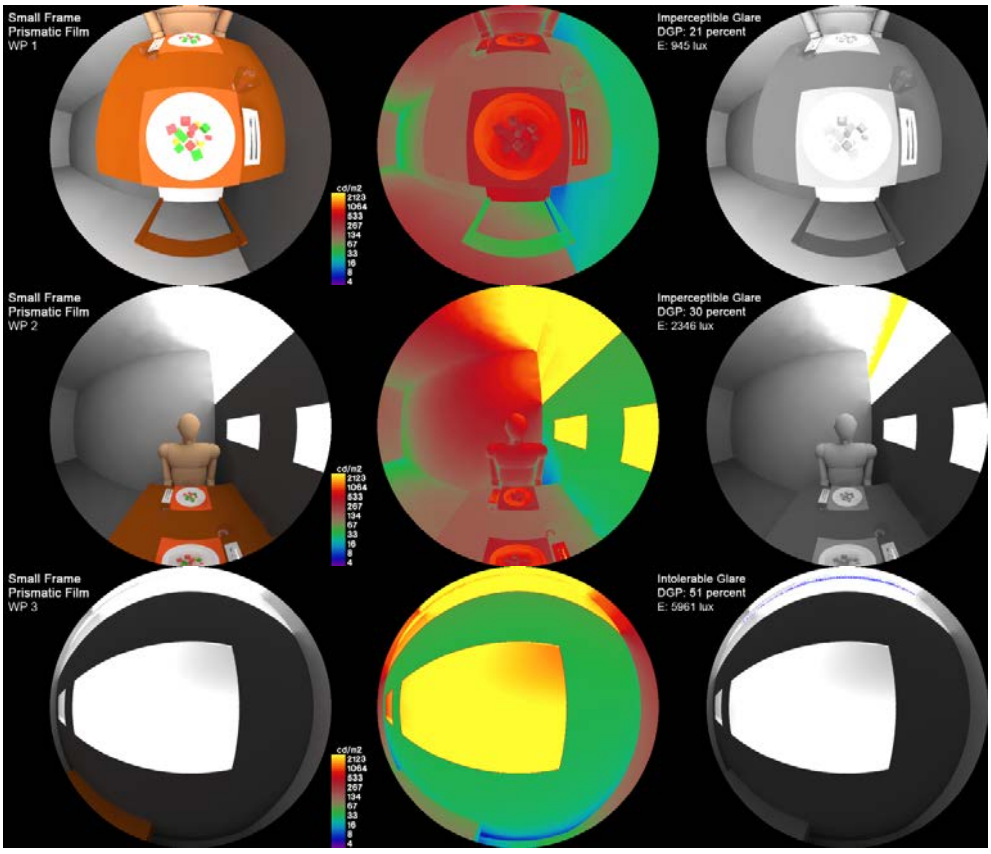

Figure 4. 33 The images of WP1, WP2 and WP3 for Small Frame WS with Prismatic Film CFS from VRP

4.3 Summary tables of Mean DGP results of each case and the relations between them

In this section the Mean DGP of each case and the relation between them are explained. In the following table the summary of all Mean DGP are described:

			Daylight Glare Probability (DGP) index			
Restaurants	Window Systems	Complex Fenestration System	WP1 (table)	WP2 (person)	WP3 (window)	**MEAN**
Restaurant 1 (Sal Café)	No Frame	-	30 E≈ 2350	36 E≈ 3500	69 E≈ 9350	**45**
	Large Frame	-	29 E≈ 1810	32 E≈ 2840	68 E≈ 7840	**43**
	Small Frame	-	17 E≈ 780	24 E≈ 1240	43 E≈ 4073	**28**
Restaurant 2 (Azurmendi)	No Frame	-	28 E≈ 2540	28 E≈ 1860	44 E≈ 4700	**33**
	Large Frame	-	24 E≈ 1639	27 E≈ 1810	40 E≈ 3790	**30**
	Small Frame	-	22 E≈ 1287	25 E≈ 1350	28 E≈ 2420	**25**
Virtual Restaurant	No Frame	No CFS	36 E= 3164	44 E= 4803	80 E= 10870	**53**
		Light Shelf	36 E= 3170	44 E= 4763	81 E= 11044	**54**
		Prismatic Film	38 E= 3717	49 E= 5570	83 E= 11404	**57**
	Large Frame	No CFS	31 E= 2314	43 E= 4661	79 E= 10824	**51**
		Light Shelf	30 E= 2002	43 E= 4589	80 E= 10991	**51**
		Prismatic Film	33 E= 2655	48 E= 5386	82 E= 11327	**54**
	Small Frame	No CFS	20 E= 677	27 E= 1703	50 E= 5844	**32**
		Light Shelf	19 E= 505	27 E= 1535	50 E= 5830	**32**
		Prismatic Film	21 E= 945	30 E= 2346	51 E= 5961	**34**

Table 4. 8 Daylight Glare Probability of each workplane, window systems and restaurant in addition to mean Daylight Glare Probability

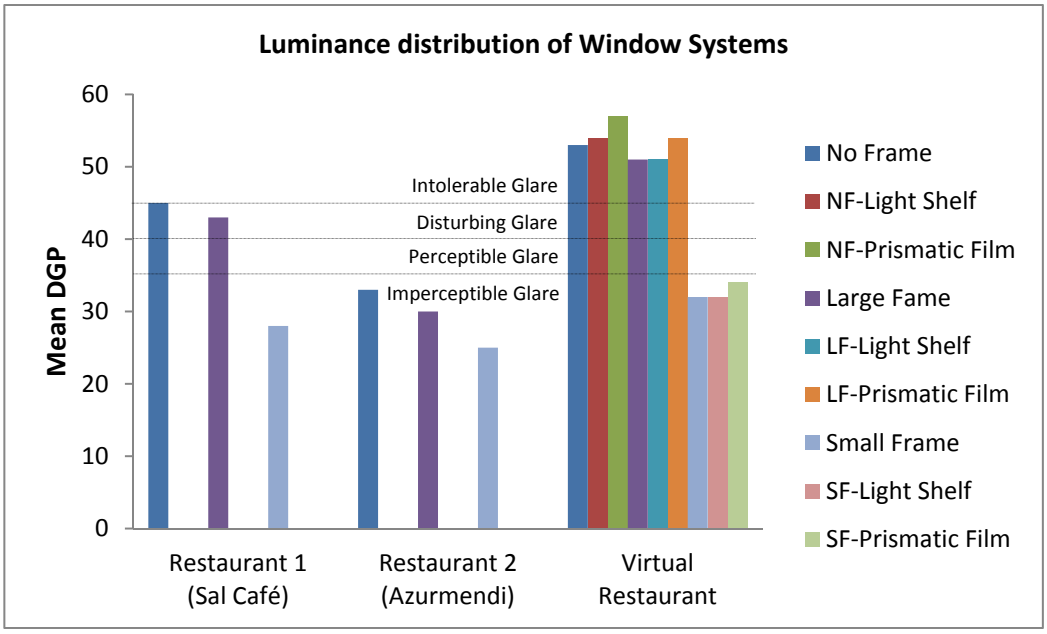

Figure 4. 34 Luminance distribution by mean Daylight Glare Probability of each window system and restaurant

In a simple way Mean DGP of three defined workplanes has been obtained to take into account in detail the different workplanes' Daylight Glare Probability. So, it has been useful in a simple way to test particular workplanes' light contribution in overall perception. Note that, the introduction of third workplane to the glare analysis could approximate to consider more the adaptation aspects, smoothing extreme situations.

According to Mean DGP results, the restaurant 1 (Sal Café) in Mediterranean climate with Clear Sky with Sun (CIE Clear Sky) and with Southeast orientation, in the No Frame Window System that it means fully Glazed Façade there is Disturbing glare probability (Mean DGP 45%), on the border with Intolerable glare probability. In the Large Frame, there is a little less glare probability but it keeps having Disturbing glare probability (Mean DGP 43%). In the Small Frame, the glare probability decreases notably up to Impercptible glare probability (Mean DGP 28%).

The restaurant 2 (Azurmendi) in Atlantic climate with Intermediante Sky with Sun and with North orientation, in the three Window Systems barely there is glare probability with Imperceptible. In the Small Frame there is the least glare probability (Mean DGP 25%), in the Large Frame there is a lilttle more (Mean DGP 30%) and in No Frame Window Systems on border to perceive something (Mean DGP 33%).

The virtual restaurant with Clear Sky with Sun (CIE Clear Sky) and with South orientation, in No Frame and Large Frame there is Intolerable glare probability, although in Large Frame there is a little less (Mean DGP 51%,53%). However, in Small Frame Window System the glare probability decreases notably up to Imperceptible glare probability (Mean DGP 32%). Regarding Complex Fenestartion Systems, Light Shelf increases a little in No Frame Window System because the bottom part of the shelf reflect the light coming from the paviment. Nerverthenles, in Large and Small Frame the light coming from paviment is bloqued the glare porbability decrease a llittle. The Prismatic Film Complex Fenestration System tends to increase the glare probability a little noticing more in No Frame Window System owing to global illuminance data but the Small Frame Window System even has higher luminace data in CFS because it has not top overhang. Anyway, the variation on glare perception with Complex Fenestartion System is minimun, in any case the perception state is changed.

In the following tables are summed up the relation between Workplane's DGP and the Mean and the relation between the Window Systems and Complex Fenestration Systems:

	Restaurant 1 (Sal Café)			Restaurant 2 (Sal Café)			Virtual Restaurant Prototype									$\overline{a}$
	NF	LF	SF	NF	LF	SF	No Frame			Large Frame			Small Frame			
	-	-	-	-	-	-	-	LS	PF	-	LS	PF	-	LS	PF	
$\frac{DGP_{Mean}}{DGP_{WP1}}$	1.50	1.48	1.65	1.18	1.25	1.14	1.47	1.50	1.50	1.64	1.70	1.64	1.60	1.68	1.62	**1.50**
$\frac{DGP_{Mean}}{DGP_{WP2}}$	1.25	1.34	1.17	1.18	1.11	1	1.20	1.23	1.16	1.19	1.19	1.12	1.18	1.18	1.13	**1.17**
$\frac{DGP_{Mean}}{DGP_{WP3}}$	0.65	0.63	0.65	0.75	0.75	0.89	0.66	0.67	0.69	0.64	0.64	0.66	0.64	0.64	0.67	**0.68**

Table 4. 9 Relation between each workplane (table, person and window) Daylight Glare Probability and mean Daylight Glare Probability

A posible *a* factor could refer to the adpatation of different target in a visual field. It could help to include diffent workplanes of a visual field, smoothing the extreme values but adding its contribution in the overall visual field. It seems that WP1 DGP is approximately 50% less than Mean DGP, when the pavement reflection is high it tends to be lower. WP2 DGP is approximately 20% less than Mean DGP, when there is lighter

or CFS with high reflection it tends to be higher, so the decrease is less. WP3 DGP is approximately 30% more than Mean DGP, when there are many luminous surfaces the increment tends to be higher. Therefore, the possible *a* factor could be summed up as:

$a_{maximun}$ $(a_{ma}) \approx 1.5$

a_{medium} $(a_{me}) \approx 1.20$

$a_{minimun}$ $(a_{mi}) \approx 0.7$

In the following table the realtion of DGP of studied No Frame, Large and Small Frame with Clear Sky are presented:

	$DGP_{No\ Frame}$	$DGP_{Large\ Frame}$	$DGP_{Small\ Frame}$	$\frac{DGP_{NF}}{DGP_{LF}}$	$\frac{DGP_{NF}}{DGP_{SF}}$	$\frac{DGP_{LF}}{DGP_{SF}}$
Restaurant 1 (Sal Café)	45	43	28	1.05	1.61	1.54
Restaurant 2 (Azurmendi)	33	30	25	1.10	1.32	1.2
Virtual Restaurant	53	51	32	1.04	1.66	1.59
Mean	**≈ 44 Disturbing**	**≈ 41 Disturbing**	**≈ 28 Imperceptible**	**1.06**	**1.53**	**1.44**

Table 4. 10 Mean Daylight Glare Probability between all restaurants and relations between the three window systems without Complex Fenestration Systems

The worst case of reference Clear Sky and South orientation is the Restaurant 2 (Azurmendi) because it has Intermediate Sky and North orientation. Therefore, No Frame case mean DGP is between Disturbing and Intolerable glare probability as well as Large Frame case. However, Small Frame case DGP is Imperceptible glare probability. In addition, according to DGP relation, between No Frame and Large Frame there is not almost difference and No Frame or Large Frame and Small Frame between there is approximately 1.5 (half more) of difference changing the visual glare perception from Disturbing/Intolerable to Imperceptible.

Note that to have a reference, the DGP of Uniform Sky of 22 of July at 11:00 Standard Time is tested, although this sky is for cloudy sky. The day and time is important because the Uniform Sky is built with Horizontal Illuminance data and the location as well, so *a* factor of No Frame, No CFS and No masks Window System's DGP in Barcelona and in Bilbao is checked as in the following (The images of each case there are all together at the end of the chapter):

	DGP Uniform Sky, No Frame, No CFS, No Masks (22 July at 11:00)				$\frac{DGP_{Mean}}{DGP_{WP1}}$	$\frac{DGP_{Mean}}{DGP_{WP2}}$	$\frac{DGP_{Mean}}{DGP_{WP3}}$
	WP1	WP2	WP3	Mean			
Barcelona	29 E=2278	39 E=3876	69 E=9063	46	1.59	1.18	0.67
Bilbao	29 E=2140	38 E=3684	67 E=8626	45	1.55	1.18	0.67

Table 4. 11 The mean Daylight Glare Probability of Virtual Restaurant Prototype and relation between it and each workplane DGP with Uniform Sky at 22 July and 11:00 standard time in Barcelona and Bilbao

	DGP Uniform Sky, No Frame, No CFS, No Masks (December 21 at 11:00)				$\frac{DGP_{Mean}}{DGP_{WP1}}$	$\frac{DGP_{Mean}}{DGP_{WP2}}$	$\frac{DGP_{Mean}}{DGP_{WP3}}$
	WP1	WP2	WP3	Mean			
Barcelona	22 E=968	26 E=1662	39 E=3891	29	1.32	1.11	0.74
Bilbao	21 E=820	24 E=1396	35 E=3267	27	1.29	1.12	0.77

Table 4. 12 The mean Daylight Glare Probability of Virtual Restaurant Prototype and relation between it and each workplane DGP with Uniform Sky at 21 December and 11:00 standard time in Barcelona and Bilbao

Add that the results of Mean DGP at July are Intolerable but it is on the border with Disturbing, which it approximates more to glare perception. Uniform Sky is for diffuse cloudy radiance and for winter Skies it changes a lot. At December de Mean DGP is Imperceptible. According to *gensky* with –u option script of above results,it has not –B global diffuse irradiance data option to fix time, day and location because it makes sense only with Overcast Sky. In consequence, two examples for any time, day and location of CIE Overcast Sky (-c) with –B 55.866 (Diffuse irradiance of E_H 10 000 lux) is presented.

	DGP No Frame, No CFS and No Masks				$\frac{DGP_{Mean}}{DGP_{WP1}}$	$\frac{DGP_{Mean}}{DGP_{WP2}}$	$\frac{DGP_{Mean}}{DGP_{WP3}}$
	WP1	WP2	WP3	Mean			
Overcast Sky E_H = 10 000 lux	22 E=1032	25 E=1519	37 E=3592	28	1.27	1.12	0.76

Table 4. 13 No Frame WS's mean Daylight Glare Probability of Virtual Restaurant Prototype and relation between it and each workplane DGP with Overcast Sky

	DGP Small Frame, No CFS and No Masks				$\frac{DGP_{Mean}}{DGP_{WP1}}$	$\frac{DGP_{Mean}}{DGP_{WP2}}$	$\frac{DGP_{Mean}}{DGP_{WP3}}$
	WP1	WP2	WP3	Mean			
Overcast Sky E_H = 10 000 lux	17 E=304	20 E=718	36 E=3451	24	1.41	1.20	0.67

Table 4. 14 Small Frame WS's mean Daylight Glare Probability of Virtual Restaurant Prototype and relation between it and each workplane DGP with Overcast Sky

Note that, the Mean DGP for Overcast Sky with No Frame is Imperceptible. According to *a* factor the trend continues also with Overcast Sky, although the difference between the Mean and Workplanes is less. It seems that WP1 DGP is less than Mean DGP, WP2 DGP is a little less than Mean DGP and WP3 DGP is more than Mean DGP.

Furthermore, the Mean DGP for Overcast Sky with Small Frame is Imperceptible. However, the difference between Workplanes is a little higher than No Frame-Overcast Sky case because the Out View of WP3 has more sky in proportion than WP2 and WP1.

In addition there are some aspects to take into account in the future:

· Local contrast: The Small Frame has lower glare probability than fully glazed façade window, but it provides more local contrast. In the future, the assessment of local contrast with the agreed methodology will be useful to done, although in the flowing pictures is sensed that Small Window has more local contrast.

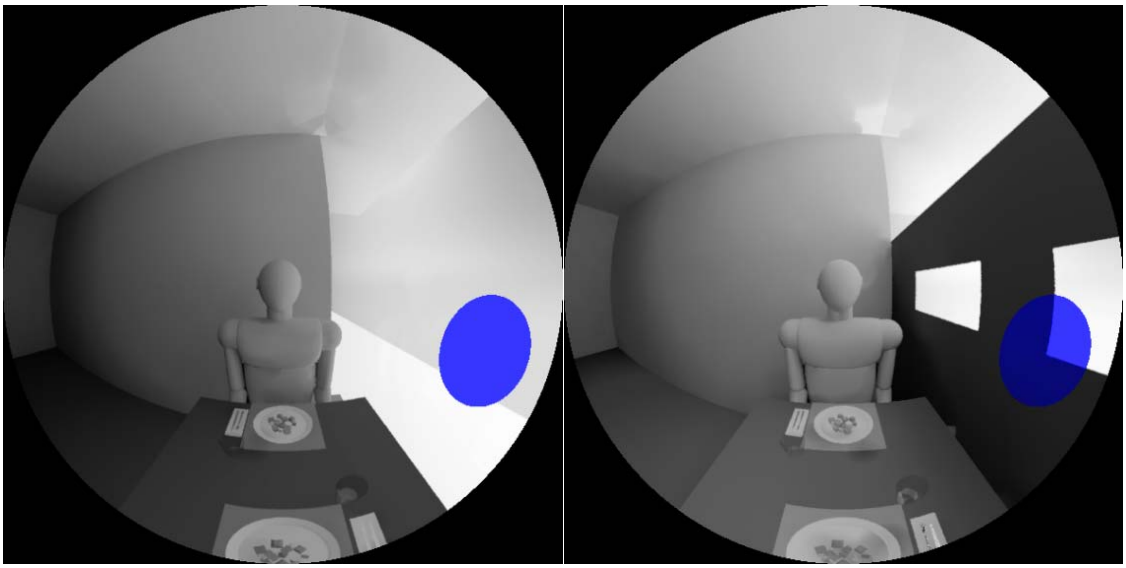

Figure 4. 35 Comparison of local contrast between No Frame and Small Frame Window Systems

· Out View: A simple way to take into account the Out View percentage is comparing the each Window System overture. In the future, the assessment of Out View with the agreed methodology will be useful to done, although in the flowing pictures is sensed that Large Window WS has less overture than No Frame WS and Small Frame WS has the least overture percentage.

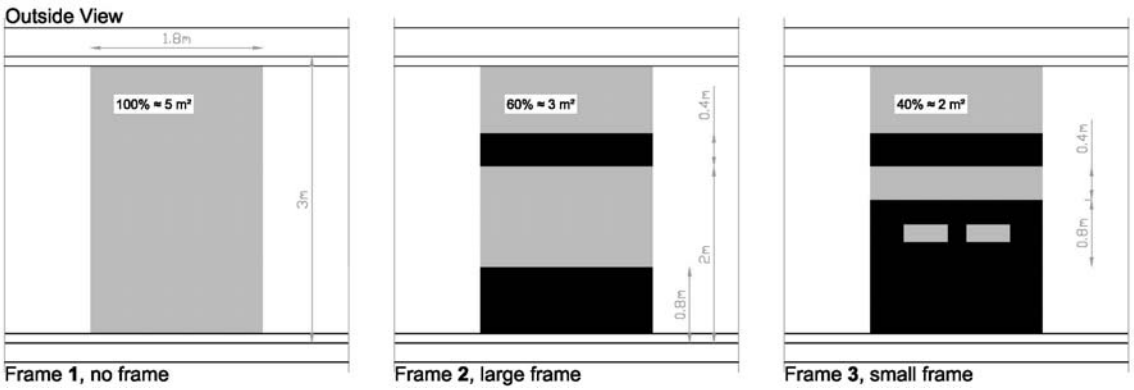

Figure 4. 36 Out view percentage of each window system

· Annual Daylight Glare Probability: According to the occupancy schedule, from 11:00 to 17:00 and throughout the all year, the Point-in-Time Glare could change considerable. For example, in No Frame Window System of virtual Restaurant Prototype according to WP2, person view, Point-in-Time DGP has been Disturbing (44%) and simulating the Annual Glare prediction in winter reaches Intolerable Daylighting Glare Probability, as it is described in the following image. However, Small

Frame Window Systems, removing some spring mornings, has Imperceptible Daylighting Glare Probability throughout the year, as it is described in the next image. The Annual Glare prediction is the aspect that in the future should be taken account.

Figure 4. 37 Annual Daylight Glare Probability of No Frame window system at Workplane 2 for Virtual Restaurant Prototype in Barcelona

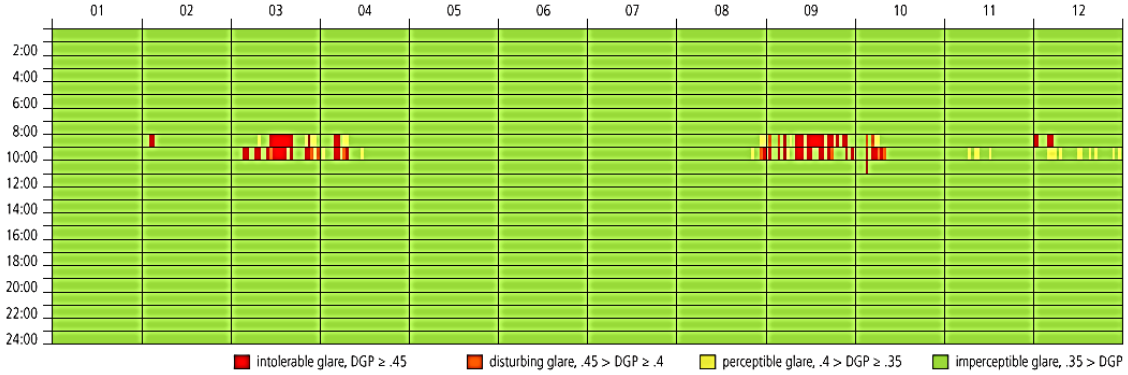

Figure 4. 38 Annual Daylight Glare Probability of Small Frame window system at Workplane 2 for Virtual Restaurant Prototype in Barcelona

· Surveys: A simple survey was done as indicative survey, 8 people have been polled at the restaurants, Sal Café and Azurmedi. The surveyed have been seated at a table next to the glazed façade, in the same position and with workplanes defined previously. They have been asked the following questions; QA, Does out view disturb you?; QB, Does front and outside view interaction disturb you?; QC, Is high contrast between outside and inside lighting?; QD, Are you able to watch accurate out view?; QE, Are in the out view undesirable visual elements?; QF, Do you think with less out luminance (brightness) value and visual elements you would have more concentration and privacy?

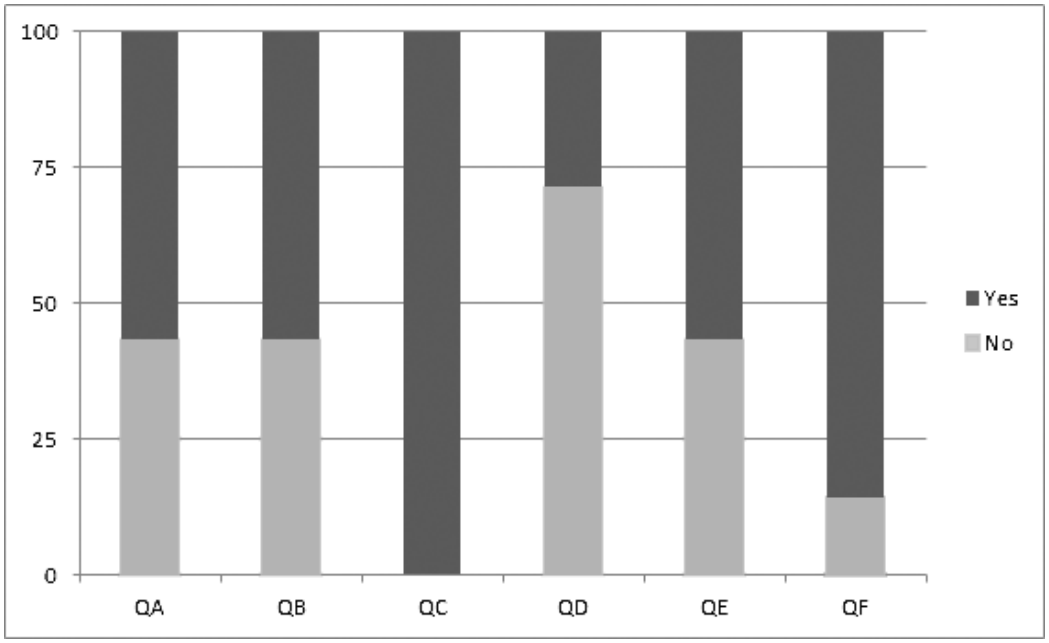

Figure 4. 39 Conducted survey polling 8 people at the restaurants. Results in %

They results indicate, on one hand, that there is high contrast between inside and outside lighting, causing glare probability. On the other hand, they demonstrate that there are undesirable visual elements. Lastly, people think that with less out luminous surfaces and visual elements they will have more concentration at the activity and in consequence more privacy. In the future will be useful to do more surveys with more polled people, because to get accurate visual comfort results, they will be compared with thorough satisfaction surveys.

Figure 4. 40 Polled people answering the survey; in the left at Restaurant 1 (Sal Café) and in the right at Restaurant 2 (Azurmendi)

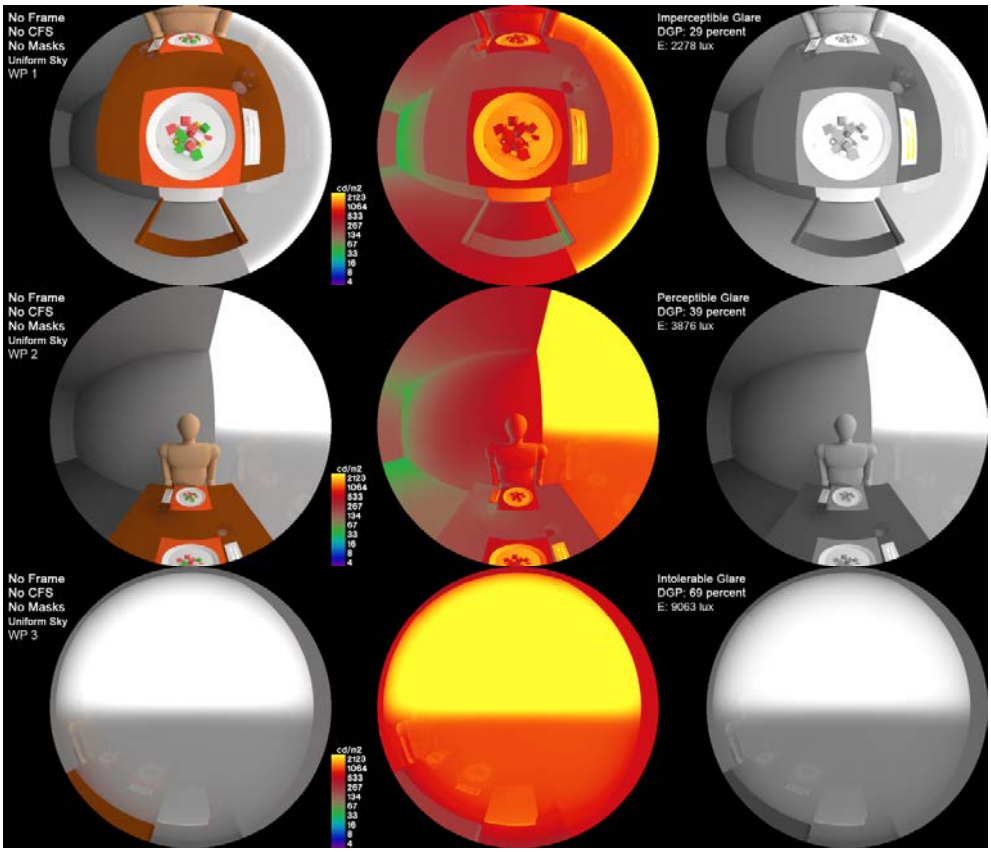

Figure 4. 41 Images of each WP for VRP with Uniform Sky at 22 July and 11:00 standard time in Barcelona

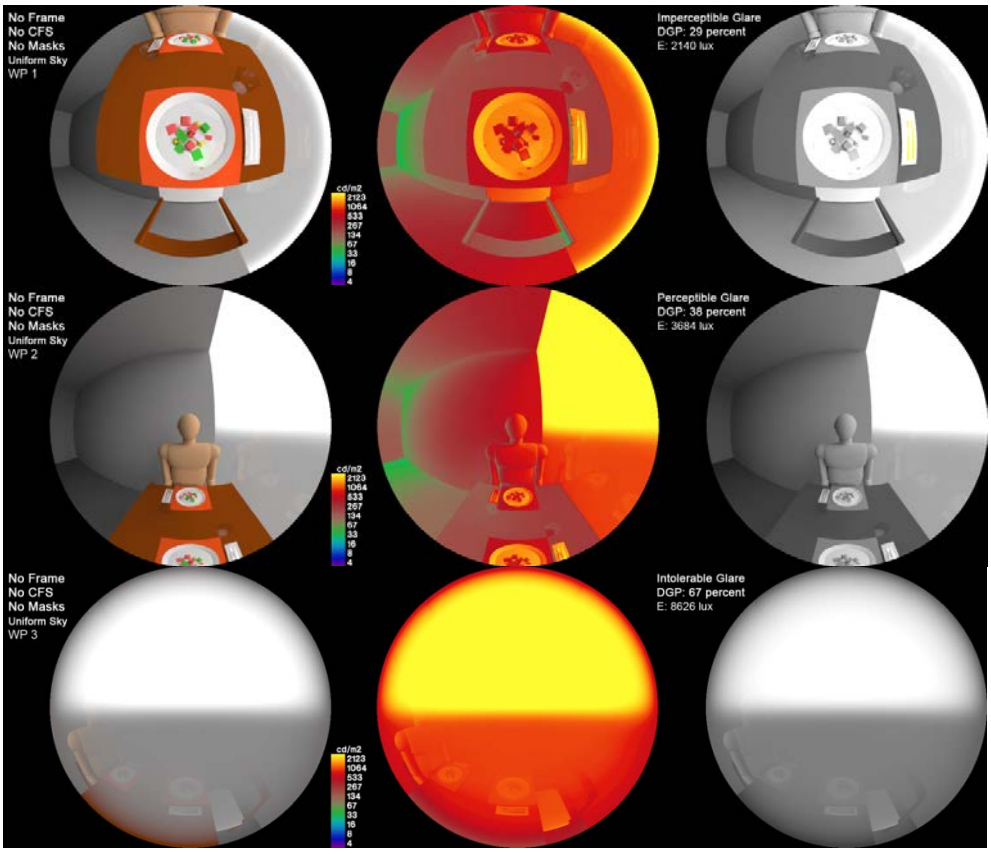

Figure 4. 42 Images of each WP for VRP with Uniform Sky at 22 July and 11:00 standard time in Bilbao

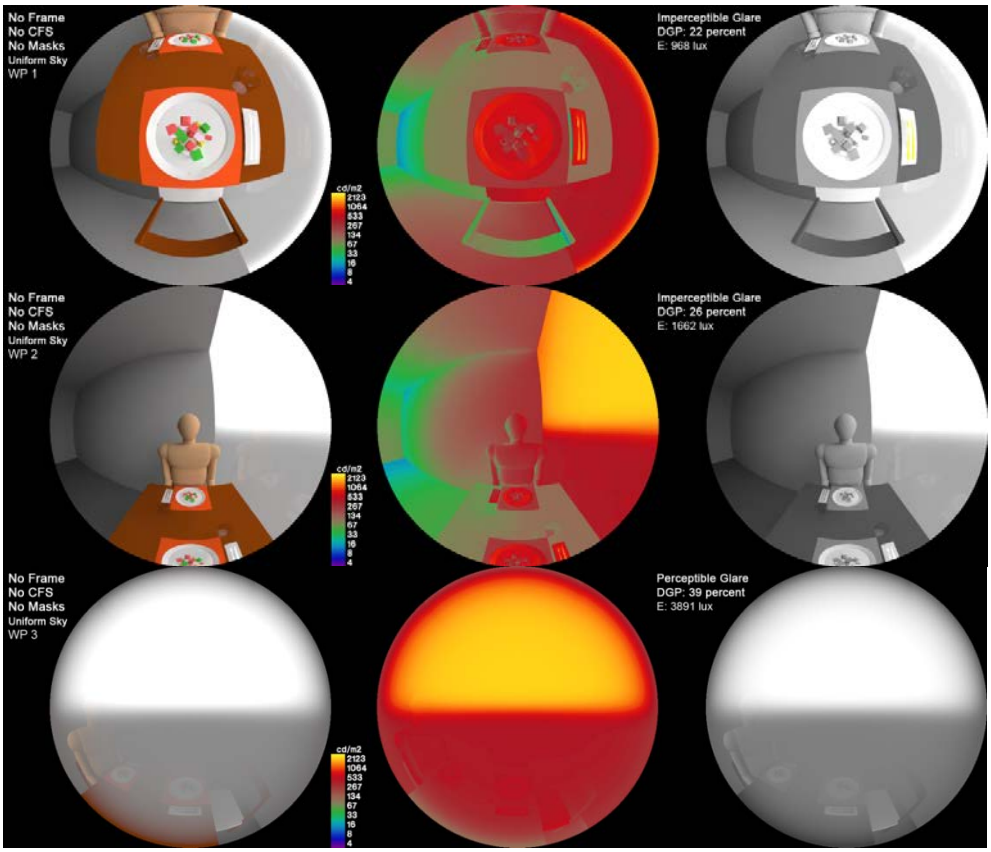

Figure 4. 43 Images of each WP for VRP with Uniform Sky at 21 December and 11:00 standard time in Barcelona

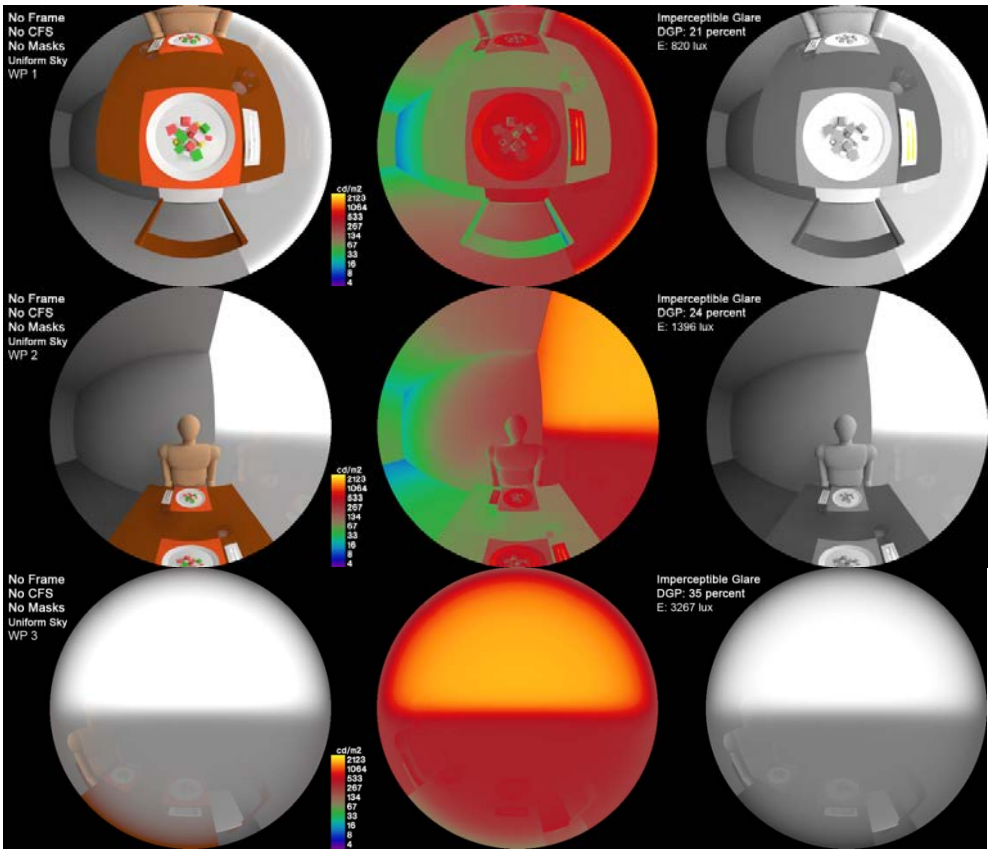

Figure 4. 44 Images of each WP for VRP with Uniform Sky at 21 December and 11:00 standard time in Bilbao

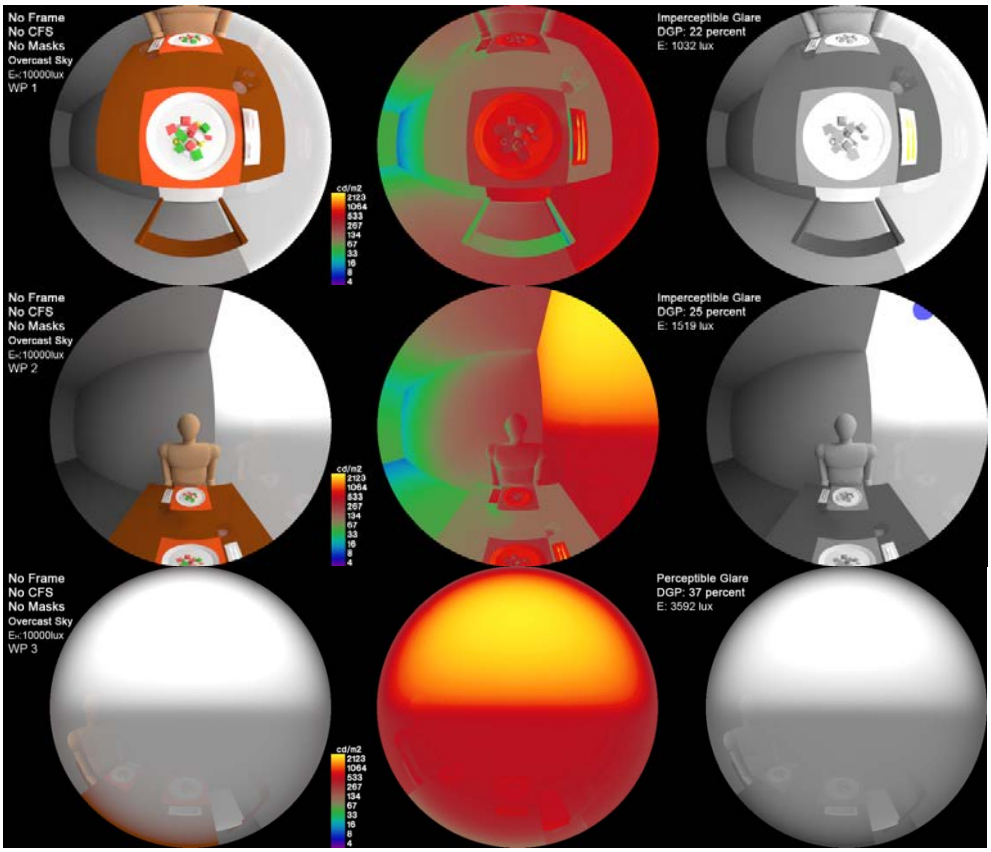

Figure 4. 45 Images of each WP for No Frame WS from VRP with Overcast Sky

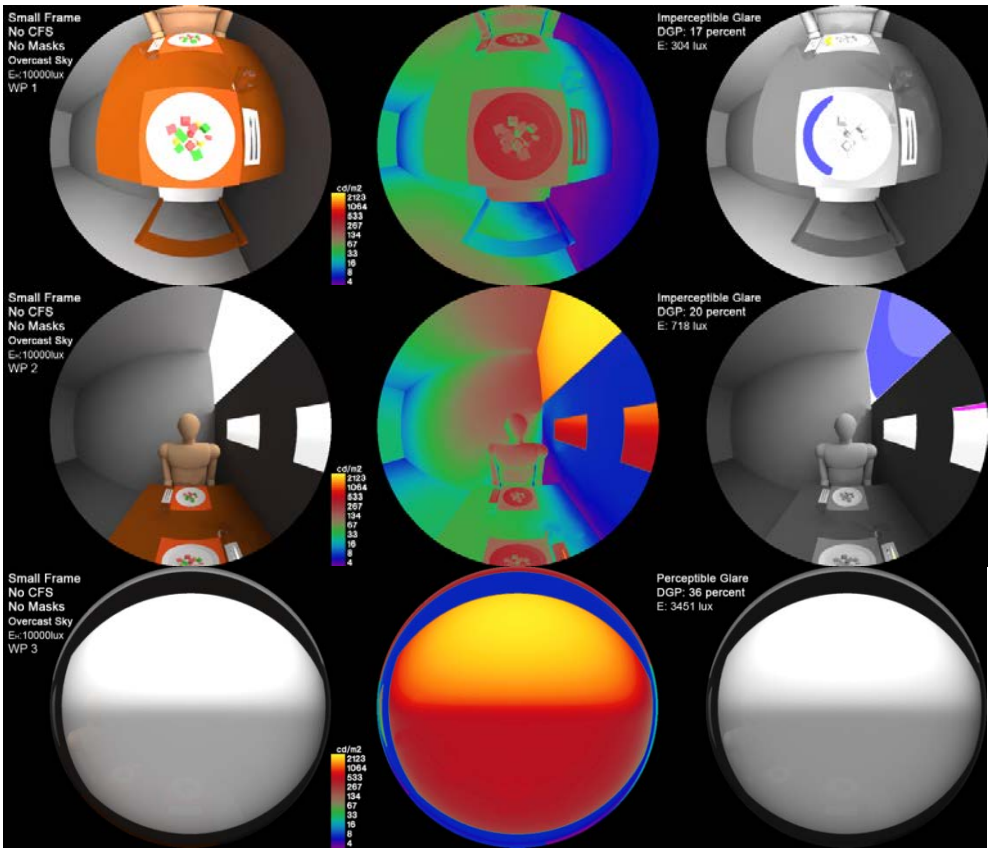

Figure 4. 46 Images of each WP for Small Frame WS from VRP with Overcast Sky

Chapter V

RESULTS OF PARAMETER 2: illuminance distribution evaluated by Daylight Autonomy (DA) index

This chapter deals with illuminance distribution. According to Climate Based Daylighting Modelling (CBDM), the Daylight Autonomy (DA) index will be used for assess illuminance distribution. The DA will be applied to workplane, which is a plane that sets the table throughout the 5m X 5m of the space, as well as, the index will be applied to each window system and to each case study.

The simulation method is chosen to get illuminance data. Therefore, the virtual models of selected two restaurants, Sal Café (R1) and Azurmendi (R2), and the virtual prototype are used to get simulated DA. The aim is, first to get the DA index of each virtual model restaurant and after to get the DA index of virtual prototype (VRP) to get more accurate lighting performance results. Note that, the virtual prototype's workplane has 2m X 5m and in consequence the grid has 286 sensor points, approximately a half of virtual models of real restaurants. So, the aim is to analyse Daylight Autonomy in each sensor point for each window system and after to get the average of sensor points Daylight Autonomy.

As referred in Material and Methods chapter 2, Daylight Autonomy of Complex Fenestration System is not possible to obtain by DIVA, Radiance interface, although the Point-in-Time illuminance data yes. Therefore, Three-Phase Method is required to get DA of Complex Fenestration System. For the virtual models of the two restaurants, all Window Systems DA except DA of CFS are simulated by DIVA and CFSs are simulated by TPM. However, all Window Systems even the Window Systems with Complex Fenestration Systems DA of virtual prototype are got by Three Phase Method.

5.1 Scripts of DA simulation

In de following section the scripts that have been used are explained. The scripts for DIVA simulation and Three-Phase Method simulation will be explained separated:

DA by DIVA scripts process:

1) Starting with DIVA, Radiance and Daysim program based plugin for Rhino. The program can be obtained from DIVA FOR RHINO website http://diva4rhino.com/ (The program for Windows OS is used for thesis's visualizations). The DIVA plugin has 4 tabs; *Location*, *Nodes*, *Materials* and *Metrics*:

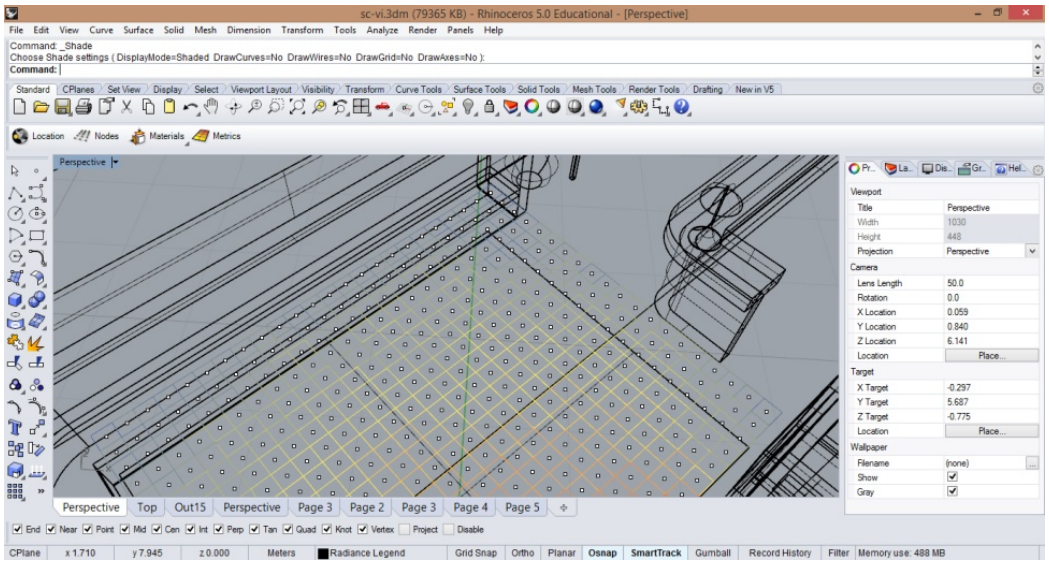

Figure 5. 1 Options of DIVA plugin into Rhinoceros program

· *Location* tab: The *.epw weather data file of the location is necessary; it could download from EnergyPlus website https://energyplus.net/weather . It must be put in DIVA's *WeatherData* folder as C:\DIVA\WeatherData. Once the location is set *-DIVA folder is created, where Rhino file is saved and DIVA's default files are saved.

· *Nodes* tab: the surface that it works as workplane and sensor points' grid is necessary to define. Then, clicking nodes tab the surface, the distance between the surface and sensor points grid and the distance between sensor points are required.

· *Materials* tab: the materials specifications are defined as Radiance's material description. Other materials have been needed, so the material specifications have been added to *material.rad* file, where it is in Resources' folder in previous *-DIVA created folder. The file *.xml that has the scattering function must be placed in *lib* folder C:\DIVA\Radiance\lib.

· *Metrics* tab: In *Daylight Grid-Based* tab selecting *Climate-Based* tab and then defining in *Metric* option Daylight Autonomy the index is obtained.

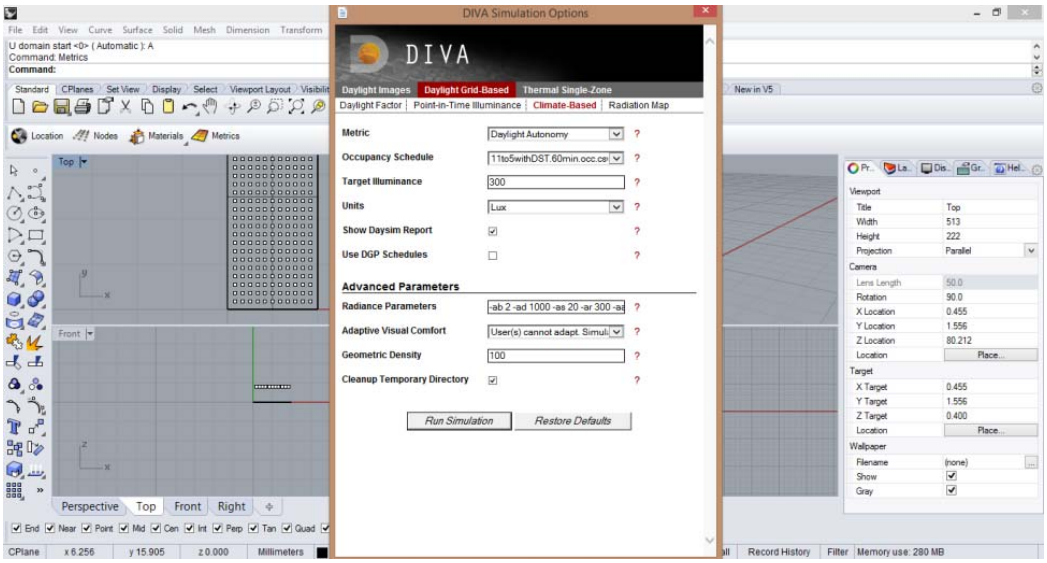

Figure 5. 2 Daylight Autonomy calculation by Climate-Based option at Daylight Grid-Based option

Therefore, the *.DA file in Grid-Based folder inside of *-DIVA folder is saved, this last folder it generates automatically in the same directory of 3D model when the location is set.

2) The parameters of Daylight Autonomy have been the following:

· Metric: Daylight Autonomy

· Occupancy Schedule: In this file there is the information of the space utilization hours. First the time step must be selected; hourly is selected for the cases study. Then, occupancy must be set with 0 or 1 hourly; from 11:00 to 17:00 in all year is selected. This file must be saved in C:\DIVA\Schedules directory in data format.

· Target Illuminance: 300

· Unit: Lux

· Radiance parameters: All Radiance parameters are changeable:

```
-ab 2 -ad 1000 -as 20 -ar 300 -aa 0.1
```

· Geometry Density: 100

· Cleanup Temporary Directory

3) Once the simulation is run the *Load DIVA Metrics Dialog* is open to set the visualization map of DA throughout the grid.

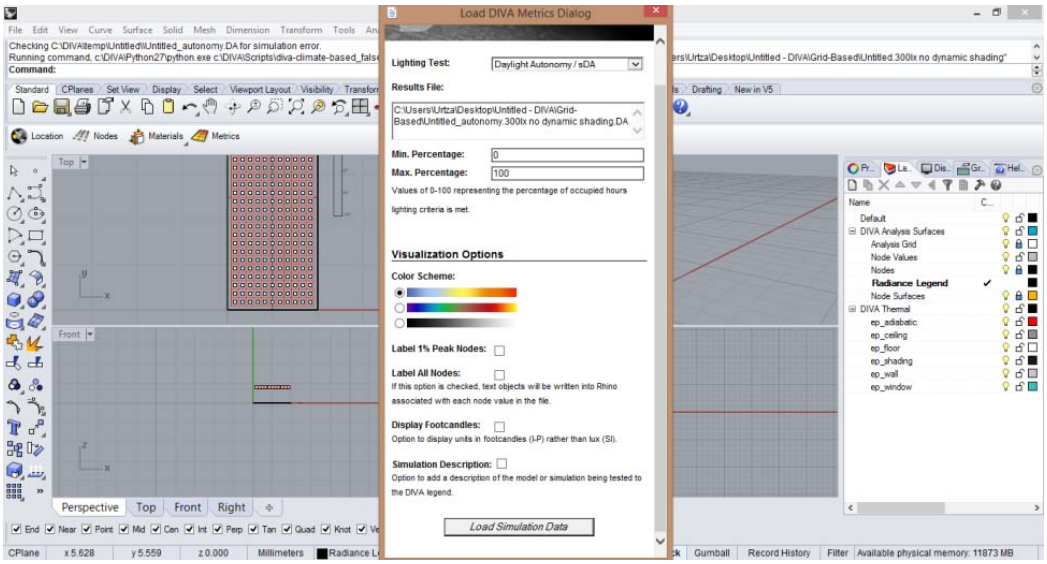

Figure 5. 3 Options for visualization of Daylight Autonomy results

4) The used settings of visualization map have been the following:

· Min. Percentage: 0

· Max. Percentage: 100

· Colour Scheme: the first option

Note that, there is an option to load other DA file that is obtained from other software as Radiance, but it must be have the same format. Clicking with the right button to *Metrics* tab there is the option to load the file.

5) Add that Point-in-Time Illuminance data is used to compare with measured illuminance data. Then it is a reference to know the margin of error of DA results.

Instead of selecting Climate Based tab, clicking Point-in-Time Illuminance tab the illuminance data is obtained.

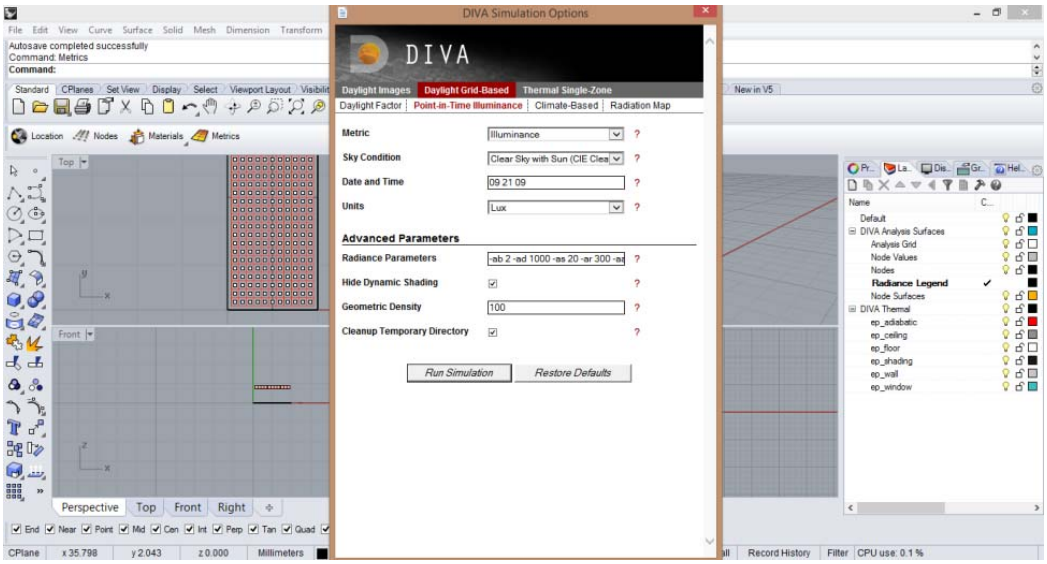

Figure 5. 4 Point-in-Time Illuminance calculation at Daylight Grid-Based option

Therefore, the *.dat file in Grid-Based folder inside of *-DIVA folder is saved. The results are in RGB irradiance values. The results should be multiply by luminous efficacy to get illuminance results. Therefore, using the same octree file and *rtrace* command by *rcalc* command with Radiance the illuminance data is obtained.

6) The parameters of Point-in-Time Illuminance data have been the following:

· Metric: Illuminance

· Sky Condition: Clear Sky with Sun (CIE Clear Sky)

· Data and Time: 07 22 11

· Units: Lux

· Radiance parameters: All Radiance parameters are changeable:

```
-ab 2 -ad 1000 -as 20 -ar 300 -aa 0.1
```

· Geometry Density: 100
· Cleanup Temporary Directory
Note that the visualization map in this study does not use, but there is a possibility. Once the simulation is run *Load DIVA Metrics Dialog* is run again and the parameters could be the following:

· Min. Illuminance: 0

· Max. Illuminance: 5000 (It should be always the same is the results are wanted to compare)

· Colour Scheme: the first option

Note that there is also the option to load other illuminance data.

DA by Three-Phase Method scripts process:

1) The material file description, *.rad, and geometry file, *.rad, should be separately from a window as light pipe. Then for each Window System View Matrix, Daylight Matrix, Transmission Matrix and Sky Matrix phases are required.

```
# windowNF.rad


void glow windowglow

0

0

4 1 1 1 0


windowglow polygon windowNF

0

0

12 0.000 0.000 0.000

   0.000 0.000 2.700

   2.000 0.000 2.700

   2.000 0.000 0.000

…
```

2) View Matrix:

The window, which works as flux transfer, should be *glow* material. Therefore for each Window System the window part will be different. Description of *glow* material and geometry of each Window System will be in window file, *.rad, separately.

First, the octree scene description by *oconv* program is required:

```
$ oconv res1_material.rad res1_geometry.rad windowNF.rad > \
res1NF_vmx.oct

$ oconv res1_material.rad res1_geometry.rad windowNF_LS.rad > \
res1NF_LS_vmx.oct

$ oconv res1_material.rad res1_geometry.rad windowNF_PF.rad > \
res1NF_PF_vmx.oct

…

$ oconv res2_material.rad res2_geometry.rad windowLF_LS.rad > \
res2LF_LS_vmx.oct

…

$ oconv resPro_material.rad resPro_geometry.rad windowSF_PF.rad \

> resProSF_PF_vmx.oct

…
```

After, the View Matrix is generated by *rcontrib* program. The orientation of Window System of each restaurant is different. Therefore the *rcontrib* has been different for each orientation:

Restaurant 1, Sal Café: Southeast orientation:

```
$ rcontrib -f klems_int.cal -b 'kbin(-sqrt(.5),sqrt(.5),0,0,0,1)' \
-bn Nkbins -m windowglow -I+ -ab 2 -ad 1000 -lw 2e-5 \
res1NF_vmx.oct < res1NF.pts > res1NF.vmx

…
```

Restaurant 2, Azurmendi: North orientation:

```
$ rcontrib -f klems_int.cal -b kbinN -bn Nkbins -m windowglow -I+ \
-ab 2 -ad 1000 -lw 2e-5 res2LF_LS_vmx.oct < res2LF_LS.pts > \ res2LF_LS.vmx
```

```
…
```

Restaurant Prototype: South orientation:

```
$ rcontrib -f klems_int.cal -b kbinS -bn Nkbins -m windowglow -I+ \
-ab 2 -ad 1000 -lw 2e-5 resProSF_PF_vmx.oct < resProSF_PF.pts > \
resProSF_PF.vmx

…
```

3) Daylight Matrix:

The *rfluxmtx* program is used to get Daylight Matrix. It generalizes sampling for light pipes. It is composed by single sender objects and one or more receiver objects. The sender is considered the window and the receiver the sky.

Sender file, following window description is used:

```
#@rfluxmtx h=kf u=+Z

Translucent_20 polygon windowNF
0
0
12 0.000 0.000 0.000
    0.000 0.000 2.700
    2.000 0.000 2.700
    2.000 0.000 0.000

…
```

Receiver file, following sky description is used:

```
#@rfluxmtx h=u
void glow groundglow
0
0
4 1 1 1 0

groundglow source ground
0
0
4 0 0 -1 180
```

```
#@rfluxmtx h=r4 u=+Y
void glow skyglow
0
0
4 1 1 1 0

skyglow source sky
0
0
4 0 0 1 180

…
```

The *rfluxmtx* program needs restaurant material and geometry file and rendering parameters. The used rendering parameter are; ab 4 -lw 1e-4 -ad 1000. The used script of *rfluxmtx* program for each Window System is the following:

```
$ rfluxmtx -v -n 2 -c 20000 -ff -ab 4 -lw 1e-4 -ad 1000 windowNF.rad \
dummysky.rad -w res1NF_material.rad res1NF_geometry.rad > res1NF.dmx

…
```

4) Transmission Matrix:

This matrix should be of 145x145, which based on Klems divisions. Two types of Complex Fenestration are used; a simple pane of clear glass and a prismatic film.

The simple pane of clear sky is obtained by WINDOW 7 software:

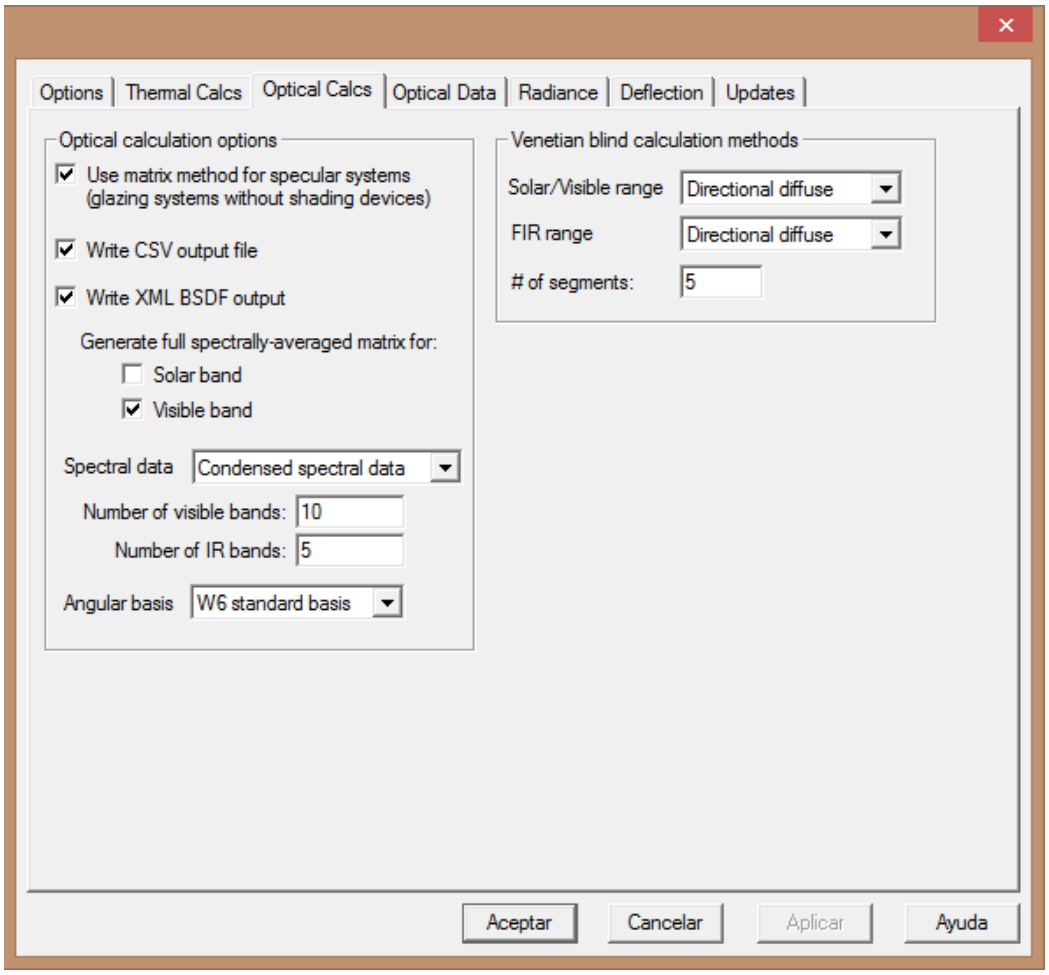

Figure 5. 5 Preference settings of BSDF for WINDOW 7 program

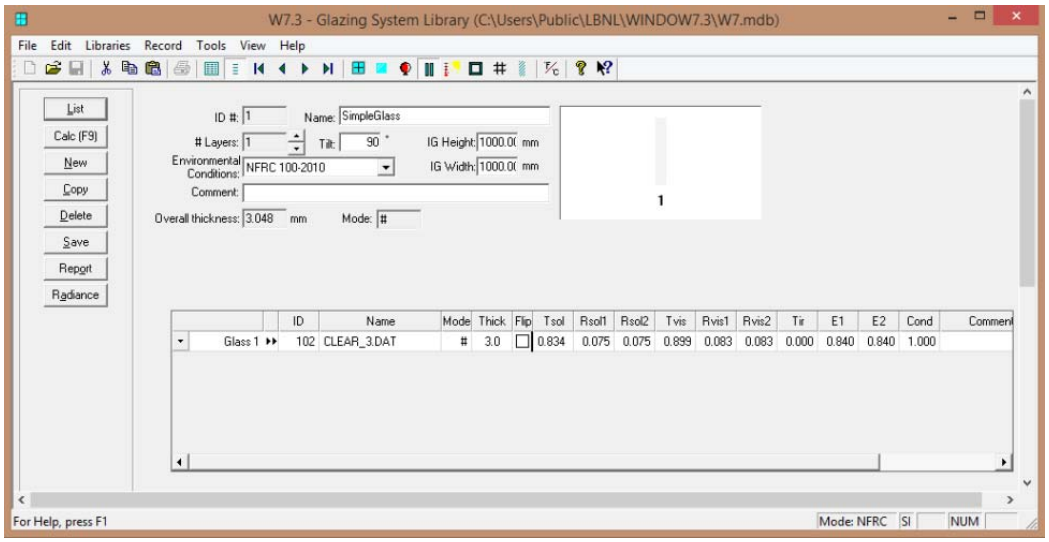

Figure 5. 6 Settings for Glazing Systems in WINDOW 7 program

The obtained file of SimpleGlass.xml is created in C:\Users\Public\LBNL\BSDFs.

The prismatic film is of Fim3M and it is obtained from Chantal Basurto Dávila's PhD. The PhD was done in EPFL and they used gonio-photometer. The file name is klems145x145_9-14-2012_t.xml.

5) Sky Matrix:

Two Sky Matrix have been used; from Barcelona and Bilbao. The weather data is obtained from Energy Plus web in *.epw format; ESP_Barcelona.081810_IWEC.epw and ESP_Bilbao.08250_SWEC.epw.

First, with epw2wea program *.epw format has been changed:

```
$ epw2wea ESP_Barcelona.081810_IWEC.epw Barcelona.wea

$ epw2wea ESP_Bilbao.08250_SWEC.epw Bilbao.wea
```

After, with *gendaymtx* program the Sky Matrix file is obtained:

```
$ gendaymtx Barcelona.wea > Barcelona.smx

$ gendaymtx Bilbao.wea > Bilbao.smx
```

Note that, although the location in Spain is not determining for Clear Sky with Sun simulation (CIE Clear Sky), the Restaurant 1, Sal Café, is from Barcelona, the Restaurant 2, Azurmendi, is from Bilbao and Restaurant Prototype is placed in Barcelona but it is not significant.

6) Final results with *dctimestep* program

The *dctimestep* is the program to compote all matrix together to have RGB irradiance values for each of the 8760 hours/year simulated time steps. The *rmtxop* is the program to convert RGB irradiance values to illuminance values for each of the 8760 hours/year simulated time steps. The used script is the following:

```
$ dctimestep res1NF.vmx SimpleGlass.xml res1NF.dmx Barcelona.smx | \
rmtxop \  -fa -c 47.4 119.9 11.6 - > res1NF.dat

$ dctimestep res2LF_LS.vmx SimpleGlass.xml res2LF_LS.dmx Bilbao.smx | \
rmtxop -fa -c 47.4 119.9 11.6 - > res2LF_LS.dat
```

```
$ dctimestep resProSF_PF.vmx klems145x145_9-14-2012_t.xml \
resProSF_PF.dmx Barcelona.smx | rmtxop -fa -c 47.4 119.9 11.6 - > \
resProSF_PF.dat

…
```

5.2 Mean DA index and distribution map throughout the space

In this section the pictures of mean Daylight Autonomy throughout the grid for each window system and restaurants will be shown.

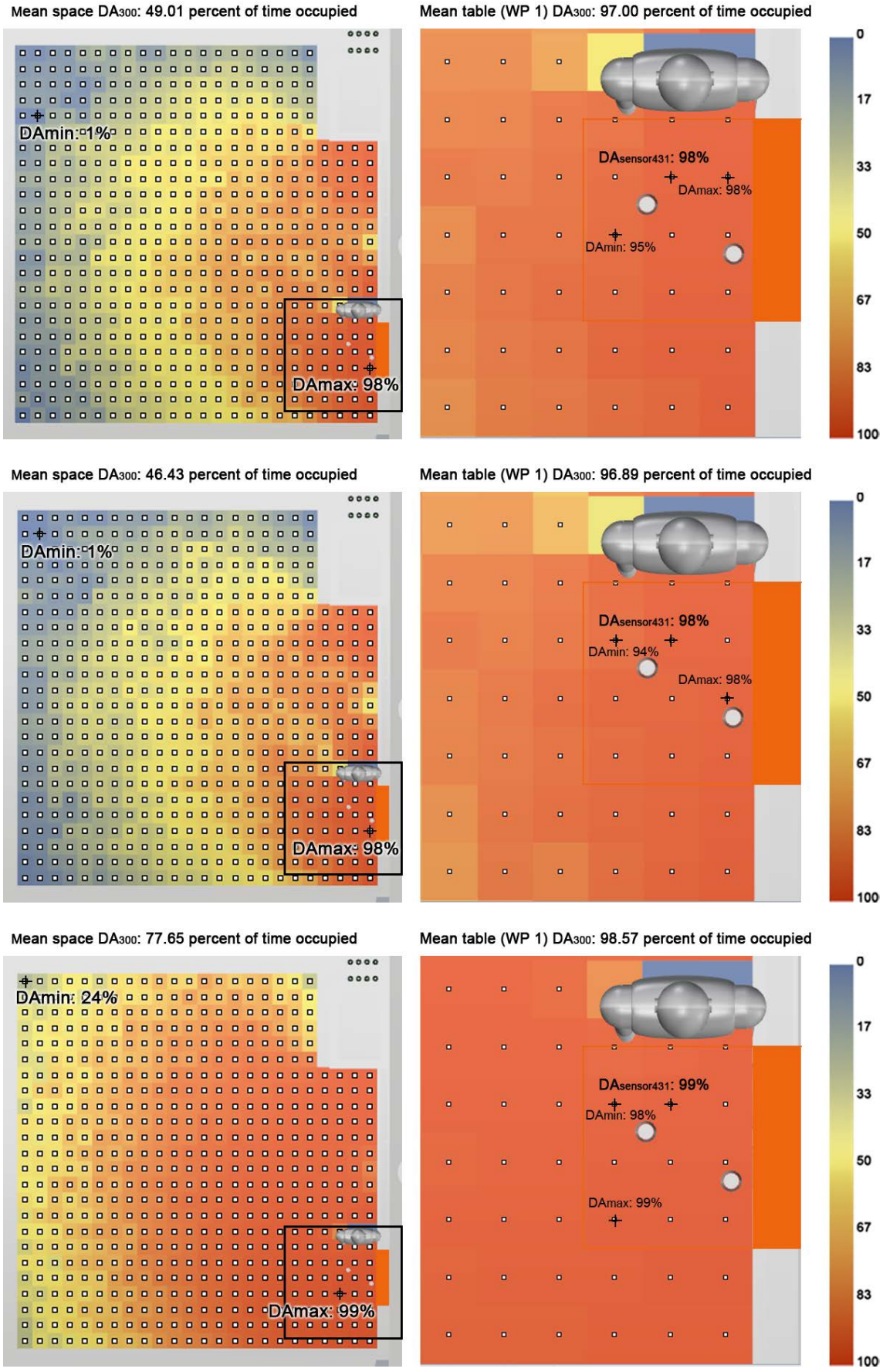

Figure 5. 7 The mean DA of No Frame WS without CFS, with Light Shelf CFS and with Prismatic Film CFS for R1

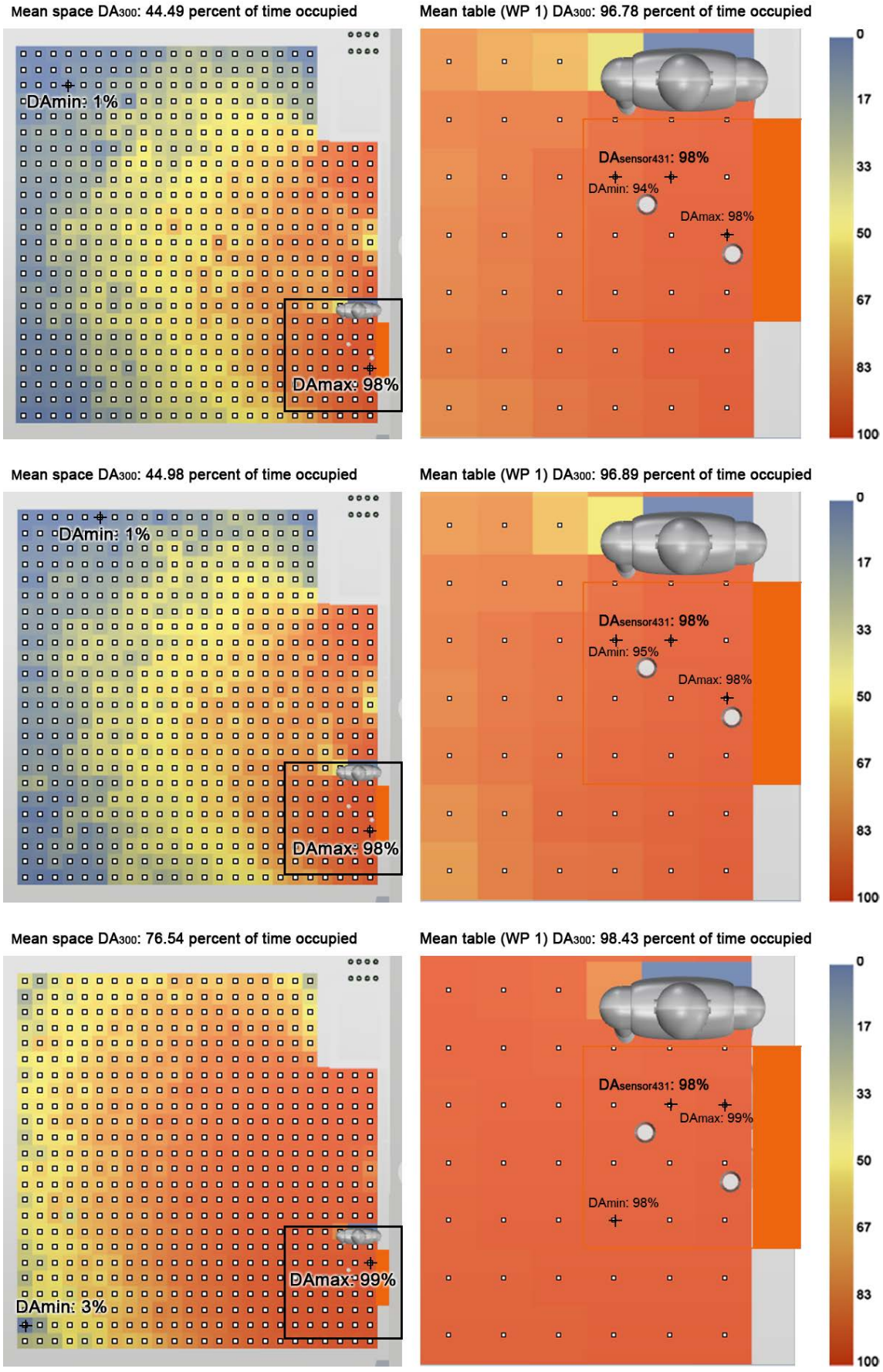

Figure 5. 8 The mean DA of Large Frame WS without CFS, with Light Shelf CFS and with Prismatic Film CFS for R1

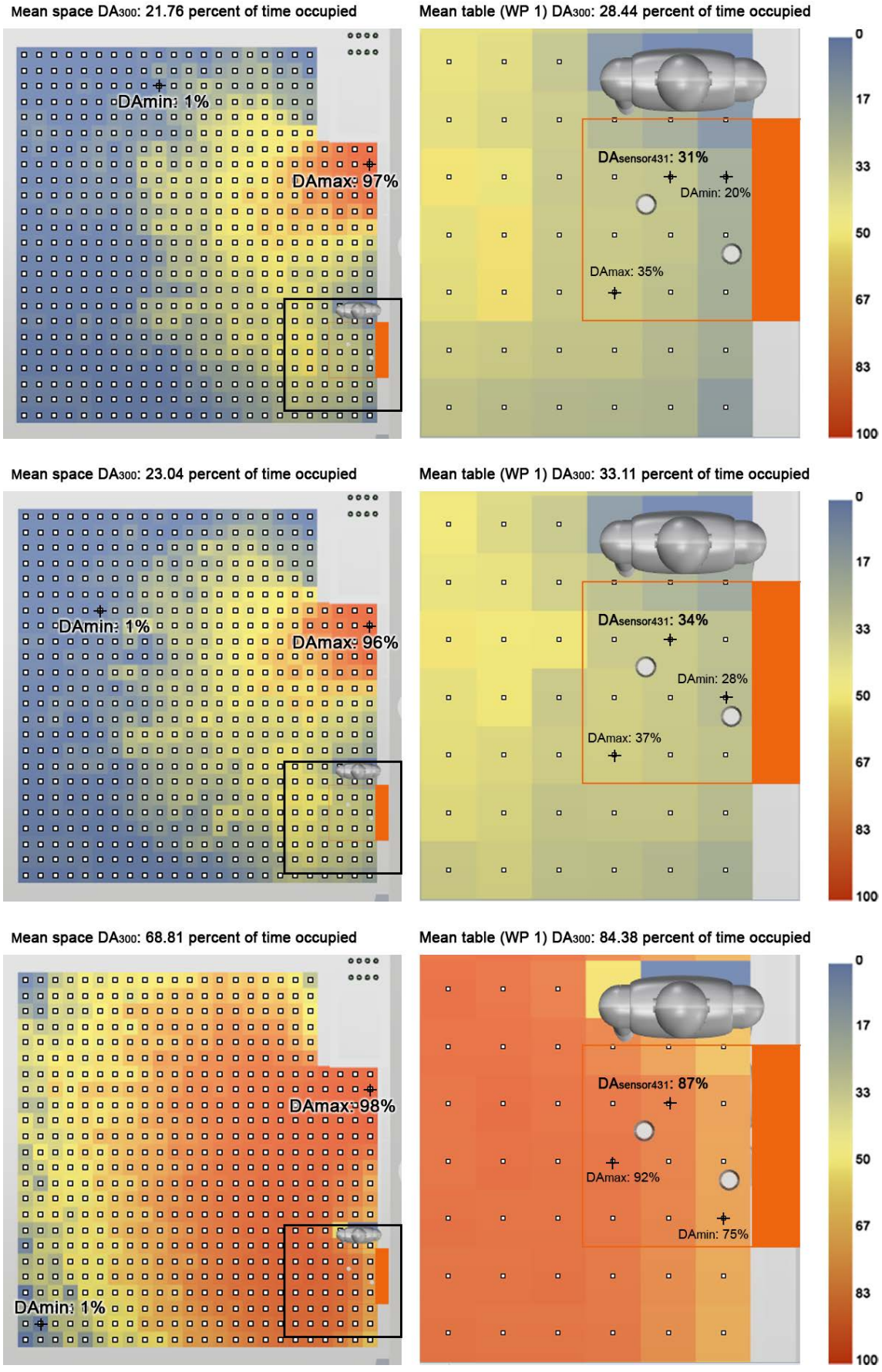

Figure 5. 9 The mean DA of Small Frame WS without CFS, with Light Shelf CFS and with Prismatic Film CFS for R1

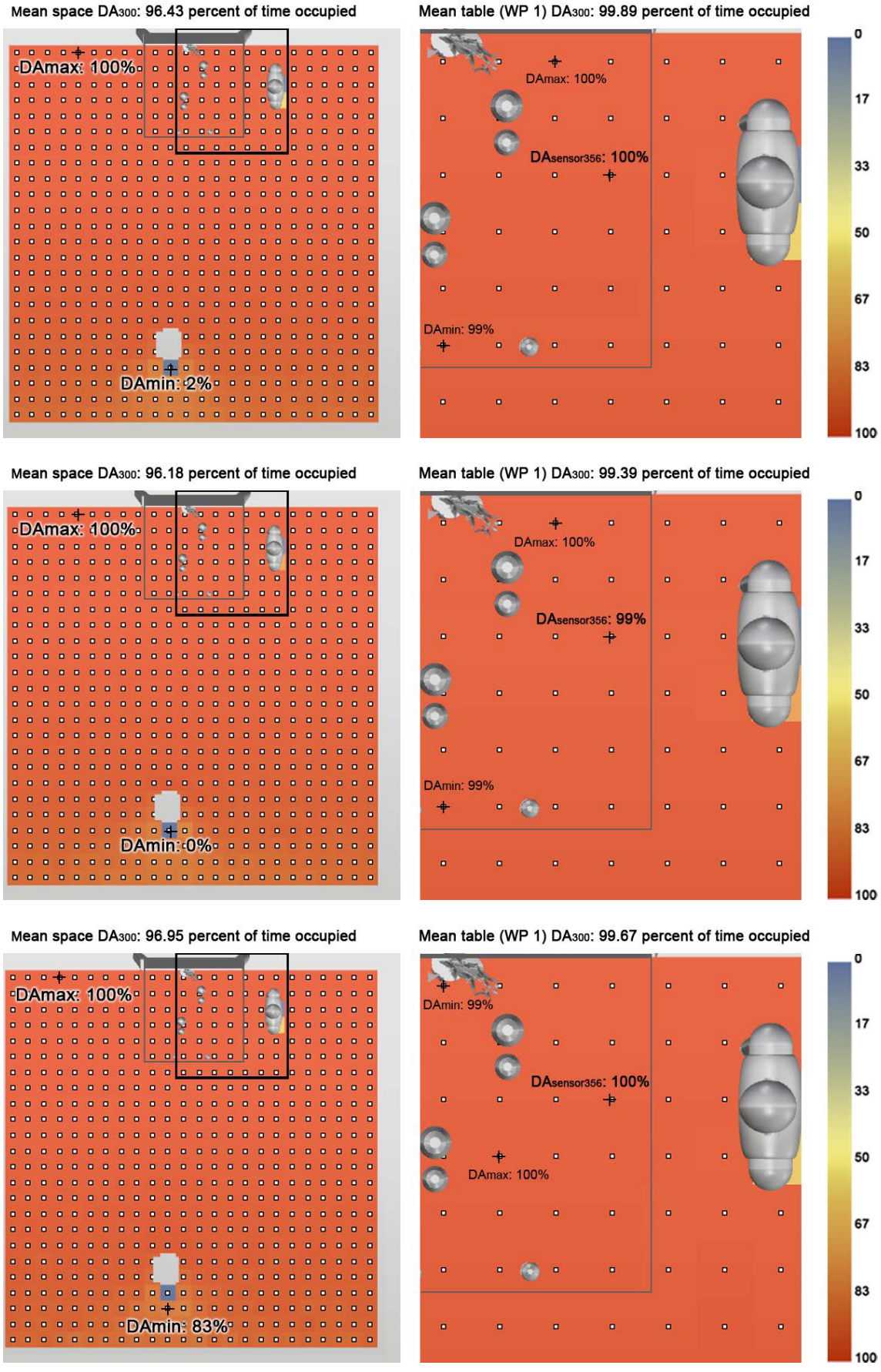

Figure 5. 10 The mean DA of No Frame WS without CFS, with Light Shelf CFS and with Prismatic Film CFS for R2

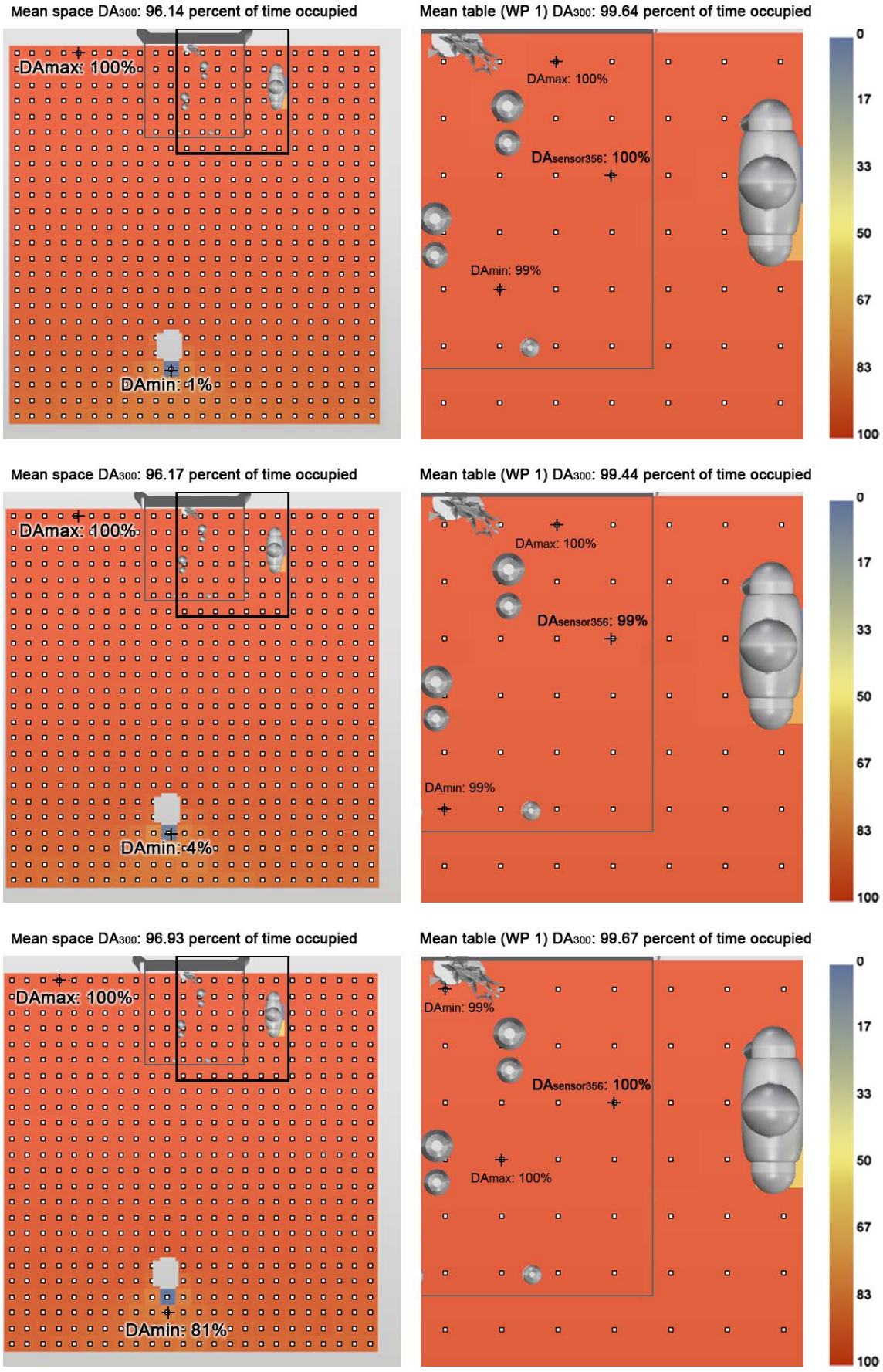

Figure 5. 11 The mean DA of Large Frame WS without CFS, with Light Shelf CFS and with Prismatic Film CFS for R2

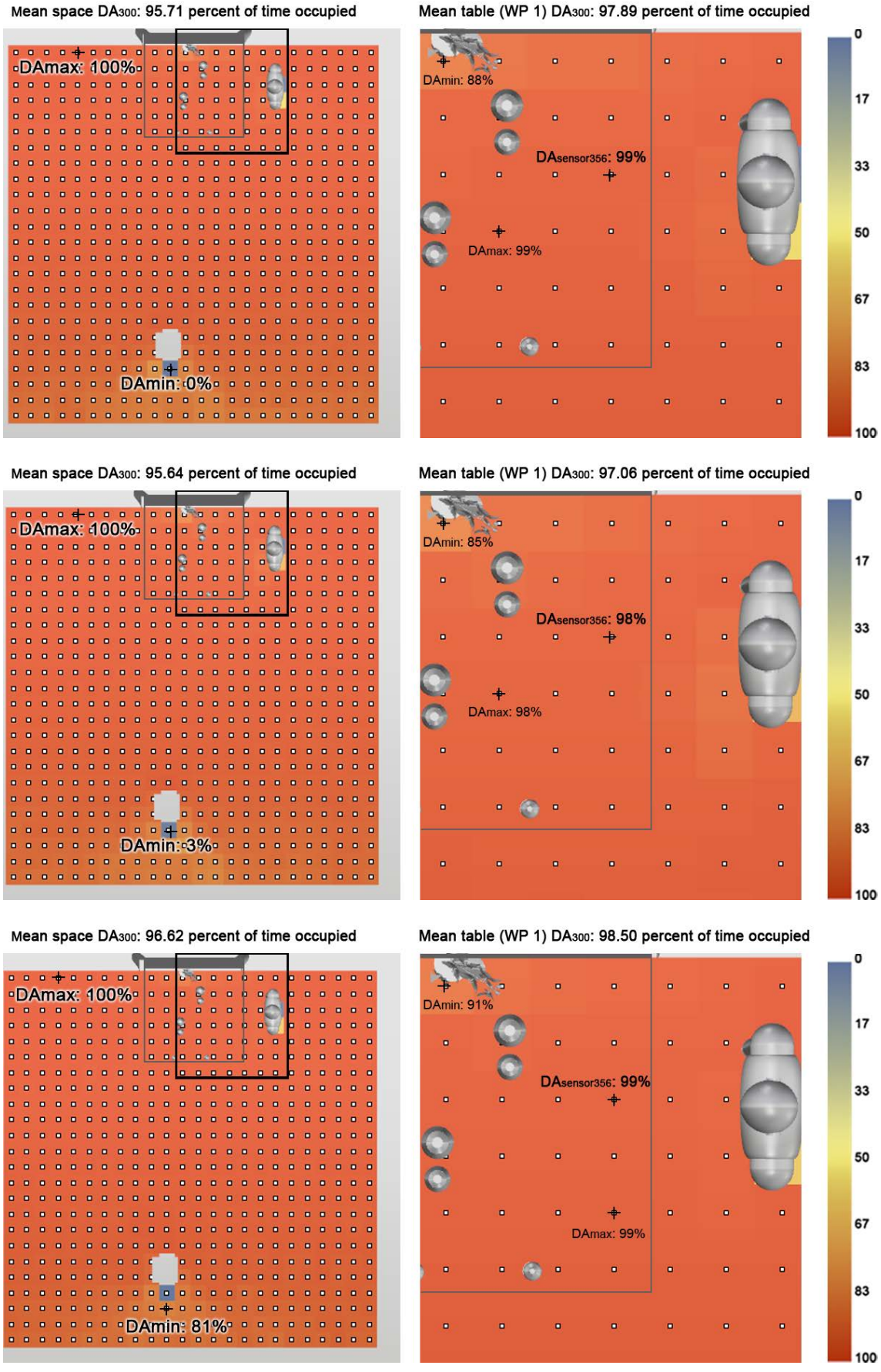

Figure 5. 12 The mean DA of Small Frame WS without CFS, with Light Shelf CFS and with Prismatic Film CFS for R2

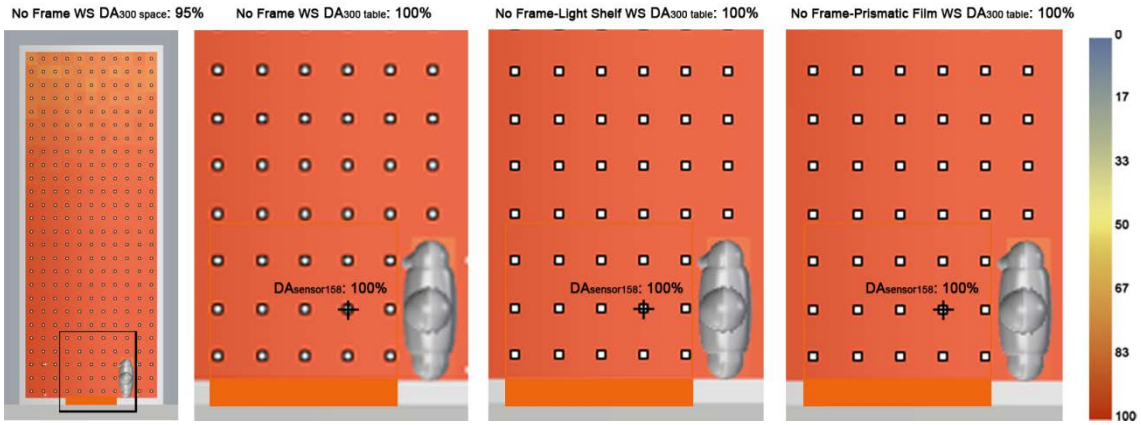

Figure 5. 13 The mean DA of No Frame WS without CFS, with Light Shelf CFS and with Prismatic Film CFS for VRP

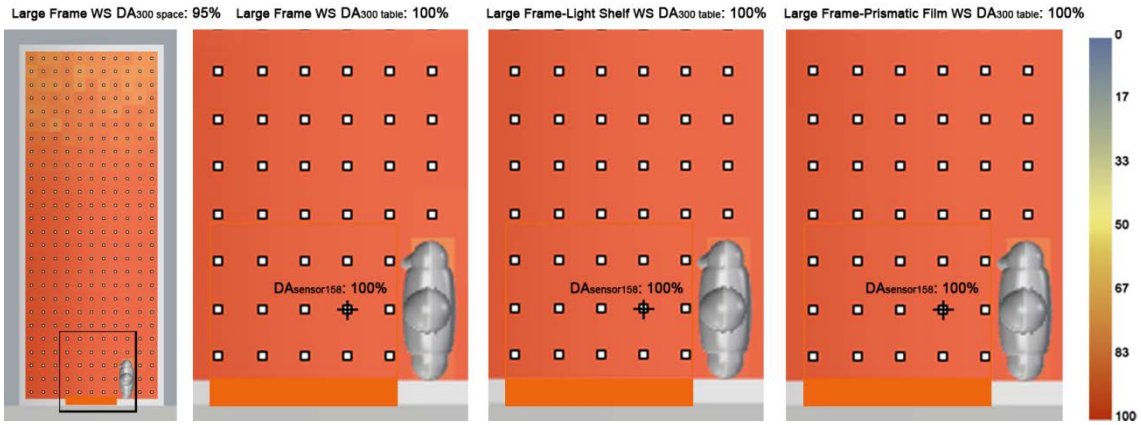

Figure 5. 14 The mean DA of Large Frame WS without CFS, with Light Shelf CFS and with Prismatic Film CFS for VRP

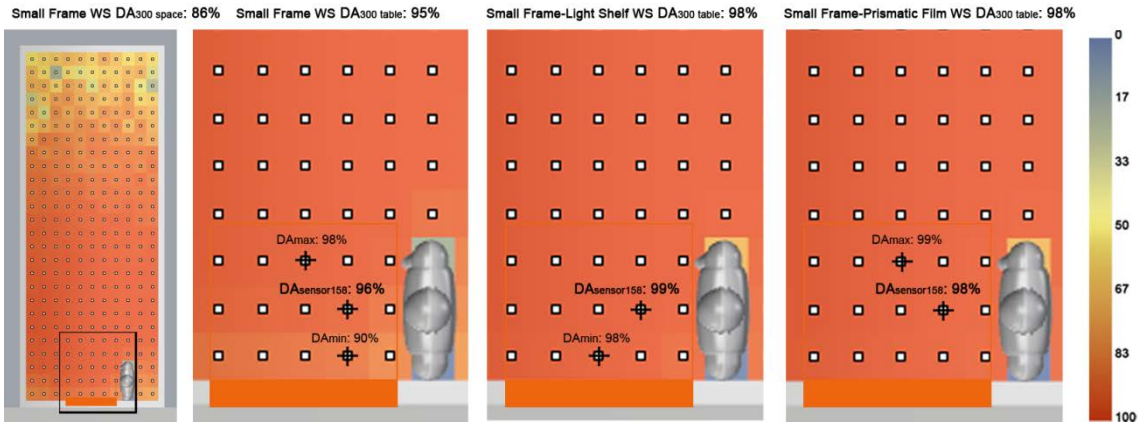

Figure 5. 15 The mean DA of Small Frame WS without CFS, with Light Shelf CFS and with Prismatic Film CFS for VRP

5.3 Summary tables of Mean DA results of each case and the relations between them

In the following section simulated illuminance data and Daylight Autonomy of restaurant will be explained. The illuminance data is used to have a reference. The tables of each restaurant follow the same outline:

- Point-in-Time Illuminance data of each Window System throughout the row of table location. In bold there are the sensor points placed on the table and the others there are in the same row from the window up to the indoor front wall
- Mean and Standard Deviation of illuminance data in different sensor point groups; all sensor points of the space (WP pane); sensor points of the row that belongs the table; and sensor points of the table in row
- The graphic of illuminance data of each Window System results
- Daylight Autonomy data of each Window System throughout the row of table location. In bold there are the sensor points placed on the table and the others there are in the same row from the window up to the indoor front wall
- Mean and Standard Deviation of Daylight Autonomy in different sensor point groups; all sensor points of the space (WP pane); sensor points of the row that belongs the table; and sensor points of the table in row
- The graphic of Daylight Autonomy of each Window System results

The restaurants are those studied, so far:

- Restaurant 1 (Sal Café) of Barcelona under Clear Sky with Sun (CIE Clear Sky)
- Restaurant 2 (Azurmedi) of Bilbao under Intermediate Sky
- Restaurant Prototype in Barcelona under Clear Sky with Sun (CIE Clear Sky). However, there would not be huge difference if it were in Bilbao under Clear Sky with Sun (CIE Clear Sky)

Note that, Restaurant 1 and Restaurant 2 results are simulated by DIVA except the Window Systems by Prismatic Film Complex Fenestration System. However, to have more accurate results, the results of Restaurant Prototype are simulated by Three-Phase Method (In case to have a reference, there are Illuminance data by DIVA, as well). In the following the results of Restaurant 1 (Sal Café), Restaurant 2 (Azurmendi) and Restaurant Prototype are explained:

RESTAURANT 1, R1 (Sal Café)

In the following tables there are results of Illuminance data and Daylight Autonomy index.

Nº Sensor	Point-in-Time Illuminance (lux) by DIVA, 22 July at 12:00 local time (SAL CAFÉ)								
	No Frame			Large Frame			Small Frame		
	No CFSnf	Light Shelf	3M Prismatic Film	No CFSlf	Light Shelf	3M Prismatic Film	No CFSsf	Light Shelf	3M Prismatic Film
409	221	171	220	181	167	179	109	137	131
410	240	221	196	196	181	216	112	150	142
411	242	239	230	200	231	234	130	153	165
412	296	256	266	234	235	233	145	150	215
413	322	256	303	250	248	293	158	162	207
414	325	279	332	297	265	320	180	177	248
415	352	291	320	309	292	302	209	199	272
416	387	317	323	336	315	330	208	232	242
417	436	367	466	390	360	433	228	246	311
418	493	415	510	416	395	464	271	258	324
419	543	450	498	457	440	511	270	276	393
420	599	488	505	481	455	593	285	314	389
421	644	486	663	523	535	607	335	343	404
422	703	534	732	577	524	692	367	356	520
423	804	639	817	618	612	837	420	399	554
424	836	692	884	705	698	877	442	430	613
425	940	786	1134	782	751	1009	473	467	712
426	1041	842	1122	851	847	1119	569	513	733
427	1157	963	1242	951	960	1223	613	532	851
428	1208	1080	1316	1067	1075	1312	531	573	763
429	1385	1246	1460	1203	1222	1310	569	587	791
430	**1524**	**1403**	**1504**	**1331**	**1386**	**1506**	**540**	**566**	**644**
431	**1866**	**1797**	**1787**	**1675**	**1781**	**1791**	**493**	**564**	**608**
432	**2123**	**2118**	**1983**	**1974**	**2060**	**1984**	**358**	**460**	**339**

Table 5. 1 Point-in-Time Illuminance data by DIVA of each window system for Restaurant 1, Sal Café. The results are of sensor-row from the outside to the inside that contains reference sensors of the table. Sensor points in bold are on the table

Note that, the results have the trend to be a little underestimated comparing to measurements. In No Frame No CFS case, at Sensor Point 431; measured, 2350 lux; and simulated by DIVA 1866. In addition, at Sensor Point 409; measured, 414 lux; and

simulated 221 lux. Taking into account the model errors and other approximations the trend of results of DIVA are indicative and useful.

Point-in-Time Illuminance (lux) by DIVA, 22 July at 12:00 local time (SAL CAFÉ)

	No Frame			Large Frame			Small Frame		
	No CFSnf	Light Shelf	3M Prismatic Film	No CFSlf	Light Shelf	3M Prismatic Film	No CFSsf	Light Shelf	3M Prismatic Film
$Mean_{1\text{-}552}$	609	541	601	528	532	597	350	360	421
$Mean_{409\text{-}432}$	779	681	784	667	668	766	334	344	440
$SD_{409\text{-}432}$	533	520	536	485	514	530	164	159	228
$SD_{409\text{-}432}/M_{409\text{-}432}$	0.68	0.76	0.68	0.73	0.77	0.69	0.49	0.46	0.52
$Mean_{430\text{-}432}$	1838	1773	1758	1660	1743	1760	464	530	530

Table 5. 2 Mean (M) and Standard Deviation (SD) calculation from illuminance data obtained by DIVA of each window system for Restaurant 1, Sal Café

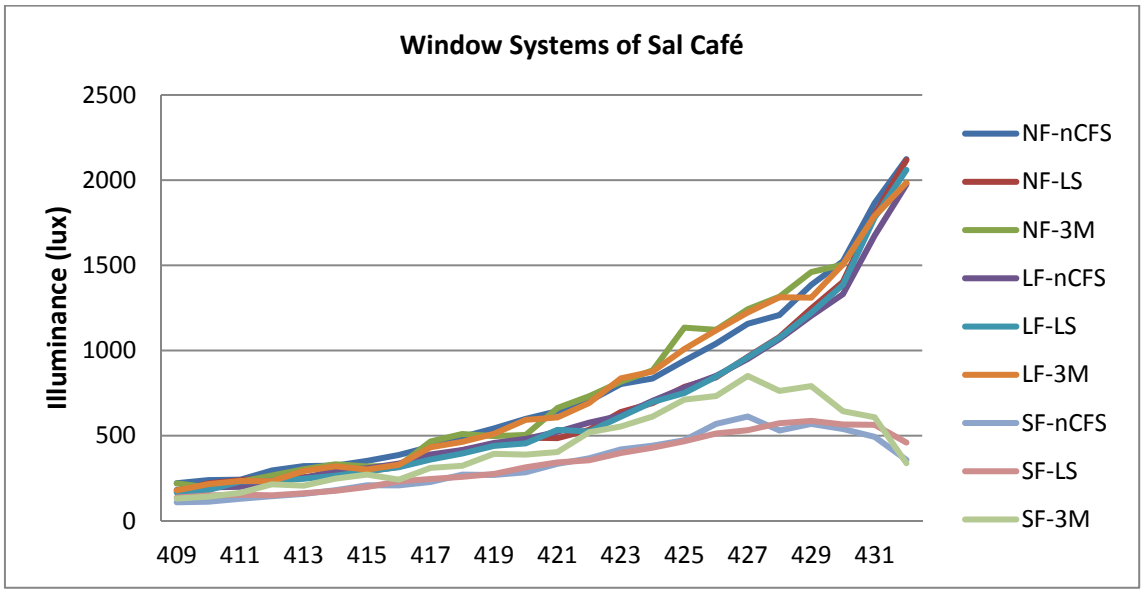

Figure 5. 16 According to sensor, Point-in-Time Illuminance data by DIVA of each window system for Restaurant 1, Sal Café

The illuminance data are on 22 of July at 11:00 Standard Time (12:00 Local Time) in Restaurant 1 (Sal Café), Barcelona under Clear Sky. The results show that the illuminance values of No Frame Window System are higher but there is not huge difference with Large Frame WS. The difference between No Frame WS and Small WS is higher (779/334= 2.33), about twice. However, the mean of the space, the row followed by the table, and the table are higher than 300 lux, which could be a

minimum to have comfort. Regarding Complex Fenestration System, the Light Shelf does not make a huge improvement on light level, but the Prismatic Film 3M improves the mean light level and the uniformity of the space, smoothing the fall on illuminance according to the deep.

Daylight Autonomy (DA, %) by DIVA and TPM, 11:00-17:00 (SAL CAFÉ)

Nº Sensor	No Frame			Large Frame			Small Frame		
	No CFSnf	Light Shelf	3M Prismatic Film (TPM)	No CFSlf	Light Shelf	3M Prismatic Film (TPM)	No CFSsf	Light Shelf	3M Prismatic Film (TPM)
409	13	6	51	4	6	38	0	0	26
410	14	7	52	4	7	38	0	0	34
411	13	22	44	6	4	54	0	3	26
412	20	9	62	9	7	57	2	0	52
413	31	21	66	19	18	65	4	1	52
414	33	35	69	29	19	60	0	1	48
415	42	31	68	24	39	64	4	5	59
416	45	41	77	28	41	77	5	8	62
417	51	39	82	42	43	79	7	17	65
418	50	42	84	38	45	84	15	19	74
419	54	49	88	50	45	87	16	26	76
420	57	51	89	56	51	88	18	30	75
421	64	52	93	56	59	91	24	18	84
422	65	62	92	56	58	91	22	22	86
423	66	60	94	58	66	95	38	26	89
424	68	72	96	68	74	95	42	35	92
425	79	75	96	75	78	96	38	38	92
426	82	80	97	80	83	97	43	48	93
427	90	90	98	83	87	97	52	52	93
428	89	88	98	88	90	98	47	49	95
429	92	91	98	93	93	98	33	48	93
430	**95**	**94**	**98**	**94**	**95**	**98**	**32**	**34**	**91**
431	**98**	**98**	**99**	**98**	**98**	**98**	**31**	**34**	**87**
432	**98**	**98**	**99**	**98**	**98**	**99**	**20**	**29**	**76**

Table 5. 3 Daylight Autonomy data for Restaurant 1, Sal Café, by DIVA of each window system, but the Prismatic Film CFS window system by TPM. The results are of sensor-row from the outside to the inside that contains reference sensors of the table. Sensor points in bold are on the table

Daylight Autonomy (DA, %) by DIVA and TPM, 11:00-17:00 (SAL CAFÉ)

	No Frame			Large Frame			Small Frame		
	No CFSnf	Light Shelf	3M Prismatic Film (TPM)	No CFSlf	Light Shelf	3M Prismatic Film (TPM)	No CFSsf	Light Shelf	3M Prismatic Film (TPM)
$Mean_{1\text{-}552}$	49.01	46.43	77.65	44.49	44.98	76.54	21.76	23.04	68.81
$Mean_{409\text{-}432}$	58.71	54.71	82.96	52.33	54.33	81.02	20.54	22.63	71.63
$SD_{409\text{-}432}$	28.21	30.17	17.51	31.92	32.23	19.73	17.11	17.52	22.19
$SD_{409\text{-}432}/M_{409\text{-}432}$	0.48	0.55	0.21	0.61	0.59	0.24	0.83	0.77	0.31
$Mean_{430\text{-}432}$	97.00	96.67	98.55	96.67	97.00	98.40	27.67	32.33	84.59

Table 5. 4 Mean (M) and Standard Deviation (SD) calculation from Daylight Autonomy for Restaurant 1, Sal Café. Data obtained by DIVA of each window system, but 3M Prismatic Film window system CFS by TPM

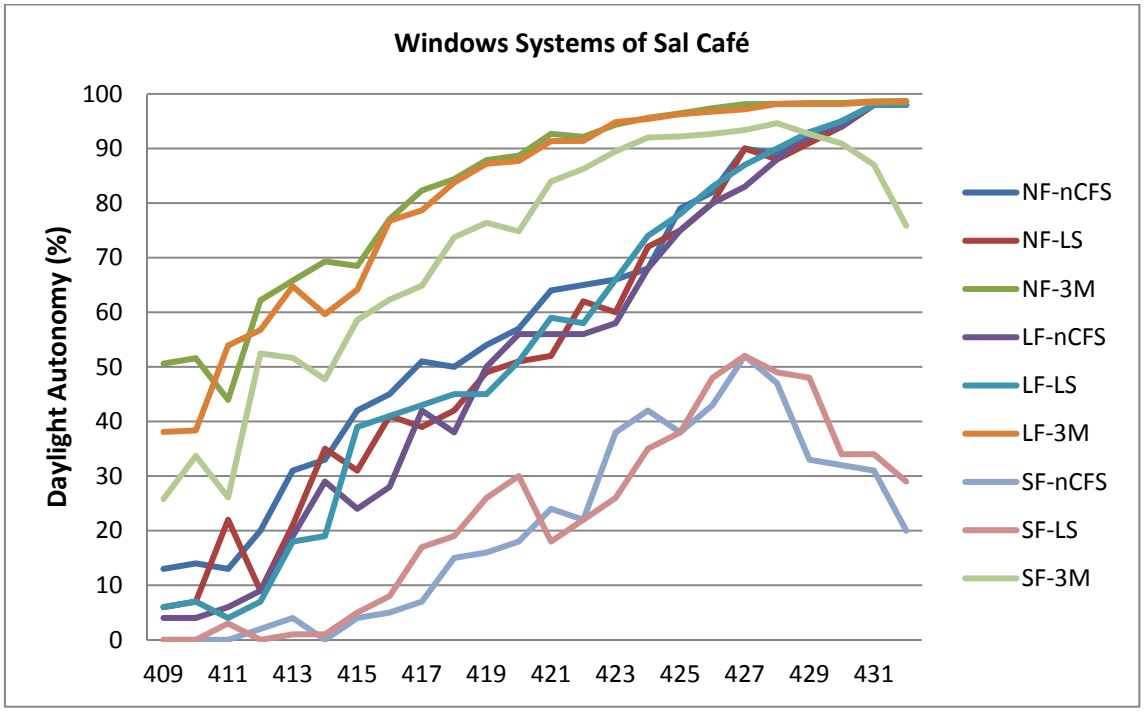

Figure 5. 17 According to sensor, Daylight Autonomy for Restaurant 1, Sal Café. Data obtained by DIVA of each window system, but 3M Prismatic Film CFS window system by TPM

The Daylight Autonomy values are of all year round from 11:00 a.m. to 17:00 p.m. in Restaurant 1 (Sal Café), Barcelona. The results of Daylight Autonomy follow the illuminance values trend, but there is difference with Prismatic Film 3M CFS because it is simulated by Three-Phase Method. In Annex 3 the comparison of illuminance data of PF-3M CFS between DIVA and TPM are explained. According to TMP results, they tend to be a little overestimated comparing with measurements. However, taking into

account some model errors and approximations the results are very closed to real results, so they are indicative and useful.

RESTAURANT 2 (Azurmendi)

In the following tables there are results of Illuminance data and Daylight Autonomy index.

	Point-in-Time Illuminance (lux) by DIVA, 25 August 12:00 local time (AZURMENDI)								
Nº Sensor	No Frame			Large Frame			Small Frame		
	No CFSnf	Light Shelf	3M Prismatic Film	No CFSlf	Light Shelf	3M Prismatic Film	No CFSsf	Light Shelf	3M Prismatic Film
335	300	280	284	248	254	273	282	264	269
336	312	323	308	319	292	279	302	282	299
337	363	332	349	323	332	324	300	315	300
338	402	379	413	381	402	432	385	379	390
339	469	408	427	426	414	427	443	413	403
340	477	469	465	472	458	464	448	443	449
341	561	470	514	488	522	504	481	468	486
342	595	527	540	537	555	565	528	507	535
343	636	611	601	606	613	611	560	586	580
344	697	663	659	653	670	676	605	601	694
345	757	744	720	719	718	751	676	659	752
346	839	757	793	798	763	828	758	739	746
347	945	831	858	862	844	869	784	791	867
348	1007	918	941	945	913	967	836	799	944
349	1055	993	1046	1047	969	1024	884	859	1026
350	1150	1013	1124	1093	1050	1115	946	887	1087
351	1250	1090	1223	1178	1040	1179	1101	922	1056
352	1351	1063	1236	1158	1086	1256	1037	887	1115
353	**1378**	**1106**	**1302**	**1209**	**1082**	**1300**	**1071**	**889**	**1122**
354	**1460**	**1055**	**1368**	**1334**	**1124**	**1344**	**1051**	**860**	**1133**
355	**1675**	**1252**	**1540**	**1508**	**1264**	**1500**	**1167**	**889**	**1179**
356	**1937**	**1580**	**1840**	**1791**	**1582**	**1818**	**1236**	**1040**	**1323**
357	**1639**	**1940**	**2121**	**2059**	**1908**	**2119**	**1289**	**1016**	**1310**
358	**2314**	**2148**	**2236**	**2213**	**2155**	**2262**	**881**	**840**	**906**

Table 5. 5 Point-in-Time Illuminance data by DIVA of each window system for Restaurant 2, Azurmendi. The results are of sensor-row from the outside to the inside that contains reference sensors of the table. Sensor points in bold are on the table

Note that, in this case as well, the results have the trend to be a little underestimated comparing to measurements. In No Frame No CFS case, at Sensor Point 356; measured, 2540 lux; and simulated by DIVA 1937. In addition, at Sensor Point 335; measured, 880 lux; and simulated 300 lux. Taking into account the model errors and other approximations the trend of results of DIVA are indicative and useful.

Point-in-Time Illuminance (lux) by DIVA, 25 August 12:00 local time (AZURMENDI)

	No Frame			Large Frame			Small Frame		
	No CFSnf	Light Shelf	3M Prismatic Film	No CFSlf	Light Shelf	3M Prismatic Film	No CFSsf	Light Shelf	3M Prismatic Film
$Mean_{1\text{-}574}$	1019	915	972	958	913	973	857	809	867
$Mean_{335\text{-}358}$	982	873	955	932	875	954	752	681	790
$SD_{335\text{-}358}$	551	494	564	550	493	562	317	244	342
$SD_{335\text{-}358}/M_{335\text{-}358}$	0.56	0.57	0.59	0.59	0.56	0.59	0.42	0.36	0.43
$Mean_{353\text{-}358}$	1734	1513	1735	1686	1519	1724	1116	922	1162

Table 5. 6 Mean (M) and Standard Deviation (SD) calculation from illuminance data obtained by DIVA of each window system for Restaurant 2, Azurmendi

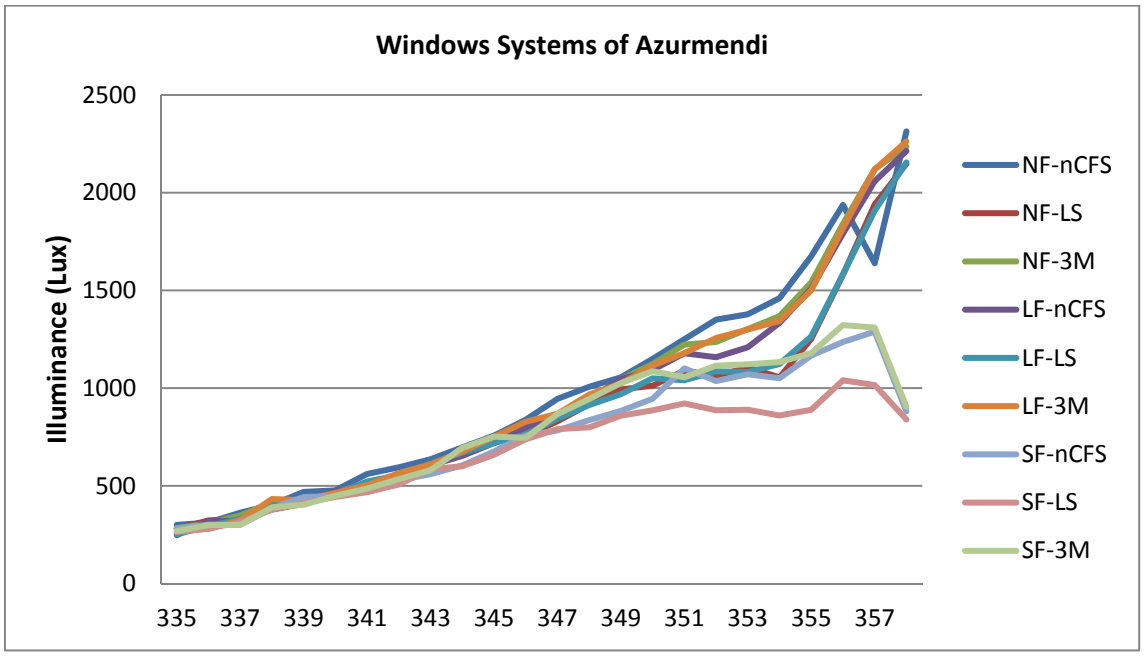

Figure 5. 18 According to sensor, Point-in-Time Illuminance data by DIVA of each window system for Restaurant 2, Azurmendi

The illuminance data are on 25 of August at 11:00 Standard Time (12:00 Local Time) in Restaurant 2 (Azurmendi), Bilbao under Intermediate Sky. In this case the difference is not huge between different Window Systems because the most of the façade of the room is transparent. However, it seems that Small Frame Window System continue contributing less light but with enough light level throughout the space, row and table. Regarding Complex Fenestrations Systems, the Prismatic Film 3M CFS contribution improves the light level and uniformity.

Daylight Autonomy (DA, %) by DIVA and TPM, 11:00-17:00 (AZURMENDI)

Nº Sensor	No Frame			Large Frame			Small Frame		
	No CFSnf	Light Shelf	3M Prismatic Film (TPM)	No CFSlf	Light Shelf	3M Prismatic Film (TPM)	No CFSsf	Light Shelf	3M Prismatic Film (TPM)
335	87	85	87	85	84	90	85	85	88
336	89	89	91	87	89	91	88	87	90
337	91	90	90	90	90	92	90	89	91
338	93	93	93	93	92	94	92	91	94
339	94	94	94	94	94	95	93	93	95
340	95	95	95	95	94	95	94	94	96
341	96	95	95	95	95	96	95	95	97
342	97	96	96	97	96	97	96	96	97
343	97	97	97	97	97	98	96	97	97
344	98	97	97	97	97	98	97	97	98
345	98	98	98	98	98	98	98	97	98
346	99	98	98	98	98	99	98	98	99
347	99	98	98	99	98	99	98	98	99
348	99	99	99	99	99	99	99	98	99
349	99	99	99	99	99	99	99	98	99
350	99	99	99	99	99	99	99	99	99
351	99	99	99	99	99	99	99	98	99
352	99	99	99	99	99	99	99	98	99
353	**99**	**99**	**99**	**99**	**99**	**100**	**99**	**98**	**99**
354	**100**	**99**	**99**	**99**	**99**	**100**	**99**	**98**	**99**
355	**100**	**99**	**99**	**100**	**99**	**100**	**99**	**98**	**99**
356	**100**	**99**	**99**	**100**	**99**	**100**	**99**	**98**	**99**
357	**100**	**100**	**100**	**100**	**100**	**100**	**98**	**98**	**99**
358	**100**	**100**	**100**	**100**	**100**	**100**	**95**	**96**	**98**

Table 5. 7 Daylight Autonomy data for Restaurant 2, Azurmendi, by DIVA of each window system, but the Prismatic Film CFS window system by TPM. The results are of sensor-row from the outside to the inside that contains reference sensors of the table. Sensor points in bold are on the table

Daylight Autonomy (DA, %) by DIVA and TPM, 11:00-17:00 (AZURMENDI)

	No Frame			Large Frame			Small Frame		
	No CFSnf	Light Shelf	3M Prismatic Film (TPM)	No CFSlf	Light Shelf	3M Prismatic Film (TPM)	No CFSsf	Light Shelf	3M Prismatic Film (TPM)
$Mean_{1\text{-}574}$	96.43	96.18	96.95	96.14	96.17	96.93	95.71	95.64	96.62
$Mean_{335\text{-}358}$	96.96	96.50	96.66	96.58	96.38	97.41	96.00	95.58	96.95
$SD_{335\text{-}358}$	3.67	3.86	3.46	4.13	4.05	2.99	3.90	3.86	3.14
$SD_{335\text{-}358}/M_{335\text{-}358}$	0.04	0.04	0.04	0.04	0.04	0.03	0.04	0.04	0.03
$Mean_{353\text{-}358}$	99.83	99.33	99.33	99.67	99.33	99.72	98.17	97.67	98.81

Table 5. 8 Mean (M) and Standard Deviation (SD) calculation from Daylight Autonomy for Restaurant 2, Azurmendi. Data obtained by DIVA of each window system, but 3M Prismatic Film window system CFS by TPM

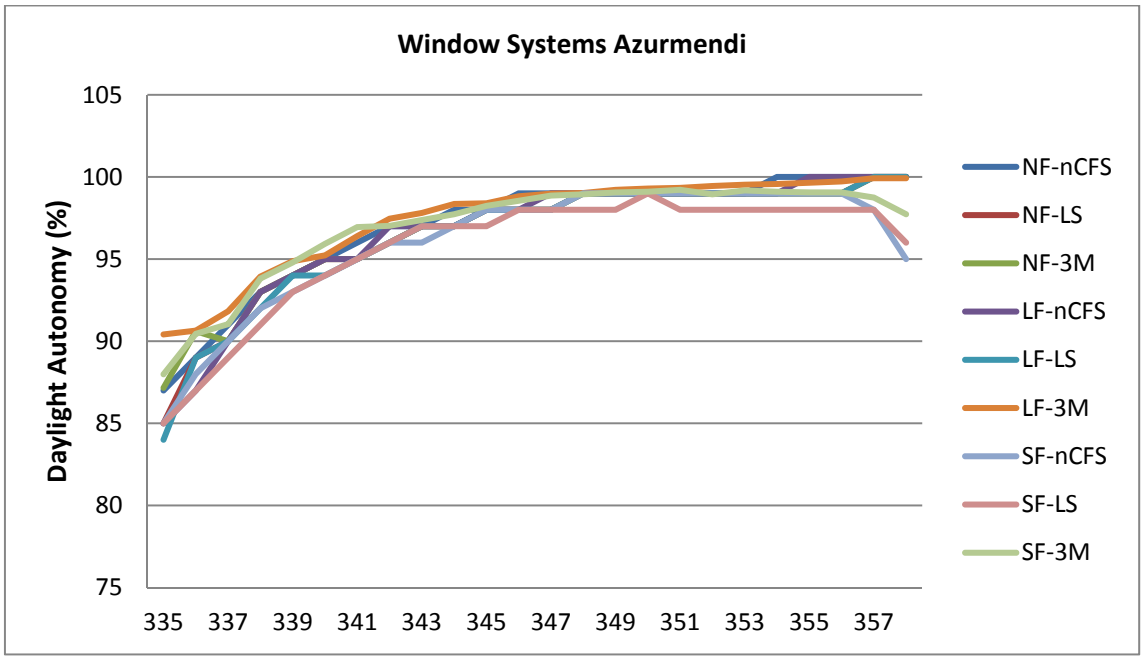

Figure 5. 19 According to sensor, Daylight Autonomy for Restaurant 2, Azurmendi. Data obtained by DIVA of each window system, but 3M Prismatic Film CFS window system by TPM

The Daylight Autonomy values are of all year round from 11:00 a.m. to 17:00 p.m. in Restaurant 2 (Azurmendi), Bilbao. The results of Daylight Autonomy follow the illuminance values trend, but as there is much transparent part there is enough level in the most room and majorities of time with all Window Systems. However, the Small Frame WS continue having the least light level performance and PF-3M CFS have the best light level performance. Note that, the difference between PF-3M CFS performance by TPM and the other WSs is lower, that is explained better in Annex 3.

	Illuminance measurements (lux)	
	Restaurant1 (Sal Café)	Restaurant2 (Azurmendi)
Exterior horizontal plane	82 000	73 500
Exterior vertical plane	13 200	9 760
Sensor Point $431_{SalCafé}$ and $356_{Azurmendi}$	2350	2 540
Sensor Point $409_{SalCafé}$ and $335_{Azurmendi}$	414	880

Table 5. 9 Illuminance measurements; in Restaurant 1 (Sal Café), 22 July at 12:00 local time; and in Restaurant 2 (Azurmendi), 25 August at 12:00 local time

Regarding Daylight Autonomy of different window system performance results of Restaurant 1 (Sal Café) and Restaurant 2 (Azurmendi), they are very different case to compare but it seems that they have the same trend. There is not huge difference between No Frame SW and Large Frame WS. However, the difference is more between No Frame SW and Small Frame WS, but in both case there is enough level at 11:00 a.m with Small Frame WS. The Complex Fenestration Systems increase mean light level lighting better table workplane, although Light Shelf's contribution is not as much as 3M Prismatic Film contribution and in No Frame case the improvement of CFS is not considerable.

Restaurant 1 (Sal Café) has less Daylight Autonomy than Restaurant 2 (Azurmendi), due to the amount of glass façade of each room. On one hand the Restaurant 1 (Sal Café) has almost 50% of DA with No Frame and Large Frame WSs and almost 20% of DA with Small Frame WS. Taking into account the contribution of PF-3M CFS, the Small Frame's Daylight Autonomy increases more than twice approaching No Frame without CFS WS DA results. On the other hand, in Restaurant 2 (Azurmendi) the results between different Window Systems almost are the same approximately 95%, due to many windows light contribution.

Taking into account that the studied real restaurants are different and the Daylight Autonomy (DA) data are obtained by different methods, virtual restaurant prototype is proposed to get DA performance. As the Three-Phase Method results trend is reasonable, all Window Systems' Daylight Autonomy of virtual restaurant prototype have been got by Three-Phase Method. It is explained in the following section.

RESTAURANT PROTOTYPE

In the following tables there are results of Illuminance data and Daylight Autonomy index.

Point-in-Time Illuminance (lux) by DIVA, 22 July at 12:00 local time (PROTOTYPE)

Nº Sensor	No Frame			Large Frame			Small Frame		
	No CFSnf	Light Shelf	3M Prismatic Film	No CFSlf	Light Shelf	3M Prismatic Film	No CFSsf	Light Shelf	3M Prismatic Film
157	**3409**	**3324**	**4531**	**3297**	**3218**	**4328**	**807**	**856**	**1826**
158	**2852**	**2741**	**4025**	**2750**	**2710**	**3900**	**1135**	**1126**	**2312**
159	**2354**	**2331**	**3869**	**2258**	**2245**	**3572**	**1122**	**1187**	**2388**
160	2030	2046	3630	1915	2016	3360	1138	1215	2603
161	1807	1879	3130	1722	1808	3282	1100	1171	2810
162	1661	1664	2842	1562	1605	2820	1037	1149	2186
163	1452	1495	2726	1413	1445	2547	957	1018	2087
164	1336	1314	2518	1248	1282	2309	825	909	2012
165	1150	1163	2176	1085	1113	2066	752	801	1729
166	1017	1022	1923	955	988	1818	634	686	1523
167	929	898	1633	821	854	1561	548	608	1394
168	800	787	1425	718	742	1232	506	514	1117
169	720	708	1294	631	667	1238	445	460	818
170	645	612	1087	564	592	996	385	417	801
171	578	518	845	492	540	964	319	345	689
172	479	480	829	448	442	756	284	323	644
173	466	427	674	401	400	603	260	271	463
174	417	390	590	351	361	520	233	248	477
175	382	354	693	322	328	512	204	217	386
176	348	323	467	289	300	457	182	187	350
177	320	304	432	268	271	482	170	179	382
178	302	288	417	243	254	448	150	167	355
179	282	274	411	229	230	303	146	147	273
180	281	240	357	219	216	355	142	135	223
181	250	249	332	221	211	322	132	133	214
182	250	230	313	196	208	310	129	126	244

Table 5. 10 Point-in-Time Illuminance data by DIVA of each window system for Virtual Restaurant Prototype. The results are of sensor-row from the outside to the inside that contains reference sensors of the table. Sensor points in bold are on the table

	Point-in-Time Illuminance (lux) by DIVA (PROTOTYPE)								
	No Frame			Large Frame			Small Frame		
	No CFSnf	Light Shelf	3M Prismatic Film	No CFSlf	Light Shelf	3M Prismatic Film	No CFSsf	Light Shelf	3M Prismatic Film
$Mean_{1-286}$	962	948	1568	886	900	1487	481	503	1105
$Mean_{157-182}$	1020	1002	1660	947	963	1579	528	561	1166
$SD_{157-182}$	867	860	1336	850	845	1284	373	397	868
$SD_{157-182}/M_{157-182}$	0.85	0.86	0.80	0.90	0.88	0.81	0.71	0.71	0.74
$Mean_{157-159}$	2872	2799	4142	2768	2724	3933	1021	1056	2175

Table 5. 11 Mean (M) and Standard Deviation (SD) calculation from illuminance data obtained by DIVA of each window system for Virtual Restaurant Prototype

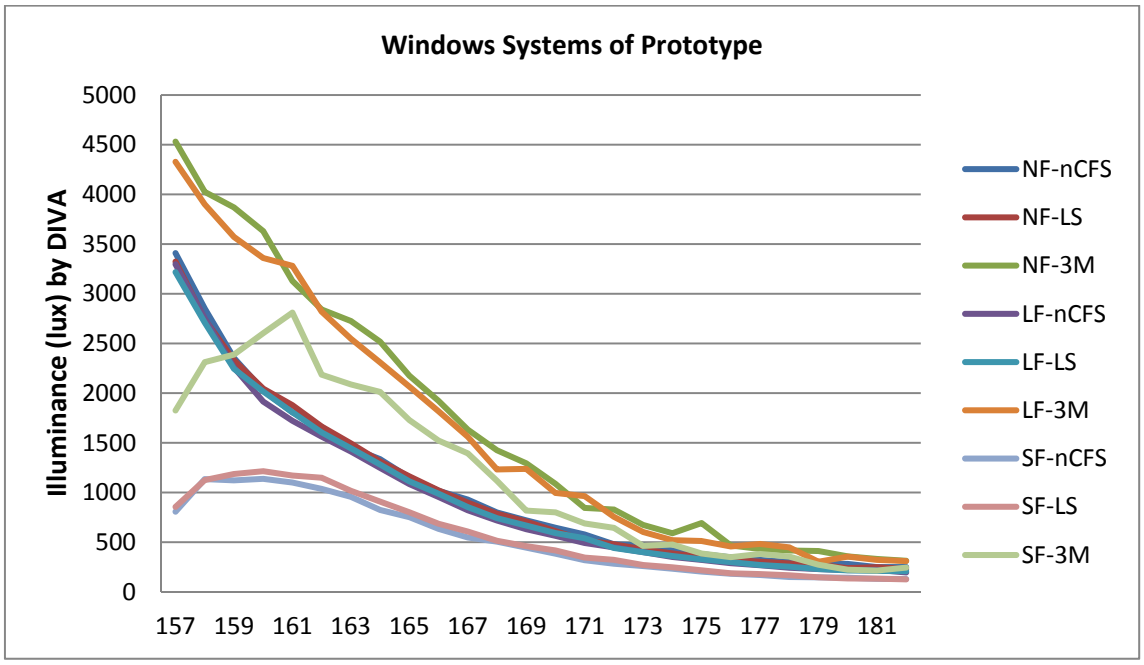

Figure 5. 20 According to sensor, Point-in-Time Illuminance data by DIVA of each window system for Virtual Restaurant Prototype

The illuminance data are on 22 of July at 11:00 Standard Time (12:00 Local Time) in Restaurant Prototype, Barcelona under Clear Sky with Sun (CIE Clear Sky). The results show that the illuminance values of No Frame Window System are higher but there is not huge difference with Large Frame WS. The difference between No Frame WS and Small WS is higher (962/481= 2), about twice. However, the mean of the space, the row followed by the table, and the table are higher than 300 lux, which could be a minimum to have comfort. Regarding Complex Fenestration System, the Light Shelf does not make a huge improvement on light level, but the Prismatic Film 3M improves

the mean light level and the uniformity of the space, smoothing the fall on illuminance according to the deep.

Point-in-Time Illuminance (lux) by TPM, 22 July at 12:00 local time (PROTOTYPE)

Nº Sensor	No Frame			Large Frame			Small Frame		
	No CFSnf	Light Shelf	3M Prismatic Film	No CFSlf	Light Shelf	3M Prismatic Film	No CFSsf	Light Shelf	3M Prismatic Film
157	**7002**	**8581**	**8232**	**5903**	**8000**	**6701**	**1092**	**1993**	**1651**
158	**5951**	**7360**	**7333**	**5162**	**6894**	**6110**	**1522**	**3046**	**2580**
159	**5087**	**6197**	**6317**	**4377**	**5874**	**5521**	**1708**	**3498**	**2815**
160	4307	5264	5596	3713	5041	5096	1817	3342	3076
161	3980	4826	5167	3459	4548	4652	1867	3363	3219
162	3653	4289	4729	3216	4045	4403	1784	2980	3200
163	3340	3796	4200	2918	3613	4040	1632	2779	2904
164	2816	3367	3896	2625	3157	3392	1522	2306	2479
165	2522	2852	3472	2332	2701	3078	1337	2086	2296
166	2205	2536	2881	2016	2309	2549	1250	1852	2066
167	1962	2120	2491	1681	2034	2355	1092	1576	1852
168	1722	1881	2068	1586	1761	2002	1018	1315	1477
169	1472	1681	2032	1306	1557	1767	903	1158	1213
170	1332	1473	1704	1204	1418	1597	845	1063	1001
171	1156	1264	1499	1116	1128	1265	656	898	1104
172	1051	1202	1329	992	1018	1184	611	810	942
173	973	1020	1074	826	875	1080	570	583	860
174	818	896	1059	714	836	920	502	612	800
175	773	888	897	688	728	874	498	612	699
176	775	721	843	682	675	784	492	489	539
177	680	687	779	596	617	724	355	468	499
178	569	619	830	527	597	647	398	429	516
179	580	704	683	506	494	532	311	409	330
180	548	578	641	446	547	550	326	365	415
181	498	550	685	472	505	557	290	366	463
182	490	549	679	425	431	449	332	337	457

Table 5. 12 Point-in-Time Illuminance data by TPM of each window system for Virtual Restaurant Prototype. The results are of sensor-row from the outside to the inside that contains reference sensors of the table. Sensor points in bold are on the table

Point-in-Time Illuminance (lux) by TPM, 22 July at 12:00 local time (PROTOTYPE)									
	No Frame			Large Frame			Small Frame		
	No CFSnf	Light Shelf	3M Prismatic Film	No CFSlf	Light Shelf	3M Prismatic Film	No CFSsf	Light Shelf	3M Prismatic Film
$Mean_{1-286}$	2108	2432	2579	1823	2244	2298	881	1348	1398
$Mean_{157-182}$	2164	2535	2735	1903	2362	2416	951	1490	1517
$SD_{157-182}$	1839	2284	2271	1572	2166	1953	548	1102	1004
$SD_{157-182}/M_{157-182}$	0.85	0.90	0.83	0.83	0.92	0.81	0.58	0.74	0.66
$Mean_{157-159}$	6013	7379	7294	5147	6923	6111	1441	2846	2348

Table 5. 13 Mean (M) and Standard Deviation (SD) calculation from illuminance data obtained by TPM of each window system for Virtual Restaurant Prototype

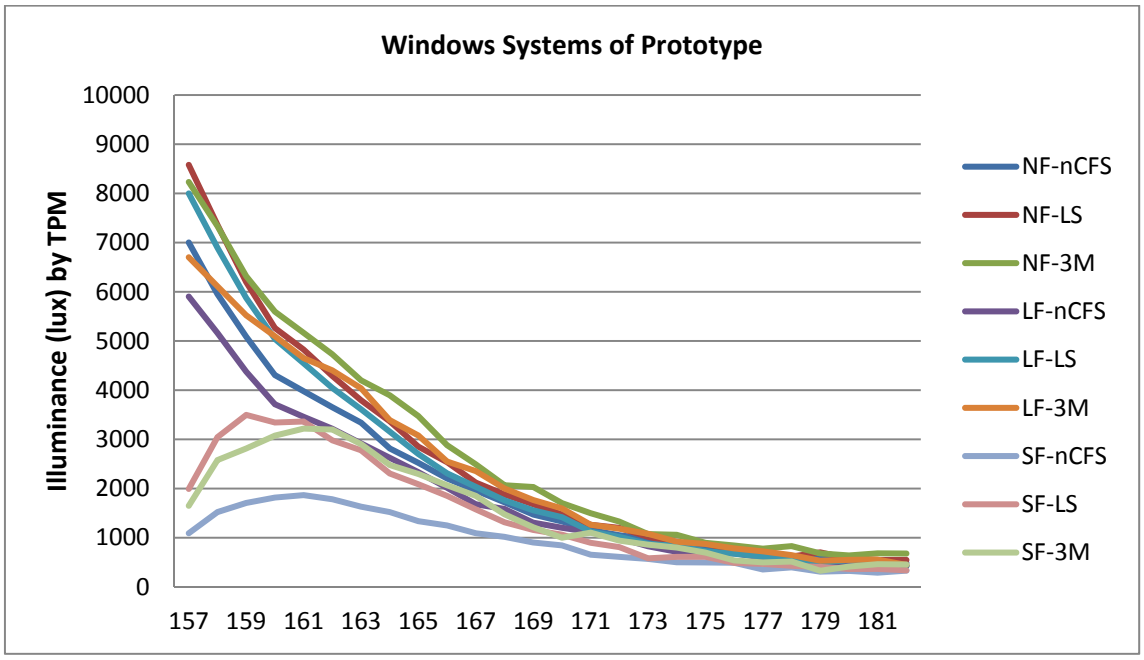

Figure 5. 21 According to sensor, Point-in-Time Illuminance data by TPM of each window system for Virtual Restaurant Prototype

The Illuminance data obtained by Three-Phase Method follow almost the same trend of Illuminance data obtained by DIVA, although Three-Phase Method values are higher. However, there is a difference with Light Shelf Complex Fenestration System. That is because in Three-Phase Method the Light Shelf is not simulated as Glow and Translucent_20 light source material. Therefore, the back Clear Glass has only the little overhang of Light Shelf protection. The Light Shelf Complex Fenestration System simulation should be improved.

	DIVA and TPM illuminance (lux) results comparison							
Nº Sensor	DIVA NF nCFS	TPM NF nCFS	DIVA NF 3M	TPM NF 3M	DIVA SF nCFS	TPM SF nCFS	DIVA SF 3M	TPM SF 3M
157	**3409**	**7002**	**4531**	**8232**	**807**	**1092**	**1826**	**1651**
158	**2852**	**5951**	**4025**	**7333**	**1135**	**1522**	**2312**	**2580**
159	**2354**	**5087**	**3869**	**6317**	**1122**	**1708**	**2388**	**2815**
160	2030	4307	3630	5596	1138	1817	2603	3076
161	1807	3980	3130	5167	1100	1867	2810	3219
162	1661	3653	2842	4729	1037	1784	2186	3200
163	1452	3340	2726	4200	957	1632	2087	2904
164	1336	2816	2518	3896	825	1522	2012	2479
165	1150	2522	2176	3472	752	1337	1729	2296
166	1017	2205	1923	2881	634	1250	1523	2066
167	929	1962	1633	2491	548	1092	1394	1852
168	800	1722	1425	2068	506	1018	1117	1477
169	720	1472	1294	2032	445	903	818	1213
170	645	1332	1087	1704	385	845	801	1001
171	578	1156	845	1499	319	656	689	1104
172	479	1051	829	1329	284	611	644	942
173	466	973	674	1074	260	570	463	860
174	417	818	590	1059	233	502	477	800
175	382	773	693	897	204	498	386	699
176	348	775	467	843	182	492	350	539
177	320	680	432	779	170	355	382	499
178	302	569	417	830	150	398	355	516
179	282	580	411	683	146	311	273	330
180	281	548	357	641	142	326	223	415
181	250	498	332	685	132	290	214	463
182	250	490	313	679	129	332	244	457

Table 5. 14 Comparison of Point-in-Time Illuminance results between DIVA and TPM for No Frame window Systems without CFS and No Frame window system with 3M Prismatic Film CFS. Sensor points in bold are on the table

	DIVA and TPM illuminance (lux) comparison (PROTOTYPE)								
	No Frame			Large Frame			Small Frame		
	No CFSnf	Light Shelf	3M Prismatic Film	No CFSlf	Light Shelf	3M Prismatic Film	No CFSsf	Light Shelf	3M Prismatic Film
$Mean_{157\text{-}182}TPM/ Mean_{157\text{-}182}DIVA$	2.12	2.53	1.65	2.00	2.45	1.53	1.80	2.66	1.30

Table 5. 15 Relation of mean illuminance results between DIVA and TPM for each window systems

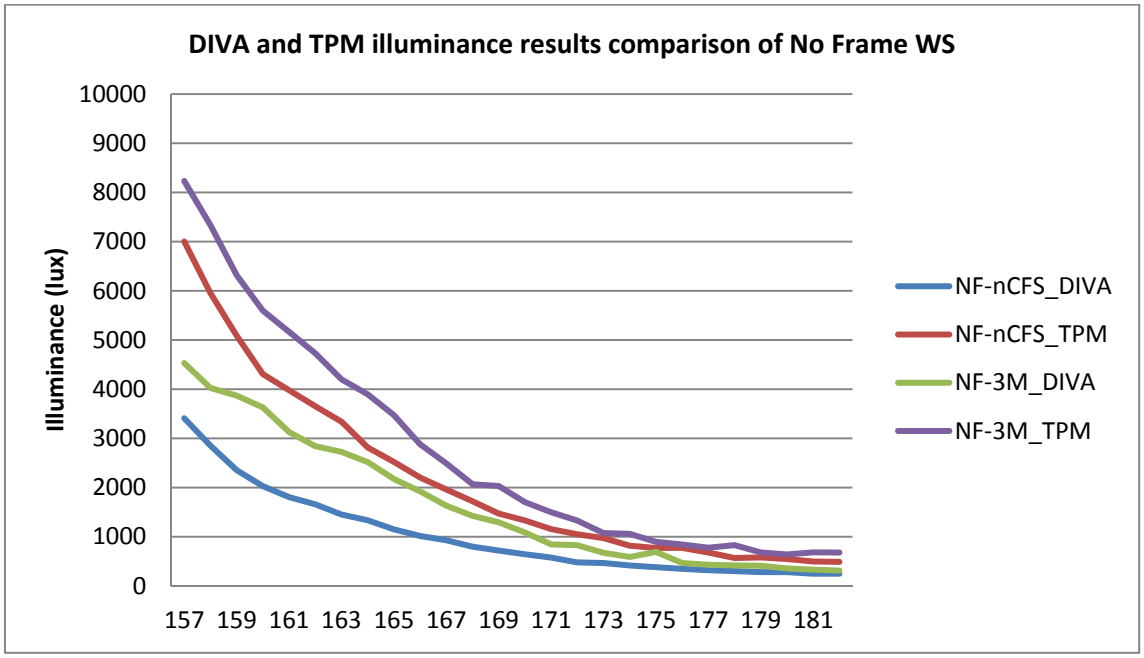

Figure 5. 22 Comparison of Point-in-Time Illuminance results between DIVA and TPM for No Frame window Systems without CFS and No Frame window system with 3M Prismatic Film CFS

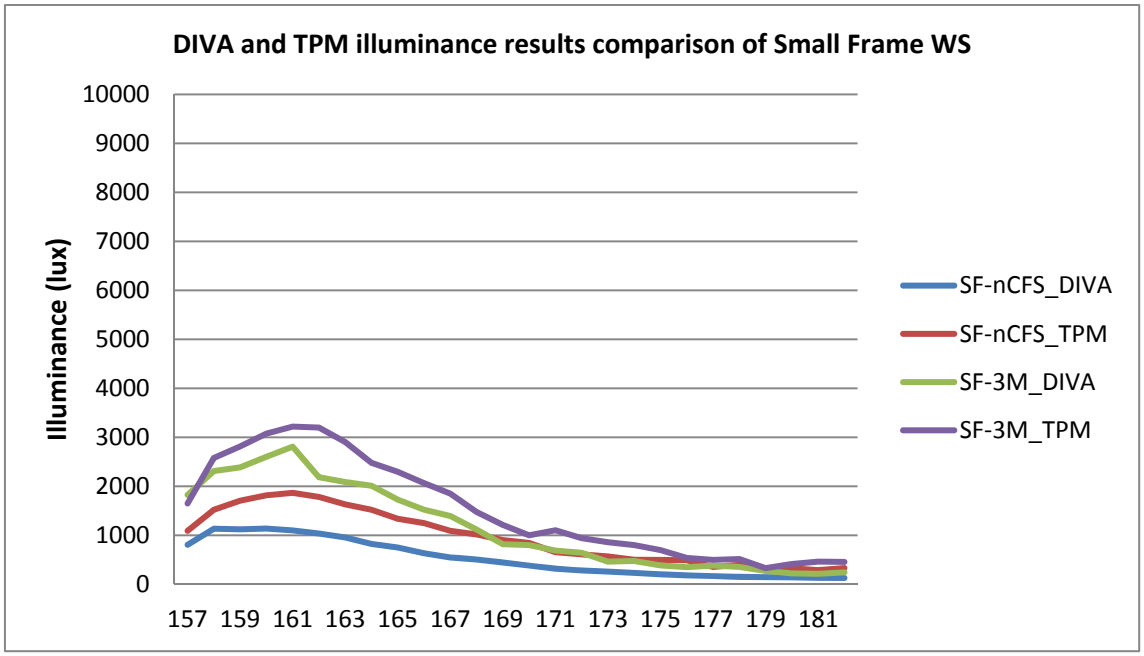

Figure 5. 23 Comparison of Point-in-Time Illuminance results between DIVA and TPM for Small Frame window Systems without CFS and Small Frame window system with 3M Prismatic Film CFS

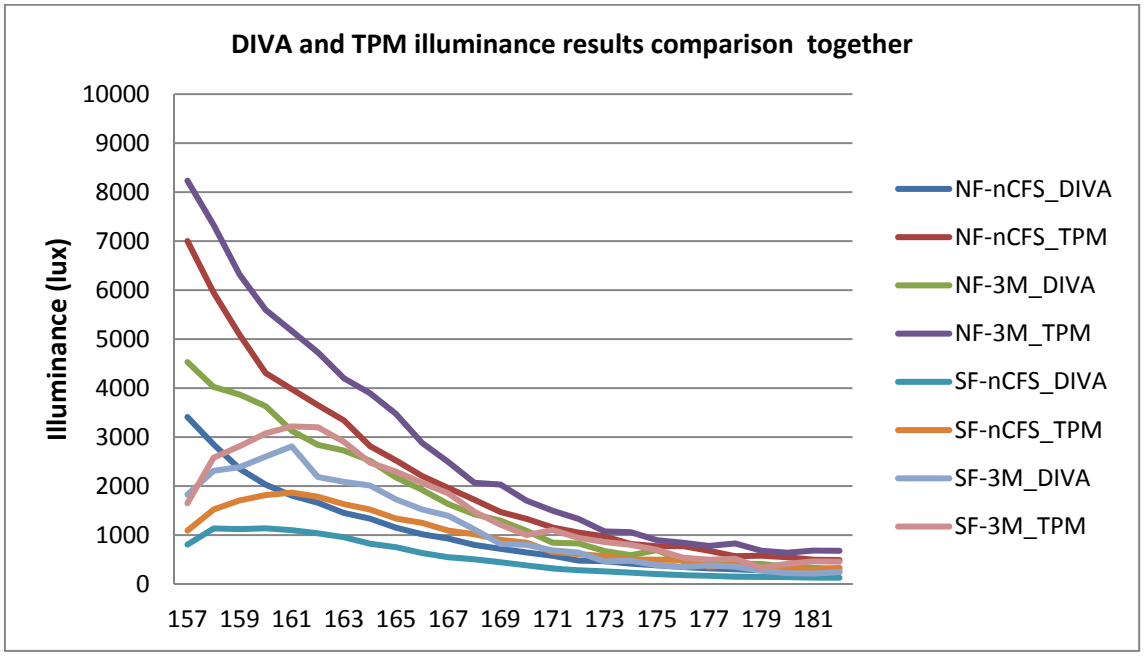

Figure 5. 24 Comparison of Point-in-Time Illuminance results between DIVA and TPM for No Frame window Systems without CFS, No Frame window system with 3M Prismatic Film CFS, Small Frame window Systems without CFS and Small Frame window system with 3M Prismatic Film CFS

The difference of Illuminance data between Three-Phase Method and DIVA is considerable. Taking into account that the real measurements are in the middle between both methods, the absolute values of simulations should not be very accurate but the trend of different window system performances and the comparison among them should be indicative and useful.

	Daylight Autonomy (DA, %) by TPM, 11:00-17:00 (PROTOTYPE)								
Nº Sensor	No Frame			Large Frame			Small Frame		
	No CFSnf	Light Shelf	3M Prismatic Film	No CFSlf	Light Shelf	3M Prismatic Film	No CFSsf	Light Shelf	3M Prismatic Film
157	**100**	**100**	**100**	**100**	**100**	**100**	**90**	**98**	**98**
158	**100**	**100**	**100**	**100**	**100**	**100**	**96**	**99**	**98**
159	**100**	**100**	**100**	**100**	**100**	**100**	**98**	**99**	**99**
160	100	100	100	100	100	100	98	99	99
161	100	100	100	100	100	100	98	99	99
162	100	100	100	100	100	100	98	99	99
163	100	100	100	100	100	100	98	99	99
164	100	100	100	100	100	100	98	99	99
165	100	100	100	99	100	100	98	99	99
166	99	100	99	99	99	99	98	99	99
167	99	99	99	99	99	99	97	98	98
168	99	99	99	99	99	99	97	98	98
169	99	99	99	98	99	98	97	98	97
170	98	99	98	98	98	98	96	97	94
171	98	98	98	98	98	97	92	95	96
172	98	98	98	98	98	97	92	94	92
173	97	98	96	96	97	96	90	89	92
174	96	96	96	95	96	95	87	90	91
175	94	97	93	94	95	92	88	91	87
176	95	93	92	93	92	91	87	85	82
177	93	92	91	91	91	90	77	85	79
178	88	91	91	87	91	87	81	82	81
179	90	93	87	87	86	83	66	81	63
180	88	89	86	82	90	83	70	75	71
181	87	89	89	85	88	85	61	75	79
182	86	89	89	84	84	77	73	72	78

Table 5. 16 Daylight Autonomy data of each window system by TPM for Virtual Restaurant Prototype. The results are of sensor-row from the outside to the inside that contains reference sensors of the table. Sensor points in bold are on the table

Daylight Autonomy (DA, %) by TPM, 11:00-17:00 (PROTOTYPE)									
	No Frame			Large Frame			Small Frame		
	No CFSnf	Light Shelf	3M Prismatic Film	No CFSlf	Light Shelf	3M Prismatic Film	No CFSsf	Light Shelf	3M Prismatic Film
$Mean_{1\text{-}286}$	95	96	95	95	95	94	86	90	89
$Mean_{157\text{-}182}$	96	97	96	95	96	95	89	92	91
$SD_{157\text{-}182}$	4.67	4.00	4.68	5.72	4.87	6.71	11.10	8.73	10.14
$SD_{157\text{-}182}/M_{157\text{-}182}$	0.05	0.04	0.05	0.06	0.05	0.07	0.12	0.09	0.11
$Mean_{157\text{-}159}$	100	100	100	100	100	100	95	98	98

Table 5. 17 Mean (M) and Standard Deviation (SD) calculation from Daylight Autonomy for Virtual Restaurant Prototype. Data of each window systems obtained by TPM

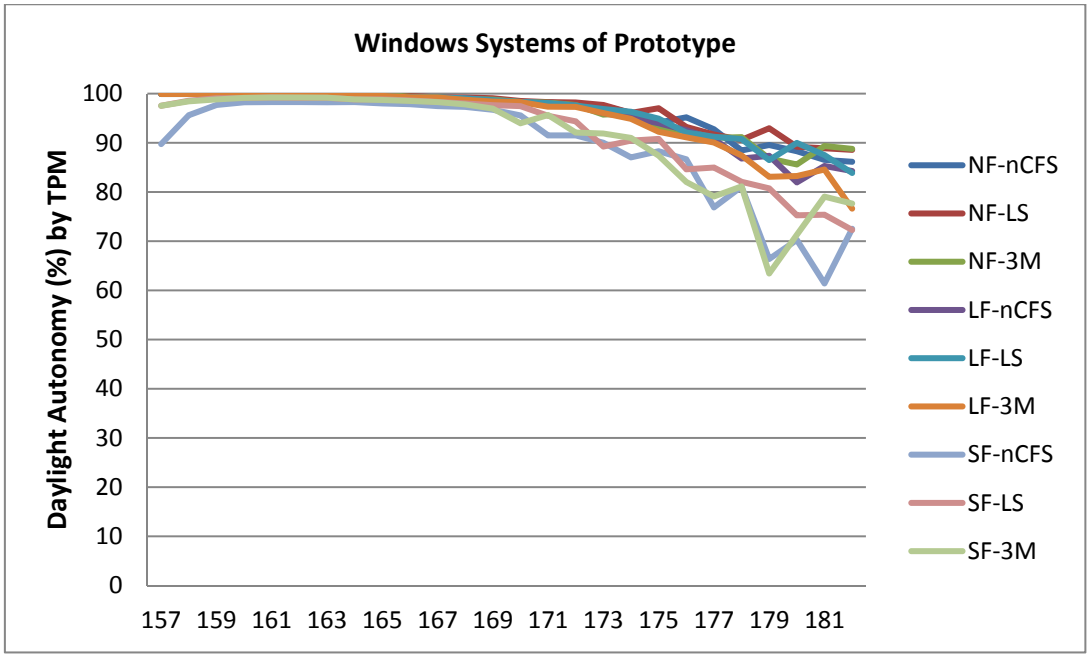

Figure 5. 25 According to sensor, Daylight Autonomy for Virtual Restaurant Prototype. Data of each window system obtained by TPM

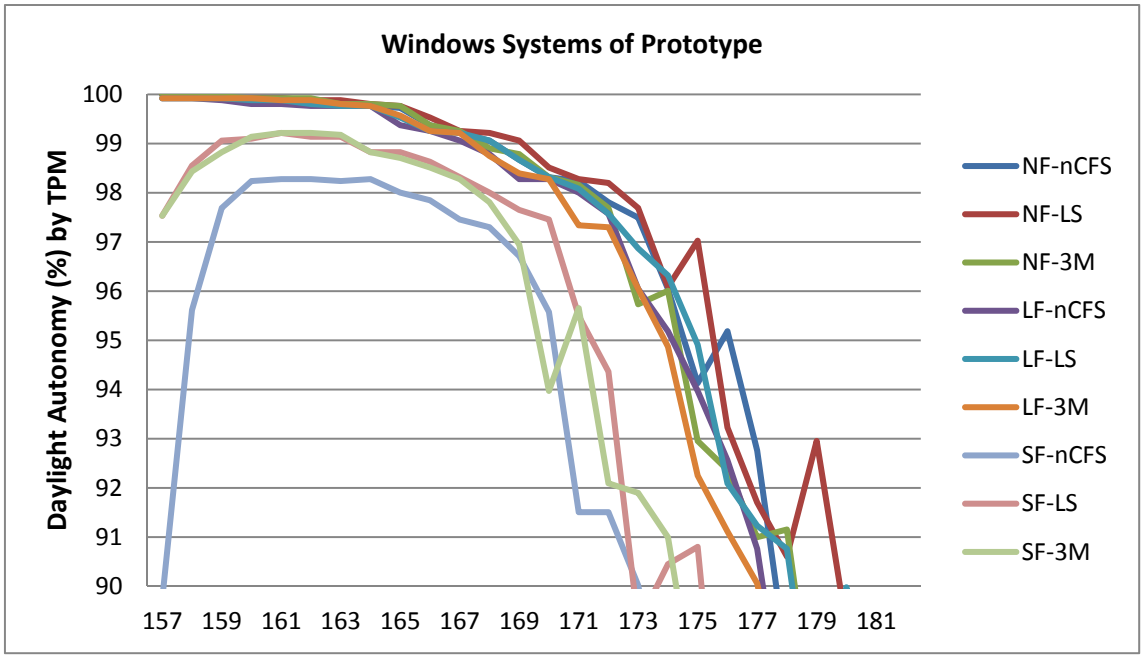

Figure 5. 26 According to sensor, Daylight Autonomy for Virtual Restaurant Prototype. Data of each window system obtained by TPM. DA results from 90%

The Daylight Autonomy values are of all year round from 11:00 a.m. to 17:00 p.m. in Restaurant Prototype, Barcelona. The results of Daylight Autonomy follow the illuminance values trend of each Window System. The Daylight Autonomy of different Window Systems is similar between 86% and 95%. The performance of Light-Shelf CFS is not very accurate, so it has not been taken into account.

Therefore, all Window System has good DA results. The Small Frame has the lowest DA results but they are good, 86 % of DA. In addition, with Prismatic Film 3M CFS the results improve a little, 89 % of DA.

Note that, in the table there is not almost difference between different Window System DA results, taking into account 300 lux as target illuminance value. In consequence, if Out View is smaller than fully glazed façade but if it has other light penetration the light level and the distribution throughout the room should be enough for visual comfort.

In the following tables there are relations between different Window Systems. They should be useful to evaluate them.

Point-in-Time Illuminance by DIVA (SAL CAFÉ)

	No Frame			Large Frame			Small Frame		
	No CFSnf	Light Shelf/ No CFSnf	3M Prismatic Film/ No CFSnf	No CFSlf/ No CFSnf	Light Shelf/ No CFSlf	3M Prismatic Film/ No CFSlf	No CFSsf/ No CFSnf	Light Shelf/ No CFSsf	3M Prismatic Film/ No CFSsf
$Mean_{409-432}$	1	0.87	1.01	0.86	1.00	1.15	0.43	1.03	1.32

Daylight Autonomy (SAL CAFÉ)

	DIVA		TPM	DIVA		TPM	DIVA		TPM
	No CFSnf	Light Shelf/ No CFSnf	3M Prismatic Film/ No CFSnf	No CFSlf/ No CFSnf	Light Shelf/ No CFSlf	3M Prismatic Film/ No CFSlf	No CFSsf/ No CFSnf	Light Shelf/ No CFSsf	3M Prismatic Film/ No CFSsf
$Mean_{409-432}$	1	0.93	1.41	0.89	1.04	1.55	0.35	1.10	3.49

Table 5. 18 Relation of mean illuminance results between window systems for Restaurant 1, Sal Café

Point-in-Time Illuminance by DIVA (AZURMENDI)

	No Frame			Large Frame			Small Frame		
	No CFSnf	Light Shelf/ No CFSnf	3M Prismatic Film/ No CFSnf	No CFSlf/ No CFSnf	Light Shelf/ No CFSlf	3M Prismatic Film/ No CFSlf	No CFSsf/ No CFSnf	Light Shelf/ No CFSsf	3M Prismatic Film/ No CFSsf
$Mean_{335-358}$	1	0.89	1.00	0.95	0.94	1.02	0.77	0.90	1.05

Daylight Autonomy (AZURMENDI)

	DIVA		TPM	DIVA		TPM	DIVA		TPM
	No CFSnf	Light Shelf/ No CFSnf	3M Prismatic Film/ No CFSnf	No CFSlf/ No CFSnf	Light Shelf/ No CFSlf	3M Prismatic Film/ No CFSlf	No CFSsf/ No CFSnf	Light Shelf/ No CFSsf	3M Prismatic Film/ No CFSsf
$Mean_{335-358}$	1	1.00	1.00	1.00	1.00	1.01	0.99	1.00	1.01

Table 5. 19 Relation of mean illuminance results between window systems for Restaurant 2, Azurmendi

To take into account the contribution of only proposed Window Systems the Restaurant Prototype is more reliable. Therefore, in the following table there are results of relation between different Window Systems.

Point-in-Time Illuminance by TPM (PROTOTYPE)

	No Frame			Large Frame			Small Frame		
	No CFSnf	Light Shelf/ No CFSnf	3M Prismatic Film/ No CFSnf	No CFSlf/ No CFSnf	Light Shelf/ No CFSlf	3M Prismatic Film/ No CFSlf	No CFSsf/ No CFSnf	Light Shelf/ No CFSsf	3M Prismatic Film/ No CFSsf
$Mean_{157\text{-}182}$	1	1.17	1.26	0.88	1.24	1.27	0.44	1.57	1.59

Daylight Autonomy by TPM (PROTOTYPE)

	DIVA		TPM	DIVA		TPM	DIVA		TPM
	No CFSnf	Light Shelf/ No CFSnf	3M Prismatic Film/ No CFSnf	No CFSlf/ No CFSnf	Light Shelf/ No CFSlf	3M Prismatic Film/ No CFSlf	No CFSsf/ No CFSnf	Light Shelf/ No CFSsf	3M Prismatic Film/ No CFSsf
$Mean_{157\text{-}182}$	1	1.01	1.00	0.99	1.01	1.00	0.93	1.03	1.02

Table 5. 20 Relation of mean illuminance results between window systems for Virtual Restaurant Prototype, Azurmendi

It seems that with studied virtual prototype if the window is smaller the Prismatic Film CFS improves more the light performance, from almost 25% of improvement to almost 60% of improvement. The improvement is not very notably in DA because in all Window Systems get to almost 300 lux level. Add that, there is not huge difference between No Frame and Large Frame in lighting contribution to the workplane.

Chapter VI

CONCLUSIONS

This chapter will be divided into four parts. The conclusions on each parameter, luminance and illuminance distributions, will be presented separately. In another section at the end, the general conclusions and future works will be discussed.

6.1 Conclusions on Parameter 1: luminance distribution evaluated by the Daylight Glare Probability (DGP) index

The Daylight Glare Probability index was used to assess luminance distribution. Three workplanes were selected for a table next to the façade at the restaurant: WP1, toward to down visual field; WP2, toward to front visual field; and WP3, toward to out visual field. The Daylight Glare Probability index was used for the indoor luminance range. Accordingly, the largest part of the outside view (WP3), which is close to the façade view, is the outdoor portion. Therefore, the DGP of the outside view (WP3) is a little overestimated, but the trend in this workplane's DGP helped to predict approximately the overall glare perception. Furthermore, in a simple way, the mean DGP of the three defined workplanes was obtained to consider in detail the different workplanes' Daylight Glare Probability. So, the index was useful for a basic test of the overall quality of indoor atmospheres.

Two real restaurants and a virtual restaurant were evaluated with Clear Sky. For the real restaurants, three window systems were analysed. The three window systems were a No Frame fully glazed façade, a façade with a Large Frame window, and a façade with a Small Frame window. In this case, there were no Complex Fenestration Systems. The real restaurants were compared with simulated pictures. The simulated pictures results were fairly close to the real ones, although in the real pictures, the fisheye lens captured less than the simulated fisheye projection, and the real pictures had some top and bottom black pixels. However, the trend in the results obtained from both pictures systems was same. Thus, the simulated picture results make sense and the virtual restaurant was used to assess all the window systems' luminance distribution. In addition, under the same Clear Sky with Sun in Spain, the location of the virtual restaurant was not a determining factor. Barcelona with its Mediterranean climate was selected to test all of the window systems at virtual restaurant.

The simulations of the virtual restaurant took place on 22 July at 11:00 standard time (12:00 local time) and the façade faced south. The Daylight Glare Probability (DGP) of each three workplanes (table, person and window) was assessed for each three window systems (fully glazed façade, large window and small window) and two Complex Fenestration Systems (Light Shelf and Prismatic Film) under a Clear Sky with Sun (CIE Clear Sky). Then, the hypothetical Mean DGP of the three workplanes was

calculated to obtain the trend in general glare perception. The conclusions of each window system are as follows:

· No Frame WS (fully glazed façade): in WP1 (table), there was a Perceptible probability of glare; in WP2 (person), there was a Disturbing probability of glare; and in WP3 (window), there was an Intolerable probability of glare (this value was overestimated) (see Table 4.8). According to the Mean DGP, there was an Intolerable probability of glare (Mean DGP 53%, Intolerable), but taking into account the overestimation, this result was on the borderline with Disturbing. The trend in Mean DGP for No Frame window system was a Disturbing probability of glare, owing to the fully glazed window's contribution to the overall field. Therefore, the Mean DGP for the overall perception was more than WP1, a little more than WP2, and less than WP3.

· No Frame (fully glazed façade) with a Light Shelf CFS: in WP1 (table), there was a Perceptible probability of glare; in WP2 (person), there was a Disturbing probability of glare; and in WP3 (window), there was an Intolerable probability of glare (this value was overestimated) (see Table 4.8). According to the Mean DGP, there was an Intolerable probability of glare (Mean DGP 54%, Intolerable), but taking into account the overestimation, this result was on the borderline with Disturbing. The trend in Mean DGP for No Frame window system with a Light Shelf was a Disturbing probability of glare, owing to the fully glazed window's contribution to the overall field. Therefore, the Mean DGP for the overall perception was more than WP1, a little more than WP2, and less than WP3. In addition, the Light Shelf increased the DGP of WP3 slightly, owing to the reflection of the under part of the Light Shelf.

· No Frame (fully glazed façade) with a Prismatic Film CFS: in WP1 (table), there was a Perceptible probability of glare; in WP2 (person), there was an Intolerable probability of glare; and in WP3 (window), there was an Intolerable probability of glare (these last two values were overestimated) (see Table 4.8). According to the Mean DGP, there was an Intolerable probability of glare (Mean DGP 57%, Intolerable), but taking into account the overestimation, this result was on the borderline with Disturbing. The trend in Mean DGP for No Frame window systems with Prismatic Film was a Disturbing probability of glare, owing to the fully glazed window's contribution to the overall field. Therefore, the Mean DGP for the overall perception was more than WP1, a little more than WP2, and less than WP3. In addition, the Prismatic Film increased the DGP of all WPs slightly, owing to scattering reflections.

· Large Frame (façade with a large window): in WP1 (table), there was an Imperceptible probability of glare; in WP2 (person), there was a Disturbing probability of glare; and in WP3 (window), there was an Intolerable probability of glare (this value was overestimated) (see Table 4.8). According to the Mean DGP, there was an Intolerable probability of glare (Mean DGP 51%, Intolerable). The trend in Mean DGP for Large Frame window system was a Disturbing probability of glare, owing to the fully glazed

window's contribution to the overall field, but there was less probability of glare than the No Frame WS in WP1 (table), because the incoming light from the pavement was blocked. Therefore, the Mean DGP for the overall perception was more than WP1, a little more than WP2, and less than WP3.

· Large Frame (façade with a large window) with a Light Shelf CFS: in WP1 (table), there was an Imperceptible probability of glare; in WP2 (person), there was a Disturbing probability of glare; and in WP3 (window), there was an Intolerable probability of glare (this value was overestimated) (see Table 4.8). According to the Mean DGP, there was an Intolerable probability of glare (Mean DGP 51%, Intolerable), but taking into account the overestimation, this result was on the borderline with Disturbing. The trend in Mean DGP for the Large Frame window systems with a Light Shelf was a Disturbing probability of glare, owing to the fully glazed window's contribution to the overall field, but there was less probability of glare than in the No Frame WS in WP1 (table), because the incoming light from the pavement was blocked. Therefore, the Mean DGP of the overall perception was more than WP1, a little more than WP2, and less than WP3. In addition, the Light Shelf increased the DGP of WP3 slightly, owing to the reflection of the underneath of the Light Shelf.

· Large Frame (façade with a large window) with a Prismatic Film CFS: in WP1 (table), there was an Imperceptible probability of glare; in WP2 (person), there was an Intolerable probability of glare; and in WP3 (window) there was an Intolerable probability of glare (these last two values were overestimated) (see Table 4.8). According to the Mean DGP, there was an Intolerable probability of glare (Mean DGP 54%, Intolerable), but taking into account the overestimation, this result was on the borderline with Disturbing. The trend in Mean DGP for Large Frame window system with Prismatic Film was a Disturbing probability of glare, owing to the fully glazed window's contribution to the overall field, but there was less probability of glare than with No Frame WS in WP1 (table), because the incoming light from the pavement was blocked. Therefore, the Mean DGP of the overall perception was more than WP1, a little more than WP2, and less than WP3. In addition, the Prismatic Film increased the DGP of all WPs a little, owing to scattering reflections.

· Small Frame (façade with a small window): in WP1 (table), there was an Imperceptible probability of glare probability; in WP2 (person), there was an Imperceptible probability of glare; and in WP3 (window), there was an Intolerable probability of glare (this value continued to be overestimated) (see Table 4.8). According to the Mean DGP, there was an Imperceptible probability of glare (Mean DGP 32%, Imperceptible). The trend in the Mean DGP for Small Frame window system was an Imperceptible probability of glare, owing to the small window's contribution to the overall field. Therefore, the Mean DGP for the overall perception was more than WP1, a little more than WP2, and less than WP3.

· Small Frame (façade with a small window) with a Light Shelf CFS: in WP1 (table), there was an Imperceptible probability of glare; in WP2 (person) there was an Imperceptible probability of glare; and in WP3 (window), there was Intolerable probability of glare (this value was overestimated) (see Table 4.8). According to the Mean DGP, there was an Imperceptible probability of glare (Mean DGP 32%, Imperceptible). The trend in the Mean DGP of Small Frame window system with a Light Shelf was an Imperceptible probability of glare, owing to the small window's contribution to the overall field. Therefore, the Mean DGP of the overall perception was more than WP1, a little more than WP2, and less than WP3. In addition, the Light Shelf did not increase the DGP of WP3 slightly, because the reflection of the underneath of the Light Shelf did not contribute.

· Small Frame (façade with a small window) with Prismatic Film CFS: In WP1 (table), there was an Imperceptible probability of glare; in WP2 (person), there was an Imperceptible probability of glare; and in WP3 (window), there was an Intolerable probability of glare (this value was overestimated) (see Table 4.8). According to the Mean DGP, there was an Imperceptible probability of glare (Mean DGP 34%, Imperceptible). The trend in Mean DGP of Small Frame window systems with Prismatic Film was an Imperceptible probability of glare, owing to the small window's contribution to the overall field. Therefore, the Mean DGP of the overall perception was more than WP1, a little more than WP2, and less than WP3. In addition, the Prismatic Film increased the DGP of all WPs slightly, owing to scattering reflections.

In conclusion, it is difficult to assess and calculate the visual comfort of different window systems in absolute terms due to the diverse and personal factors of the perception. However, Daylight Glare Probability (DGP) assessment was useful to obtain the trends for each window system. In consequence, there is not much difference in overall DGP between No Frame WS (fully glazed façade) and Large Frame WS (façade with a large window), but the Large Frame WS has a lower DGP on WP1 (table). Nevertheless, a Small Frame WS (façade with a small window) has significantly less overall DGP than No Frame or Large Frame WSs (see Table 4.8 see Figure 4.34). Moreover, the Small Frame WS may cover up some views and select a particular outdoor view, and the opportunity to light particular workplanes. Note that the exterior horizontal surfaces, the out ground, and the sky are the most probable sources of glare.

In the Small Frame window system (façade with a small window), there could be a higher probability of more local contrast between the opaque façade and the outdoor view than in a No Frame window system (fully glazed façade), and a lower proportion of outside view. Moreover, the Small Frame provides dark background and higher

contrast. However, this could create a calm indoor visual atmosphere to concentrate on eating, chatting and viewing the outdoor area.

Regarding the contribution of Complex Fenestration Systems, the trend is difficult to define, due to the large number of design possibilities. Depending on the window size and position, the underneath of the used Light Shelf CFS could make reflections that increase the DGP of WP3 (window). However, the Light Shelf that was used decreased the DGP of WP1 (table), because the light input was low. Nevertheless, the trend in Prismatic Film CFS is easier to define, as there are fewer design options. Therefore, it contributes to a slight increase in overall DGP, but not enough to change the general glare perception (see Table 4.8). Nonetheless, it should be considered that it could be the glare source. Therefore, it could be a good option to avoid the direct view of it from the point of view.

The Mean DGP is a simple way to take into account different workplanes. When there are many points of view to analyse, the Mean DGP would not be a very practical measure. However, when the visual comfort evaluation of a particular atmosphere has to be considered, the Mean DGP could be helpful. Regarding the Mean DGP results, although the WP3 (window) DGPs are overestimated, the final results make sense and they seem to be close to the overall glare perception. Thus, the Mean DGP of the overall perception is more than WP1, a little more than WP2, and significantly less than WP3. This makes sense, because the outdoor view contributes more to the overall perception, and it is more accurate than only taking into account the intermediate common view (WP2), because it increases more the window's contribution. However, if practicality prevails, defining right point of view the DGP of WP2 (average view) should be enough.

Therefore, the Mean DGP of the overall perception is approximately 50% more than WP1; approximately 20% more than WP2; and approximately 30% less than WP3 (see Table 4.9). When the range between outdoor and indoor luminance is higher, the percentages are higher, and if the range between outdoor and indoor luminance is less as in the CIE Overcast Sky (see Table 4.13 and 4.14), the percentages are lower, but the trend continued in the same way. Therefore, the Mean DGP is more relevant for a less balanced luminance distribution. The DGP calculation for different workplanes should include the contribution to overall perception and help to smooth the perception of extreme luminance values. Changing to different workplanes helps to reduce the glare perception and avoid constant extreme luminance values. Thus, three workplanes allow differentiating more extreme luminance values than two workplanes .The Mean DGP could be closer to overall glare perception, to dynamic glare state and to take into account the adaptation aspect.

6.2 Conclusions on Parameter 2: illuminance distribution evaluated by Daylight Autonomy (DA) index

The Daylight Autonomy index was used to assess illuminance distribution. One workplane was selected: a horizontal plane at 0.8 m along the room. The grid of sensor points included points at the table next to the restaurant's façade as well.

The simulation method was selected to obtain the Daylight Autonomy index. Two virtual models of real restaurants and a virtual restaurant prototype were evaluated. In all of the restaurant models, nine window systems were analysed: No Frame (fully glazed façade) without any Complex Fenestration System, No Frame with a Light Shelf CFS, No Frame with a Prismatic Film 3M CFS, Large Frame (façade with a large window) without any Complex Fenestration System, Large Frame with a Light Shelf CFS, Large Frame with a Prismatic Film 3M CFS, Small Frame (façade with a small window) without any Complex Fenestration System, Small Frame with a Light Shelf CFS and Small Frame with a Prismatic Film 3M CFS. The light contribution of all window systems followed the same trend in each restaurant. There were not great differences between No Frame and Large Frame WSs, a greater difference between No Frame and Small Frame WSs, and if the window was smaller, a greater contribution of light and uniformity of Complex Fenestration Systems.

However, Restaurant 1 (a virtual model of the Sal Café) of Barcelona has a large overhang and more windows along the façade and Restaurant 2 (a virtual model of Azurmendi) has a large amount of glass façade. In this context, it is difficult to obtain the contribution of each window system's light contribution. In consequence, a virtual Restaurant Prototype was built to obtain more accurate results. In addition, in Restaurant 1 and 2, the DA was obtained by DIVA and the Three-Phase Method for CFSs. Taking this into account the TPM results are reasonable, the DA of the virtual Restaurant Prototype for all the window systems was obtained by TPM. Thus, the results are more comparable. Illuminance data for 22 July at 11:00 standard time (12:00 local time) in Barcelona was obtained by DIVA and TPM (as a reference, the illuminance data from DIVA was selected, because the simulation of the Light Shelf CFS is confusing in TPM). Accordingly, the conclusions for each window systems in the virtual Restaurant Prototype were as follows:

· No Frame WS (fully glazed façade): the mean Daylight Autonomy along the row that follows the table was almost 96% (see Table 5.17 and Figure 5.25). It was one of the highest DA of all window systems. According to the illuminance data (see Table 5.11 and Figure 5.20), the standard deviation in relation to the mean was high (0.85). Therefore, the uniformity was low in comparison with other window systems. In addition, the extreme standard deviation was high (867).

· No Frame WS (fully glazed façade) with a Light Shelf CFS: the DA results were not accurate, because the shelf had not been simulated as a light source. Therefore, the results were a little overestimated. The mean Daylight Autonomy along the row that follows the table was almost 97% (see Table 5.17 and Figure 5.25). According to the illuminance data (see Table 5.11 and Figure 5.20), the standard deviation in relation with the mean was high (0.86). Therefore, the uniformity was slightly lower in comparison with No Frame WS. However, the extreme standard deviation was lower than No Frame WS (860). This may be because there should be some low illuminance data.

· No Frame WS (fully glazed façade) with a Prismatic Film 3M CFS: the mean Daylight Autonomy along the row that follows the table was almost 96% (see Table 5.17 and Figure 5.25). The DA was high between all window systems. According to the illuminance data (see Table 5.11 and Figure 5.20), the standard deviation in relation with the mean was lower than the No Frame WS (0.80). Therefore, the uniformity was slightly higher in comparison with No Frame WS. However, the extreme standard deviation was higher than the No Frame WS (1336). This may be because the Prismatic Film redirected direct sunlight, moving the overhang to the bottom.

· Large Frame WS (façade with a large window): the mean Daylight Autonomy along the row that follows the table was almost 95% (see Table 5.17 and Figure 5.25). The DA was high between all window systems, although the bottom part was obstructed. According to the illuminance data (see Table 5.11 and Figure 5.20), the standard deviation in relation with the mean was higher than in the No Frame WS (0.90). Therefore, the uniformity was slightly lower in comparison with No Frame WS. However, the extreme standard deviation was slightly lower than in the No Frame WS (850). This may be because there could be some low illuminance data, due to the bottom, opaque part of the façade.

· Large Frame WS (façade with a large window) with a Light Shelf CFS: the DA results were not accurate, because the shelf was not simulated as a light source. Therefore, the results were a little overestimated. The mean Daylight Autonomy along the row that follows the table was almost 96% (see Table 5.17 and Figure 5.25). The DA was high between all window systems. According to the illuminance data (see Table 5.11 and Figure 5.20), the standard deviation in relation with the mean was higher than in the No Frame WS and slightly lower than in the Large Frame WS (0.88). Therefore, the uniformity was slightly lower than in the No Frame WS and slightly higher than in the Large Frame WS. In addition, the extreme standard deviation was slightly lower than in the Large Frame WS (845). This may be because there could be slightly more distributed light contribution.

· Large Frame WS (façade with a large window) with a Prismatic Film 3M CFS: the mean Daylight Autonomy along the row that follows the table was almost 95% (see Table

5.17 and Figure 5.25). The DA was high between all window systems. According to the illuminance data (see Table 5.11 and Figure 5.20), the standard deviation in relation with the mean was lower than in the No Frame WS and Large Frame WS (0.81). Therefore, the uniformity was higher than in the No Frame WS and Large Frame WS. However, the extreme standard deviation was higher than in the No Frame WS and Large Frame WS (1284). This may be because there could be slightly more distributed light contribution.

· Small Frame WS (façade with a small window): the mean Daylight Autonomy along the row that follows the table was almost 89% (see Table 5.17 and Figure 5.25). The DA was quite high, although the window was small. According to the illuminance data (see Table 5.11 and Figure 5.20), the standard deviation in relation with the mean was significantly lower than in the No Frame WS and Large Frame WS (0.71). Therefore, the uniformity was higher than in the No Frame WS and Large Frame WS. In addition, the extreme standard deviation was lower than in the No Frame WS and Large Frame WS (373). This may be because there could be less light contribution, and light came from the upper part of façade.

· Small Frame WS (façade with a large window) with a Light Shelf CFS: the DA results were not accurate, because the shelf had not been simulated as a light source. Therefore, the results were a little overestimated. The mean Daylight Autonomy along the row that follows the table was almost 92% (see Table 5.17 and Figure 5.25). The DA was high, although the window was small. According to the illuminance data (see Table 5.11 and Figure 5.20), the standard deviation in relation with the mean was similar to the Small Frame WS, but lower than the No Frame WS and Large Frame WS (0.71). Therefore, the uniformity was similar to the Small Frame WS, but higher than the No Frame WS and Large Frame WS. In addition, the extreme standard deviation was slightly higher for the Small Frame WS and lower than the No Frame WS and Large Frame WS (397). There was not a huge difference between the Small Frame WS, but it seems that the trend was more light contribution and slightly less uniformity than the Small Frame WS, whereas the light distribution was better than the No Frame and Large Frame WSs.

· Small Frame WS (façade with a large window) with a Prismatic Film 3M CFS: the mean Daylight Autonomy along the row that follows the table was almost 91% (see Table 5.17 and Figure 5.25). The DA was high, although the window was small. According to illuminance data (see Table 5.11 and Figure 5.20), the standard deviation in relation with the mean was slightly higher than in the Small Frame WS, but lower than in the No Frame WS and Large Frame WS (0.74). Therefore, the uniformity was slightly lower than in the Small Frame WS, but higher than in the No Frame WS and Large Frame WS. In addition, the extreme standard deviation was higher than in the Small Frame WS, and slightly similar to the No Frame WS and Large Frame WS (868). Therefore,

although it had slightly less uniformity than the Small Frame WS, it provided more light than the Small Frame WS and slightly less than the No Frame and Large Frame WSs, but better distributed.

Illuminance data from DIVA seemed a little lower than the measurements and illuminance data from the Three-Phase Method seemed a little higher than measurements. Regarding Daylight Autonomy, DIVA could not simulate the DA of a Complex Fenestration System, but otherwise the DA simulations were regular. However, the Three Phase Method allowed obtaining annual illuminance data of the Complex Fenestration Systems.

In conclusion, the absolute mean Daylight Autonomy value of each Window System performance is difficult to determine, owing to simulation variations. However, the trend for each Window System could be obtained. In this context, the bottom part of the façade does not contribute to lighting workplane and the Small Window decreases the light contribution. However, with accurate redirecting systems and other light penetration, the light level could be enough and the light distribution throughout the space could be improved. Note that, if the light level increases significantly throughout the room, the contrast should tend to decrease, although the glare probability could increase. In addition, an overhang design is determining to avoid direct sunlight on workplanes and to use direct sunlight for redirecting systems. Therefore, the trend of used CFS performance is that they improve light contribution and distribution. It seems that the proposed CFS designs works better for Clear Sky with Sun as shown by the illuminance data. The simulation of a Light Shelf should be defined better with another more complex Phase Method, because it would work well for thick façade. The Prismatic Film 3M seems to works well, it is effective at redirecting lighting and practical to implement.

6.3 General conclusions

Different workplanes' contribution as a third plane, in addition to the source and background planes, could get closer to the final glare perception, because it takes into account adaptation aspects. Three workplanes combination could allow differentiating more extreme luminance values than having only two workplanes. Therefore, the required concentration on the activity and initial luminance value or in consequence initial illuminance data or different luminance ranges could be interesting indicators to consider in Daylight Glare Methods. The study could be useful for other activities that

require three workplanes, such as a down view (e. g. tablet/paper), front view (e. g. person) and far view (e. g. entrance).

In any location, in a context of high outdoor midday luminance, small windows tend to provide less probability of daylight glare, but they tend to provide less light amount. In addition, small windows could create dark background and more contrast, due to unchanged high outdoor luminance, and less outside view, but the outside view can be selected to include desirable elements and the specific workplanes can be better lit. Therefore, an accurate side-view size and direction, according to the user's point of view, could provide a nice outdoor view and a comfortable overall light atmosphere, keeping a good level of concentration. Furthermore, if redirecting systems are added to the façade composition, and the probably of glare as a light source is avoided, more distributed light throughout the workplanes could be achieved. Therefore, a small window combined with a Complex Fenestration System can provide indoor sidelight, with an intimate and comfortable atmosphere.

Note that, it seems that independently of glare, appreciations of contrast aspect were founded. The lowest contrast there is in the extremes situations; with low light and with much light. According to; no light (all black), low contrast; a small window's light behaviour, quite contrast; more light contribution with a larger window's light behaviour, the highest contrast; but much light contribution with a fully glazed façade's light behaviour, less light contrast; up to fully light, low contrast (all white).

If the two functions of outdoor view and light requirements of the glazed façade are separated, they may work better. The management of luminance distribution could be more accurate at eye level in the visual field. In addition, the light contribution could come from the other part, usually the upper part of the room, although not necessarily, which would increase the light level and distribution. Moreover, direct light could be comfortable in a place that does not disturb visual workplanes, and could increase the visual comfort, warming the atmosphere. Therefore, a daylighting complex design could improve the indoor atmosphere for visual comfort and reduce the electric light demand. Electric lighting should only be used when it is necessary for visual comfort and services or light contribution.

In conclusion, a complex daylight design, combining an outside view, redirected light, indirect light and direct light with the workplanes, could provide a different atmosphere with an appropriate level of visual comfort, according to the activity. In this context, the façade and the indoor component designs of light driving are highly relevant. Therefore, the design of the split façade defining the height, divisions, geometry and position of each part could improve the indoor light perception for a specific activity. It was found that height is important to obtain good light redirection; window size is significant to decrease glare and visual elements; the overhang position is key to avoid direct light and to allow the entry of redirected light.

6.4 Future works

In the future, the effects of third plane incorporation into glare methods should be assessed with more projection systems, which get closer to the behaviour of two eyes, and different activities. Annual glare metrics should also be incorporated. Façade systems should work throughout the year, taking into account the low sun position in winter. The outside view, window WP, should be evaluated by the outdoor luminance range to determine more real glare situation. Virtual pictures with more accurate sky simulation and real pictures with the necessary calibration and more measurements should be compared. The local or spatial contrast and outside view percentage should be studied using agreed methodology.

Complex Fenestration System simulation should be tested more times, and the test results should be compared with real measurements to verify the final results. Furthermore, other indexes results as Continuous Daylight Autonomy (cDA), Daylight Availability (DAvailability), Useful Daylight Illuminance (UDI) and Annual Sunlight Exposure (ASE) could ensure better daylight performance of the proposed window systems.

In addition, indoor colour aspects should be studied. This Parameter 3 might improve indoor visual comfort in Small Window Systems. For a low, but enough illuminance level, a warm atmosphere might improve the indoor visual comfort. Moreover, thorough satisfaction surveys should be carried out to obtain a more real opinion about visual comfort.

Finally, according to design aspects, it would be interesting to analyse the thickness of a façade, and its impact in combination with windows and Complex Fenestration Systems. A thick façade might make it easier to frame the outside view. Furthermore, it would be interesting to test other light entries, because they could compose an atmosphere with different planes of light that balance the light distribution and the light level throughout the visual environment.

References and Bibliography

In the following, the references will be sorted by date and three general topics; daylighting, window, Complex Fenestration Systems, and restaurants and others.

DAYLIGHTING

Plummer H. Cosmos of light: the sacred architecture of Le Corbusier. Bloomington and Indianapolis: Indiana University Press, 2013. ISBN 9780253007261.

Tregenza P., Wilson M. Daylighting: architecture and lighting design. London; New York: Routledge, 2011. ISBN 9780419257004.

Silvester J. Konstantinou E. Lighting, Well-being and Performance at Work. Centre for Performance at Work, City University London 2010.

Mardaljevic J., Heschong L., Lee E. Daylight metrics and energy savings. Lighting Research and Technology 2009; 261-283.

Plummer H. La Arquitectura de la luz natural. Barcelona: Blume, 2009. ISBN 9788498014358.

Rogora A., Locatelli A. L'Illuminazione canalizzata in architettura: progettazione, tecniche, esempi. Napoli: Sistemi editoriali, 2008. ISBN 9788851305000.

Bodart M., Peñaranda R., Deneyer A., Flamant G. Photometry and colorimetry characterisation of materials in daylighting evaluation tools. Building and Environment 2008; 43: 12: 2046-2058.

Reinhart C., Mardaljevic J., Rogers Z. Dynamic Daylight Performance Metrics For Sustainable Building Design. LEUKOS: The Journal of the Illuminating Engineering Society of North America 2006; 3-1: 7-31.

Zumthor P. Peter Zumthor: atmospheres: architectural environments, surrounding objects. Birkhäuser 2006. ISBN 3764374950.

Caminada G. Cul zuffel e l'aura dado. Luzern : Quart, cop. 2005. ISBN 3907631692.

Spanish Lighting Committee (CEI), Institute for Diversification and Saving of Energy (IDAE), with the collaboration of the Superior Council of Colleges of Architects of Spain (CSCAE). Guía técnica para el aprovechamiento de la luz natural en la iluminación de edificios. Madrid: IDAE, Institute for Diversification and Saving of Energy, 2005. ISBN 8486850924.

Köster H. Dynamic daylighting architecture: basics, systems, projects. Basel [etc.]: Birkhäuser, cop., 2004. ISBN 376436730X.

M. Bodart, De Herde A. Global energy savings in offices buildings by the use of daylighting. Energy and Buildings 2002; 34: 5: 421-429.

Campo A. Estereotómico y tectónico: unidad docente Alberto Campo Baeza. Madrid: Escuela Técnica Superior de Arquitectura de Madrid, Department of Architectural Design; Maireia Libros, 2001. ISBN 849308607X.

Littlefair P.J. Site layout planning for daylight and sunlight: a guide to good practice. Watford: Construction Research Communications, cop., 1995. ISBN 1860810411.

Torres E. (PhD supervised by Serra R.). Luz cenital. PhD of Escola Tècnica Superior d'Arquitectura de Barcelona, 1993.

Serra R. Les energies a l'arquitectura. Barcelona: Editions UPC, 1993.

Commission of the European communities. Daylighting in architecture. Brussels and Luxembourg: ECSC-EECEAEC, 1993.

Lawson F. Restaurants, clubs and bars; planning, design and investment. The Architectural Press: London: 1987. ISBN 0-85139-970-3.

Lam W. Sunlighting as formgiver for architecture. New York: Van Nostrand Reinhold, cop., 1986. ISBN 0442259417.

Moore, Fuller. Concepts and practise of architectural daylighting. Van Nostrand Reinhold Co., 1985. ISBN 0442264399.

Illuminating Engineering Society of North America (IESNA). Recommended Practice for Daylighting Buildings. ISBN 978-0-87995-281-5.

Illuminating Engineering Society of North America (IESNA). Lighting Handbook-Application and Reference Volume. New York (USA), 1984.

Casas J. Óptica. Zaragoza: 1983. ISBN 8430024484.

Wyszecki G, Stiles W.S. Color science: concepts and methods, quantitative data and formulae. New York: John Wiley & Sons, 1982. ISBN 0471021067.

Arizmendi L.J. Electricidad en Arquitectura. San Sebastián: Gráficas Herza, 1982.

Lam W. Perception and Lighting as Formgivers for Architecture. New York: McGraw-Hill Book, cop., 1977. ISBN 0070360944.

Commission Internationale de l'Éclairage. Standardization of Luminance Distribution on Clear Skies. Paris: CIE Publication no. 22, 1973.

Commission internationale de l'éclairage. Daylight. Vienna: Commission Internationale de l'éclairage, 1970.

Serra R. Instalaciones: alumbrado natural. Barcelona: E.T.S.A.B., 1969-70.

Einhorn H.D., A new method for the assessment of discomfort glare. Lighting Research and Technology. 1969;1:235-247.

Hopkinson R.G., Petherbridge P., Longmore J. Daylighting. London: Heinemann, 1966.

WINDOW

Altomonte S., Ken M.G., Tregenza P.R., Wilson R. Visual task difficulty and temporal influences in glare response. Building and Environment 2016; 95; 209-226.

Uriarte U., Hernández R.J., Zamora J.L. Light and outside vision at restaurants. Proceedings Advanced Building Skins, Bern 2015; 314-323.

Yamin Garretón J.A., Rodriguez R.G., Ruiz A., Pattini A.E. Degree of eye opening: A new discomfort glare indicator. Building and Environment 2015; 88: 142-150.

Karlsen L., Heiselberg P., Bryn I., Johra H. Verification of simple illuminance based measures for indication of discomfort glare from windows. Building and Environment 2015; 615-626.

Rockcastle S., Andersen M. Measuring the dynamics of contrast & daylighting variability in architecture: A proof-of-concept methodology. Building and Environment 2014; 84: 320-333.

Konis K. Evaluating daylighting effectiveness and occupant visual comfort in a side-lit open-plan office building in San Francisco, California. Building and Environment 2013; 59: 662-677.

Aguilar A., Uriarte U, Isalgue A., Coch H., Serra R. Luminances and vision related to daylighting. WREF 2012; Denver, Colorado. Publication: Proceedings of World Renewable Energy Forum.

Young Shin J., Young Yun G., Tai Kim J. View types and luminance effects on discomfort glare assessment from windows. Energy and Buildings 2012; 46:139-145.

Kim W., Kim J. A prediction method to identify the glare source in a window with non-uniform luminance distribution. Energy and Buildings 2012; 46: 132–138.

SareyKhanie M., Andersen M., Hart B.M., Stoll J., Einhäuser W. Integration of eyetracking methods in visual comfort assessment. Proceedings CISBAT, 2011.

ASEFAVE. Manual de instalación de ventanas. Barcelona: TPE Tecnopressediciones, 2011. ISBN 9788493902308.

Agüero R., El balcón y la celosía. Elementos de confort lumínico y térmico en el clima de la ciudad de Lima. Master thesis of Arquitectura, Energia i Medi Ambient 2009.

Wienold J. Daylight Glare in Offices (PhD thesis). Universität Karlsruhe 2009.

Ruggiero F., Serra R., Dimundo A. Re-interpretation of traditional architecture for visual comfort. Building and Environment 2009; 44:1886-1891.

Kim W., Tae Ahn H., Tai Kim J. A first approach to discomfort glare in the presence of non-uniform luminance. Building and Environment 2008; 43: 1953–1960.

Velds M., Knupp D. Glare from windows. Report of CIE Division, 3–R3: 2006.

Osterhaus W. Discomfort glare assessment and prevention for daylight applications in office environments. Solar Energy 2005; 79: 140-158.

ASEFAVE. Ventanas: manual de producto. Madrid: AENOR, 2005. ISBN 8481434272.

Garcíarramos F., Alonso J.M. La Ventana tradicional: análisis morfológico. Santa Cruz de Tenerife: Colegio Oficial de Aparejadores y Arquitectos Técnicos, DL 2003. ISBN 846078158.

Chauvel P., Collins J.B., Dogniaux R., Longmore J. Glare from windows: current views of the problem. Lighting Research and Technology. 1998; 30: 89-93.

Torricelli M., Sala M., Secchi S. Daylight-technologies and instruments to design. Florence: Alinea 1995.

Ayuso C. 260 modelos de ventanas. Barcelona: CEAC, 1989. ISBN 843297515X.

Mendizábal M. Manual de la ventana. Madrid: Ministerio de Obras Públicas y Urbanismo, 1988. ISBN 8474335752.

Pracht K. Fenêtres. Denges (Suisse): Delta Et Spes, 1984.

Espinet M. El Espacio culinario: de la taberna romana a la cocina profesional y doméstica del siglo XX. Barcelona: Tusquets, 1984. ISBN 8472238202.

Romanelli F., Scapaccino E. Dalla finestra al curtain wall: ricerche sulle tecnologie del discontinuo. Roma: Officina, 1979.

Turner D.F. Windows glass design guide. London: Architectural Press; New York: Nichols, 1977. ISBN 0851397093.

Hopkinson R.G. Glare from daylighting in buildings. Applied Ergonomics 1972, 3-4: 206-215.

COMPLEX FENESTRATION SYSTEMS

Hoffmann S., Lee ES., McNeil A., Fernandes L., Vidanovic D., Thanachareonkit A. Balancing daylight, glare, and energy-efficiency goals: An evaluation of exterior coplanar shading systems using complex fenestration modeling tools. Energy and Buildings 2016; 112:279-298.

Konis K., Lee E.S. Measured daylighting potential of a static optical louver system under real sun and sky conditions. Building and Environment 2015; 92: 347-359.

González J., Fiorito F. Daylight Design of Office Buildings: Optimisation of External Solar Shadings by Using Combined Simulation Methods. Buildings 2015; 5: 560-580.

Basurto C. On advanced daylighting simulations and integrated performance assessment of complex fenestration systems for sunny climates Author. Thesis of Laboratoire d'énergie solaire et physique du bâtiment, École polytechnique fédérale de Lausanne, 2014; Nº 6425.

Rao S., Tzempelikos A. The Impact of Exterior Overhangs on the Daylighting Performance of Office Spaces. International High Performance Building Conference 2010.

Linhart F, Scartezzini J.-L. Minimizing lighting power density in office rooms equipped with anidolic daylighting systems. Solar Energy 2010; 84: 4: 587-595.

Thanachareonkit A. Comparing Physical and Virtual Methods for Daylight Performance Modelling Including Complex Fenestration Systems. Thesis of Laboratoire d'énergie solaire et physique du bâtiment, École polytechnique fédérale de Lausanne, 2008; Nº 4130.

Lee E., Selkowitz S., (and others from Lawrence Berkeley National Laboratory). Advancement of electrochromic windows. Scientific report for California Energy Commission Public Interest Energy Research (PIER) Program, 2006.

Ochoa C.E., Guedi I. Evaluating visual comfort and performance of three natural lighting systems for deep office buildings in highly luminous climates. Building and Environment 2006; 41:1128-1135.

Canziani R., Peron F., Rossi G. Daylight and energy performances of a new type of light pipe. Energy and Buildings 2004; 36: 1163–1176.

Selkowitz S, Lee E. Integrating automated shading and smart glazings with daylight controls. International Symposium on Daylighting Buildings; 2004: IEA SHC TASK 31.

Scartezzini J.L. Advanced in Daylighting and Artificial Lighting. Proc. Of Research in Building Physics, Technologisch Instituut, Leuven (Belgium): 2003.

Scartezzini J.L., Courret G. Anidolic daylighting systems. Solar Energy 2002; 73-2:123-135.

Ruck N., Aschehoug Oe., Aydinli S., (and others). Daylight in buildings: a source book on daylighting systems and components. A Report of IEA SHC Task 21 / ECBCS Annex 29. Int Energy Agency, 2000.

Coch H., Serra R., Isalgué A. The Mediterranean blind: Less light, better vision. Renewable Energy 1998; 15:431-436.

Selkowitz S, Lee ES. Advanced fenestration systems for improved daylight performance. Daylighting' 98 Conference Proceedings, Ontario, Canada; 1998.

H.F.O. Müller, Prof. Dr.-Ing. Application of holographic optical elements in buildings for various purposes like daylighting, solar shading and photovoltaic power generation. Renewable Energy 1994; 5, Part II: 935-941.

Scartezzini J.-L., Paule B., Lausselet J., Perrottet C. and Simos S. Office Lighting. Swiss Action Programme on Rational Use of Energy, Bern (Switzerland): RAVEL Publication, 1994; N° 724.329.2f.

SIMULATION

Radiance software website: http://www.radiance-online.org/ (accessed September 2016)

DIVA for Rhino software website: http://diva4rhino.com/ (accessed September 2016)

WebHDR website: http://www.jaloxa.eu/webhdr/index.shtml (January 2016)

Recognition Demo website: http://places.csail.mit.edu/demo.html (accessed March 2016)

Chan Y.C., Tzempelikos A. A hybrid ray-tracing and radiosity method for calculating radiation transport and illuminance distribution in spaces with venetian blinds. Solar Energy 2012; 86: 3109–3124.

Reinhart C.F., Wienold J. The daylighting dashboard – A simulation based design analysis for daylit spaces. Building and Environment 2011; 46: 386-396.

Jacobs A. UNIX for Radiance Tutorial. Tutorial for Radinace.

McNeil A. The Three-Phase Method for Simulating Complex Fenestration with Radiance. Tutorial of Lawrence Berkeley National Laboratory.

Wienold J., Christoffersen J. Evaluation methods and development of a new glare prediction model for daylight environments with the use of CCD cameras. Energy and Buildings 2006; 38: 743–757.

Bodart M., Deneyer A. A guide for the building of daylight scale models. PLEA, Geneva, Switzerland: 2006.

Reinhart C.F., Walkenhorst O.. Dynamic RADIANCE-Based Daylight Simulations for a Full-scale Test Office with Outer Venetian Blinds. Energy & Buildings 2001; 33(7): 683–697.

Ward G., Shakespeare R.A. (with contributions from Apian-Bennewitz P., Ehrlich C., Mardaljevic J., Phillip E.). Rendering with Radiance: The Art and Science of Lighting Visualization. Morgan Kaufmann Publishers, 1998. ISBN 0-9745381-0-8.

RESTAURAMTS AND OTHERS

Fontoynont M., Ramananarivo K., Soreze T., Guldhammer Skov K. Economic feasibility of maximising daylighting of a standard office building with efficient electric lighting. Energy and Buildings 2016; 110:435-442.

Okuda S., Okajima K., Arce-Lopera C. Visual Palatability of Food Dishes in Color Appearance, Glossiness and Convexo-concave Perception Depending on Light Source. Journal of Light & Visual Environment 2015; 39.

Napier J. Climate Based Façade Design for Business Buildings with Examples from Central London. Buildings 2015; 5:16-38.

Irulegi O., Torres L., Serra A., Mendizabal I., Hernández R. The Ekihouse: An energy self-sufficient house based on passive design strategies. Energy and Buildings 2014;83:57-69.

López-Besora J., Isalgué A., Coch H., Crespo I., Alonso C. Yellow is green: An opportunity for energy savings through colour in architectural spaces. Energy and Buildings 2014; 78: 105–112.

Münch M., Plomp G., Thunell E., Kawasaki A., Scartezzini J.L., Herzog M.H. Different colors of light lead to different adaptation and activation as determined by high-density EEG. NeuroImage 2014; 101:547–554.

Trubiano F. Performance Based Envelopes: A Theory of Spatialized Skins and the Emergence of the Integrated Design Professional. Buildings 2013; 3: 689-712.

Krauel J. Bars et restaurants. Barcelona: Links, 2013.

Mostaedi A. Cafes, bars & restaurants. Barcelona: Linksbooks International, cop. 2013.

Byrd H. Post-occupancy evaluation of green buildings: the measured impact of over-glazing. Architectural Science Review. 2012; 55:206-212.

Heung V., Gu T. Influence of restaurants atmospherics on patron satisfaction and behavioral intentions. International Journal of Hospitality Management 2012; 31:1167-1177.

Ariffin H.F., Bibon M.F., Abdullah R.P.S.R. Restaurant's Atmospheric Elements: What the Customer Wants. Procedia - Social and Behavioral Sciences 2012; 38:380-387.

Wardono P., Hibino H., Koyama S. Effects of Interior Colors, Lighting and Decors on Perceived Sociability, Emotion and Behavior Related to Social Dining. Procedia - Social and Behavioral Sciences 2012; 38: 362-372.

Talotte C., Ségrétain S., Gonac'h J., Le Rohellec J. Improvement of lighting ambience on board trains: experimental results on the combined effect of light parameters and seat colours on perception. WCRR Lille 2011 9th World Congress.

Grobe L., Wittkopf S., Rana Pandey A., Xiaoming Y., Kian Seng A., Scartezzini J.L., Selkowitz S. Singapore's Zero-Energy Building's Daylight Monitoring System. International Conference on Applied Energy 2010, Energy Solutions for a Sustainable World, Singapore: 2010; 21–23.

Viénot F., Durand M-L., Mahler E. Kruithof's rule revisited using LED illumination. Journal of Modern Optics 2009; 56:13: 1433-1446.

Hong T., Selkowitz S., Yazdanian M. Assessment of Energy Impact of Window Technologies for Commercial Buildings. Assistant Secretary for Energy Efficiency and Renewable Energy of the U.S. Department of Energy under Contract, Nº DE-AC02-05CH11231: 2009; LBNL-6035E.

Cohen E., Avieli N. Foodintourism, attraction and impediment. Annals of Tourism Research 2004; 31-4: 755–778.

Coch H., Serra R., (in collaboration with Solsona X., Isalgué A., Roset J.). El disseny energètic a l`arquiectura. UPC Editions, Barcelona: 1994. ISBN 8476533780.

Taylor S.E., Fiske S.T. Salience, Attention, and Attribution: Top of the Head Phenomena. Advances in Experimental Social Psychology 1978; 11: 249-288.

Kruithof, A.-A. Tubular Luminescence Lamps for General Illumination. Philips Technical Review 1941; 6 (3): 65–96. ISSN 0031-7926.

Annex 1: Principal aspect of Radiance software

The central programs of Radiance are; ***rtrace***, which computes single ray value and ***rpict***, which produces a picture from a scene description. However, first, a scene description is necessary. For that, the texture of materials, the material of objects, the geometry of objects, the Sky geometry and the Sky material is required. Always keeping the order mentioned; textures, materials and surfaces (geometry).The program to get scene description is ***oconv***. Moreover, the program principal to get the brightness as texture of the sky is ***gensky***. Note that, the sky needs more description as glow material and source surface (this surface is a solid angle). The all textures, materials and surfaces options there are explained in Radiance Reference Manual obtained from http://radsite.lbl.gov/radiance/refer/ray.html. In the new website, http://www.radiance-online.org/learning/tutorials, there are more updates tutorials.

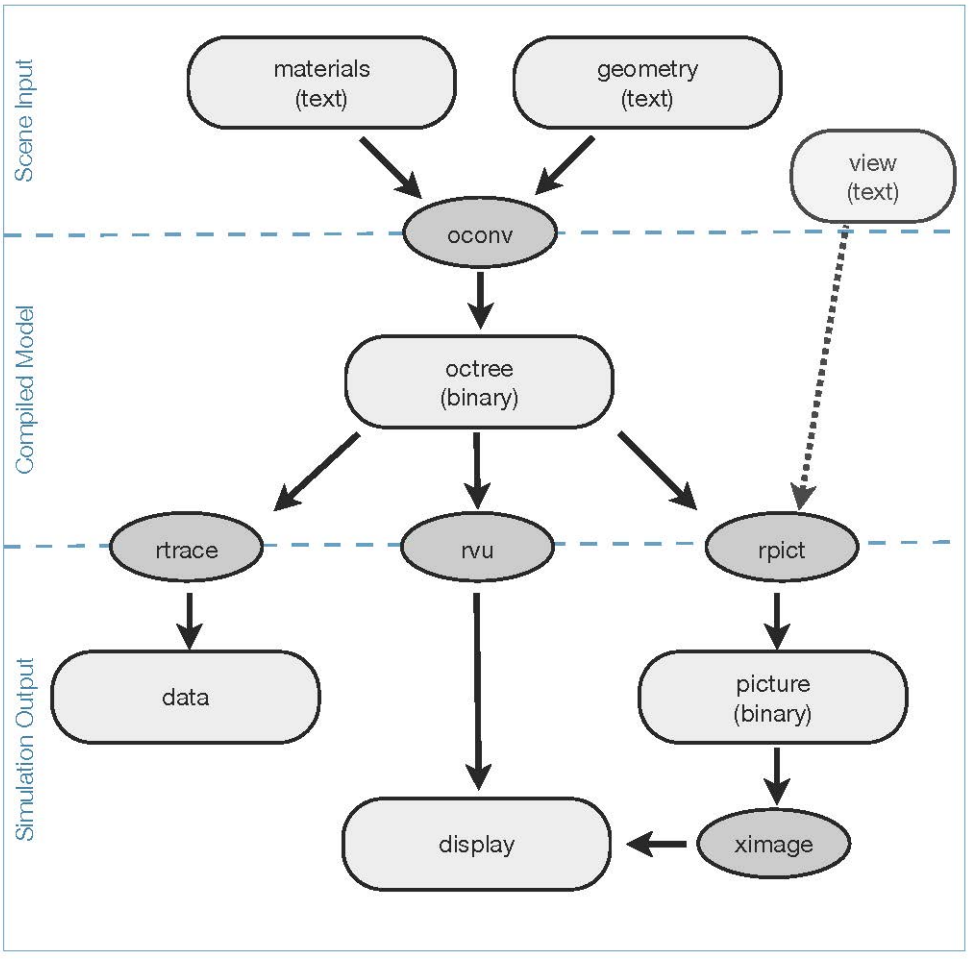

Figure A1. 1 Radiance Flowchart. Obtained from Radiance Primer tutorial of Giulio Antonutto & Andrew McNeil

Note that, *rvu* is a command which displays images interactively and *ximage* program is used to get different pictures options. Furthermore, a comment line begins with a pound sign, “#”. It does not execute, it is only for information. A **modifier** [mod] is either the identifier of a previously defined primitive, or "void". An **identifier** [id] can be any string (i.e., any sequence of non-white characters). A line beginning with an exclamation point, “!”, is interpreted as a command. It is executed by the shell, and its output is read as input to the program. White space is generally ignored, except as a separator.

All text inputs are files with text descriptions and the extension is not important, but, it helps to know what type the information is. Usually the extension is *.rad. So the three principal command lines are:

1) *oconv*:

```
$ oconv material.rad object.rad sky.rad > *scene_description.oct
```

material.rad file:

There are many material types the most common is Plastic.

Plastic is a material with uncoloured highlights. It is given by its RGB reflectance, its fraction of specularity, and its roughness value. Roughness is specified as the rms slope of surface facets. A value of 0 corresponds to a perfectly smooth surface, and a value of 1 would be a very rough surface. Specularity fractions greater than 0.1 and roughness values greater than 0.2 are not very realistic. (A pattern modifying plastic will affect the material color.):

mod plastic id
0
0
5 red green blue spec rough

```
# material.rad
void plastic orange_tile
0
0
5 1 0.1 0.1 0 0
(…)
```

object.rad file:

There are many surfaces types the most common is Polygon.

A polygon is given by a list of three-dimensional vertices, which are ordered counter-clockwise as viewed from the front side (into the surface normal). The last vertex is automatically connected to the first. Holes are represented in polygons as interior vertices connected to the outer perimeter by coincident edges (seams):

mod polygon id
0
0
3n x1 y1 z1
x2 y2 z2
x3 y3 z3
…
xn yn zn

```
# object.rad
orange_tile plastic wall.1
0
0
12 0.00 0.00 0.00
    0.00 0.00 2.00
    2.00 0.00 2.00
    2.00 0.00 0.00
```

sky.rad file:

Usually the sky brightness is got by *gensky* command. It has ±s for Clear Sky and -c for Overcast Sky. With –B option horizontal diffuse irradiation can be added (-B 55.866). However, *gendaylit* command is used when the input is other, as global horizontal irradiation data (-E). The “skyfunc” is the modifier, texture, of material data.

The material data is used to be glow.

Glow is used for surfaces that are self-luminous, but limited in their effect. In addition to the radiance value, a maximum radius for shadow testing is given:

mod glow id
0
0
4 red green blue maxrad

The surface as geometry is used to be source as solid angle description.

A source is not really a surface, but a solid angle. It is used for specifying light sources that are very distant. The direction to the center of the source and the number of degrees subtended by its disk are given as follows:

mod source id
0
0
4 xdir ydir zdir angle

The ground description is necessary as well. It has the same description as the sky but with inverted geometry. In the following there is all text together:

```
# sky.rad
# textures, material and geometry description followed

!gensky 07 22 11 +s –a 41 –o -2 –m -15

skyfunc glow sky_mat
0
0
4 1 1 1 0

sky_mat source sky
0
0
4 0 0 1 180

skyfunc glow ground_mat
0
0
4 1 1 1 0

ground_mat source ground
0
0
4 0 0 -1 180
```

2) *rtrace*:

```
$ rtrace -I -h -ab 2 -aa 0.15 -ar 128 -ad 512 -as 256 *scene_description.oct <*grid.pts |
rcalc -e '$1=179*(.265*$1+.670*$2+.065*$3)' > illuminance.dat
```

“ ’ ” Is used for Linux. For Windows OS it must be “. All parameter can be set. In the following there are all commands specifications.

3) *rpict*:

```
$ rpict -vth -vh 180 -vv 180 -vp 1 4 1.35 -vd 1 0 0 –vu 0 0 1 -ab 2 -aa 0.15 -ar 128 -ad
512 -as 256 -av 0 0 0 scene_description.oct > picture.pic
```

The view specifications can be set as a *.vf file. –vth parameter is for fisheye projection. All parameter can be set. In the following there are all commands specifications.

Regarding *.pic format, usually *.tif format is more common. ra_tiff is a program to change from *.pic format to *.tif format:

```
$ ra_tiff picture.pic picture.tif
```

Other common programs as *hdrgen*, *getinfo*, *evalglare*, *pfilt*, *falsecolor* script as follow:

```
$ hdrgen –o *.hdr -2exposure.JPG 0exposure.JPG +2exposure.JPG
```

```
$ getinfo –d *.hdr
```

```
$ evalglare –i 2350 *.hdr > *.glr
```

*.glr is a file to save the outputs.

```
$ pfilt *.hdr > *pfilt.hdr
```

```
$ falsecolor –s 3000 –log 3 –n 10 –lw 400 –lh 800 –ip *.hdr > *_fc.hdr
```

All parameter can be set. In the following there are all commands specifications. The specifications are obtained from http://www.radiance-online.org/learning/documentation/manual-pages . There can be found all program descriptions with their all parameter specifications.

NAME

rtrace - trace rays in RADIANCE scene

SYNOPSIS

rtrace [options] [$EVAR] [@file] octree
rtrace [options] −defaults

DESCRIPTION

Rtrace traces rays from the standard input through the RADIANCE scene given by *octree* and sends the results to the standard output. (The octree may be given as the output of a command enclosed in quotes and preceded by a '!'.) Input for each ray is:

xorg yorg zorg xdir ydir zdir

If the direction vector is (0,0,0), a bogus record is printed and the output is flushed if the *-x* value is one or zero. (See the notes on this option below.) This may be useful for programs that run *rtrace* as a separate process. In the second form, the default values for the options (modified by those options present) are printed with a brief explanation.

Options may be given on the command line and/or read from the environment and/or read from a file. A command argument beginning with a dollar sign ('$') is immediately replaced by the contents of the given environment variable. A command argument beginning with an at sign ('@') is immediately replaced by the contents of the given file. Most options are followed by one or more arguments, which must be separated from the option and each other by white space. The exceptions to this rule are the boolean options. Normally, the appearance of a boolean option causes a feature to be "toggled", that is switched from off to on or on to off depending on its previous state. Boolean options may also be set explicitly by following them immediately with a '+' or '-', meaning on or off, respectively. Synonyms for '+' are any of the characters "yYtT1", and synonyms for '-' are any of the characters "nNfF0". All other characters will generate an error.

-f*io* Format input according to the character *i* and output according to the character *o*. *Rtrace* understands the following input and output formats: 'a' for ascii, 'f' for single-precision floating point, and 'd' for double-precision floating point. In addition to these three choices, the character 'c' may be used to denote 4-byte floating point (Radiance) color format for the output of values only *(−ov* option, below). If the output character is missing, the input format is used.

Note that there is no space between this option and its argument.

-o*spec* Produce output fields according to *spec*. Characters are interpreted as follows:

o	origin (input)
d	direction (normalized)
v	value (radiance)
V	contribution (radiance)
w	weight
W	color coefficient
l	effective length of ray
L	first intersection distance
c	local (u,v) coordinates
p	point of intersection
n	normal at intersection (perturbed)
N	normal at intersection (unperturbed)
s	surface name

m modifier name

M material name

~ tilde (end of trace marker)

If the letter 't' appears in *spec*, then the fields following will be printed for every ray traced, not just the final result. If the capital letter 'T' is given instead of 't', then all rays will be reported, including shadow testing rays to light sources. Spawned rays are indented one tab for each level. The tilde marker ('~') is a handy way of differentiating the final ray value from daughter values in a traced ray tree, and usually appears right before the 't' or 'T' output flags. E.g., *−ov~TmW* will emit a tilde followed by a tab at the end of each trace, which can be easily distinguished even in binary output.

Note that there is no space between this option and its argument.

-te *mod* Append *mod* to the trace exclude list, so that it will not be reported by the trace option *(−o*t*)*. Any ray striking an object having *mod* as its modifier will not be reported to the standard output with the rest of the rays being traced. This option has no effect unless either the 't' or 'T' option has been given as part of the output specifier. Any number of excluded modifiers may be given, but each must appear in a separate option.

-ti *mod* Add *mod* to the trace include list, so that it will be reported by the trace option. The program can use either an include list or an exclude list, but not both.

-tE *file* Same as *−te*, except read modifiers to be excluded from *file*. The RAYPATH environment variable determines which directories are searched for this file. The modifier names are separated by white space in the file.

-tI *file* Same as *−ti*, except read modifiers to be included from *file*.

−i Boolean switch to compute irradiance rather than radiance values. This only affects the final result, substituting a Lambertian surface and multiplying the radiance by pi. Glass and other transparent surfaces are ignored during this stage. Light sources still appear with their original radiance values, though the *−dv* option (below) may be used to override this. This option is especially useful in conjunction with ximage(1) for computing illuminance at scene points.

−u Boolean switch to control uncorrelated random sampling. When "off", a low-discrepancy sequence is used, which reduces variance but can result in a brushed appearance in specular highlights. When "on", pure Monte Carlo sampling is used in all calculations.

−I Boolean switch to compute irradiance rather than radiance, with the input origin and direction interpreted instead as measurement point and orientation.

−h Boolean switch for information header on output.

-x *res* Set the x resolution to *res*. The output will be flushed after every *res* input rays if *−y* is set to zero. A value of one means that every ray will be flushed, whatever the setting of *−y*. A value of zero means that no output flushing will take place.

-y *res* Set the y resolution to *res*. The program will exit after *res* scanlines have been processed, where a scanline is the number of rays given by the *−x* option, or 1 if *−x* is zero. A value of zero means the program will not halt until the end of file is reached.

If both *−x* and *−y* options are given, a resolution string is printed at the beginning of the output. This is mostly useful for recovering image dimensions with *pvalue(1)*, and for creating valid Radiance picture files using the color output format. (See the *−f* option, above.)

-n *nproc* Execute in parallel on *nproc* local processes. This option is incompatible with the *−P* and *−PP*, options. Multiple processes also do not work properly with ray tree output using any of the *−o*t** options. There is no benefit from specifying more processes than there are cores available on the system or the *−x* setting, which forces a wait at each flush.

-dj *frac* Set the direct jittering to *frac*. A value of zero samples each source at specific sample points (see the *−ds* option below), giving a smoother but somewhat less accurate rendering. A

positive value causes rays to be distributed over each source sample according to its size, resulting in more accurate penumbras. This option should never be greater than 1, and may even cause problems (such as speckle) when the value is smaller. A warning about aiming failure will issued if *frac* is too large.

-ds *frac* Set the direct sampling ratio to *frac*. A light source will be subdivided until the width of each sample area divided by the distance to the illuminated point is below this ratio. This assures accuracy in regions close to large area sources at a slight computational expense. A value of zero turns source subdivision off, sending at most one shadow ray to each light source.

-dt *frac* Set the direct threshold to *frac*. Shadow testing will stop when the potential contribution of at least the next and at most all remaining light sources is less than this fraction of the accumulated value. (See the *−dc* option below.) The remaining light source contributions are approximated statistically. A value of zero means that all light sources will be tested for shadow.

−dc *frac* Set the direct certainty to *frac*. A value of one guarantees that the absolute accuracy of the direct calculation will be equal to or better than that given in the *−dt* specification. A value of zero only insures that all shadow lines resulting in a contrast change greater than the *−dt* specification will be calculated.

-dr *N* Set the number of relays for secondary sources to *N*. A value of 0 means that secondary sources will be ignored. A value of 1 means that sources will be made into first generation secondary sources; a value of 2 means that first generation secondary sources will also be made into second generation secondary sources, and so on.

-dp *D* Set the secondary source presampling density to D. This is the number of samples per steradian that will be used to determine ahead of time whether or not it is worth following shadow rays through all the reflections and/or transmissions associated with a secondary source path. A value of 0 means that the full secondary source path will always be tested for shadows if it is tested at all.

−dv Boolean switch for light source visibility. With this switch off, sources will be black when viewed directly although they will still participate in the direct calculation. This option is mostly for the program *mkillum(1)* to avoid inappropriate counting of light sources, but it may also be desirable in conjunction with the *−i* option.

-ss *samp* Set the specular sampling to *samp*. For values less than 1, this is the degree to which the highlights are sampled for rough specular materials. A value greater than one causes multiple ray samples to be sent to reduce noise at a commmesurate cost. A value of zero means that no jittering will take place, and all reflections will appear sharp even when they should be diffuse.

-st *frac* Set the specular sampling threshold to *frac*. This is the minimum fraction of reflection or transmission, under which no specular sampling is performed. A value of zero means that highlights will always be sampled by tracing reflected or transmitted rays. A value of one means that specular sampling is never used. Highlights from light sources will always be correct, but reflections from other surfaces will be approximated using an ambient value. A sampling threshold between zero and one offers a compromise between image accuracy and rendering time.

-bv Boolean switch for back face visibility. With this switch off, back faces of all objects will be invisible to view rays. This is dangerous unless the model was constructed such that all surface normals face outward. Although turning off back face visibility does not save much computation time under most circumstances, it may be useful as a tool for scene debugging, or for seeing through one-sided walls from the outside.

-av *red grn blu*
Set the ambient value to a radiance of *red grn blu* . This is the final value used in place of an indirect light calculation. If the number of ambient bounces is one or greater and the ambient value weight is non-zero (see *-aw* and *-ab* below), this value may be modified by the computed indirect values to improve overall accuracy.

-aw *N* Set the relative weight of the ambient value given with the *-av* option to *N*. As new indirect irradiances are computed, they will modify the default ambient value in a moving average, with the specified weight assigned to the initial value given on the command and all other weights set to 1. If a value of 0 is given with this option, then the initial ambient value is never modified. This is the safest value for scenes with large differences in indirect contributions, such as when both indoor and outdoor (daylight) areas are visible.

-ab *N* Set the number of ambient bounces to *N*. This is the maximum number of diffuse bounces computed by the indirect calculation. A value of zero implies no indirect calculation.

-ar *res* Set the ambient resolution to *res*. This number will determine the maximum density of ambient values used in interpolation. Error will start to increase on surfaces spaced closer than the scene size divided by the ambient resolution. The maximum ambient value density is the scene size times the ambient accuracy (see the *−aa* option below) divided by the ambient resolution. The scene size can be determined using *getinfo(1)* with the *−d* option on the input octree.

-aa *acc* Set the ambient accuracy to *acc*. This value will approximately equal the error from indirect illuminance interpolation. A value of zero implies no interpolation.

-ad *N* Set the number of ambient divisions to *N*. The error in the Monte Carlo calculation of indirect illuminance will be inversely proportional to the square root of this number. A value of zero implies no indirect calculation.

-as *N* Set the number of ambient super-samples to *N*. Super-samples are applied only to the ambient divisions which show a significant change.

-af *fname* Set the ambient file to *fname*. This is where indirect illuminance will be stored and retrieved. Normally, indirect illuminance values are kept in memory and lost when the program finishes or dies. By using a file, different invocations can share illuminance values, saving time in the computation. The ambient file is in a machine-independent binary format which can be examined with *lookamb(1)*.

The ambient file may also be used as a means of communication and data sharing between simultaneously executing processes. The same file may be used by multiple processes, possibly running on different machines and accessing the file via the network (ie. *nfs(4)*). The network lock manager *lockd(8)* is used to insure that this information is used consistently.

If any calculation parameters are changed or the scene is modified, the old ambient file should be removed so that the calculation can start over from scratch. For convenience, the original ambient parameters are listed in the header of the ambient file. *Getinfo(1)* may be used to print out this information.

-ae *mod* Append *mod* to the ambient exclude list, so that it will not be considered during the indirect calculation. This is a hack for speeding the indirect computation by ignoring certain objects. Any object having *mod* as its modifier will get the default ambient level rather than a calculated value. Any number of excluded modifiers may be given, but each must appear in a separate option.

-ai *mod* Add *mod* to the ambient include list, so that it will be considered during the indirect calculation. The program can use either an include list or an exclude list, but not both.

-aE *file* Same as *−ae*, except read modifiers to be excluded from *file*. The RAYPATH environment variable determines which directories are searched for this file. The modifier names are separated by white space in the file.

-aI *file* Same as *−ai*, except read modifiers to be included from *file*.

-me *rext gext bext*

Set the global medium extinction coefficient to the indicated color, in units of 1/distance (distance in world coordinates). Light will be scattered or absorbed over distance according to this value. The ratio of scattering to total scattering plus absorption is set by the albedo parameter, described below.

-ma *ralb galb balb*
Set the global medium albedo to the given value between 0 0 0 and 1 1 1. A zero value means that all light not transmitted by the medium is absorbed. A unitary value means that all light not transmitted by the medium is scattered in some new direction. The isotropy of scattering is determined by the Heyney-Greenstein parameter, described below.

−mg *gecc* Set the medium Heyney-Greenstein eccentricity parameter to *gecc*. This parameter determines how strongly scattering favors the forward direction. A value of 0 indicates perfectly isotropic scattering. As this parameter approaches 1, scattering tends to prefer the forward direction.

−ms *sampdist*
Set the medium sampling distance to *sampdist*, in world coordinate units. During source scattering, this will be the average distance between adjacent samples. A value of 0 means that only one sample will be taken per light source within a given scattering volume.

-lr *N* Limit reflections to a maximum of *N*, if N is a positive integer. If *N* is zero or negative, then Russian roulette is used for ray termination, and the *-lw* setting (below) must be positive. If N is a negative integer, then this sets the upper limit of reflections past which Russian roulette will be used. In scenes with dielectrics and total internal reflection, a setting of 0 (no limit) may cause a stack overflow.

-lw *frac* Limit the weight of each ray to a minimum of *frac*. During ray-tracing, a record is kept of the estimated contribution (weight) a ray would have in the image. If this weight is less than the specified minimum and the *-lr* setting (above) is positive, the ray is not traced. Otherwise, Russian roulette is used to continue rays with a probability equal to the ray weight divided by the given *frac*.

-ld Boolean switch to limit ray distance. If this option is set, then rays will only be traced as far as the magnitude of each direction vector. Otherwise, vector magnitude is ignored and rays are traced to infinity.

-e *efile* Send error messages and progress reports to *efile* instead of the standard error.

−w Boolean switch to suppress warning messages.

−P *pfile* Execute in a persistent mode, using *pfile* as the control file. Persistent execution means that after reaching end-of-file on its input, *rtrace* will fork a child process that will wait for another *rtrace* command with the same *−P* option to attach to it. (Note that since the rest of the command line options will be those of the original invocation, it is not necessary to give any arguments besides *−P* for subsequent calls.) Killing the process is achieved with the *kill(1)* command. (The process ID in the first line of *pfile* may be used to identify the waiting *rtrace* process.) This option may be used with the *−fr* option of *pinterp(1)* to avoid the cost of starting up *rtrace* many times.

−PP *pfile* Execute in continuous-forking persistent mode, using *pfile* as the control file. The difference between this option and the *−P* option described above is the creation of multiple duplicate processes to handle any number of attaches. This provides a simple and reliable mechanism of memory sharing on most multiprocessing platforms, since the *fork(2)* system call will share memory on a copy-on-write basis.

EXAMPLES

To compute radiance values for the rays listed in samples.inp:

```
rtrace −ov scene.oct < samples.inp > radiance.out
```

To compute illuminance values at locations selected with the 't' command of *ximage(1):*

```
ximage scene.hdr | rtrace −h −x 1 −i scene.oct | rcalc −e '$1=47.4*$1+120*$2+11.6*$3'
```

To record the object identifier corresponding to each pixel in an image:

```
vwrays −fd scene.hdr | rtrace −fda `vwrays −d scene.hdr` −os scene.oct
```

To compute an image with an unusual view mapping:

```
cnt 480 640 | rcalc -e 'xr:640;yr:480' -f unusual_view.cal | rtrace -x 640 -y 480 -fac scene.oct >
unusual.hdr
```

ENVIRONMENT

RAYPATH	the directories to check for auxiliary files.

FILES

/tmp/rtXXXXXX	common header information for picture sequence

DIAGNOSTICS

If the program terminates from an input related error, the exit status will be 1. A system related error results in an exit status of 2. If the program receives a signal that is caught, it will exit with a status of 3. In each case, an error message will be printed to the standard error, or to the file designated by the *-e* option.

AUTHOR

Greg Ward

SEE ALSO

getinfo(1), lookamb(1), oconv(1), pfilt(1), pinterp(1), pvalue(1), rpict(1), rcontrib(1), rvu(1), vwrays(1), ximage(1)

NAME

rpict - generate a RADIANCE picture

SYNOPSIS

rpict [options] [$EVAR] [@file] [octree]
rpict [options] −defaults

DESCRIPTION

Rpict generates a picture from the RADIANCE scene given in *octree* and sends it to the standard output. If no *octree* is given, the standard input is read. (The octree may also be specified as the output of a command enclosed in quotes and preceded by a '!'.) Options specify the viewing parameters as well as giving some control over the calculation. Options may be given on the command line and/or read from the environment and/or read from a file. A command argument beginning with a dollar sign ('$') is immediately replaced by the contents of the given environment variable. A command argument beginning with an at sign ('@') is immediately replaced by the contents of the given file.

In the second form shown above, the default values for the options (modified by those options present) are printed with a brief explanation.

Most options are followed by one or more arguments, which must be separated from the option and each other by white space. The exceptions to this rule are the *−vt* option and the boolean options. Normally, the appearance of a boolean option causes a feature to be "toggled", that is switched from off to on or on to off depending on its previous state. Boolean options may also be set explicitly by following them immediately with a '+' or '-', meaning on or off, respectively. Synonyms for '+' are any of the characters "yYtT1", and synonyms for '-' are any of the characters "nNfF0". All other characters will generate an error.

-vt*t* Set view type to *t*. If *t* is 'v', a perspective view is selected. If *t* is 'l', a parallel view is used. A cylindrical panorma may be selected by setting *t* to the letter 'c'. This view is like a standard perspective vertically, but projected on a cylinder horizontally (like a soupcan's-eye view). Three fisheye views are provided as well; 'h' yields a hemispherical fisheye view, 'a' results in angular fisheye distortion, and 's' results in a planisphere (stereographic) projection. A hemispherical fisheye is a projection of the hemisphere onto a circle. The maximum view angle for this type is 180 degrees. An angular fisheye view is defined such that distance from the center of the image is proportional to the angle from the central view direction. An angular fisheye can display a full 360 degrees. A planisphere fisheye view maintains angular relationships between lines, and is commonly used for sun path analysis. This is more commonly known as a "stereographic projection," but we avoid the term here so as not to confuse it with a stereoscopic pair. A planisphere fisheye can display up to (but not including) 360 degrees, although distortion becomes extreme as this limit is approached. Note that there is no space between the view type option and its single letter argument.

-vp *x y z* Set the view point to *x y z*. This is the focal point of a perspective view or the center of a parallel projection.

-vd *xd yd zd*
Set the view direction vector to *xd yd zd*. The length of this vector indicates the focal distance as needed by the *−pd* option, described below.

-vu *xd yd zd*
Set the view up vector (vertical direction) to *xd yd zd*.

-vh *val* Set the view horizontal size to *val*. For a perspective projection (including fisheye views), *val* is the horizontal field of view (in degrees). For a parallel projection, *val* is the view width in world coordinates.

-vv *val* Set the view vertical size to *val*.

-vo *val* Set the view fore clipping plane at a distance of *val* from the view point. The plane will be perpendicular to the view direction for perspective and parallel view types. For fisheye view types, the clipping plane is actually a clipping sphere, centered on the view point with radius *val*. Objects in front of this imaginary surface will not be visible. This may be useful for

seeing through walls (to get a longer perspective from an exterior view point) or for incremental rendering. A value of zero implies no foreground clipping. A negative value produces some interesting effects, since it creates an inverted image for objects behind the viewpoint. This possibility is provided mostly for the purpose of rendering stereographic holograms.

-va *val* Set the view aft clipping plane at a distance of *val* from the view point. Like the view fore plane, it will be perpendicular to the view direction for perspective and parallel view types. For fisheye view types, the clipping plane is actually a clipping sphere, centered on the view point with radius *val*. Objects behind this imaginary surface will not be visible. A value of zero means no aft clipping, and is the only way to see infinitely distant objects such as the sky.

-vs *val* Set the view shift to *val*. This is the amount the actual image will be shifted to the right of the specified view. This is option is useful for generating skewed perspectives or rendering an image a piece at a time. A value of 1 means that the rendered image starts just to the right of the normal view. A value of −1 would be to the left. Larger or fractional values are permitted as well.

-vl *val* Set the view lift to *val*. This is the amount the actual image will be lifted up from the specified view, similar to the *−vs* option.

-vf *file* Get view parameters from *file*, which may be a picture or a file created by rvu (with the "view" command).

-x *res* Set the maximum x resolution to *res*.

-y *res* Set the maximum y resolution to *res*.

-pa *rat* Set the pixel aspect ratio (height over width) to *rat*. Either the x or the y resolution will be reduced so that the pixels have this ratio for the specified view. If *rat* is zero, then the x and y resolutions will adhere to the given maxima.

-ps *size* Set the pixel sample spacing to the integer *size*. This specifies the sample spacing (in pixels) for adaptive subdivision on the image plane.

-pt *frac* Set the pixel sample tolerance to *frac*. If two samples differ by more than this amount, a third sample is taken between them.

-pj *frac* Set the pixel sample jitter to *frac*. Distributed ray-tracing performs anti-aliasing by randomly sampling over pixels. A value of one will randomly distribute samples over full pixels. A value of zero samples pixel centers only. A value between zero and one is usually best for low-resolution images.

-pm *frac* Set the pixel motion blur to *frac*. In an animated sequence, the exact view will be blurred between the previous view and the next view as though a shutter were open this fraction of a frame time. (See the *−S* option regarding animated sequences.) The first view will be blurred according to the difference between the initial view set on the command line and the first view taken from the standard input. It is not advisable to use this option in combination with the *pmblur(1)* program, since one takes the place of the other. However, it may improve results with *pmblur* to use a very small fraction with the *−pm* option, to avoid the ghosting effect of too few time samples.

-pd *dia* Set the pixel depth-of-field aperture to a diameter of *dia* (in world coordinates). This will be used in conjunction with the view focal distance, indicated by the length of the view direction vector given in the *−vd* option. It is not advisable to use this option in combination with the *pdfblur(1)* program, since one takes the place of the other. However, it may improve results with *pdfblur* to use a very small fraction with the *−pd* option, to avoid the ghosting effect of too few samples.

-dj *frac* Set the direct jittering to *frac*. A value of zero samples each source at specific sample points (see the *−ds* option below), giving a smoother but somewhat less accurate rendering. A positive value causes rays to be distributed over each source sample according to its size, resulting in more accurate penumbras. This option should never be greater than 1, and may even cause

problems (such as speckle) when the value is smaller. A warning about aiming failure will issued if *frac* is too large. It is usually wise to turn off image sampling when using direct jitter by setting −ps to 1.

-ds *frac* Set the direct sampling ratio to *frac*. A light source will be subdivided until the width of each sample area divided by the distance to the illuminated point is below this ratio. This assures accuracy in regions close to large area sources at a slight computational expense. A value of zero turns source subdivision off, sending at most one shadow ray to each light source.

-dt *frac* Set the direct threshold to *frac*. Shadow testing will stop when the potential contribution of at least the next and at most all remaining light source samples is less than this fraction of the accumulated value. (See the −*dc* option below.) The remaining light source contributions are approximated statistically. A value of zero means that all light source samples will be tested for shadow.

−dc *frac* Set the direct certainty to *frac*. A value of one guarantees that the absolute accuracy of the direct calculation will be equal to or better than that given in the −*dt* specification. A value of zero only insures that all shadow lines resulting in a contrast change greater than the −*dt* specification will be calculated.

-dr *N* Set the number of relays for secondary sources to *N*. A value of 0 means that secondary sources will be ignored. A value of 1 means that sources will be made into first generation secondary sources; a value of 2 means that first generation secondary sources will also be made into second generation secondary sources, and so on.

-dp *D* Set the secondary source presampling density to D. This is the number of samples per steradian that will be used to determine ahead of time whether or not it is worth following shadow rays through all the reflections and/or transmissions associated with a secondary source path. A value of 0 means that the full secondary source path will always be tested for shadows if it is tested at all.

−dv Boolean switch for light source visibility. With this switch off, sources will be black when viewed directly although they will still participate in the direct calculation. This option may be desirable in conjunction with the −*i* option so that light sources do not appear in the output.

-ss *samp* Set the specular sampling to *samp*. For values less than 1, this is the degree to which the highlights are sampled for rough specular materials. A value greater than one causes multiple ray samples to be sent to reduce noise at a commmesurate cost. A value of zero means that no jittering will take place, and all reflections will appear sharp even when they should be diffuse. This may be desirable when used in combination with image sampling (see −*ps* option above) to obtain faster renderings.

-st *frac* Set the specular sampling threshold to *frac*. This is the minimum fraction of reflection or transmission, under which no specular sampling is performed. A value of zero means that highlights will always be sampled by tracing reflected or transmitted rays. A value of one means that specular sampling is never used. Highlights from light sources will always be correct, but reflections from other surfaces will be approximated using an ambient value. A sampling threshold between zero and one offers a compromise between image accuracy and rendering time.

-bv Boolean switch for back face visibility. With this switch off, back faces of all objects will be invisible to view rays. This is dangerous unless the model was constructed such that all surface normals face outward. Although turning off back face visibility does not save much computation time under most circumstances, it may be useful as a tool for scene debugging, or for seeing through one-sided walls from the outside.

-av *red grn blu*
Set the ambient value to a radiance of *red grn blu*. This is the final value used in place of an indirect light calculation. If the number of ambient bounces is one or greater and the ambient value weight is non-zero (see *-aw* and *-ab* below), this value may be modified by the computed

indirect values to improve overall accuracy.

-aw *N* Set the relative weight of the ambient value given with the *-av* option to *N*. As new indirect irradiances are computed, they will modify the default ambient value in a moving average, with the specified weight assigned to the initial value given on the command and all other weights set to 1. If a value of 0 is given with this option, then the initial ambient value is never modified. This is the safest value for scenes with large differences in indirect contributions, such as when both indoor and outdoor (daylight) areas are visible.

-ab *N* Set the number of ambient bounces to *N*. This is the maximum number of diffuse bounces computed by the indirect calculation. A value of zero implies no indirect calculation.

-ar *res* Set the ambient resolution to *res*. This number will determine the maximum density of ambient values used in interpolation. Error will start to increase on surfaces spaced closer than the scene size divided by the ambient resolution. The maximum ambient value density is the scene size times the ambient accuracy (see the *−aa* option below) divided by the ambient resolution. The scene size can be determined using *getinfo(1)* with the *−d* option on the input octree. A value of zero is interpreted as unlimited resolution.

-aa *acc* Set the ambient accuracy to *acc*. This value will approximately equal the error from indirect illuminance interpolation. A value of zero implies no interpolation.

-ad *N* Set the number of ambient divisions to *N*. The error in the Monte Carlo calculation of indirect illuminance will be inversely proportional to the square root of this number. A value of zero implies no indirect calculation.

-as *N* Set the number of ambient super-samples to *N*. Super-samples are applied only to the ambient divisions which show a significant change.

-af *fname* Set the ambient file to *fname*. This is where indirect illuminance will be stored and retrieved. Normally, indirect illuminance values are kept in memory and lost when the program finishes or dies. By using a file, different invocations can share illuminance values, saving time in the computation. Also, by creating an ambient file during a low resolution rendering, better results can be obtained in a second high resolution pass. The ambient file is in a machine-independent binary format which may be examined with *lookamb(1)*.

The ambient file may also be used as a means of communication and data sharing between simultaneously executing processes. The same file may be used by multiple processes, possibly running on different machines and accessing the file via the network (ie. *nfs(4)*). The network lock manager *lockd(8)* is used to insure that this information is used consistently.

If any calculation parameters are changed or the scene is modified, the old ambient file should be removed so that the calculation can start over from scratch. For convenience, the original ambient parameters are listed in the header of the ambient file. *Getinfo(1)* may be used to print out this information.

-ae *mod* Append *mod* to the ambient exclude list, so that it will not be considered during the indirect calculation. This is a hack for speeding the indirect computation by ignoring certain objects. Any object having *mod* as its modifier will get the default ambient level rather than a calculated value. Any number of excluded modifiers may be given, but each must appear in a separate option.

-ai *mod* Add *mod* to the ambient include list, so that it will be considered during the indirect calculation. The program can use either an include list or an exclude list, but not both.

-aE *file* Same as *−ae*, except read modifiers to be excluded from *file*. The RAYPATH environment variable determines which directories are searched for this file. The modifier names are separated by white space in the file.

-aI *file* Same as *−ai*, except read modifiers to be included from *file*.

-me *rext gext bext*
Set the global medium extinction coefficient to the indicated color, in units of 1/distance (distance in world coordinates). Light will be scattered or absorbed over distance according to this value. The ratio of scattering to total scattering plus absorption is set by the albedo parameter, described below.

-ma *ralb galb balb*
Set the global medium albedo to the given value between 0 0 0 and 1 1 1. A zero value means that all light not transmitted by the medium is absorbed. A unitary value means that all light not transmitted by the medium is scattered in some new direction. The isotropy of scattering is determined by the Heyney-Greenstein parameter, described below.

−mg *gecc* Set the medium Heyney-Greenstein eccentricity parameter to *gecc*. This parameter determines how strongly scattering favors the forward direction. A value of 0 indicates perfectly isotropic scattering. As this parameter approaches 1, scattering tends to prefer the forward direction.

−ms *sampdist*
Set the medium sampling distance to *sampdist*, in world coordinate units. During source scattering, this will be the average distance between adjacent samples. A value of 0 means that only one sample will be taken per light source within a given scattering volume.

−i Boolean switch to compute irradiance rather than radiance values. This only affects the final result, substituting a Lambertian surface and multiplying the radiance by pi. Glass and other transparent surfaces are ignored during this stage. Light sources still appear with their original radiance values, though the *−dv* option (above) may be used to override this.

−u Boolean switch to control uncorrelated random sampling. When "off", a low-discrepancy sequence is used, which reduces variance but can result in a dithered appearance in specular highlights. When "on", pure Monte Carlo sampling is used in all calculations.

-lr *N* Limit reflections to a maximum of *N*, if N is a positive integer. If *N* is zero, then Russian roulette is used for ray termination, and the *-lw* setting (below) must be positive. If N is a negative integer, then this sets the upper limit of reflections past which Russian roulette will be used. In scenes with dielectrics and total internal reflection, a setting of 0 (no limit) may cause a stack overflow.

-lw *frac* Limit the weight of each ray to a minimum of *frac*. During ray-tracing, a record is kept of the estimated contribution (weight) a ray would have in the image. If this weight is less than the specified minimum and the *-lr* setting (above) is positive, the ray is not traced. Otherwise, Russian roulette is used to continue rays with a probability equal to the ray weight divided by the given *frac*.

-S *seqstart* Instead of generating a single picture based only on the view parameters given on the command line, this option causes *rpict* to read view options from the standard input and for each line containing a valid view specification, generate a corresponding picture. This option is most useful for generating animated sequences, though it may also be used to control rpict from a remote process for network-distributed rendering. *Seqstart* is a positive integer that will be associated with the first output frame, and incremented for successive output frames. By default, each frame is concatenated to the output stream, but it is possible to change this action using the *−o* option (described below). Multiple frames may be later extracted from the output using *ra_rgbe(1)*.

Note that the octree may not be read from the standard input when using this option.

-o *fspec* Send the picture(s) to the file(s) given by *fspec* instead of the standard output. If this option is used in combination with *−S* and *fspec* contains an integer field for *printf(3)* (eg. "%03d") then the actual output file name will include the current frame number. *Rpict* will not allow a picture file to be clobbered (overwritten) with this option. If an image in a sequence already exists *(−S* option), *rpict* will skip until it reaches an image that doesn't, or the end of the sequence. This is useful for running rpict on multiple machines or processors to render the

same sequence, as each process will skip to the next frame that needs rendering.

-r *fn* Recover pixel information from the file *fn*. If the program gets killed during picture generation, the information may be recovered using this option. The view parameters and picture dimensions are also recovered from *fn* if possible. The other options should be identical to those which created *fn*, or an inconsistent picture may result. If *fn* is identical to the file specification given with the −*o* option, *rpict* will rename the file prior to copying its contents. This insures that the old file is not overwritten accidentally. (See also the −*ro* option, below.)

If *fn* is an integer and the recover option is used in combination with the −*S* option, then *rpict* skips a number of view specifications on its input equal to the difference between *fn* and *seqstart*. *Rpict* then performs a recovery operation on the file constructed from the frame number *fn* and the output file specification given with the −*o* option. This provides a convenient mechanism for recovering in the middle of an aborted picture sequence.

The recovered file will be removed if the operation is successful. If the recover operation fails (due to lack of disk space) and the output file and recover file specifications are the same, then the original information may be left in a renamed temporary file. (See FILES section, below.)

-ro *fspec* This option causes pixel information to be recovered from and subsequently returned to the picture file *fspec*. The effect is the same as specifying identical recover and output file names with the −*r* and −*o* options.

-z *fspec* Write pixel distances out to the file *fspec*. The values are written as short floats, one per pixel in scanline order, as required by *pinterp(1)*. Similar to the −*o* option, the actual file name will be constructed using *printf* and the frame number from the −*S* option. If used with the −*r* option, −*z* also recovers information from an aborted rendering.

−P *pfile* Execute in a persistent mode, using *pfile* as the control file. This option must be used together with −*S*, and is incompatible with the recover option *(−r)*. Persistent execution means that after reaching end-of-file on its input, *rpict* will fork a child process that will wait for another *rpict* command with the same −*P* option to attach to it. (Note that since the rest of the command line options will be those of the original invocation, it is not necessary to give any arguments besides −*P* for subsequent calls.) Killing the process is achieved with the *kill(1)* command. (The process ID in the first line of *pfile* may be used to identify the waiting *rpict* process.) This option may be less useful than the −*PP* variation, explained below.

−PP *pfile* Execute in continuous-forking persistent mode, using *pfile* as the control file. The difference between this option and the −*P* option described above is the creation of multiple duplicate processes to handle any number of attaches. This provides a simple and reliable mechanism of memory sharing on most multiprocessing platforms, since the *fork(2)* system call will share memory on a copy-on-write basis. This option may be used with *rpiece(1)* to efficiently render a single image using multiple processors on the same host.

-t *sec* Set the time between progress reports to *sec*. A progress report writes the number of rays traced, the percentage completed, and the CPU usage to the standard error. Reports are given either automatically after the specified interval, or when the process receives a continue (−CONT) signal (see *kill(1)*). A value of zero turns automatic reporting off.

-e *efile* Send error messages and progress reports to *efile* instead of the standard error.

−w Boolean switch for warning messages. The default is to print warnings, so the first appearance of this option turns them off.

EXAMPLE

rpict −vp 10 5 3 −vd 1 −.5 0 scene.oct > scene.hdr

rpict −S 1 −o frame%02d.hdr scene.oct < keyframes.vf

ENVIRONMENT

RAYPATH the directories to check for auxiliary files.

FILES

/tmp/rtXXXXXX	common header information for picture sequence
rfXXXXXX	temporary name for recover file

DIAGNOSTICS

If the program terminates from an input related error, the exit status will be 1. A system related error results in an exit status of 2. If the program receives a signal that is caught, it will exit with a status of 3. In each case, an error message will be printed to the standard error, or to the file designated by the *−e* option.

AUTHOR

Greg Ward

SEE ALSO

getinfo(1), lookamb(1), oconv(1), pdfblur(1), pfilt(1), pinterp(1), pmblur(1), printf(3), ra_rgbe(1), rad(1), rtrace(1), rvu(1)

NAME

oconv - create an octree from a RADIANCE scene description

SYNOPSIS

oconv [−i octree | −b xmin ymin zmin size][−n objlim][−r maxres][−f][−w][-] [input ..]

DESCRIPTION

Oconv adds each scene description *input* to *octree* and sends the result to the standard output. Each *input* can be either a file name, or a command (enclosed in quotes and preceded by a '!'). Similarly, the octree input may be given as a command preceded by a '!'. If any of the surfaces will not fit in *octree*, an error message is printed and the program aborts. If no *octree* is given, a new one is created large enough for all of the surfaces.

The *−b* option allows the user to give a bounding cube for the scene, starting at *xmin ymin zmin* and having a side length *size*. If the cube does not contain all of the surfaces, an error results. The *−b* and *−i* options are mutually exclusive.

The *−n* option specifies the maximum surface set size for each voxel. Larger numbers result in quicker octree generation, but potentially slower rendering. Smaller values may or may not produce faster renderings, since the default number (6) is close to optimal for most scenes.

The *−r* option specifies the maximum octree resolution. This should be greater than or equal to the ratio of the largest and smallest dimensions in the scene (ie. surface size or distance between surfaces). The default is 16384.

The *−f* option produces a frozen octree containing all the scene information. Normally, only a reference to the scene files is stored in the octree, and changes to those files may invalidate the result. The freeze option is useful when the octree file's integrity and loading speed is more important than its size, or when the octree is to be relocated to another directory, and is especially useful for creating library objects for the "instance" primitive type. If the input octree is frozen, the output will be also.

The *−w* option suppresses warnings.

A hyphen by itself ('-') tells *oconv* to read scene data from its standard input. This also implies the *−f* option.

The only scene file changes that do not require octree regeneration are modifications to non-surface parameters. If the coordinates of a surface are changed, or any primitives are added or deleted, oconv must be run again. Programs will abort with a "stale octree" message if they detect any dangerous inconsistencies between the octree and the input files.

Although the octree file format is binary, it is meant to be portable between machines. The only limitation is that machines with radically different integer sizes will not work together. For the best results, the −f option should be used if an octree is to be used in different environments.

DIAGNOSTICS

There are four basic error types reported by oconv:

warning - a non-fatal input-related error

fatal - an unrecoverable input-related error

system - a system-related error

internal - a fatal error related to program limitations

consistency - a program-caused error

Most errors are self-explanatory. However, the following internal errors should be mentioned:

Too many scene files

Reduce the number of scene files by combining them or using calls to xform(1) within files to create a hierarchy.

Set overflow in addobject (id)

This error occurs when too many surfaces are close together in a scene. Either too many surfaces are lying right on top of each other, or the bounding cube is inflated from an oversized object or an improper *−b* specification. If hundreds of triangles come together at a common vertex, it may not be possible to create an octree from the object. This happens most often when inane CAD systems create spheres using a polar tessellation. Chances are, the surface "id" is near one of those causing the problem.

Hash table overflow in fullnode

This error is caused by too many surfaces. If it is possible to create an octree for the scene at all, it will have to be done in stages using the *−i* option.

EXAMPLE

To add book1, book2 and a transformed book3 to the octree "scene.oct":

```
oconv −i scene.oct book1 book2 '\!xform −rz 30 book3' > newscene.oct
```

AUTHOR

Greg Ward

NOTES

In the octree, the names of the scene files are stored rather than the scene information. This means that a new octree must be generated whenever the scene files are changed or moved. Also, an octree that has been moved to a new directory will not be able to find scene files with relative pathnames. The freeze option avoids these problems. *make(1)* or *rad(1)* can be used to automate octree creation and maintenance.

SEE ALSO

getbbox(1), getinfo(1), make(1), obj2mesh(1), rad(1), rpict(1), rvu(1), rtrace(1), xform(1)

NAME

ra_tiff - convert RADIANCE picture to/from a TIFF color or greyscale image

SYNOPSIS

ra_tiff [**-z|-L|-l|-f|-w**][**-b**][**-e +/-stops**][**-g gamma**] { **in.hdr|-** } **out.tif**
ra_tiff -r [**−x**][**−g gamma**][**−e +/-stops**] **in.tif** [**out.hdr|-**]

DESCRIPTION

Ra_tiff converts between RADIANCE and TIFF image formats. The *−g* option specifies the exponent used in gamma correction; the default value is 2.2, which is the recommended value for TIFF images.

The *−b* option can be used to specify an 8-bit greyscale TIFF output file. The type of input file is determined automatically.

The *−z* option will result in LZW compression of the TIFF output file. The *−L* option specifies SGILOG compression, which is recommended to capture the full dynamic range of the Radiance picture. However, since many TIFF readers do not yet support this format, use this option under advisement. The *−l* option specifies SGILOG24 compressed output, which has less dynamic range than SGILOG, but may be smaller in some cases. (It is usually larger.) The *−f* option specifies 32-bit IEEE floating-point/primary output, which is the highest resolution format but results in very large files, since each RGB pixel takes 96 bits (12 bytes) and does not compress well. The *−w* option specifies 16-bit/primary output, which is understood by some photo editing software, such as Adobe Photoshop. Decompression is automatically determined for TIFF input.

The *−e* option specifies an exposure compensation in f-stops (powers of two). Only integer stops are allowed, for efficiency.

The *−r* option invokes a reverse conversion, from a TIFF image to a RADIANCE picture. The RADIANCE picture file can be taken from the standard input or sent to the standard output by using a hyphen ('-') in place of the file name, but the TIFF image must be to or from a file. The *−x* option can be used to specify an XYZE Radiance output file, rather than the default RGBE.

EXAMPLES

To convert a Radiance picture to SGILOG-compressed TIFF format:

```
ra_tiff −L scene1.hdr scene1.tif
```

To later convert this image back into Radiance and display using human visibility tone-mapping:

```
ra_tiff −r scene1.tif scene1.hdr
ximage −e human scene1.hdr
```

AUTHOR

Greg Ward Larson
Sam Leffler

ACKNOWLEDGEMENT

Work on this program was initiated and sponsored by the LESO group at EPFL in Switzerland. Additions for the SGILOG data encoding were sponsored by Silicon Graphics, Inc.

BUGS

Many TIFF file subtypes are not supported.
A gamma value other than 2.2 is not properly recorded or understood if recorded in the TIFF file.

SEE ALSO

pfilt(1), ra_bmp(1), ra_bn(1), ra_ppm(1), ra_pr(1), ra_pr24(1), ra_t8(1), ra_t16(1), ximage(1)

NAME

gensky - generate a RADIANCE description of the sky

SYNOPSIS

gensky month day time [options]
gensky -ang altitude azimuth [options]
gensky -defaults

DESCRIPTION

Gensky produces a RADIANCE scene description for the CIE standard sky distribution at the given month, day and time. By default, the time is interpreted as local standard time on a 24-hour clock. The time value may be given either as decimal hours, or using a colon to separate hours and minutes. If the time is immediately followed (no white space) by a North American or European time zone designation, then this determines the standard meridian, which may be specified alternatively with the *−m* option. The following time zones are understood, with their corresponding hour differences from Greenwich Mean Time:

Standard time:
YST PST MST CST EST GMT
9 8 7 6 5 0

CET EET AST GST IST JST NZST
−1 −2 −3 −4 −5.5 −9 −12

Daylight savings time:
YDT PDT MDT CDT EDT BST
8 7 6 5 4 −1

CEST EEST ADT GDT IDT JDT NZDT
−2 −3 −4 −5 −6.5 −10 −13

If the time is preceded by a plus sign ('+'), then it is interpreted as local solar time instead. It is very important to specify the correct latitude and longitude (unless local solar time is given) using the *−a* and *−o* options to get the correct solar angles.

The second form gives the solar angles explicitly. The altitude is measured in degrees above the horizon, and the azimuth is measured in degrees west of South.

The third form prints the default option values.

The output sky distribution is given as a brightness function, *skyfunc*. Its value is in watts/steradian/meter2. The x axis points east, the y axis points north, and the z axis corresponds to the zenith. The actual material and surface(s) used for the sky is left up to the user. For a hemispherical blue sky, the description might be:

```
!gensky 4 1 14

skyfunc glow skyglow
0
0
4 .99 .99 1.1 0

skyglow source sky
0
0
4 0 0 1 180
```

Often, *skyfunc* will actually be used to characterize the light coming in from a window.

In addition to the specification of a sky distribution function, *gensky* suggests an ambient value in a comment at the beginning of the description to use with the *−av* option of the RADIANCE rendering programs.

(See rvu(1) and rpict(1).) This value is the cosine-weighted radiance of the sky in watts/steradian/meter2.

Gensky supports the following options.

−s Sunny sky without sun. The sky distribution will correspond to a standard CIE clear day.

+s Sunny sky with sun. In addition to the sky distribution function, a source description of the sun is generated.

−c Cloudy sky. The sky distribution will correspond to a standard CIE overcast day.

−i Intermediate sky without sun. The sky will correspond to a standard CIE intermediate day.

+i Intermediate sky with sun. In addition to the sky distribution, a (somewhat subdued) sun is generated.

−u Uniform cloudy sky. The sky distribution will be completely uniform.

-g *rfl* Average ground reflectance is *rfl*. This value is used to compute *skyfunc* when Dz is negative. Ground plane brightness is the same for *−s* as for *+s*. (Likewise for *−i* and *+i*, but see the *−r* option below.)

-b *brt* The zenith brightness is *brt*. Zenith radiance (in watts/steradian/meter2) is normally computed from the sun angle and sky turbidity (for sunny sky). It can be given directly instead, using this option.

-B *irrad* Same as *−b*, except zenith brightness is computed from the horizontal diffuse irradiance (in watts/meter2).

-r *rad* The solar radiance is *rad*. Solar radiance (in watts/steradian/meter2) is normally computed from the solar altitude. This option may be used to override the default calculation. If a value of zero is given, no sun description is produced, and the contribution of direct solar to ground brightness is neglected.

-R *irrad* Same as *−r*, except solar radiance is computed from the horizontal direct irradiance (in watts/meter2).

-t *trb* The turbidity factor is *trb*. Greater turbidity factors correspond to greater atmospheric scattering. A turbidity factor of 1.0 indicates an ideal clear atmosphere (i.e. a completely dark sky). Values less than 1.0 are physically impossible.

The following options do not apply when the solar altitude and azimuth are given explicitly.

-a *lat* The site latitude is *lat* degrees north. (Use negative angle for south latitude.) This is used in the calculation of sun angle.

-o *lon* The site longitude is *lon* degrees west. (Use negative angle for east longitude.) This is used in the calculation of solar time and sun angle. Be sure to give the corresponding standard meridian also! If solar time is given directly, then this option has no effect.

-m *mer* The site standard meridian is *mer* degrees west of Greenwich. (Use negative angle for east.) This is used in the calculation of solar time. Be sure to give the correct longitude also! If a time zone or solar time is given directly, then this option has no effect.

EXAMPLE

To produce a sunny sky for July 4th at 2:30pm Eastern daylight time at a site latitude of 42 degrees, 89 degrees west longitude:

```
gensky 7 4 14:30EDT +s −a 42 −o 89
```

To produce a sunny sky distribution for a specific sun position but without the sun description:

```
gensky −ang 23 −40 −s
```

FILES

/usr/local/lib/ray/skybright.cal

AUTHOR

Greg Ward

SEE ALSO

rpict(1), rvu(1), xform(1)

NAME

gendaylit - generates a RADIANCE description of the daylight sources using Perez models for direct and diffuse components

SYNOPSIS

gendaylit month day hour [-P|-W|-L|-G|-E] input_value(s) [options]
gendaylit -ang altitude azimuth [-P|-W|-L|-G|-E] input_value(s) [options]

DESCRIPTION

Gendaylit produces a RADIANCE scene description based on an angular distribution of the daylight sources (direct+diffuse) for the given atmospheric conditions (direct and diffuse component of the solar radiation), date and local standard time. The default output is the radiance of the sun (direct) and the sky (diffuse) integrated over the visible spectral range (380-780 nm). We have used the calculation of the sun's position and the ground brightness models which were programmed in *gensky*.

The diffuse angular distribution is calculated using the Perez et al. sky luminance distribution model (see Solar Energy Vol. 50, No. 3, pp. 235-245, 1993) which, quoting Perez, describes "the mean instantaneous sky luminance angular distribution patterns for all sky conditions from overcast to clear, through partly cloudy, skies". The correctness of the resulting sky radiance/luminance values in this simulation is ensured through the normalization of the modelled sky diffuse to the measured sky diffuse irradiances/illuminances.

As described below, the radiation can be defined with the pairs direct-normal and diffuse-horizontal irradiance (-W option), direct-horizontal and diffuse-horizontal irradiance (-G option), direct-normal and diffuse-horizontal illuminance (-L option) or global-horizontal irradiation alone (-E option). The direct-normal radiation is understood here as the radiant flux coming from the sun and an area of approximately 3 degrees around the sun (World Meteorological Organisation specifications for measuring the direct radiation. The aperture angle of a pyrheliometer is approximately 6 degrees). To simplify the calculations for the direct radiation, the sun is represented as a disk and no circumsolar radiation is modelled in the 3 degrees around the sun. This means that all the measured/evaluated direct radiation is added to the 0.5 degree sun source.

The direct and diffuse solar irradiances/illuminances are the inputs needed for the calculation. These quantities are the commonly accessible data from radiometric measurement centres or from the Test Reference Year. The use of such data is the recommended method for achieving the most accurate simulation results.

The atmospheric conditions are modelled with the Perez et al. parametrization (see Solar Energy Vol. 44, No 5, pp. 271-289, 1990), which is dependent on the values for the direct-normal and the diffuse-horizontal irradiances. The three parameters are epsilon, delta and the solar zenith angle. "Epsilon variations express the transition from a totally overcast sky (epsilon=1) to a low turbidity clear sky (epsilon>6); delta variations reflect the opacity/thickness of the clouds". Delta can vary from 0.05 representing a dark sky to 0.5 for a very bright sky. Not every combination of epsilon, delta and solar zenith angle is possible. For a clear day, if epsilon and the solar zenith angle are known, then delta can be determined. For intermediate or overcast days, the sky can be dark or bright, giving a range of possible values for delta when epsilon and the solar zenith are fixed. The relation between epsilon and delta is represented in a figure on page 393 in Solar Energy Vol.42, No 5, 1989. Note that the epsilon parameter is a function of the solar zenith angle. It means that a clear day will not be defined by fixed values of epsilon and delta. Consequently the input parameters, epsilon, delta and the solar zenith angle, have to be determined on a graph. It might be easier to work with the measured direct and diffuse components (direct normal irradiance/illuminance and diffuse horizontal irradiance/illuminance) than with the epsilon and delta parameters.

The conversion of irradiance into illuminance for the direct and the diffuse components is determined by the luminous efficacy models of Perez et al. (see Solar Energy Vol. 44, No 5, pp. 271-289, 1990). To convert the luminance values into radiance integrated over the visible range of the spectrum, we devide the luminance by the white light efficacy factor of 179 lm/W. This is consistent with the RADIANCE calculation because the luminance will be recalculated from the radiance integrated over the visible range by:

luminance = radiance_integrated_over_visible_range * 179 or luminance = (RED*.263 + GREEN*.655 + BLUE*.082) * 179 with the capability to model colour (where radiance_integrated_over_visible_range == (RED + GREEN + BLUE)/3).

From *gensky, if the hour is preceded by a plus sign ('+'), then it is interpreted as local solar time instead of standard time.* The second form gives the solar angles explicitly. The altitude is measured in degrees above the horizon, and the azimuth is measured in degrees west of South. The x axis points east, the y axis points north, and the z axis corresponds to the zenith. The actual material and surface(s) used for the sky is left up to the user. In addition to the specification of a sky distribution function, *gendaylit* suggests an ambient value in a comment at the beginning of the description to use with the *−av* option of the RADIANCE rendering programs. (See rview(1) and rpict(1).) This value is the cosine-weighted radiance of the sky in W/sr/m^2.

Gendaylit can be used with the following input parameters. They offer three possibilities to run it: with the Perez parametrization, with irradiance values and with illuminance values.

−P *epsilon delta* (these are the Perez parameters)

−W *direct-normal-irradiance* (W/m^2), *diffuse-horizontal-irradiance* (W/m^2)

−G *direct-horizontal-irradiance* (W/m^2), *diffuse-horizontal-irradiance* (W/m^2)

−L *direct-normal-illuminance* (lm/m^2), *diffuse-horizontal-illuminance* (lm/m^2)

−E *global-horizontal-irradiance* (W/m^2)

The -E option calculates the diffuse irradiance fraction with the model of Erbs, Klein and Duffie (Solar Energy 28/4, 1982), being followed by the calculation of the -G option. Due to the high uncertainty of the model, the results have to be handled with care. A second irradiance value, if available, is definitely recommended.

The output can be set to either the radiance of the visible radiation, the solar radiance (full spectrum) or the luminance.

−O[0|1|2] (0=output in W/m^2/sr visible radiation (default), 1=output in W/m^2/sr solar radiation, 2=output in lm/m^2/sr luminance).

Gendaylit supports the following options.

−s The source description of the sun is not generated.

−w Suppress warning messages

-g *rfl* Average ground reflectance is *rfl.* This value is used to compute *skyfunc* when Dz is negative.

The following options do not apply when the solar altitude and azimuth are given explicitly.

-a *lat* The site latitude is *lat* degrees north. (Use negative angle for south latitude.) This is used in the calculation of sun angle.

-o *lon* The site longitude is *lon* degrees west. (Use negative angle for east longitude.) This is used in the calculation of solar time and sun angle. Be sure to give the corresponding standard meridian also! If solar time is given directly, then this option has no effect.

-m *mer* The site standard meridian is *mer* degrees west of Greenwich. (Use negative angle for east.) This is used in the calculation of solar time. Be sure to give the correct longitude also! If solar time is given directly, then this option has no effect.

-i *time_interval* **[min]**
If gendaylit is used with weather files, the specified instantaneous points of time may be incorrect. This error occurs due to the fact that measurement results are frequently defined for time intervals, not for specific points of time. Although gendaylit is working correctly, this may lead to wrong outputs especially at low sun altitudes. The -i option allows to specify the time interval of the measurements in minutes, causing the solar position to be corrected for low sun altitudes. A warning message is returned if a correction has been performed.

EXAMPLES

A clear non-turbid sky for a solar altitude of 60 degrees and an azimut of 0 degree might be defined by:

gendaylit -ang 60 0 -P 6.3 0.12 or gendaylit -ang 60 0 -W 840 135 This sky description corresponds to the clear sky standard of the CIE.

The corresponding sky with a high turbidity is:

gendaylit -ang 60 0 -P 3.2 0.24 or gendaylit -ang 60 0 -W 720 280

The dark overcast sky (corresponding to the CIE overcast standard, see CIE draft standard, Pub. No. CIE DS 003, 1st Edition, 1994) is obtained by:

gendaylit -ang 60 0 -P 1 0.08

A bright overcast sky is modelled with a larger value of delta, for example:

gendaylit -ang 60 0 -P 1 0.35

To generate the same bright overcast sky for March 2th at 3:15pm standard time at a site latitude of 42 degrees, 108 degrees west longitude, and a 110 degrees standard meridian:

gendaylit 3 2 15.25 -a 42 -o 108 -m 110 -P 1 0.35

FILES

/usr/local/lib/ray/perezlum.cal

AUTHOR

Jean-Jacques Delaunay, Jan Wienold, Wendelin Sprenger, Fraunhofer ISE (Freiburg i.B., Germany) (wendelin.sprenger@ise.fhg.de)

ACKNOWLEDGEMENTS

The first work on this program was supported by the German Federal Ministry for Research and Technology (BMFT) under contract No. 0329294A, and a scholarship from the French Environment and Energy Agency (ADEME) which was co-funded by Bouygues. Many thanks to Peter Apian-Bennewitz, Arndt Berger, Christian Reetz, Ann Kovach, R. Perez, C. Gueymard and G. Ward for their help.

SEE ALSO

gensky(1), rpict(1), rview(1), xform(1)

hdrgen

Create a high dynamic-range image from multiple exposures of a static scene. The input files may be JPEG or TIFF, but must be 24-bit RGB (trichromatic) images. The output is your choice of a Radiance HDR picture or a 32-bit LogLuv TIFF image. The syntax of the hdrgen command is:

hdrgen –o *out_file* [–r *cam.rsp*] [–m *cachesiz*] [–a] [–e] [–s *stonits1*] *image1* [–s *stonits2*] *image2* …

As many exposures may be given as necessary, and should ideally be spaced within two f–stops of each other. The brightest exposure should have no black pixels, and the darkest exposure should have no white pixels, but there is little point in extending beyond these limits, which may cause problems in determining the camera response function. The order of options and input files is unimportant, with the exception of the –s option, which must preceed the corresponding exposure. Following is an explanation of the options and their meanings:

–o *out_file*
Write high dynamic-range image to the given file. If the file has a '.tif' suffix, it will be written out as a LogLuv TIFF image. If it has a '.exr' suffix, it will be written out as an ILM OpenEXR image. If it has a '.jpg' suffix, it will be written out in JPEG-HDR format. If it has any other suffix or none at all, it will be written out as an RLE RGBE Radiance picture.

-k *var_file*
Write variance image to the given file, using the same format rules as the output file. This image indicates where the input deviates from an ideal exposure sequence, and may be useful for diagnostic purposes or further image processing.

-q *quality*
Set output quality to *quality* (0-100). This affects the JPEG output compression, and potentially the details of the other formats written as well. (For example, writing out a TIFF with –q 100 results in a 96-bit/pixel IEEE floating-point file rather than a LogLuv encoding.)

–r *cam.rsp*
Use the given file for the camera's response curves. If this file exists, it must contain the coefficients of three polynomials, one for each color primary. If the file does not exist, hdrgen will use its principal algorithm to derive these coefficients and write them out to this file for later use. If a scene contains no low frequency content or gradations of intensity, it may be impossible to derive the response curve from the exposure sequence. Thus it is better to create this information once for a given camera and reuse it for other sequences.

–m *cachesiz*
Specify the cache size to use in megabytes. No more than this much memory will be allocated to hold image data during processing. The default value is 100. Using a smaller value may require longer processing if many input images are used, since some will need to be read in twice rather than once, but specifying a larger value than there is memory available will definitely be worse, due to virtual memory swapping.

–a Toggle automatic exposure alignment. The default value is "on," so giving this option one time switches it off. The alignment algorithm examines neighboring exposures and finds the pixel offset in x and y that minimizes the difference in the two images. It may be necessary to switch this option off when dealing with very dark or very bright exposures taken in a tripod-stabilized sequence.

–e Toggle exposure adjustment. Normally "on," exposure adjustment fine-tunes the scale difference between adjacent images to account for slight inaccuracies in the aperture or speed settings of the camera.

-x Toggle over- and under-exposed image removal. Normally "off," this option causes unnecessary exposures that are too light or too dark to contribute useful information to be automatically

ignored.

–f Toggle lens flare removal. Normally, "off," this option is designed to reduce the scattered light from a camera's lens and aperture, which results in a slightly fogged appearance in high dynamic-range images.

-g Toggle ghost removal. Normally "off," this option attempts to remove moving or changing objects in a scene, which cause ghosts in the combined output.

–s *stonits*

Set the sample-to-nits (cd/m^2) conversion factor for the following image to the floating-point value *stonits*. This is normally determined automatically by the program from camera information stored in the Exif image header. If the image did not come directly from a digital camera, then it will be necessary to use this option for each image. If the absolute conversion is unknown, then simply pick a value for the brightest image, and increase it subsequently for each exposure in the sequence. One f-stop requires doubling this conversion factor, and two f-stops requires quadrupling.

Diagnostics

The primary failure mode for this algorithm is the one mentioned in the description of the –r option, when the exposures contain too little information to solve for the camera response function. The best solution to this problem is to take off the exposures that are very light and very dark, or to use a different sequence of images to generate a response file. This file may then be used to combine the entire set of images, since the program no longer needs to solve for the responses.

Most of the other diagnostics you will encounter are "warnings," which means that the final image will be written, but may have problems. In particular, when the alignment algorithm fails on a hand-held sequence, some ghosting may be visible on high contrast edges in the output. Using the –a option to turn off automatic alignment will eliminate the warning, but unless the sequence was taken on a very stable tripod, the results will usually be worse rather than better.

Example

To combine all JPEG images matching a given wildcard and put into a LogLuv TIFF:

hdrgen P13351?.JPG –o testimg.tif

Author

This software was written by Greg Ward of Exponent Corporation. Send comments or questions to gward@exponent.com or gward@lmi.net.

References

Tomoo Mitsunaga and Shree Nayar, "Radiometric Self-Calibration," *Proceedings of IEEE Conference on Computer Vision and Pattern Recognition*, June, 1999.
Greg Ward, "LogLuv encoding for full-gamut, high-dynamic range images," *Journal of Graphics Tools*, 3(1):15-31 1998.
Greg Ward, High Dynamic Range Images, web page.
Paul Debevec, web page.

NAME

getinfo - get header information from a RADIANCE file

SYNOPSIS

getinfo [**-d**][**file ..**]
getinfo -
getinfo -c command ..

DESCRIPTION

Getinfo reads the header of each RADIANCE *file* and writes it to the standard output. Octree and picture files are in a binary format, which makes it difficult to determine their content. Therefore, a few lines of text are placed at the beginning of each file by the RADIANCE program that creates it. The end of the header information and the start of the data is indicated by an empty line. The *−d* option can be used to print the dimensions of an octree or picture file instead. For an octree, *getinfo −d* prints the bounding cube (xmin ymin zmin size). For a picture, *getinfo −d* prints the y and x resolution (−Y yres +X xres). If no *file* is given, the standard input is read.

The second form of *getinfo* with a hyphen simply removes the header and copies the body of the file from the standard input to the standard output.

The third form of *getinfo −c* is followed by a command and its arguments, which is executed on the data segment of the standard input. The header is passed along, with the addition of the command at the end. This is roughly equivalent to the following sequence, but does not require the input to be in a file:

(getinfo < input ; getinfo - < input | command ..)

EXAMPLE

To print the header information from scene1.oct and scene2.hdr:

getinfo scene1.oct scene2.hdr

AUTHOR

Greg Ward

SEE ALSO

oconv(1), pfilt(1), rcalc(1), rhinfo(1), rpict(1), rvu(1)

NAME

evalglare − determines and evaluates glare sources within a 180 degree fish−eye−image, given in the RADIANCE RGBE (.hdr) image format.

SYNOPSIS

evalglare [−s] [−y] [−Y value] [−B angle] [−b factor] [−c checkfile] [−t xpos ypos angle] [−T xpos ypos angle] [−d] [−r angle] [−i Ev] [−I Ev yfill_max y_fill_min] [−v] [−V] [−g type] [−G type] [−u r g b] [−vf viewfile] [−vtt] [−vv vertangle] [−vh horzangle] hdrfile

or

hdr|evalglare [−s] [−y] [−Y value] [−B angle] [−b factor] [−c checkfile] [−t xpos ypos angle][−T xpos ypos angle] [−d] [−r angle] [−i Ev] [−I Ev yfill_max y_fill_min] [−v] [−V]] [−g type] [−G type] [−u r g b] [−vf viewfile][−vtt] [−vv vertangle] [−vh horzangle]

DESCRIPTION

evalglare determines and evaluates glare sources within a 180 degree fish−eye−image, given in the RADIANCE image format (.pic or .hdr). The image should be rendered as fish eye (e.g. using the −vta or −vth option) using 180 degree for the horizontal and vertical view angle (−vv =180, −vh=180). Due to performance reasons of the evalglare code, the image should be smaller than 1200x1200 pixels. The recommended size is 800x800 pixels. In the first step, the program uses a given threshold to determine all glare sources. Three different threshold methods are implemented. The recommended method is to define a task area by −t or −T option. In this (task) area the average luminance is calculated Each pixel, exceeding this value multiplied by the −b factor [default=5] is treated as a potential glare source. The other two methods are described below [see −b]. In the second step the program tries to merge glare source pixels to one glare source, when they are placed nearby each other. This merging is performed in−between a search area, given by an opening angle (−r, default =0.2 in radiant). If a check file is written (−c fname), the detected glare sources will be colored to different colors where the rest of the image is set to gray. The luminance values of all pixels are kept to the initial value. The color is chosen by chance, no significance is given by the color. To enable a unform coloring for all glare sources, the −u option can be used. Luminance peaks can be extracted to separate glare sources by using the −y or −Y value option (default since version v0.9c). Default value (−y) is 50000 cd/m2, can be changed by using −Y value. A smoothing option (−s) counts initial non−glare source pixels to glare sources, when they are surrounded by a glare source.

The program calculates the daylight glare probability (DGP) as well as other glare indexes (dgi,ugr,vcp,cgi) to the standard output. The DGP describes the fraction of persons disturbed, caused by glare from daylight (range 0...1). Values lower than 0.2 are out of the range of the user assessment tests, where the program is based on and should be interpreted carefully. A low light correction is applied to the DGP when the vertical illumiance is lower than 500 lux. By the use of −g or −G the field of view is cut according the the definition of Guth. The option −B angle (in rad) calculates the average luminance of a horizontal band. In the case of non−180 degree images, an external measured illuminance value can be provided by using the −i or −I option. The use of the −I option enables the filling up of images, which are horizontally cut. The age correction is not supported any more and disabled. If the option −d is used, all found glare sources and their position, size, and luminance values are printed to the standard output, too. The last line gives following values: 1. dgp, 2. average luminance of image,3. vertical eye illuminance, 4. background luminance, 5. direct vertical eye illuminance, 6. dgi, 7. ugr, 8. vcp, 9. cgi, 10. average luminance of all glare sources, 11. sum of solid angles of all glare sources 12. Veiling luminance (disability glare) 13. x−direction of glare source 14. y−direction of glare source 15. z−direction of glare source 16. band luminance

The program is based on the studies from J. Christoffersen and J. Wienold (see âEvaluation methods and development of a new glare prediction model for daylight environments with the use of CCD cameras and RADIANCEâ , Energy and Buildings, 2006. More details can be also found in following issertation: J. Wienold, âDaylight glare in officesâ, Fraunhofer IRB, 2010. URL for download: http://publica.fraunhofer.de/eprints/urn:nbn:de:0011−n−1414579.pdf

−B *angle*,
Calculate average luminance of a horizontal band. The angle is in rad. Output only when using the −d option.

−b *factor*,
Threshold factor; if factor >100, it is used as constant threshold in cd/m2, regardless if a task position is given or not if factor is <= 100 and a task position is given, this factor multiplied by the average task luminance will be used as threshold for detecting the glare sources if factor is <= 100 and no task position is given, this factor multiplied by the average luminance in the entire picture will be used as threshold for detecting the glare sources, default value=5.

−c *fname*
writes a checkfile in the RADIANCE picture format

−d enables detailed output (default: disabled)

−g *type* cut field of view according to Guth, write checkfile specified by –c and exit without any glare evaluation. type=1: total field of view type=2: field of view seen by both eyes

−G *type*
cut field of view according to Guth, perform glare evaluation. type=1: total field of view type=2: field of view seen by both eyes

−i *Ev* The vertical illuminance is measured externally. This value will be used for calculating the dgp.

−I *Ev y_max y_min*
The vertical illuminance is measured externally. This value will be used for calculating the dgp. Below y_min and above y_max, the picture is filled up by the last known value. This option should be used, when the provided picture is cut horizontally.

−r *angle*
search radius (angle in radiant) between pixels, where evalglare tries to merge glare source pixels to the same glare source (default value: 0.2 radiant)

−s enables smoothing function (default: disabled)

−t *xpos ypos angle*
definition of task position in x and y coordinates, and its opening angle in radiant

−T *xpos ypos angle*
same as −t, except that the task area is colored bluish in the checkfile

−u *r g b*
color glare sources unfiformly when writing check file (implies −c option). Color given in r g b.

−v show version of evalglare and exit

−V Just calculate the vertical illuminance and exit

−x disable peak extraction

−y enables peak extraction (default: enabled)

−Y *value*
enables peak extraction with value as threshold for extracted peaks

In case, the view settings within the image are missing or are not valid (e.g. after the use of pcompos or pcomb), the view options can be set by command line options. As soon as view options are set within the command line, view options within the image are ignored. The view options are implemented according to the RADIANCE definition (please read man page of rpict for details):

−vtt Set view type to t (for fish−eye views, please use –vta or –vth preferably)

−vf *viewfile*
Get view parameters from file

−vv *val* Set the view vertical size to val

−vh *val* Set the view horizontal size to *val*

ACKNOWLEDGEMENTS

The evalglare program was developped by Jan Wienold originally at the Fraunhofer Institute for Solar Energy Systems in Freiburg, Germany. It is further developped and maintained by the same author at EPFL, Lausanne, Switzerland.

The author would like to thank C. Reetz for his generous help and his support of providing libraries for the program. The EU Commission supported this work as part of the EU project âEnergy and Comfort Control for Building management systemsâ (ECCO-Build, Contract NÂ°: ENK6-CT-2002-00656).

The dfg-foundation (contract WI 1304/7-2) supported the research for the extension of evalglare for low-light scenes.

AUTHORS

Jan Wienold.

NAME

pfilt - filter a RADIANCE picture

SYNOPSIS

pfilt [**options**] [**file**]

DESCRIPTION

Pfilt performs anti-aliasing and scaling on a RADIANCE picture. The program makes two passes on the picture file in order to set the exposure to the correct average value. If no *file* is given, the standard input is read.

-x *res* Set the output x resolution to *res*. This must be less than or equal to the x dimension of the target device. If *res* is given as a slash followed by a real number, the input resolution is divided by this number to get the output resolution. By default, the output resolution is the same as the input.

-y *res* Set the output y resolution to *res*, similar to the specification of the x resolution above.

-p *rat* Set the pixel aspect ratio to *rat*. Either the x or the y resolution will be reduced so that the pixels have this ratio for the specified picture. If *rat* is zero, then the x and y resolutions will adhere to the given maxima. Zero is the default.

-c Pixel aspect ratio is being corrected, so do not write PIXASPECT variable to output file.

-e *exp* Adjust the exposure. If *exp* is preceded by a '+' or '-', the exposure is interpreted in f-stops (ie. the power of two). Otherwise, *exp* is interpreted as a straight multiplier. The individual primaries can be changed using *−er, −eg* and *−eb*. Multiple exposure options have a cumulative effect.

-t lamp Color-balance the image as if it were illuminated by fixtures of the given type. The specification must match a pattern listed in the lamp lookup table (see the −f option below).

-f lampdat Use the specified lamp lookup table rather than the default (lamp.tab).

−1 Use only one pass on the file. This allows the exposure to be controlled absolutely, without any averaging. Note that a single pass is much quicker and should be used whenever the desired exposure is known and star patterns are not required.

−2 Use two passes on the input. This is the default.

−b Use box filtering (default). Box filtering averages the input pixels corresponding to each separate output pixel.

-r *rad* Use Gaussian filtering with a radius of *rad* relative to the output pixel size. This option with a radius around 0.6 and a reduction in image width and height of 2 or 3 produces the highest quality pictures. A radius greater than 0.7 results in a defocused picture.

-m *frac* Limit the influence of any given input pixel to *frac* of any given output pixel. This option may be used to mitigate the problems associated with inadequate image sampling, at the expense of a slightly blurred image. The fraction given should not be less than the output picture dimensions over the input picture dimensions (x_o*y_o/x_i/y_i), or blurring will occur over the entire image. This option implies the *−r* option for Gaussian filtering, which defaults to a radius of 0.6.

-h *lvl* Set intensity considered "hot" to *lvl*. This is the level above which areas of the image will begin to exhibit star diffraction patterns (see below). The default is 100 watts/sr/m2.

-n *N* Set the number of points on star patterns to *N*. A value of zero turns star patterns off. The default is 0. (Note that two passes are required for star patterns.)

-s *val* Set the spread for star patterns to *val*. This is the value a star pattern will have at the edge of the image. The default is .0001.

−a Average hot spots as well. By default, the areas of the picture above the hot level are not used in setting the exposure.

ENVIRONMENT

RAYPATH directories to search for lamp lookup table

FILES

/tmp/rt??????

AUTHOR

Greg Ward

SEE ALSO

getinfo(1), ies2rad(1), pcompos(1), pflip(1), pinterp(1), pvalue(1), protate(1), rad(1), rpict(1), ximage(1)

NAME

falsecolor − make a false color RADIANCE picture

SYNOPSIS

falsecolor [**−i input**][**−p picture**][**−cb** | **−cl** | **−cp**][**−e**][**−s scale**][**−l label**][**−n ndivs**][**−lw lwidth**][**−lh lheight**][**−log decades**][**−m mult**][**−pal palette**][**−r redv**][**−g grnv**][**−b bluv**]

falsecolor −palettes

DESCRIPTION

Falsecolor produces a false color picture for lighting analysis. Input is a rendered Radiance picture.

By default, luminance is displayed on a linear scale from 0 to 1000 cd/m2, where dark areas are purple and brighter areas move through blue, green, red to yellow. A different scale can be given with the *−s* option. If the argument given to *−s* begins with an "a" for "auto," then the maximum is used for scaling the result. The default multiplier is 179, which converts from radiance or irradiance to luminance or illuminance, respectively. A different multiplier can be given with *−m* to get daylight factors or whatever. For a logarithmic rather than a linear mapping, the *−log* option can be used, where *decades* is the number of decades below the maximum scale desired.

A legend is produced for the new image with a label given by the *−l* option. The default label is "cd/m2", which is appropriate for standard Radiance images. If the *−i* option of *rpict(1)* was used to produce the image, then the appropriate label would be "Lux".

If contour lines are desired rather than just false color, the *−cl* option can be used. These lines can be placed over another Radiance picture using the *−p* option. If the input picture is given with *−ip* instead of *−i*, then it will be used both as the source of values and as the picture to overlay with contours. The *−cb* option produces contour bands instead of lines, where the thickness of the bands is related to the rate of change in the image. The *−cp* option creates a posterization effect where colours are banded without the background image showing through. The *−n* option can be used to change the number of contours (and corresponding legend entries) from the default value of 8. The *−lw* and *−lh* options may be used to change the legend dimensions from the default width and height of 100x200. A value of zero in either eliminates the legend in the output.

The *−e* option causes extrema points to be printed on the brightest and darkest pixels of the input picture.

The *−pal* option provides different color palettes for *falsecolor*. The current choices are *spec* for the old spectral mapping, *hot* for a thermal scale, *eco* for a blue-red-yellow scale, and *pm3d* for a variation of the default mapping, *def*. A Radiance HDR image of all available palettes can be created with the *−palettes* option. The remaining options, *−r*, *−g*, and *−b* are for changing the mapping of values to colors. These are expressions of the variable *v*, where *v* varies from 0 to 1. These options are not recommended for the casual user.

If no *−i* or *−ip* option is used, input is taken from the standard input. The output image is always written to standard output, which should be redirected.

EXAMPLES

To create a false color image directly from *rpict(1)*:

```
rpict −vf default.vp scene.oct | falsecolor > scene.hdr
```

To show the available color palettes:

```
falsecolor -palettes | ximage
```

To create a logarithmic contour plot of illuminance values on a Radiance image:

```
rpict −i −vf default.vp scene.oct > irrad.hdr
rpict −vf default.vp scene.oct > rad.hdr
falsecolor −i irrad.hdr −p rad.hdr −cl −log 2 −l Lux > lux.hdr
```

AUTHOR

Greg Ward
Axel Jacobs (Perl translation and −pal options)

ACKNOWLEDGEMENT

Work on this program was initiated and sponsored by the LESO group at EPFL in Switzerland. The 'eco' palette was sponsored by Foster + Partners in London.

SEE ALSO

getinfo(1), pcomb(1), pcompos(1), pextrem(1), pfilt(1), pflip(1), protate(1), psign(1), rpict(1), ximage(1)

NAME

epw2wea - weather file converter

SYNOPSIS

epw2wea file_name.epw file_name.wea

DESCRIPTION

epw2wea transforms an EnergyPlus weather data (.epw) file into the DAYSIM weather file format, for use with the RADIANCE gendaymtx program.

AUTHOR

Christoph Reinhart, Jason Turner

SEE ALSO

gendaymtx(1)

NAME

gendaymtx - generate an annual Perez sky matrix from a weather tape

SYNOPSIS

gendaymtx [**−v**][**−h**][**−d|−s**][**−r deg**][**−m N**][**−g r g b**][**−c r g b**][**-o{f|d}**][**-O{0|1}**] [**tape.wea**]

DESCRIPTION

Gendaymtx takes a weather tape as input and produces a matrix of sky patch values using the Perez all-weather model. The weather tape is assumed to be in the simple ASCII format understood by DAYSIM, which contains a short header with the site parameters followed by the month, day, standard time, direct normal and diffuse horizontal irradiance values, one time step per line. Each time step line is used to compute a column in the output matrix, where rows correspond to sky patch positions, starting with 0 for the ground and continuing to 145 for the zenith using the default *−m 1* parameter setting.

Increasing the *−m* parameter, typically by factors of two, yields a higher resolution sky using the Reinhart patch subdivision. For example, setting *−m 4* yields a sky with 2305 patches plus one patch for the ground. Each matrix entry is in fact three values, corresponding to red green and blue radiance channels (watts/sr/meter^2). Thus, an hourly weather tape for an entire year would yield 8760x3 (26280) values per output line (row).

The *−c* option may be used to specify a color for the sky. The gray value should equal 1 for proper energy balance. The default sky color is *−c 0.960 1.004 1.118* . Similarly, the *−g* option may be used to specify a ground color. The default value is *−g 0.2 0.2 0.2* corresponding to a 20% gray.

The *−d* option may be used to produce a sun-only matrix, with no sky contributions. Alternatively, the *−s* option may be used to exclude any direct solar component from the output.

By default, *gendaymtx* assumes the positive Y-axis points north such that the first sky patch is in the Y-axis direction on the horizon, the second patch is just west of that, and so on spiraling around to the final patch near the zenith. The *−r* (or *−rz)* option rotates the sky the specified number of degrees counter-clockwise about the zenith, i.e., west of north. This is in keeping with the effect of passing the output of *gensky(1)* or *gendaylit(1)* through *xform(1)* using a similar transform.

The *−of* or *−od* option may be used to specify binary float or double output, respectively. This is much faster to write and to read, and is therefore preferred on systems that support it. (MS Windows is not one of them.) The *−O1* option specifies that output should be total solar radiance rather than visible radiance. The *−h* option prevents the output of the usual header information. Finally, the *−v* option will enable verbose reporting, which is mostly useful for finding out how many time steps are actually in the weather tape.

EXAMPLES

Produce an uncolored Tregenza sky matrix without solar direct:

```
gendaymtx -m 1 -c 1 1 1 -s Detroit.wea > Detroit.mtx
```

Produce an hourly, annual Reinhart sky matrix with 2306 patches including solar contributions and send float output to *dctimestep(1)* to compute a sensor value matrix:

```
gendaymtx -m 4 -of VancouverBC.wea | dctimestep -if -n 8760 DCoef.mtx > res.dat
```

AUTHORS

Ian Ashdown wrote most of the code, based on Jean-Jacques Delaunay's original gendaylit(1) implementation. Greg Ward wrote the final parameter parsing and weather tape conversion.

SEE ALSO

dctimestep(1), genBSDF(1), gendaylit(1), gensky(1), genskyvec(1), rcollate(1), rcontrib(1), xform(1)

NAME

rcontrib - compute contribution coefficients in a RADIANCE scene

SYNOPSIS

rcontrib [**−n nprocs**][**−V**][**−c count**][**−fo** | **−r**][**−e expr**][**−f source**][**−o ospec**][**−p p1=V1,p2=V2**][**−b binv**][**−bn nbins**] { **−m mod** | **−M file** } [**SEVAR**] [**@file**] [rtrace options] **octree**
rcontrib [options] −defaults

DESCRIPTION

Rcontrib computes ray coefficients for objects whose modifiers are named in one or more *−m* settings. These modifiers are usually materials associated with light sources or sky domes, and must directly modify some geometric primitives to be considered in the output. A modifier list may also be read from a file using the *−M* option. The RAYPATH environment variable determines directories to search for this file. (No search takes place if a file name begins with a '.', '/' or '~' character.)

If the *−n* option is specified with a value greater than 1, multiple processes will be used to accelerate computation on a shared memory machine. Note that there is no benefit to using more processes than there are local CPUs available to do the work, and the *rcontrib* process itself may use a considerable amount of CPU time.

By setting the boolean *−V* option, you may instruct *rcontrib* to report the contribution from each material rather than the ray coefficient. This is particularly useful for light sources with directional output distributions, whose value would otherwise be lost in the shuffle. With the default *-V-* setting, the output of rcontrib is a coefficient that must be multiplied by the radiance of each material to arrive at a final contribution. This is more convenient for computing daylight coefficeints, or cases where the actual radiance is not desired. Use the *-V+* setting when you wish to simply sum together contributions (with possible adjustment factors) to obtain a final radiance value. Combined with the *−i* or *−I* option, irradiance contributions are reported by *−V+* rather than radiance, and *−V-* coefficients contain an additonal factor of PI.

The *−c* option tells *rcontrib* how many rays to accumulate for each record. The default value is one, meaning a full record will be produced for each input ray. For values greater than one, contributions will be averaged together over the given number of input rays. If set to zero, only a single record will be produced at the very end, corresponding to the sum of all rays given on the input (rather than the average). This is equivalent to passing all the output records through a program like *total(1)* to sum RGB values together, but is much more efficient. Using this option, it is possible to reverse sampling, sending rays from a parallel source such as the sun to a diffuse surface, for example. Note that output flushing via zero-direction rays is disabled with *−c* set to zero.

The output of *rcontrib* has many potential uses. Source contributions can be used as components in linear combination to reproduce any desired variation, e.g., simulating lighting controls or changing sky conditions via daylight coefficients. More generally, *rcontrib* can be used to compute arbitrary input-output relationships in optical systems, such as luminaires, light pipes, and shading devices.

Rcontrib sends the accumulated rays tallies to one or more destinations according to the given *−o* specification. If a destination begins with an exclamation mark ('!'), then a pipe is opened to a command and data is sent to its standard input. Otherwise, the destination is treated as a file. An existing file of the same name will not be clobbered, unless the *−fo* option is given. If instead the *−r* option is specified, data recovery is attempted on existing files. (If *−c 0* is used together with the *−r* option, existing files are read in and new ray evaluations are added to the previous results, providing a convenient means for progressive simulation.) If an output specification contains a "%s" format, this will be replaced by the modifier name. The *−b* option may be used to further define a "bin number" within each object if finer resolution is needed, and this will be applied to a "%d" format in the output file specification if present. The actual bin number is computed at run time based on ray direction and surface intersection, as described below. The number of bins must be specified in advance with the *−bn* option, and this is critical for output files containing multiple values per record. A variable or constant name may be given for this parameter if it has been defined via a previous *−f* or *−e* option. Since bin numbers start from zero, the bin count is always equal to the last bin plus one. The most recent *−p, −b, −bn* and *−o* options to the left of each *−m* setting are the ones used for that modifier. The ordering of other options is unimportant, except for *−x* and *−y* if the *−c* is zero, when they control the resolution string produced in the corresponding output.

If a *−b* expression is defined for a particular modifier, the bin number will be evaluated at run time for each ray contribution. Specifically, each ray's world intersection point will be assigned to the variables Px, Py, and Pz, and the normalized ray direction will be assigned to Dx, Dy, and Dz. These parameters may be combined with definitions given in *−e* arguments and files read using the *−f* option. Additional parameter values that apply only to this modifier may be specified with a *−p* option, which contains a list of variable names and assigned values, separated by commas or semicolons. The computed bin value will be rounded to the nearest whole number. (Negative bin values will be silently ignored.) For a single bin, you may specify *−b 0*, which is the default. This mechanism allows the user to define precise regions or directions they wish to accumulate, such as the Tregenza sky discretization, which would be otherwise impossible to specify as a set of RADIANCE primitives. The rules and predefined functions available for these expressions are described in the *rcalc(1)* man page. Like *rcalc, rcontrib* will search the RADIANCE library directories for each file given in a *−f* option.

If no *−o* specification is given, results are written on the standard output in order of modifier (as given on the command line) then bin number. Concatenated data is also sent to a single destination (i.e., an initial *−o* specification without formatting strings). If a "%s" format appears but no "%d" in the *−o* specification, then each modifier will have its own output file, with multiple values per record in the case of a non-zero *−b* definition. If a "%d" format appears but no "%s", then each bin will get its own output file, with modifiers output in order in each record. For text output, each RGB coefficient triple is separated by a tab, with a newline at the end of each ray record. For binary output formats, there is no such delimiter to mark the end of each record.

Input and output format defaults to plain text, where each ray's origin and direction (6 real values) are given on input, and one line is produced per output file per ray. Alternative data representations may be specified by the *−f[io]* option, which is described in the *rtrace* man page along with the associated *−x* and *−y* resolution settings. In particular, the color ('c') output data representation together with positive dimensions for *−x* and *−y* will produce an uncompressed RADIANCE picture, suitable for manipulation with *pcomb(1)* and related tools.

Options may be given on the command line and/or read from the environment and/or read from a file. A command argument beginning with a dollar sign ('$') is immediately replaced by the contents of the given environment variable. A command argument beginning with an at sign ('@') is immediately replaced by the contents of the given file.

EXAMPLES

To compute the proportional contributions from sources modified by "light1" vs. "light2" on a set of illuminance values:

```
rcontrib −I+ @render.opt −o c_%s.dat −m light1 −m light2 scene.oct < test.dat
```

To generate a pair of images corresponding to these two lights' contributions:

```
vwrays −ff −x 1024 −y 1024 −vf best.vf | rcontrib −ffc 'vwrays −d −x 1024 −y 1024 −vf best.vf' @render.opt −o c_%s.hdr −m light1 −m light2 scene.oct
```

These images may then be recombined using the desired outputs of light1 and light2:

```
pcomb −c 100 90 75 c_light1.hdr −c 50 55 57 c_light2.hdr > combined.hdr
```

To compute an array of illuminance contributions according to a Tregenza sky:

```
rcontrib −I+ −f tregenza.cal −b tbin −bn Ntbins −o sky.dat −m skyglow −b 0 −o ground.dat −m groundglow @render.opt scene.oct < test.dat
```

ENVIRONMENT

RAYPATH path to search for −f and −M files

AUTHOR

Greg Ward

SEE ALSO

cnt(1), genklemsamp(1), getinfo(1), pcomb(1), pfilt(1), ra_rgbe(1), rcalc(1), rfluxmtx(1), rmtxop(1), rpict(1), rsensor(1), rtrace(1), total(1), vwrays(1), ximage(1)

NAME

rfluxmtx - compute flux transfer matrix(es) for RADIANCE scene

SYNOPSIS

rfluxmtx [−v][rcontrib options] { sender.rad | - } receivers.rad [-i system.oct] [system.rad ..]

DESCRIPTION

Rfluxmtx samples rays uniformly over the surface given in *sender.rad* and records rays arriving at surfaces in the file *receivers.rad*, producing a flux transfer matrix per receiver. A system octree to which the receivers will be appended may be given with a *−i* option following the receiver file. Additional system surfaces may be given in one or more *system.rad* files, which are compiled before the receiver file into an octree sent to the *rcontrib(1)* program to do the actual work. If a single hyphen ('-') is given in place of the sender file, then *rfluxmtx* passes ray samples from its standard input directly to *rcontrib* without interpretation. By default, all resulting matrix data are interleaved and sent to the standard output in ASCII format, but this behavior is typically overridden using inline options as described below.

The *−v* option turns on verbose reporting for the number of samples and the executed *rcontrib* command. All other supported options are passed on to *rcontrib(1)*. However, the *−f, −e, −p, −b, −bn, −m,* and *−M* options are controlled by *rfluxmtx* and may not be set by the user. Also, the *−x, −y,* and *−ld* options are ignored unless *rfluxmtx* is invoked in the pass-through mode, in which case they may be needed to generate RADIANCE views from *vwrays(1)*. The sample count, unless set by the *−c* option, defaults to 10000 when a sender file is given, or to 1 for pass-through mode.

VARIABLES

The sender and receiver scene files given to *rfluxmtx* contain controlling parameters in special comments of the form:

```
#@rfluxmtx variable=value ..
```

At minimum, both sender and receiver must specify one of the hemisphere sampling types, and there must be at least one surface in each file.

h=*u* Set hemisphere sampling to "uniform," meaning a single bin of (cosine-distributed) samples. In the case of distant "source" primitives, this is the only sampling method that supports arbitrary receiver sizes. The other methods below require a full hemispherical source.

h=*kf* Divide the hemisphere using the LBNL/Klems "full" sampling basis.

h=*kh* Divide the hemisphere using the LBNL/Klems "half" sampling basis.

h=*kq* Divide the hemisphere using the LBNL/Klems "quarter" sampling basis.

h=*rN* Divide the hemisphere using Reinhart's substructuring of the Tregenza sky pattern with *N* divisions in each dimension. If it is not given, *N* defaults to 1, which is just the Tregenza sky.

h=*scN* Subdivide the hemisphere using the Shirley-Chiu square-to-disk mapping with an *NxN* grid over the square.

u=*[-]{X|Y|Z|ux,uy,uz}*
Orient the "up" direction for the hemisphere using the indicated axis or direction vector.

o=*output.mtx*
Send the matrix data for this receiver to the indicated output file. The file format will be determined by the command-line *−fio* option and will include an information header unless the *−h* option was used to turn headers off. (The output file specification is ignored for senders.)

In normal execution, only a single sender surface is sampled, but it may be comprised of any number of subsurfaces, as in a triangle mesh or similar. The surface normal will be computed as the average of all the constituent subsurfaces. The subsurfaces themselves must be planar, thus only *polygon* and *ring* surface primitives are supported. Other primitives will be silently ignored and will have no effect on the calculation.

In the receiver file, the *source* primitive is supported as well, and multiple receivers (and multiple output

matrices) are identified by different modifier names. Though it may be counter-intuitive, receivers are often light sources, since samples end up there in a backwards ray-tracing system such as RADIANCE. When using local geometry, the overall aperture shape should be close to flat. Large displacements may give rise to errors due to a convex receiver's larger profile at low angles of incidence.

Rays always emanate from the back side of the sender surface and arrive at the front side of receiver surfaces. In this way, a receiver surface may be reused as a sender in a subsequent *rfluxmtx* calculation and the resulting matrices will concatenate properly. (Note that it is important to keep receiver surfaces together, otherwise a "duplicate modifier" error will result.)

EXAMPLES

To generate a flux transfer matrix connecting input and output apertures on a light pipe:

```
rfluxmtx int_aperture.rad ext_aperture.rad lpipe.rad > lpipe.mtx
```

AUTHOR

Greg Ward

SEE ALSO

genBSDF(1), getinfo(1), rcalc(1), rcollate(1), rcontrib(1), rmtxop(1), vwrays(1)

NAME

dctimestep - compute annual simulation time-step(s) via matrix multiplication

SYNOPSIS

dctimestep [**−n nsteps**][**−h**][**−o ospec**][**−i{f|d}**][**−o{f|d}**] **DCspec** [**skyf**]
dctimestep [**−n nsteps**][**−h**][**−o ospec**][**−i{f|d}**][**−o{f|d}**] **Vspec Tbsdf.xml Dmat.dat** [**skyf**]

DESCRIPTION

Dctimestep has two invocation forms. In the first form, *dctimestep* is given a daylight coefficient specification and an optional sky vector or matrix, which may be read from the standard input if unspecified. The daylight coefficients are multiplied against these sky values and the results are written to the standard output. This may be a list of color values or a combined Radiance image, as explained below.

In the second form, *dctimestep* takes four input files, forming a matrix expression. The first argument is the View matrix file that specifies how window output directions are related to some set of measured values, such as an array of illuminance points or images. This matrix is usually computed by *rcontrib(1)* for a particular set of windows or skylight openings. The second argument is the window transmission matrix, or BSDF, given as a standard XML description. The third argument is the Daylight matrix file that defines how sky patches relate to input directions on the same opening. This is usually computed using *genklemsamp(1)* with *rcontrib* in a separate run for each window or skylight orientation. The last file is the sky contribution vector or matrix, typically computed by *genskyvec(1)* or *gendaymtx(1),* and may be passed on the standard input. This data is assumed by default to be in ASCII format, whereas the formats of the View and Daylight matrices are detected automatically if given as binary data.

If the input sky data lacks a header, the *−n* option may be used to indicate the number of time steps, which will be 1 for a sky vector. The sky input file must contain the number of columns specified in each sky patch row, whether it is read from the standard input or from a file. Input starts from the first patch at the first time step, then the first patch at the second time step, and so on. The *−if* or *−id* option may be used to specify that sky data is in float or double format, respectively, which is more efficient for large matrices. These options are unnecessary in the when the sky input has a header.

The standard output of *dctimestep* is either a color vector with as many RGB triplets as there are rows in the View matrix, or a combined *Radiance* picture. Which output is produced depends on the first argument. A regular file name will be loaded and interpreted as a matrix to generate a color results vector. A file specification containing a '%d' format string will be interpreted as a list of *Radiance* component pictures, which will be summed according to the computed vector.

The *−o* option may be used to specify a file or a set of output files to use rather than the standard output. If the given specification contains a '%d' format string, this will be replaced by the time step index, starting from 1. In this way, multiple output pictures may be produced, or separate result vectors (one per time step).

A header will normally be produced on the output, unless the *−h* option is specified. The *−of* or *−od* option may be used to specify IEEE float or double binary output data, respectively.

EXAMPLES

To compute workplane illuminances at 3:30pm on Feb 10th:

gensky 2 10 15:30 | genskyvec | dctimestep workplaneDC.dmx > Ill_02-10-1530.dat

To compute an image at 10am on the equinox from a set of component images:

gensky 3 21 10 | genskyvec | dctimestep dcomp%03d.hdr > view_03-21-10.hdr

To compute a set of illuminance contributions for Window 1 on the Winter solstice at 2pm:

gensky 12 21 14 | genskyvec | dctimestep IllPts.vmx Blinds20.xml Window1.dmx > Ill_12-21-14.dat

To compute Window2's contribution to an interior view at 12 noon on the Summer solstice:

gensky 6 21 12 | genskyvec | dctimestep view%03d.hdr Blinds30.xml Window2.dmx > view_6-21-12.hdr

To generate an hourly matrix of sensor value contributions from Skylight3 using a 3-phase calculation,

where output columns are time steps:

gendaymtx -of Tampa.wea | dctimestep WPpts.vmx shade3.xml Skylight3.dmx > wp_win3.dat

Generate a series of pictures corresponding to timesteps in an annual simulation:

gendaymtx NYCity.wea | dctimestep -o tstep%04d.hdr dcomp%03d.hdr

To multiply two matrices into a IEEE-float result with header:

dctimestep -of Inp1.fmx Inp2.fmx > Inp1xInp2.fmx

AUTHOR

Greg Ward

SEE ALSO

gendaymtx(1), genklemsamp(1), genskyvec(1), getinfo(1), mkillum(1), rcollate(1), rcontrib(1), rmtxop(1), rtrace(1), vwrays(1)

Annex 2: White Balance of fisheye projection photographs

Taking into account that the digital camera (Canon EOS 600D with Canon objective EFS 18-55mm) has many light source types, from the same point of view and with three exposures (-1, 0, 1) photographs have been taken with fisheye projection (Lens-Gloxy; Front Filter Size, 67 mm; conversion factor, 0.42x; thread Size, 46mm) according to different light source types. In the following table there are listed the used light sources.

	Light Measurements in the picture		
LIGHT TYPE	One point: Middle	One point: Right Extreme Middle	All points of camera: (It chooses automatically)
Auto	3 (-1,0,+1)	3 (-1,0,+1)	3 (-1,0,+1)
Daylight (5 200 K)	3 (-1,0,+1)	3 (-1,0,+1)	3 (-1,0,+1)
Shadow (7 000 K	3 (-1,0,+1)	3 (-1,0,+1)	3 (-1,0,+1)
Cloudy (6 000 K)	3 (-1,0,+1)	3 (-1,0,+1)	3 (-1,0,+1)
Tungsten (3 200 K)	3 (-1,0,+1)	3 (-1,0,+1)	3 (-1,0,+1)
White Fluorescent (4 000 K)	3 (-1,0,+1)	3 (-1,0,+1)	3 (-1,0,+1)
Flash	3 (-1,0,+1)	3 (-1,0,+1)	3 (-1,0,+1)
Personalized	3 (-1,0,+1)	3 (-1,0,+1)	3 (-1,0,+1)

Table A2. 1 Light measurements in the picture for white balance

The results show that the white colours (according to Hue (Red, Blue and Green), Saturation and Brightness) of different daylight spectrum are not very different for checking the luminance distribution from human eye conditions. In addition, with Auto option and Daylighting options there are not a huge difference, as well. In the following there are all pictures obtained. Regarding electric lighting, the spectrum is quite different and as well as, the colour temperature. So, white colour provided by electric lighting is different to white colour provided by daylighting. As in the case studio is for daylighting the auto option could be acceptable choice.

The pictures provided by electric lighting are cold because the light is thought for low flux. The personalized option is strange because it is not calibrated.

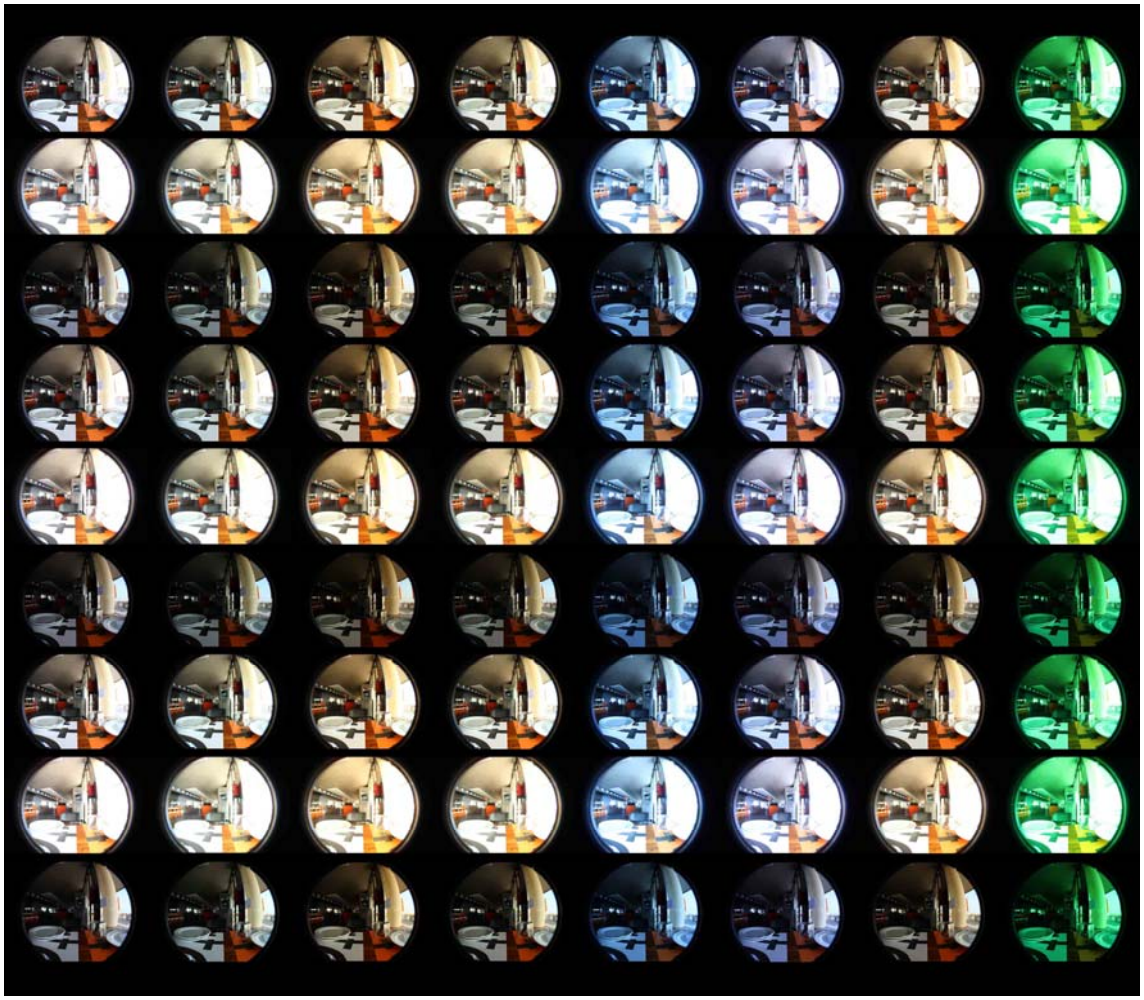

Figure A2. 1 Photographs with different light source type to check white colour difference

Annex 3: Calibration of illuminance obtained by TPM results according to illuminance obtained by DIVA

Comparing with illuminance measurements, it seems that DIVA has a little lower results and TPM has a little higher results. In both simulation methods is very important the calibration with real data.

	Illuminance measurements (lux)	
	Restaurant1 (Sal Café)	Restaurant2 (Azurmendi)
Exterior horizontal plane	82 000	73 500
Exterior vertical plane	13 200	9 760
Sensor Point $431_{SalCafé}$ and $356_{Azurmendi}$	2350	2 540
Sensor Point $409_{SalCafé}$ and $335_{Azurmendi}$	414	880

Table A3. 1 The illuminance measurements for Restaurant 1 (Sal Café) and Restaurants 2 (Azurmendi)

	Point-in-Time Illuminance (lux) of 3M Prismatic Film CFS (SAL CAFÉ)					
Nº Sensor	No Frame		Large Frame		Small Frame	
	DIVA	TPM	DIVA	TPM	DIVA	TPM
409	221	470	179	391	131	355
410	240	482	216	383	142	372
411	242	421	234	497	165	337
412	296	557	233	519	215	485
413	322	622	293	610	207	477
414	325	643	320	555	248	462
415	352	696	302	610	272	551
416	387	809	330	770	242	563
417	436	919	433	824	311	609
418	493	977	464	922	324	726
419	543	1085	511	1007	393	771
420	599	1115	593	1044	389	764
421	644	1382	607	1260	404	945
422	703	1371	692	1280	520	1003
423	804	1562	837	1584	554	1199
424	836	1722	877	1688	613	1332
425	940	1889	1009	1861	712	1363
426	1041	2135	1119	1987	733	1445
427	1157	2297	1223	2125	851	1521
428	1208	2386	1312	2353	763	1663

429	1385	2511	1310	2395	791	1491
430	**1524**	**2651**	**1506**	**2471**	**644**	**1375**
431	**1866**	**2960**	**1791**	**2797**	**608**	**1128**
432	**2123**	**3135**	**1984**	**3017**	**339**	**790**

Table A3. 2 Point-in-Time Illuminance (lux) of 3M Prismatic Film CFS by DIVA and TPM (SAL CAFÉ). Sensor points in bold are on the table

	Point-in-Time Illuminance (lux) of 3M Prismatic Film CFS (AZURMENDI)					
Nº	No Frame		Large Frame		Small Frame	
Sensor	DIVA	TPM	DIVA	TPM	DIVA	TPM
335	284	801	273	950	269	824
336	308	947	279	950	299	941
337	349	1051	324	1002	300	973
338	413	1191	432	1173	390	1163
339	427	1313	427	1287	403	1261
340	465	1437	464	1328	449	1412
341	514	1503	504	1505	486	1596
342	540	1748	565	1744	535	1604
343	601	1868	611	1812	580	1751
344	659	1924	676	2084	694	1853
345	720	2116	751	2082	752	1979
346	793	2321	828	2357	746	2267
347	858	2503	869	2577	867	2486
348	941	2723	967	2658	944	2572
349	1046	2963	1024	3028	1026	2761
350	1124	3200	1115	3151	1087	2845
351	1223	3367	1179	3301	1056	3120
352	1236	3549	1256	3451	1115	2868
353	**1302**	**3800**	**1300**	**3555**	**1122**	**3043**
354	**1368**	**3837**	**1344**	**3965**	**1133**	**2968**
355	**1540**	**4391**	**1500**	**4326**	**1179**	**3104**
356	**1840**	**5053**	**1818**	**4998**	**1323**	**3224**
357	**2121**	**5578**	**2119**	**5627**	**1310**	**3092**
358	**2236**	**6206**	**2262**	**6256**	**906**	**2372**

Table A3. 3 Point-in-Time Illuminance (lux) of 3M Prismatic Film CFS by DIVA and TPM (AZURMENDI). Sensor points in bold are on the table

To test the Daylight Autonomy of 3M Prismatic Film CFS, Three-Phase Method illuminance results have been calibrated according to DIVA illuminance results. In the following the calibrated 3M Prismatic Film DA of No Frame and Small Frame Window Systems is presented. The results are of both restaurants, Sal Café and Azurmendi.

	No Frame (SAL CAFÉ)				
	DA			E	
Nº Sensor	No CFS (DIVA)	3M Prismatic Film (TPM)	Calibrated 3M Prismatic Film (TPM)	3M Prismatic Film (DIVA)	Calibrated 3M Prismatic Film (TPM)
409	13	51	14	221	296
410	14	52	15	240	304
411	13	44	3	242	265
412	20	62	34	296	351
413	31	66	38	322	392
414	33	69	43	325	405
415	42	68	45	352	438
416	45	77	53	387	510
417	51	82	61	436	579
418	50	84	64	493	615
419	54	88	70	543	683
420	57	89	70	599	703
421	64	93	82	644	871
422	65	92	81	703	864
423	66	94	86	804	984
424	68	96	89	836	1085
425	79	96	91	940	1190
426	82	97	93	1041	1345
427	90	98	94	1157	1447
428	89	98	94	1208	1503
429	92	98	95	1385	1582
430	**95**	**98**	**95**	**1524**	**1670**
431	**98**	**99**	**96**	**1866**	**1865**
432	**98**	**99**	**96**	**2123**	**1975**

Table A3. 4 Calibrated TPM DA according to illuminance results of DIVA, for No Frame window system of Restaurant 1, Sal Café. Sensor points in bold are on the table

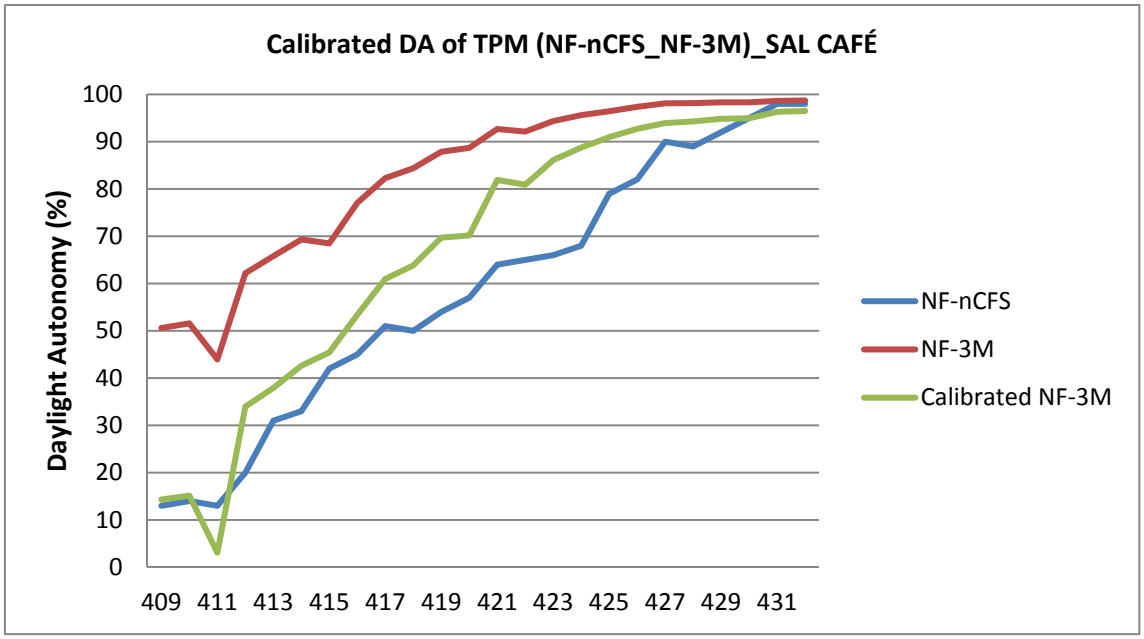

Figure A3. 1 Calibrated TPM DA according to illuminance results of DIVA, for No Frame window system of Restaurant 1, Sal Café

	Small Frame (SAL CAFÉ)				
	DA			E	
Nº Sensor	No CFS (DIVA)	3M Prismatic Film (TPM)	Calibrated 3M Prismatic Film (TPM)	3M Prismatic Film (DIVA)	Calibrated 3M Prismatic Film (TPM)
409	0	26	0	131	192
410	0	34	1	142	201
411	0	26	2	165	182
412	2	52	4	215	262
413	4	52	3	207	258
414	0	48	3	248	250
415	4	59	13	272	298
416	5	62	16	242	304
417	7	65	26	311	329
418	15	74	38	324	392
419	16	76	44	393	416
420	18	75	41	389	412
421	24	84	55	404	510
422	22	86	60	520	542
423	38	89	68	554	647
424	42	92	74	613	719
425	38	92	75	712	736
426	43	93	77	733	780
427	52	93	79	851	821
428	47	95	82	763	898
429	33	93	78	791	805
430	**32**	**91**	**74**	**644**	**742**
431	**31**	**87**	**66**	**608**	**609**
432	**20**	**76**	**46**	**339**	**427**

Table A3. 5 Calibrated TPM DA according to illuminance results of DIVA, for Small Frame window system of Restaurant 1, Sal Café. Sensor points in bold are on the table

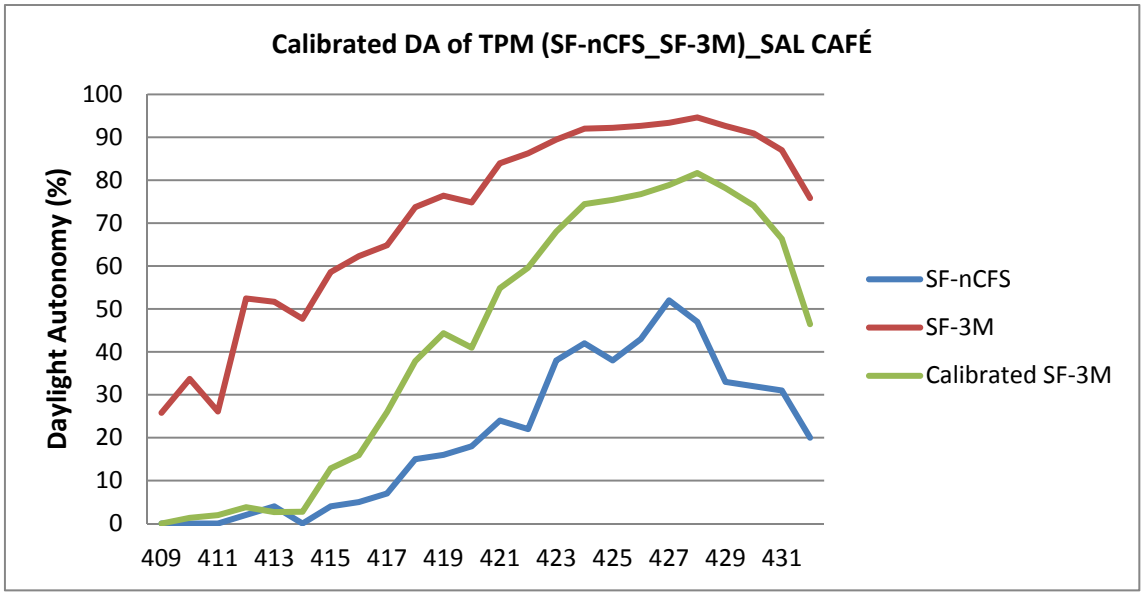

Figure A3. 2 Calibrated TPM DA according to illuminance results of DIVA, for Small Frame window system of Restaurant 1, Sal Café

	No Frame (AZURMENDI)				
	DA			E	
Nº Sensor	No CFS (DIVA)	3M Prismatic Film (TPM)	Calibrated 3M Prismatic Film (TPM)	3M Prismatic Film (DIVA)	Calibrated 3M Prismatic Film (TPM)
335	87	87	20	284	291
336	89	91	41	308	345
337	91	90	54	349	382
338	93	93	66	413	434
339	94	94	71	427	478
340	95	95	75	465	523
341	96	95	77	514	547
342	97	96	82	540	636
343	97	97	84	601	680
344	98	97	85	659	700
345	98	98	86	720	770
346	99	98	88	793	845
347	99	98	90	858	911
348	99	99	91	941	991
349	99	99	92	1046	1079
350	99	99	94	1124	1165
351	99	99	94	1223	1226
352	99	99	94	1236	1292
353	**99**	**99**	**95**	**1302**	**1383**
354	**100**	**99**	**95**	**1368**	**1397**
355	**100**	**99**	**97**	**1540**	**1598**
356	**100**	**99**	**97**	**1840**	**1839**
357	**100**	**100**	**98**	**2121**	**2030**
358	**100**	**100**	**98**	**2236**	**2259**

Table A3. 6 Calibrated TPM DA according to illuminance results of DIVA, for No Frame window system of Restaurant 2, Azurmendi. Sensor points in bold are on the table

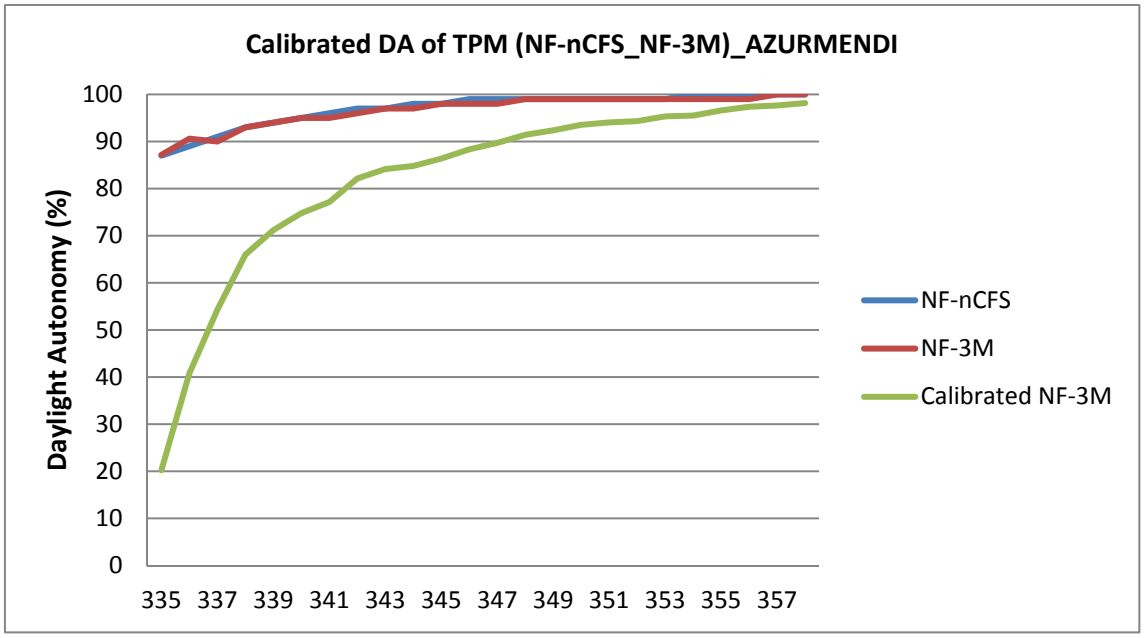

Figure A3. 3 Calibrated TPM DA according to illuminance results of DIVA, for No Frame window system of Restaurant 2, Azurmendi

Small Frame (AZURMENDI)					
	DA			E	
Nº Sensor	No CFS (DIVA)	3M Prismatic Film (TPM)	Calibrated 3M Prismatic Film (TPM)	3M Prismatic Film (DIVA)	Calibrated 3M Prismatic Film (TPM)
335	85	88	39	269	338
336	88	90	53	299	386
337	90	91	59	300	399
338	92	94	70	390	477
339	93	95	75	403	517
340	94	96	79	449	579
341	95	97	83	486	654
342	96	97	83	535	658
343	96	97	85	580	718
344	97	98	86	694	760
345	98	98	88	752	811
346	98	99	90	746	930
347	98	99	92	867	1019
348	99	99	92	944	1055
349	99	99	93	1026	1132
350	99	99	93	1087	1166
351	99	99	94	1056	1279
352	99	99	93	1115	1176
353	**99**	**99**	**94**	**1122**	**1248**
354	**99**	**99**	**93**	**1133**	**1217**
355	**99**	**99**	**93**	**1179**	**1273**
356	**99**	**99**	**93**	**1323**	**1322**
357	**98**	**99**	**92**	**1310**	**1268**
358	**95**	**98**	**87**	**906**	**973**

Table A3. 7 Calibrated TPM DA according to illuminance results of DIVA, for Small Frame window system of Restaurant 2, Azurmendi. Sensor points in bold are on the table

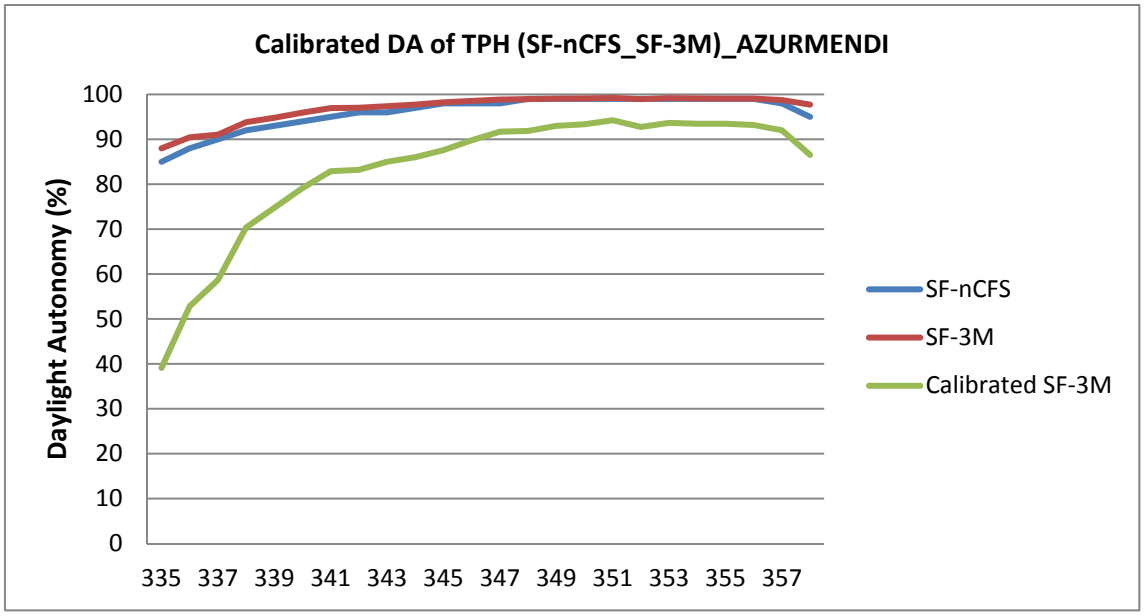

Figure A3. 4 Calibrated TPM DA according to illuminance results of DIVA, for Small Frame window system of Restaurant 2, Azurmendi

The trend of calibrated 3M Prismatic Film CFS Daylight Autonomy results, in Sal Café restaurant they are reasonable. The DA results along the space are higher with 3M Prismatic Film CF than only fully glazed No Frame Window System. However, the trend of calibrated 3M Prismatic Film CFS Daylight Autonomy results in Azurmendi restaurant is confusing. The DA results along the space are lower with 3M Prismatic Film CF Window Systems than only fully glazed No Frame Window System. It seems that, the Daylight Matrix of Three-Phase Method is not entirely completed throughout all hours of the year, although enough to have nice results. But as the difference with illuminance target, 300 lux, is not very huge with any Complex Fenestration Systems some variations have been appeared between both methods. In addition, in some direct and indirect lighting performance some variations have been appeared, as well. Anyway, both simulation methods are very useful to have the trend of different Window Systems, although daylighting is very changeable. Note that, for now the Three/Five/Six Phase Methods are the only methods to get Daylight Autonomy of Complex Fenestration Systems.

Annex 4: Illuminance and Daylight Autonomy results of all sensor-points for Virtual Restaurant Prototype

Point-in-Time Illuminance (lux) by DIVA, 22 July at 12:00 local time (PROTOTYPE)

	No Frame			Large Frame			Small Frame		
Nº Sensor	No CFSnf	Light Shelf	3M Prismatic Film	No CFSlf	Light Shelf	3M Prismatic Film	No CFSsf	Light Shelf	3M Prismatic Film
1	3148	3058	3924	3022	2947	3921	503	560	1388
2	2762	2683	3647	2588	2492	3461	736	786	1755
3	2437	2378	3524	2258	2198	3384	888	904	2174
4	2153	2092	3228	1985	1991	3390	923	978	2209
5	1904	1852	3075	1739	1772	2867	922	981	2052
6	1631	1694	2818	1519	1566	2712	853	953	2138
7	1432	1464	2637	1310	1384	2380	801	888	2037
8	1248	1275	2500	1141	1189	2446	722	792	2043
9	1111	1101	2307	994	1046	2103	667	653	1954
10	948	955	2155	879	898	1958	610	615	1506
11	857	855	1914	770	788	1692	532	528	1489
12	748	733	1725	669	689	1569	469	514	1417
13	660	675	1297	595	633	1264	403	430	1074
14	581	572	1201	537	508	1024	373	373	1162
15	526	529	925	457	484	990	313	310	922
16	492	464	845	399	435	809	283	302	710
17	408	398	743	365	383	571	252	267	570
18	386	396	665	336	337	634	227	234	542
19	351	340	679	291	301	522	203	186	442
20	307	309	428	275	275	410	191	177	346
21	278	281	479	244	247	444	156	176	323
22	276	258	488	220	225	340	126	139	272
23	245	244	353	209	212	391	139	136	392
24	265	222	334	186	190	251	115	125	259
25	232	208	383	180	191	327	143	112	254
26	228	211	309	180	179	245	103	123	213
27	3302	3237	4345	3187	3128	4063	620	647	1511
28	2901	2816	4057	2827	2765	4004	942	953	1931
29	2562	2490	3789	2434	2438	3654	1038	1108	2341
30	2281	2218	3606	2157	2147	3339	1030	1091	2548
31	1965	1971	3329	1845	1876	3015	1013	1101	2307
32	1715	1743	2897	1597	1681	2931	939	1042	2321
33	1503	1544	2800	1409	1466	2623	833	966	2385
34	1309	1325	2427	1226	1267	2569	810	835	2051
35	1151	1151	2183	1066	1078	2219	711	723	1881
36	1024	998	2033	930	978	1992	660	682	1883
37	883	892	1742	797	833	1680	552	561	1533
38	782	766	1554	715	742	1586	464	525	1295
39	694	702	1427	619	647	1366	432	464	1134
40	600	600	1112	557	558	1278	370	375	922
41	551	537	1086	493	519	972	342	357	740

42	482	480	914	441	457	755	300	289	689
43	445	442	727	388	385	668	266	276	680
44	404	387	680	347	357	710	225	245	553
45	365	353	577	315	320	557	197	208	392
46	334	319	539	267	284	491	183	173	434
47	307	285	519	253	248	422	157	167	288
48	274	281	452	228	227	320	149	154	314
49	264	241	340	216	218	333	145	164	208
50	260	239	334	210	215	274	142	126	277
51	239	223	387	197	198	353	117	146	209
52	246	226	350	187	196	301	106	129	216
53	3349	3272	4325	3246	3217	4262	748	764	1893
54	3012	2912	4218	2904	2870	4188	1101	1088	2235
55	2676	2572	4047	2563	2534	4042	1169	1237	2629
56	2321	2298	3912	2236	2229	3492	1131	1269	2477
57	2050	2054	3459	1959	1979	3329	1124	1175	2496
58	1776	1768	2998	1687	1723	3147	1003	1058	2211
59	1544	1533	2888	1462	1504	2696	950	975	2335
60	1351	1349	2711	1257	1316	2632	867	890	2365
61	1178	1202	2370	1106	1101	2163	748	739	1817
62	1041	1034	2027	928	1003	1988	648	700	1864
63	907	923	1805	831	870	1768	556	618	1500
64	801	793	1680	726	752	1453	482	557	1126
65	725	714	1368	632	648	1314	450	490	1135
66	630	604	1080	571	596	1078	367	402	1005
67	572	552	1000	498	504	946	342	353	814
68	490	471	931	444	445	758	309	316	621
69	455	424	771	393	407	722	260	285	544
70	424	395	603	348	364	621	228	228	531
71	357	361	555	326	330	498	221	225	438
72	336	336	525	288	308	471	193	217	425
73	307	292	462	255	256	377	164	169	305
74	290	281	418	235	241	513	166	165	317
75	272	258	400	226	222	336	138	162	255
76	266	238	390	215	220	343	148	125	219
77	255	237	393	204	209	319	131	140	232
78	248	238	381	193	202	300	125	120	223
79	3366	3277	4474	3267	3250	4375	791	859	1945
80	3060	2989	4365	2986	2940	4161	1151	1149	2515
81	2707	2662	3983	2620	2621	4094	1235	1296	2651
82	2322	2348	3724	2287	2284	3734	1191	1232	2921
83	2060	2050	3481	1962	1983	3406	1161	1195	2803
84	1792	1831	3346	1693	1774	3462	1047	1134	2639
85	1524	1574	2764	1468	1530	3010	956	1001	2415
86	1373	1380	2910	1302	1324	2640	867	911	2323
87	1199	1225	2468	1107	1149	2321	751	818	2006
88	1057	1059	2043	972	1010	1800	659	717	1706
89	931	928	1800	837	871	1767	578	596	1574
90	826	790	1712	740	783	1421	508	543	1279
91	716	729	1325	649	646	1233	480	477	958
92	637	637	1074	617	615	1057	398	425	804
93	570	557	962	504	527	870	343	357	713

94	522	505	947	454	464	811	307	331	647
95	463	441	728	405	403	689	274	275	572
96	412	404	618	367	340	567	234	241	590
97	383	369	551	324	339	535	202	243	431
98	340	326	489	292	303	433	185	207	410
99	315	313	463	268	269	371	188	189	346
100	291	273	454	237	254	405	150	158	267
101	281	270	386	226	217	372	136	157	234
102	274	251	359	216	220	325	146	146	240
103	263	239	360	195	205	332	128	137	266
104	249	225	382	206	188	260	112	107	198
105	3374	3321	4484	3282	3248	4375	847	889	1965
106	3060	2985	4201	3015	2943	4282	1136	1147	2432
107	2670	2671	4202	2609	2612	3938	1234	1324	2727
108	2363	2336	3786	2234	2281	3820	1227	1289	2740
109	2001	2099	3641	1940	1974	3505	1156	1244	2703
110	1760	1783	3239	1684	1737	3002	1111	1157	2635
111	1560	1550	2645	1461	1528	2535	981	1001	2395
112	1361	1362	2461	1282	1318	2372	854	929	1999
113	1205	1187	2431	1117	1150	2298	758	762	1815
114	1052	1032	1918	982	1014	1857	663	706	1775
115	935	942	1631	864	875	1537	583	646	1521
116	817	828	1509	759	766	1325	511	523	1204
117	722	718	1273	666	671	1179	466	460	962
118	650	617	1098	569	598	996	414	398	978
119	594	561	995	504	515	886	353	373	684
120	529	519	853	425	468	790	313	302	591
121	452	459	798	387	417	689	278	278	544
122	420	404	665	358	362	571	233	237	459
123	381	371	517	327	338	504	224	220	416
124	347	344	499	301	307	491	179	209	396
125	329	312	438	275	277	368	177	188	395
126	287	279	421	245	244	400	163	166	289
127	278	277	406	236	236	303	168	155	330
128	262	247	376	219	219	337	135	133	238
129	256	252	361	206	200	316	140	126	221
130	249	237	376	210	189	385	118	125	210
131	3382	3319	4538	3307	3243	4381	841	863	1906
132	3012	2960	4148	2935	2895	4091	1168	1157	2392
133	2607	2588	4182	2524	2523	3958	1259	1325	2542
134	2256	2269	3777	2148	2189	3433	1218	1286	2732
135	1969	2011	3559	1865	1907	3442	1153	1257	2579
136	1718	1719	3181	1614	1682	3107	1082	1153	2688
137	1514	1515	2704	1432	1496	2774	955	1044	2455
138	1316	1328	2366	1253	1279	2335	882	934	2060
139	1190	1208	2293	1103	1146	2101	778	797	1828
140	1047	1044	1896	967	1018	1782	671	700	1395
141	913	905	1745	837	871	1569	590	621	1304
142	813	815	1433	749	764	1385	482	528	1071
143	725	698	1436	668	674	1132	449	467	987
144	638	638	1111	565	603	1029	384	410	833
145	576	561	946	507	512	843	344	335	756

146	518	507	731	454	466	676	301	325	591
147	463	450	689	418	402	699	279	276	513
148	429	425	727	363	370	582	231	257	536
149	363	361	602	314	326	498	205	219	423
150	352	319	469	298	305	453	186	196	370
151	316	324	418	266	280	406	177	172	346
152	296	303	518	245	250	348	158	178	268
153	284	268	395	226	234	388	135	157	263
154	271	255	442	217	223	450	140	136	271
155	256	257	357	208	214	308	137	130	262
156	252	245	392	199	195	317	122	118	249
157	**3409**	**3324**	**4531**	**3297**	**3218**	**4328**	**807**	**856**	**1826**
158	**2852**	**2741**	**4025**	**2750**	**2710**	**3900**	**1135**	**1126**	**2312**
159	**2354**	**2331**	**3869**	**2258**	**2245**	**3572**	**1122**	**1187**	**2388**
160	**2030**	**2046**	**3630**	**1915**	**2016**	**3360**	**1138**	**1215**	**2603**
161	**1807**	**1879**	**3130**	**1722**	**1808**	**3282**	**1100**	**1171**	**2810**
162	**1661**	**1664**	**2842**	**1562**	**1605**	**2820**	**1037**	**1149**	**2186**
163	**1452**	**1495**	**2726**	**1413**	**1445**	**2547**	**957**	**1018**	**2087**
164	**1336**	**1314**	**2518**	**1248**	**1282**	**2309**	**825**	**909**	**2012**
165	**1150**	**1163**	**2176**	**1085**	**1113**	**2066**	**752**	**801**	**1729**
166	**1017**	**1022**	**1923**	**955**	**988**	**1818**	**634**	**686**	**1523**
167	**929**	**898**	**1633**	**821**	**854**	**1561**	**548**	**608**	**1394**
168	**800**	**787**	**1425**	**718**	**742**	**1232**	**506**	**514**	**1117**
169	**720**	**708**	**1294**	**631**	**667**	**1238**	**445**	**460**	**818**
170	**645**	**612**	**1087**	**564**	**592**	**996**	**385**	**417**	**801**
171	**578**	**518**	**845**	**492**	**540**	**964**	**319**	**345**	**689**
172	**479**	**480**	**829**	**448**	**442**	**756**	**284**	**323**	**644**
173	**466**	**427**	**674**	**401**	**400**	**603**	**260**	**271**	**463**
174	**417**	**390**	**590**	**351**	**361**	**520**	**233**	**248**	**477**
175	**382**	**354**	**693**	**322**	**328**	**512**	**204**	**217**	**386**
176	**348**	**323**	**467**	**289**	**300**	**457**	**182**	**187**	**350**
177	**320**	**304**	**432**	**268**	**271**	**482**	**170**	**179**	**382**
178	**302**	**288**	**417**	**243**	**254**	**448**	**150**	**167**	**355**
179	**282**	**274**	**411**	**229**	**230**	**303**	**146**	**147**	**273**
180	**281**	**240**	**357**	**219**	**216**	**355**	**142**	**135**	**223**
181	**250**	**249**	**332**	**221**	**211**	**322**	**132**	**133**	**214**
182	**250**	**230**	**313**	**196**	**208**	**310**	**129**	**126**	**244**
183	3346	3164	4441	3149	3081	4185	689	718	1666
184	2323	2119	3328	2053	2099	3034	872	891	1883
185	1850	1777	2922	1724	1740	2865	905	940	2148
186	1701	1736	2972	1604	1661	2884	998	1046	2390
187	1688	1737	2971	1595	1645	2844	1052	1140	2459
188	1583	1591	2899	1486	1563	2778	1021	1031	2401
189	1459	1408	2765	1334	1383	2538	921	927	2025
190	1238	1273	2394	1160	1243	2087	814	852	1890
191	1115	1118	2098	1049	1072	1830	708	739	1734
192	998	1003	1665	924	953	1643	633	639	1522
193	903	864	1531	805	846	1451	558	575	1198
194	784	781	1256	732	743	1210	497	505	962
195	725	714	1139	608	658	1092	420	433	902
196	628	592	1139	542	562	911	388	384	778
197	547	528	912	482	503	833	322	345	654

198	505	483	750	440	451	772	287	307	502
199	459	424	699	400	391	732	258	280	545
200	404	398	648	349	349	472	234	229	461
201	370	359	570	309	342	570	206	205	446
202	330	326	541	282	285	481	194	172	365
203	320	295	529	254	263	371	177	178	280
204	292	287	447	242	226	353	148	153	283
205	276	263	373	219	234	324	135	160	275
206	257	245	353	218	219	369	135	141	289
207	249	249	364	195	214	322	132	113	211
208	241	231	342	194	201	297	122	118	216
209	835	801	830	447	408	429	10	9	21
210	0	0	0	0	0	0	0	0	0
211	281	258	339	228	223	292	93	86	158
212	1453	1431	2544	1341	1422	2343	754	853	1814
213	1625	1645	2893	1542	1582	2830	982	1026	2257
214	1530	1550	2586	1399	1473	2607	945	988	2040
215	1347	1375	2381	1258	1328	2327	847	854	1945
216	1206	1206	2307	1126	1169	2156	769	791	1774
217	1095	1067	1922	984	1044	1834	687	703	1695
218	940	954	1593	874	900	1577	611	633	1228
219	852	835	1413	772	813	1355	517	546	1139
220	780	742	1223	669	697	1332	450	481	1015
221	678	667	1060	606	620	1065	425	430	860
222	616	620	951	554	535	1079	376	384	750
223	545	522	902	482	495	790	330	325	631
224	482	465	712	408	451	648	286	296	575
225	426	423	674	364	388	570	252	265	463
226	399	378	639	340	328	496	224	238	374
227	359	345	504	306	326	478	197	195	433
228	323	303	497	275	282	482	179	179	402
229	296	289	470	245	262	385	158	164	377
230	276	268	412	228	247	367	140	144	325
231	267	255	384	218	223	370	149	144	295
232	248	240	420	209	210	284	143	130	212
233	248	232	319	201	206	322	122	118	183
234	246	240	368	196	194	296	118	122	200
235	3167	3096	3620	3023	2925	3476	384	418	855
236	2098	2044	2493	1941	1920	2338	447	434	853
237	1506	1482	2031	1428	1403	1931	499	536	1316
238	1430	1438	2572	1351	1413	2370	705	776	1767
239	1473	1530	2635	1398	1391	2649	895	915	2070
240	1387	1393	2422	1314	1363	2306	845	867	2009
241	1283	1291	2319	1162	1209	2018	790	796	1747
242	1149	1147	2095	1068	1087	2056	698	725	1531
243	1024	1032	1710	933	972	1836	636	659	1369
244	919	896	1689	851	834	1518	573	564	1218
245	810	780	1349	721	744	1388	517	515	1055
246	699	720	1239	650	663	1221	432	460	896
247	639	616	1102	568	575	938	396	388	776
248	580	559	963	508	517	885	326	358	643
249	520	499	924	453	466	738	315	316	590

250	468	459	836	392	409	752	273	277	487
251	429	405	700	368	374	581	239	268	544
252	378	371	637	325	325	635	216	219	446
253	352	338	537	290	301	547	193	192	351
254	318	308	526	272	284	465	174	171	369
255	294	284	435	229	262	395	166	163	342
256	272	258	385	226	243	342	147	155	235
257	253	235	324	202	221	344	132	119	292
258	246	237	343	204	197	368	117	136	213
259	238	226	331	200	189	309	111	110	252
260	243	216	304	191	178	250	107	115	219
261	2862	2793	3474	2706	2665	3385	433	435	1086
262	2115	2065	2796	1946	1952	2538	536	581	1138
263	1638	1672	2386	1514	1515	2358	611	663	1642
264	1412	1449	2492	1297	1338	2396	692	763	1902
265	1362	1386	2609	1260	1287	2420	782	834	1812
266	1263	1284	2255	1185	1202	2096	770	796	1937
267	1188	1143	2022	1036	1076	1964	698	728	1759
268	1059	1050	1906	946	973	1938	637	693	1422
269	941	919	1752	875	890	1733	585	603	1348
270	846	841	1735	754	814	1436	529	544	1181
271	771	740	1205	696	684	1042	466	464	1020
272	679	672	1189	608	595	1090	398	405	969
273	610	589	1090	541	559	885	358	387	905
274	560	532	791	479	463	832	321	324	654
275	495	479	798	411	433	634	289	264	550
276	430	445	736	364	377	570	251	257	508
277	410	390	641	332	350	542	223	226	508
278	368	359	570	298	312	536	207	212	555
279	329	308	500	268	275	427	174	191	395
280	305	291	396	255	251	432	168	165	390
281	274	263	407	234	227	351	167	150	357
282	257	236	392	212	209	331	120	137	335
283	247	226	303	202	196	331	144	141	204
284	224	212	321	188	196	336	120	108	227
285	218	207	383	188	186	293	103	101	178
286	205	203	290	167	176	317	104	89	175
Mean	962	948	1568	886	900	1487	481	503	1105
Max	3409	3324	4538	3307	3250	4381	1259	1325	2921
Min	205	203	290	167	176	245	10	9	21
$Mean_{table}$	2969	2916	4242	2886	2848	4092	1061	1097	2277
Max_{table}	3409	3324	4538	3307	3248	4381	1259	1325	2727
Min_{table}	2354	2331	3869	2258	2245	3572	807	856	1826

Table A4. 1 Point-in-Time Illuminance data by DIVA of each window system for Virtual Restaurant Prototype. Sensor-row, that contains reference sensors of the table, is in bold

Point-in-Time Illuminance (lux) by TPM, 22 July at 12:00 local time (PROTOTYPE)

Nº Sensor	No Frame			Large Frame			Small Frame		
	No CFSnf	Light Shelf	3M Prismatic Film	No CFSlf	Light Shelf	3M Prismatic Film	No CFSsf	Light Shelf	3M Prismatic Film
1	6776	8207	7968	5564	7257	6239	747	1224	1316
2	6291	7400	7416	5002	6395	5811	1097	1950	2015
3	5877	6935	7219	4755	5802	5529	1403	2770	2420
4	5275	6156	6219	4251	5284	5396	1528	2865	2493
5	4751	5467	5542	3866	4681	5030	1534	2881	2767
6	4143	4860	4919	3421	4168	4306	1589	2779	2630
7	3659	4129	4356	3039	3582	3940	1486	2452	2543
8	3060	3443	3864	2666	3159	3462	1454	2193	2319
9	2726	3061	3151	2403	2787	2824	1235	1936	2266
10	2470	2638	2981	2166	2356	2625	1134	1660	1760
11	1924	2240	2622	1823	2008	2156	1065	1574	1638
12	1743	1901	2155	1494	1750	2032	988	1313	1490
13	1519	1670	1782	1340	1553	1542	886	1107	1259
14	1384	1409	1677	1188	1372	1647	796	971	1218
15	1123	1258	1355	1067	1205	1291	641	813	1187
16	1054	1143	1304	971	1021	1150	607	719	898
17	922	1008	1152	878	889	1122	615	562	815
18	949	871	973	752	834	933	561	581	674
19	841	821	814	643	671	953	517	545	652
20	669	767	860	625	656	733	407	553	545
21	644	688	804	532	640	714	330	434	578
22	535	558	676	483	551	499	366	390	575
23	519	605	580	451	499	578	254	395	396
24	541	487	521	453	478	412	346	371	371
25	548	488	504	440	476	456	339	382	306
26	451	476	567	469	478	485	295	305	324
27	6945	8543	8030	5919	7761	6548	867	1556	1492
28	6498	7761	7774	5469	7060	6192	1308	2448	2264
29	6035	7138	7522	5015	6433	6051	1619	2957	2601
30	5453	6447	6483	4515	5611	5609	1731	3190	3075
31	4987	5617	5959	4003	5021	5075	1776	2986	2936
32	4323	4932	5141	3710	4445	4846	1705	2832	2993
33	3838	4194	4510	3185	3874	4072	1595	2539	2676
34	3293	3575	3907	2776	3233	3571	1454	2324	2356
35	2840	3020	3304	2462	2825	3234	1381	2064	2150
36	2338	2700	2864	2139	2407	2808	1146	1803	2026
37	2019	2227	2317	1922	2160	2295	1037	1508	1617
38	1793	2031	2082	1603	1765	2020	1021	1355	1429
39	1534	1691	1987	1406	1462	1831	915	1150	1338
40	1401	1631	1558	1191	1347	1578	816	916	1123
41	1226	1410	1506	1083	1211	1466	715	895	1014
42	1053	1198	1261	891	1165	1179	688	847	989
43	995	997	1104	886	998	1089	613	638	883
44	901	904	1049	726	800	921	562	614	751
45	822	917	833	708	769	941	468	586	692
46	716	776	849	654	626	809	534	442	681
47	687	670	683	503	622	653	357	476	666

48	638	574	714	489	627	620	263	440	406
49	535	577	640	467	514	628	319	325	425
50	560	570	658	450	484	653	333	337	607
51	489	536	507	477	516	623	302	314	393
52	528	555	582	434	473	502	299	353	400
53	6984	8551	8100	6043	8063	6498	986	1903	1724
54	6611	7998	7985	5570	7304	6608	1517	2910	2247
55	6144	7424	7497	5165	6646	6238	1732	3298	3008
56	5530	6562	6665	4516	5888	5631	1830	3251	3135
57	4786	5740	5957	4198	5167	5270	1751	3375	3159
58	4345	4941	5220	3674	4554	4635	1726	3165	3086
59	3710	4199	4364	3142	3800	4137	1660	2676	2765
60	3162	3613	4122	2824	3391	3502	1482	2378	2505
61	2820	3081	3273	2527	2827	3124	1366	2105	2301
62	2361	2610	2806	2168	2519	2729	1276	1894	1954
63	2085	2302	2501	1782	2079	2600	1140	1595	1748
64	1815	2050	2179	1608	1898	2189	1008	1479	1510
65	1515	1718	1920	1484	1619	1824	903	1133	1365
66	1424	1403	1721	1258	1400	1621	812	954	1105
67	1251	1238	1476	1106	1236	1381	698	901	991
68	1132	1172	1484	960	1001	1270	631	870	908
69	1005	1063	1119	882	965	1063	520	761	880
70	821	943	1062	809	835	933	533	620	751
71	735	847	947	696	825	815	477	546	622
72	744	772	932	693	693	800	485	499	532
73	691	617	771	464	532	695	402	404	538
74	640	673	667	547	610	632	450	345	459
75	579	537	760	541	533	652	392	440	364
76	569	577	495	434	570	538	301	375	381
77	462	557	608	454	487	543	212	369	430
78	530	623	690	437	498	499	318	282	320
79	7087	8538	8229	5979	8114	6621	1092	2017	1973
80	6599	8107	7951	5701	7472	6453	1550	2995	2654
81	6211	7302	7478	5217	6694	6309	1747	3432	3010
82	5521	6475	6821	4640	5987	5826	1909	3574	3207
83	4885	5660	6041	4036	5222	5422	1902	3498	3334
84	4130	4820	5188	3656	4430	4697	1854	3314	3014
85	3777	4099	4376	3242	3815	4365	1713	2790	2961
86	3126	3585	3923	2766	3362	3618	1464	2491	2720
87	2790	3108	3409	2408	2855	3205	1475	2046	2240
88	2443	2695	2912	2077	2445	2881	1328	1857	2137
89	2111	2284	2588	1898	2213	2357	1216	1651	1830
90	1905	2041	2279	1638	1888	2053	1039	1408	1644
91	1610	1777	2057	1352	1537	1728	943	1187	1485
92	1411	1480	1645	1291	1468	1633	823	1053	1122
93	1320	1346	1536	1101	1314	1508	717	935	1048
94	1049	1179	1335	953	1152	1240	652	747	902
95	950	1125	1173	830	887	1052	608	665	799
96	883	1005	891	749	834	1021	559	591	670
97	779	898	991	731	757	919	526	611	697
98	746	790	864	588	765	713	431	428	589
99	689	697	931	563	610	666	404	402	555

100	576	694	658	553	576	629	376	385	520
101	535	616	715	493	527	696	409	411	513
102	552	575	657	499	502	539	379	359	436
103	514	506	574	485	521	575	280	269	439
104	544	570	601	479	444	594	332	388	361
105	6961	8517	8120	5982	8016	6677	1161	2068	1925
106	6554	7995	8058	5530	7461	6681	1591	3243	2557
107	6049	7274	7423	5054	6906	6333	1957	3595	3054
108	5324	6325	6706	4556	5858	5836	1978	3542	3306
109	4651	5546	5869	4004	5081	5383	1956	3443	3203
110	4048	4826	5057	3600	4460	4716	1805	3098	3144
111	3522	4140	4538	3179	3803	4148	1745	2758	2883
112	3086	3499	3865	2760	3354	3581	1513	2401	2579
113	2618	3071	3443	2304	2817	3116	1385	2197	2147
114	2349	2620	2866	2112	2463	2953	1426	1804	1908
115	2030	2272	2476	1885	2165	2464	1171	1647	1915
116	1810	2044	2301	1637	1889	2134	1117	1316	1473
117	1576	1804	1834	1434	1519	1720	965	1131	1306
118	1407	1488	1769	1221	1437	1567	812	1025	1178
119	1177	1354	1636	1083	1232	1439	776	936	1142
120	1079	1185	1305	947	1045	1300	717	783	973
121	1008	998	1254	890	954	1089	617	600	787
122	912	994	1091	760	879	939	467	630	678
123	821	840	976	754	767	824	429	639	624
124	708	814	836	594	684	721	440	507	609
125	583	695	745	558	533	786	432	464	575
126	598	615	713	551	591	468	396	455	509
127	592	591	660	566	507	562	349	342	391
128	544	584	600	434	521	548	355	365	341
129	537	602	659	380	462	636	261	367	456
130	504	615	790	454	487	472	316	366	394
131	6942	8594	8101	5865	7985	6818	1070	2039	1931
132	6474	7964	7954	5534	7382	6507	1617	3110	2686
133	5800	6902	7117	4926	6633	6174	1891	3613	3113
134	4888	5972	6391	4323	5555	5735	1876	3551	3215
135	4450	5172	5409	3712	4849	5008	1887	3520	3420
136	3871	4514	4947	3433	4196	4591	1792	3053	3263
137	3474	3965	4343	2980	3757	4069	1710	2855	2869
138	2907	3428	3892	2629	3289	3592	1590	2315	2621
139	2635	2942	3316	2277	2815	3078	1403	2055	2450
140	2328	2703	2969	2119	2468	2621	1308	1848	2017
141	1997	2240	2429	1871	2165	2494	1230	1705	1867
142	1774	2034	2194	1578	1825	1991	995	1413	1536
143	1558	1722	1899	1404	1596	1934	923	1227	1359
144	1352	1471	1632	1303	1409	1453	833	1128	1340
145	1229	1384	1406	1101	1273	1402	773	901	1132
146	1122	1268	1286	928	1057	1181	625	856	782
147	898	1008	1179	876	1003	1077	546	724	696
148	847	926	937	755	847	879	460	687	690
149	806	835	991	646	771	930	516	619	638
150	712	747	806	664	702	802	504	473	577
151	668	642	793	558	604	618	442	537	369

152	642	546	733	575	507	579	334	422	540
153	539	555	606	578	568	625	341	382	439
154	476	509	538	516	563	598	259	370	447
155	510	483	577	434	450	460	286	368	453
156	517	577	577	441	471	526	298	348	395
157	**7002**	**8581**	**8232**	**5903**	**8000**	**6701**	**1092**	**1993**	**1651**
158	**5951**	**7360**	**7333**	**5162**	**6894**	**6110**	**1522**	**3046**	**2580**
159	**5087**	**6197**	**6317**	**4377**	**5874**	**5521**	**1708**	**3498**	**2815**
160	**4307**	**5264**	**5596**	**3713**	**5041**	**5096**	**1817**	**3342**	**3076**
161	**3980**	**4826**	**5167**	**3459**	**4548**	**4652**	**1867**	**3363**	**3219**
162	**3653**	**4289**	**4729**	**3216**	**4045**	**4403**	**1784**	**2980**	**3200**
163	**3340**	**3796**	**4200**	**2918**	**3613**	**4040**	**1632**	**2779**	**2904**
164	**2816**	**3367**	**3896**	**2625**	**3157**	**3392**	**1522**	**2306**	**2479**
165	**2522**	**2852**	**3472**	**2332**	**2701**	**3078**	**1337**	**2086**	**2296**
166	**2205**	**2536**	**2881**	**2016**	**2309**	**2549**	**1250**	**1852**	**2066**
167	**1962**	**2120**	**2491**	**1681**	**2034**	**2355**	**1092**	**1576**	**1852**
168	**1722**	**1881**	**2068**	**1586**	**1761**	**2002**	**1018**	**1315**	**1477**
169	**1472**	**1681**	**2032**	**1306**	**1557**	**1767**	**903**	**1158**	**1213**
170	**1332**	**1473**	**1704**	**1204**	**1418**	**1597**	**845**	**1063**	**1001**
171	**1156**	**1264**	**1499**	**1116**	**1128**	**1265**	**656**	**898**	**1104**
172	**1051**	**1202**	**1329**	**992**	**1018**	**1184**	**611**	**810**	**942**
173	**973**	**1020**	**1074**	**826**	**875**	**1080**	**570**	**583**	**860**
174	**818**	**896**	**1059**	**714**	**836**	**920**	**502**	**612**	**800**
175	**773**	**888**	**897**	**688**	**728**	**874**	**498**	**612**	**699**
176	**775**	**721**	**843**	**682**	**675**	**784**	**492**	**489**	**539**
177	**680**	**687**	**779**	**596**	**617**	**724**	**355**	**468**	**499**
178	**569**	**619**	**830**	**527**	**597**	**647**	**398**	**429**	**516**
179	**580**	**704**	**683**	**506**	**494**	**532**	**311**	**409**	**330**
180	**548**	**578**	**641**	**446**	**547**	**550**	**326**	**365**	**415**
181	**498**	**550**	**685**	**472**	**505**	**557**	**290**	**366**	**463**
182	**490**	**549**	**679**	**425**	**431**	**449**	**332**	**337**	**457**
183	6817	8379	7799	5770	7809	6306	935	1808	1684
184	4621	5678	5662	3958	5453	4851	1235	2367	2112
185	3757	4636	4787	3281	4611	4093	1445	2748	2416
186	3427	4229	4594	3031	4189	4211	1565	2821	2788
187	3638	4417	4718	3050	4226	4462	1697	3127	3126
188	3400	4088	4473	2954	3836	4202	1772	2924	2770
189	3040	3601	4178	2727	3423	4058	1559	2559	2776
190	2821	3147	3455	2490	3033	3474	1449	2360	2451
191	2328	2703	3001	2196	2714	2873	1320	1949	2175
192	2161	2428	2683	1931	2294	2673	1233	1703	1855
193	1900	2098	2346	1647	1990	2378	1092	1493	1770
194	1631	1857	2079	1475	1723	2038	1025	1221	1503
195	1537	1567	1703	1292	1506	1660	813	1092	1297
196	1309	1400	1753	1156	1332	1485	844	1031	1171
197	1201	1334	1444	1045	1178	1394	686	802	990
198	1055	1178	1252	885	999	1142	620	803	853
199	882	953	1038	803	905	1103	564	601	705
200	861	874	1011	713	830	973	477	595	706
201	764	840	980	669	739	820	459	578	679
202	699	730	954	541	609	720	388	447	553
203	619	632	779	585	600	626	443	526	572

204	649	570	628	428	540	659	365	402	560
205	513	567	578	468	497	634	317	413	357
206	547	570	713	486	495	696	290	356	410
207	491	542	546	444	429	516	287	321	533
208	505	526	673	441	468	499	293	297	412
209	1811	2053	1746	952	1171	971	38	66	52
210	0	0	0	0	0	0	0	0	0
211	607	660	603	517	586	545	221	322	308
212	2990	3557	3804	2566	3423	3509	1192	2347	2184
213	3406	4184	4630	2978	4029	4126	1529	2890	2806
214	3186	3783	4236	2872	3691	3916	1501	2665	2742
215	2854	3319	3756	2638	3242	3772	1533	2385	2760
216	2491	3003	3536	2308	2895	3083	1343	2212	2210
217	2346	2691	2909	2066	2599	2802	1336	1854	2076
218	2097	2333	2479	1817	2179	2370	1156	1599	1889
219	1934	1970	2248	1611	1867	2046	1038	1481	1518
220	1563	1761	1988	1445	1705	1820	995	1251	1431
221	1378	1476	1678	1293	1466	1652	805	1175	1115
222	1290	1376	1637	1108	1189	1393	778	979	1050
223	1080	1256	1308	925	1137	1356	731	870	848
224	1051	1132	1237	857	982	1161	617	770	806
225	864	954	1089	840	836	932	532	578	737
226	782	908	973	713	790	912	514	576	591
227	763	803	892	645	705	865	459	504	653
228	624	755	918	585	662	717	394	455	500
229	596	696	772	579	553	720	317	476	532
230	605	603	729	552	501	588	364	354	549
231	542	580	609	432	551	525	344	326	449
232	512	539	634	416	496	569	328	318	434
233	505	491	601	389	395	449	301	320	329
234	450	441	478	451	420	522	278	381	325
235	6698	8231	7425	5602	7504	5864	575	1092	1039
236	4531	5365	5159	3792	4863	4219	678	1339	1142
237	3250	3831	3882	2709	3562	3410	841	1482	1432
238	3046	3560	4009	2625	3383	3489	1163	2077	2167
239	3146	3793	4103	2785	3610	4118	1422	2630	2561
240	3030	3526	3817	2577	3331	3539	1399	2578	2492
241	2769	3021	3630	2362	3017	3216	1360	2293	2355
242	2413	2821	3189	2192	2665	2971	1349	1925	2260
243	2275	2447	2940	1926	2318	2647	1107	1823	1866
244	1949	2209	2453	1781	2010	2500	1118	1585	1649
245	1638	1934	2185	1523	1857	2013	1017	1365	1440
246	1551	1775	1973	1449	1541	1727	795	1069	1393
247	1283	1452	1613	1187	1413	1532	775	964	1189
248	1233	1287	1477	1061	1174	1354	675	946	1027
249	1122	1198	1259	965	1032	1279	636	862	902
250	1010	975	1155	831	870	1097	598	668	838
251	900	965	1007	806	891	958	578	670	609
252	751	823	965	731	767	869	414	568	693
253	718	834	824	613	685	827	464	520	667
254	685	728	709	575	665	706	342	450	495
255	648	643	845	562	535	620	382	422	496

256	582	587	643	530	527	569	326	335	421
257	490	557	634	402	489	522	277	336	399
258	494	553	527	422	468	461	254	285	337
259	498	445	583	386	425	541	316	368	408
260	544	492	548	390	440	431	291	284	410
261	5755	7099	6361	4998	6762	5569	559	1110	1069
262	4178	5231	5032	3672	4995	4284	770	1537	1493
263	3363	4153	4172	2924	3876	3657	919	1899	1703
264	2917	3492	3823	2599	3295	3441	1101	2122	2011
265	2853	3459	3710	2436	3290	3418	1238	2429	2273
266	2633	3201	3469	2190	3106	3477	1345	2323	2366
267	2479	2860	3397	2165	2843	3093	1252	2083	2248
268	2265	2460	2920	1990	2453	2635	1087	1842	1907
269	1969	2337	2674	1840	2195	2499	1114	1601	1830
270	1798	2028	2447	1554	1977	2208	1060	1408	1595
271	1602	1756	2033	1421	1677	1877	906	1263	1335
272	1451	1540	1776	1260	1483	1733	931	1064	1216
273	1350	1382	1632	1132	1271	1325	769	980	1168
274	1095	1313	1266	1036	1168	1154	605	856	912
275	1007	1144	1281	987	1033	1100	589	772	850
276	938	944	1153	719	867	1063	529	797	736
277	818	977	1026	771	836	946	479	556	622
278	753	821	811	696	753	854	507	546	672
279	665	789	851	655	652	743	474	399	606
280	600	647	750	542	619	573	340	338	520
281	614	613	680	481	639	629	314	465	580
282	540	557	631	468	477	680	304	331	436
283	523	519	489	476	496	436	283	251	433
284	439	492	560	433	470	511	218	280	312
285	422	493	423	390	442	530	240	301	365
286	436	478	608	367	460	463	271	297	417
Mean	2108	2432	2579	1823	2244	2298	881	1348	1398
Max	7087	8594	8232	6043	8114	6818	1978	3613	3420
Min	422	441	423	367	395	412	38	66	52
$Mean_{table}$	6313	7709	7628	5370	7239	6391	1512	2912	2479
Max_{table}	7002	8594	8232	5982	8016	6818	1957	3613	3113
Min_{table}	5087	6197	6317	4377	5874	5521	1070	1993	1651

Table A4. 2 The illuminance data by TPM of each window system for Virtual Restaurant Prototype. Sensor-row, that contains reference sensors of the table, is in bold

Daylight Autonomy (DA, %) by TPM, 11:00-17:00 (PROTOTYPE)

Nº Sensor	No Frame			Large Frame			Small Frame		
	No CFSnf	Light Shelf	3M Prismatic Film	No CFSlf	Light Shelf	3M Prismatic Film	No CFSsf	Light Shelf	3M Prismatic Film
1	100	100	100	100	100	100	83	92	95
2	100	100	100	100	100	100	90	97	98
3	100	100	100	100	100	100	95	98	98
4	100	100	100	100	100	100	96	99	98
5	100	100	100	100	100	100	96	99	99
6	100	100	100	100	100	100	98	99	99
7	100	100	100	99	100	100	97	99	99
8	99	100	100	99	99	99	97	98	98
9	99	99	99	99	99	99	95	98	98
10	99	99	99	99	99	99	96	98	98
11	99	99	99	99	99	99	95	98	97
12	99	99	99	98	99	98	94	97	97
13	98	99	98	98	98	98	95	95	95
14	98	98	98	98	98	98	93	94	95
15	98	98	97	97	98	96	90	93	95
16	97	98	97	96	97	95	89	92	90
17	95	96	95	95	95	94	89	86	88
18	96	94	93	93	94	93	87	86	85
19	94	95	90	91	92	93	86	86	84
20	91	93	90	90	91	89	73	87	80
21	91	91	89	86	90	86	61	77	82
22	85	87	85	81	88	75	70	72	80
23	85	88	82	84	84	82	35	74	70
24	85	83	79	82	83	68	69	70	66
25	86	84	78	78	83	77	66	72	55
26	80	82	81	83	84	77	54	59	61
27	100	100	100	100	100	100	86	96	96
28	100	100	100	100	100	100	92	98	98
29	100	100	100	100	100	100	97	98	98
30	100	100	100	100	100	100	97	99	99
31	100	100	100	100	100	100	98	99	99
32	100	100	100	100	100	100	98	99	99
33	100	100	100	100	100	100	98	99	99
34	100	100	100	99	99	100	98	99	99
35	99	99	99	99	99	99	98	99	98
36	99	99	99	99	99	99	96	98	98
37	99	99	99	99	99	99	95	98	98
38	99	99	99	98	99	99	95	98	97
39	98	99	98	98	98	98	95	97	97
40	98	98	98	98	98	98	94	95	94
41	98	98	98	97	98	98	92	94	93
42	96	98	97	96	98	95	91	94	93
43	96	97	94	95	97	94	90	89	90
44	95	95	94	93	94	92	88	89	88
45	95	95	90	93	94	93	81	89	87
46	92	94	92	90	90	89	87	78	87
47	91	91	88	86	90	88	69	81	86

48	90	87	88	83	90	85	40	81	71
49	86	88	85	85	86	86	63	70	77
50	87	87	86	81	87	86	70	67	85
51	81	85	76	85	85	85	56	61	67
52	86	87	82	80	84	81	59	72	71
53	100	100	100	100	100	100	90	97	98
54	100	100	100	100	100	100	96	99	98
55	100	100	100	100	100	100	97	99	99
56	100	100	100	100	100	100	98	99	99
57	100	100	100	100	100	100	98	99	99
58	100	100	100	100	100	100	98	99	99
59	100	100	100	100	100	100	98	99	99
60	100	100	100	99	100	100	98	99	99
61	99	100	99	99	99	99	98	99	99
62	99	99	99	99	99	99	97	98	98
63	99	99	99	99	99	99	97	98	98
64	99	99	99	99	99	99	95	98	97
65	98	99	98	98	98	98	95	96	96
66	98	98	98	98	98	98	95	96	94
67	98	98	98	98	98	97	93	95	91
68	98	98	98	96	97	97	91	94	91
69	97	98	95	96	97	94	88	93	91
70	94	95	94	94	95	93	87	89	87
71	94	95	93	93	95	90	85	88	83
72	93	94	93	93	93	90	86	86	79
73	92	90	89	81	88	87	77	78	81
74	90	91	87	87	90	86	81	70	77
75	88	85	89	88	87	88	75	82	69
76	87	88	76	81	89	80	59	75	66
77	80	87	83	83	84	81	22	74	75
78	85	90	88	81	87	80	63	56	60
79	100	100	100	100	100	100	91	98	98
80	100	100	100	100	100	100	96	99	99
81	100	100	100	100	100	100	98	99	99
82	100	100	100	100	100	100	98	99	99
83	100	100	100	100	100	100	98	99	99
84	100	100	100	100	100	100	98	99	99
85	100	100	100	100	100	100	98	99	99
86	100	100	100	99	100	100	98	99	99
87	100	100	100	99	99	99	98	99	99
88	99	99	99	99	99	99	98	98	98
89	99	99	99	99	99	99	98	98	98
90	99	99	99	99	99	99	97	98	98
91	99	99	99	98	98	98	95	97	98
92	98	98	98	98	98	98	95	97	95
93	98	98	98	98	98	98	93	96	93
94	98	98	97	97	98	97	91	92	92
95	97	98	96	95	96	94	90	90	90
96	96	97	92	94	95	94	87	88	86
97	94	96	93	93	94	93	87	89	87
98	93	94	91	89	94	88	84	80	83
99	91	91	93	90	90	87	77	76	81

100	89	91	84	89	89	87	73	72	80
101	86	91	87	86	87	88	79	81	79
102	87	87	87	86	86	80	75	72	74
103	84	85	82	85	88	83	57	49	75
104	87	88	83	85	84	85	68	73	64
105	100	100	100	100	100	100	91	98	98
106	100	100	100	100	100	100	96	99	99
107	100	100	100	100	100	100	98	99	99
108	100	100	100	100	100	100	98	99	99
109	100	100	100	100	100	100	98	99	99
110	100	100	100	100	100	100	98	99	99
111	100	100	100	100	100	100	98	99	99
112	100	100	100	100	100	100	98	99	99
113	100	100	100	99	99	99	98	99	98
114	99	99	99	99	99	99	98	98	98
115	99	99	99	99	99	99	98	98	98
116	99	99	99	99	99	99	97	98	98
117	99	99	98	98	98	98	96	97	97
118	98	98	98	98	98	98	95	97	95
119	98	98	98	98	98	98	94	95	95
120	98	98	97	97	98	97	93	93	93
121	98	97	97	96	97	95	91	89	88
122	96	97	95	94	96	94	85	90	87
123	94	96	94	94	94	92	82	91	84
124	93	95	91	91	92	88	82	86	84
125	89	92	90	89	87	91	83	82	83
126	89	90	88	88	91	79	79	83	79
127	91	90	84	90	87	83	71	71	68
128	87	89	83	81	86	82	70	73	68
129	87	90	87	78	86	86	43	75	74
130	85	91	91	83	85	79	67	75	68
131	100	100	100	100	100	100	91	98	98
132	100	100	100	100	100	100	97	99	99
133	100	100	100	100	100	100	98	99	99
134	100	100	100	100	100	100	98	99	99
135	100	100	100	100	100	100	98	99	99
136	100	100	100	100	100	100	98	99	99
137	100	100	100	100	100	100	98	99	99
138	100	100	100	100	100	100	98	99	99
139	100	100	100	99	99	99	98	99	99
140	99	100	99	99	99	99	98	99	98
141	99	99	99	99	99	99	98	98	98
142	99	99	99	99	99	99	97	98	98
143	99	99	99	98	99	99	96	98	97
144	98	98	98	98	98	98	95	98	97
145	98	98	98	98	98	98	95	96	95
146	98	98	98	97	98	97	90	95	90
147	97	97	97	96	97	96	89	93	87
148	95	97	93	94	97	92	85	92	87
149	95	95	93	93	94	94	88	90	86
150	93	94	90	92	94	91	87	84	83
151	92	91	91	90	91	87	84	87	69

152	91	88	90	90	87	84	70	80	81
153	86	88	84	90	89	85	71	76	75
154	82	87	81	89	90	85	41	74	78
155	85	86	83	82	83	78	56	77	78
156	87	90	86	84	85	82	61	72	74
157	**100**	**100**	**100**	**100**	**100**	**100**	**90**	**98**	**98**
158	**100**	**100**	**100**	**100**	**100**	**100**	**96**	**99**	**98**
159	**100**	**100**	**100**	**100**	**100**	**100**	**98**	**99**	**99**
160	**100**	**100**	**100**	**100**	**100**	**100**	**98**	**99**	**99**
161	**100**	**100**	**100**	**100**	**100**	**100**	**98**	**99**	**99**
162	**100**	**100**	**100**	**100**	**100**	**100**	**98**	**99**	**99**
163	**100**	**100**	**100**	**100**	**100**	**100**	**98**	**99**	**99**
164	**100**	**100**	**100**	**100**	**100**	**100**	**98**	**99**	**99**
165	**100**	**100**	**100**	**99**	**100**	**100**	**98**	**99**	**99**
166	**99**	**100**	**99**	**99**	**99**	**99**	**98**	**99**	**99**
167	**99**	**99**	**99**	**99**	**99**	**99**	**97**	**98**	**98**
168	**99**	**99**	**99**	**99**	**99**	**99**	**97**	**98**	**98**
169	**99**	**99**	**99**	**98**	**99**	**98**	**97**	**98**	**97**
170	**98**	**99**	**98**	**98**	**98**	**98**	**96**	**97**	**94**
171	**98**	**98**	**98**	**98**	**98**	**97**	**92**	**95**	**96**
172	**98**	**98**	**98**	**98**	**98**	**97**	**92**	**94**	**92**
173	**97**	**98**	**96**	**96**	**97**	**96**	**90**	**89**	**92**
174	**96**	**96**	**96**	**95**	**96**	**95**	**87**	**90**	**91**
175	**94**	**97**	**93**	**94**	**95**	**92**	**88**	**91**	**87**
176	**95**	**93**	**92**	**93**	**92**	**91**	**87**	**85**	**82**
177	**93**	**92**	**91**	**91**	**91**	**90**	**77**	**85**	**79**
178	**88**	**91**	**91**	**87**	**91**	**87**	**81**	**82**	**81**
179	**90**	**93**	**87**	**87**	**86**	**83**	**66**	**81**	**63**
180	**88**	**89**	**86**	**82**	**90**	**83**	**70**	**75**	**71**
181	**87**	**89**	**89**	**85**	**88**	**85**	**61**	**75**	**79**
182	**86**	**89**	**89**	**84**	**84**	**77**	**73**	**72**	**78**
183	100	100	100	100	100	100	85	95	97
184	100	100	100	100	100	100	92	98	98
185	100	100	100	100	100	100	97	99	98
186	100	100	100	100	100	100	98	99	99
187	100	100	100	100	100	100	98	99	99
188	100	100	100	100	100	100	98	99	99
189	100	100	100	100	100	100	98	99	99
190	100	100	100	100	100	100	98	99	99
191	100	100	100	99	100	99	98	99	99
192	99	99	99	99	99	99	98	98	98
193	99	99	99	99	99	99	97	98	98
194	99	99	99	99	99	99	97	98	98
195	99	99	98	98	99	98	96	97	97
196	98	98	98	98	98	98	97	97	97
197	98	98	98	98	98	98	93	94	94
198	98	98	97	97	98	97	92	95	91
199	97	97	96	96	97	96	89	91	88
200	97	97	95	95	96	95	87	90	89
201	95	96	95	93	95	91	88	90	88
202	93	95	93	90	91	89	82	83	83
203	91	92	91	91	91	87	85	88	84

204	91	89	85	84	88	89	77	79	83
205	86	90	83	86	87	86	70	82	69
206	89	90	89	87	87	88	63	74	76
207	83	89	81	83	83	80	62	70	81
208	87	88	88	85	85	81	65	66	77
209	98	98	98	95	96	95	2	2	0
210	0	0	0	0	0	0	0	0	0
211	91	93	91	87	90	87	21	68	68
212	100	100	100	99	100	100	94	98	98
213	100	100	100	100	100	100	98	99	99
214	100	100	100	100	100	100	98	99	99
215	100	100	100	100	100	100	98	99	99
216	100	100	100	99	100	100	98	99	99
217	100	100	100	99	100	99	98	99	98
218	99	99	99	99	99	99	98	98	98
219	99	99	99	99	99	99	97	98	98
220	99	99	99	99	99	99	97	98	98
221	99	99	98	98	99	98	96	98	96
222	98	98	98	98	98	98	96	97	95
223	98	98	98	98	98	98	95	96	93
224	98	98	97	97	98	97	92	95	91
225	97	98	97	97	97	95	90	89	89
226	96	97	95	95	96	94	89	90	85
227	96	96	92	92	95	93	87	86	88
228	92	95	93	91	93	90	82	85	81
229	91	93	90	92	90	91	69	85	81
230	90	90	90	90	87	85	80	75	83
231	88	90	84	84	90	83	79	69	77
232	89	89	86	81	87	85	72	70	77
233	86	86	84	81	82	79	68	70	67
234	85	84	80	86	83	81	56	80	66
235	100	100	100	100	100	100	78	92	94
236	100	100	100	100	100	100	84	94	94
237	100	100	100	99	100	100	89	96	97
238	100	100	100	99	100	100	94	98	98
239	100	100	100	100	100	100	97	99	99
240	100	100	100	100	100	100	97	99	99
241	100	100	100	100	100	100	98	99	99
242	100	100	100	99	100	100	98	99	99
243	100	100	100	99	99	99	97	99	98
244	99	99	99	99	99	99	98	98	98
245	99	99	99	99	99	99	97	98	98
246	99	99	99	99	99	99	95	97	98
247	98	99	98	98	99	98	96	97	97
248	98	98	98	98	98	98	93	97	96
249	98	98	98	98	98	98	93	97	93
250	98	97	97	97	97	97	91	93	93
251	97	98	96	97	97	96	93	92	85
252	96	97	95	96	96	94	85	90	90
253	95	97	94	93	94	93	87	88	87
254	93	95	90	92	94	91	80	85	80
255	94	92	92	91	90	88	82	83	81

256	91	91	88	91	90	87	72	71	74
257	87	90	87	82	87	83	59	73	69
258	86	89	81	84	86	80	45	59	66
259	86	81	86	81	82	85	72	80	75
260	90	87	81	82	85	79	64	61	77
261	100	100	100	100	100	100	76	92	93
262	100	100	100	100	100	100	86	95	97
263	100	100	100	100	100	100	91	97	98
264	100	100	100	99	100	100	93	98	98
265	100	100	100	99	100	100	96	98	99
266	100	100	100	99	100	100	97	99	99
267	100	100	100	99	100	100	97	99	99
268	100	100	100	99	99	99	97	98	98
269	99	100	99	99	99	99	97	98	98
270	99	99	99	99	99	99	97	98	98
271	99	99	99	99	99	99	97	98	97
272	99	99	99	99	99	99	97	97	97
273	99	99	98	98	98	98	96	97	97
274	98	98	98	98	98	97	92	96	94
275	98	98	98	98	98	97	92	95	93
276	98	98	97	96	97	97	91	96	91
277	97	98	97	97	97	96	87	90	87
278	96	97	92	95	96	94	90	90	89
279	95	97	93	95	94	92	88	82	88
280	92	92	92	92	92	84	74	75	83
281	91	91	91	88	92	86	70	87	84
282	91	90	87	89	87	89	68	72	76
283	90	87	81	88	89	79	62	47	78
284	84	87	85	85	87	81	27	62	61
285	83	87	75	82	86	84	40	66	68
286	84	86	87	82	87	80	57	68	78
Mean	96	96	95	95	95	94	86	90	90
Max	100	100	100	100	100	100	98	99	99
Min	80	81	75	78	82	68	2	2	55
$Mean_{table}$	100	100	100	100	100	100	95	98	98
Max_{table}	100	100	100	100	100	100	98	99	99
Min_{table}	100	100	100	100	100	100	90	98	98

Table A4. 3 The Daylight Autonomy by TPM of each window system for Virtual Restaurant Prototype. Sensor-row, that contains reference sensors of the table, is in bold

Glossary

To taste the light	To perceive the light
Split façade	Divided façade
Side-view	Adjacent window view
Daylight Glare Probability	DGP
Daylight Autonomy	DA
Climate-Based Daylighting Modelling	CBDM
Three-Phase Method	TPM
Complex Fenestration System	CFS
Bi-directional Transmission Distribution Function	BTDF
Bi-directional Scattering Distribution Function	BSDF
High Dynamic Range Image	HDR
M	Mean
Standard Deviation	SD
Vertical Illuminance	E_v (lux)
Horizontal Illuminance	E_h (lux)
Luminance	L (cd/m^2)
Luminous efficacy	K_R (lm/w)
Global Horizontal Irradiance	GhI (w/m^2)
Diffuse Horizontal Irradiance	DhI (w/m^2)
Set Point	SP
WP	Workplane
R1	Restaurant 1
R2	Restaurant 2
RP	Restaurant Prototype
VRP	Virtual Restaurant Prototype
WS	Window Systems
NF	No Frame
LF	Large Frame
SF	Small Frame
LS	Light Shelf
PF	Prismatic Film
CFSnf	Complex Fenestration System - No Frame
CFSlf	Complex Fenestration System - Large Frame
CFSsf	Complex Fenestration System - Small Frame
nCFS	No Complex Fenestration System